The role of mesenchymal stem cells from adult human bone marrow in *in vitro* wound models

Nathan G. Walker

Thesis submitted to the University of Sheffield for the degree of Doctor of Philosophy

Department of Materials Science and Engineering, University of Sheffield

June 2013

Abstract

Chronic wounds present a major unmet clinical problem. They arise from wounds that fail to progress through the normal phases of healing due to factors that compound healing such as vascular complications, or diabetes. Despite improvements in treatments for difficult wounds, the incidence of limb amputation remains high. Therefore there is a need for more active therapies.

Mesenchymal stem cells (MSCs) have the capacity to differentiate into multiple cell-types, however they have also been shown to release a plethora of growth factors and cytokines which are beneficial to wound healing, consequently MSCs have shown to improve wound healing outcomes in a predominantly paracrine fashion. MSCs, for example, can increase angiogenesis/ neovascularisation, modulate inflammatory responses, accelerate re-epithelialisation, and increase collagen deposition.

The first objective of the work was to develop a synthetic material based delivery method for MSCs that could be used in the clinic. Plasma polymerisation was used to surface-functionalise medical grade silicone with acrylic acid. The acid surface chemistry enhanced cell attachment to the silicone, and cells could effectively be transferred from the silicone to model wound beds comprised of decellularised dermis (DED). Once the cells were delivered they remained viable, and the acrylic acid surface chemistry was found not to affect the MSC phenotype or their functional capacity prior to cell delivery.

The second part of the project involved developing a 3-D wound model using tissue-engineered (TE) skin, in which to assess the benefit of MSCs, and applying non-invasive imaging to monitor wound healing using optical coherence tomography (OCT). TE skin is reconstructed from DED by the addition of laboratory expanded fibroblasts and keratinocytes, and it possesses a functional epithelium. Full-thickness incisional wounds were created in TE skin, and fibrin clots containing cells could be inserted into the wound cavity; wounds healed after 14 days. OCT could clearly identity structural features of skin (including the dermis, epidermis and fibrin clot) with good correspondence to histology. Appropriate sampling of the wounds by OCT was determined, and consistency in identifying corresponding wound regions within a sample over time was addressed, so that wound volumes could be calculated and compared.

Finally MSCs were introduced to the wound model. MSCs were found not to reduce the rate of wound closure in the dermal portion of the wound, however they did accelerate re-epithelialisation and this was detectable by OCT. Additionally, cytokine analysis was performed on the surrounding medium under wound conditions. In the presence of MSCs, wound medium contained more hepatocyte growth factor (HGF) and basic fibroblast growth

factor (bFGF). Elevated levels of these beneficial factors to wound healing were associated with an early onset of epithelialisation.

Publications

- **Walker, N.G.,** Mistry, A.R., Smith, L.E., Tsaknakis, G., Eves, P.C., Forster, S., Watt, S.M., and MacNeil. S. "*A Chemically Defined Carrier for the Delivery of Human Mesenchymal/Stromal Cells to Model Wound Beds*". Tissue Engineering, ***18****,143-155, (2012)*.

- Jiang, D., Qi, Y., **Walker, N.G**., Sindrilaru, A., Hainzl, A., Wlaschek, M., MacNeil, S., and Scharffetter-Kochanek, K. "*The Effect of Adipose Tissue Derived MSCs Delivered by a Chemically Defined Carrier on Full-Thickness Cutaneous Wound Healing*". Biomaterials, ***34,*** *2501-15, (2013).*

Oral Presentations

- "*A Chemically Defined Carrier for the Delivery of MSCs"*: Biomaterials and Tissue Engineering Group (BiTEG), 12th Annual Work in Progress Meeting (2010), University of Leeds, UK.

Poster Presentations

- '*The Uses of Tissue-Engineered Skin in Translational Research*'. Tissue Engineering: The third dimension to animal replacement (2012), Royal College of Obstetricians and Gynecologists, London, UK.

- '*A Chemically Defined Carrier for the Delivery of Human Mesenchymal Stem Cell/Stromal Cells to Skin Wounds*'. 5th UK Mesenchymal Stem Cell Meeting (2011), Aston University, Birmingham, UK.

- '*A Chemically Defined Carrier for the Delivery of Human Mesenchymal Stem/Stromal Cells to Skin Wounds*'. Biomaterials & Tissue Engineering Group (BiTEG). 13th Annual White Rose Work in Progress Meeting (2011), University of York, UK.

- '*Evidence for Nanotubes in Human Mesenchymal Stem Cells*'. Quantitative Imaging for Systems Biology (2009), Oxford University, UK.

Acknowledgements

Firstly, I would like to thank my God the Lord Jesus Christ. Without His provision I would have not have been able to complete this research.

I am hugely thankful to my supervisors Dr. Gwen Reilly and Prof. Sheila MacNeil for their continuous support during the PhD. Thank you both for giving me the opportunity to salvage my PhD after my uneventful first 18 months. I especially would like to thank Sheila for endeavoring to review 'bits' of this thesis in a very timely manner, so that I could meet the deadline for the submission of this work.

I want to thank all those I worked with in the laboratory, and I would like to thank all who where in my supervisory groups for their kind support in helping me troubleshoot problems. Specifically I would like to thank: Dr. Irene Canton, for teaching me cell culture and basic assays, and for nurturing me in my early days as a student; Dr. Louise Smith, for teaching me how to isolate primary cells from skin, make tissue-engineered skin, and perform plasma polymerisation; Dr. Anthony Bullock, for teaching me to use Origin 8 software and for passing on your wisdom from years as a hardy Post-Doc; Mark Wagner and Claire Johnson, for keeping the lab tidy and for dealing with all my requests to order materials; Juliet Bell, for teaching me how to use the XPS software; and Dr. Steven Matcher, and Dr. Zenghei Liu for all their help in understanding the OCT set-up and optimising its use.

Lastly, I want to thank my family and friends for all their love and support over the course of my studies. I would especially like to thank my wife Delphine for putting up with all my stress during the write-up and for helping me out in so many little ways.

Abbreviations

%	Percent
-	Minus/ Negative
+	Plus/ Positive
<	Less than
>	Greater than
°	Degrees
1°	Primary
2°	Secondary
α	Alpha
β	Beta
μ	Micrometer
C°	Degrees Celsius
2D	Two Dimensional
3D	Three Dimensional
AA	Acrylic Acid
Ab/s	Antibody/Antibodies
ABTS	2,2'-azino-bis(3-ethylbenzothiazoline-6-sulphonic Acid)
AGE	Advanced Glycation End Products
ALI	Air-Liquid Interface
ANOVA	Analysis of Variance
APC	Adenomatous Polyposis Coli
ATP	Adenosine triphosphate
a.u.	Arbitrary Units
bFGF	Basic Fibroblast Growth Factor
BF	Birefringence
BM	Basement Membrane
BMA	Bone Marrow Aspirate
BSA	Bovine Serum Albumin
$CaCl_2$	Calcium Chloride
CD	Cluster of Differentiation
CFU-F	Colony Forming Unit Fibroblast
CO_2	Carbon Dioxide
Col IV	Collagen IV
CLSM	Confocal Laser Scanning Microscopy
CM	Conditioned Medium
CW	Chronic Wound
Cy	Cyanine Dye
dH_2O	Distilled Water
Da	Daltons
DAB	3,3' Diaminobenzidine
DAPI	4',6-diamidino-2-phenylindole
DED	De-epidermalised dermis
DFU	Diabetic Foot Ulcer
DMF	Dimethylformide
DMEM	Dulbecco's Modified Eagle's Medium
DMSO	Dimethyl Sulphoxide
DNA	Deoxyribonucleic Acid
eGFP	Enhanced Green Fluorescent Protein
ECFC	Endothelial Colony Forming Cells
ECM	Extra-Cellular Matrix
EDTA	Ethylene Diamine Tetra-acetic Acid
EGF	Epidermal Growth Factor
EGM-2	Endothelial Cell Growth Medium-2
ELISA	Enzyme-Linked Immunosorbent Assay
EPC	Endothelial Progenitor Cell
FACS	Fluorescence Activated Cell Sorting
FCS	Fetal Calf Serum

FDA	Food and Drug Administration
FD-OCT	Fourier Domain Optical Coherence Tomography
FITC	Fluorescein Isothiocyanate
FN	Fibronectin
FTDW	Full-Thickness Dermal Wound
g	gram
GAGs	Glycosaminoglycans
GFs	Growth Factors
GFP	Green Fluorescent Protein
GMP	Good Manufacturing Practice
H_2O_2	Hydrogen Peroxide
h	hours
hBM	Human Bone Marrow
HBOT	Hyperbaric Oxygen Therapy
HCl	Hydrochloric Acid
HDF	Human Dermal Fibroblasts
H&E	Heamatoxylin and Eosin
Hg	Mercury
HGF	Hepatocyte Growth Factor
HIF	Hypoxia-Inducible Factor
HLA	Human Leukocyte Antigen
HRP	Horseradish Peroxidase
HuVECs	Human vascular endothelial cells
Hz	Hertz
i3T3s	Irradiated Swiss Mouse Fibroblasts
Igs	Immunoglobulins
IGF	Insulin-like Growth Factor
IL-8	Interleukin- 8
IMS	Industrial Methylated Sprits
IU	International Units
IR	Infrared
K	Keratinocytes
L	Litre
M	Molar
mbar	millibar
MCP	Macrophage Chemoattractant Protein
mIG	Mouse Immuoglobulin
min	minutes
mm	millimeter
mM	Millimolar
MHz	Megahertz
ml	millilitre
MMP	Matrix Metalloproteinase
mRNA	Messenger Ribose Nucleic Acid
MSC	Mesenchymal Stem Cells
MSCGM	Mesenchymal Stem Cell Growth Medium
MTT	A3-(4,5-dimethylthiazol-2-yl)-2,5-diphenyltetrazolium bromide
N	Number of Independent Experiments
n	Number of Samples/ Experimental Condition
NA	Numerical Aperture
N/A	Non applicable
NaOH	Sodium Hydroxide
NIR	Near Infrared
nm	nanometer
nM	nanomolar
NPT	Negative Pressure Therapy
O_2	Oxygen
OCT	Optical Coherence Tomography
p	passage
P	Probability

ppAAc	Plasma Polymerised Acrylic Acid
PBS	Phosphate Buffered Saline
PDGF	Platelet-Derived Growth Factor
PE	Phycoerythrin
Pen/Strep	Penicillin/ Streptomycin
PFTE	Polytetrafluoroethylene
pH	Potentiometric Hydrogen Ion Concentration
PMN	Polymorphonuclear
PS-OCT	Polarisation Sensitive OCT
®	Registered Trademark
RF	Radio Frequency
RFP	Red Fluorescent Protein
ROS	Reactive Oxygen Species
rpm	revolutions per minute
RT	Room Temperature
SA	Surface Area
SAM	Self-Assembled Monolayer
S.D.	Standard Deviation
SEM	Standard Error of the Mean
SNR	Signal to Noise Ratio
SS-OCT	Swept-Source Optical Coherence Tomography
T3	3,3,5-Triiodo-L-thyronine Sodium Salt
™	Unregistered Trademark
TCP	Tissue Culture Plastic
TD-OCT	Time Domain OCT
TE	Tissue Engineered
TIMPs	Tissue Inhibitors of MMPs
TNF	Tumour Necrosis Factor
tPA	Tissue Plasminogen Activator
TRITC	Tetramethylrhodamine Isothiocyanate
uPA	Urokinase Plasminogen Activator
UV	Ultra Violet
v	Volume
VN	Vitronectin
VEGF	Vascular Endothelial Growth Factor
w	Weight
W	Watts
WBS	Wound Breaking Strength
WCA	Water Contact Angle
X	Multiplied
XPS	X-ray Photoelectron Spectroscopy

Table of Contents

Table of Figures

Chapter One: Introduction

Chapter Two: Materials and Methods

Chapter Three: Delivery of MSCs to Model Wound Beds

Chapter Four: Developing a Model Wound-Healing based on Human Tissue Engineered Skin

Chapter Five: Using OCT to Non-Invasively Image Wounds

Chapter 6: Investigating the Effects of MSCs in Model Wounds Derived from TE skin

List of Tables

Chapter One: Introduction

Chapter Two: Materials and Methods

Chapter Three: Delivery of MSCs to Model Wound Beds

Chapter One:

Literature Review

1.1 The Structure of Skin

Skin is the largest human organ. It covers an area between 1.5 and 2 m^2, comprises almost one sixth of a person's weight, and each square inch of skin is estimated to contain 4.6 m of blood vessels, 3.6 m of nerves, 1500 nervous receptors, 350 sweat glands, and 100 sebaceous glands (Marieb 2007). It is a heterogeneous tissue that is comprised of two distinct structures: the epidermis and the dermis, and they form 100 µm and 1-4 mm of the skin's thickness respectively (Figure 1.1).

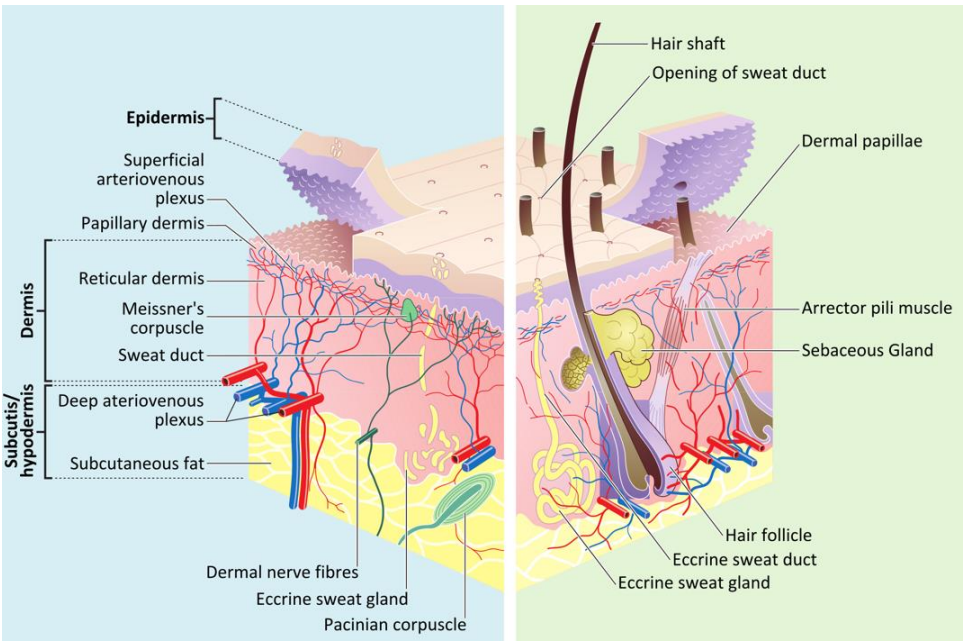

Figure 1.1. *Structure of skin. Non-hairy and hairy regions (right and left). The epidermal invaginations are called rete ridges. (Figure from Wikipedia commons, May 2013.)*

Skin provides many physiological functions which include: thermoregulation through sweat production from eccrine glands, diverting blood to and from its surface, and positioning hair follicles via erector pili muscles to trap insulative air; production of vitamin D which is essential to the body's ability to uptake dietary calcium; and shielding against ultra violet (UV) radiation via melanin production. However, its most important function is to provide a barrier between the 'inside' of the organism and the external environment for the purpose of protecting it against microbial invasion and excessive water loss (Figure 1.2).

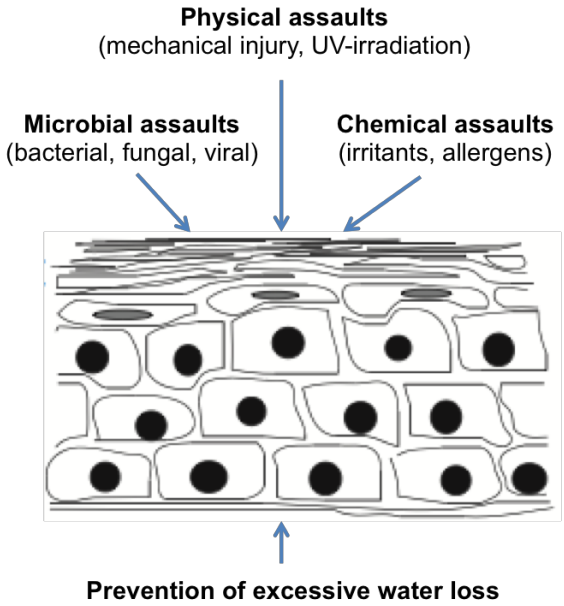

***Figure 1.2**. Barrier function of skin. The figure depicts the epidermis. (Adapted from Proksch et al, 2008)*

Structure of the Epidermis

The epidermis constitutes the physical barrier of the skin and it is comprised of five layers from the basement membrane (BM) to the surface (Figure 1.3). Each layer will be discussed in turn starting from the layer closest to the BM.

Stratum Germanitivum

The lowest layer of the epidermis, which is situated directly above the BM, is the stratum germanitium (SG). Within this layer germinative basal cells reside; these are proliferative keratinocytes that act as 'mother' cells, ensuring continuous regeneration of the epidermis as their daughter cells slowly migrate to the surface and undergo differentiation along the way. During this process, keratinocytes undergo dramatic changes in morphology due to alterations in their cytoskeletal architecture as a result of changes in the expression of keratin and filaggrin (Smith and Dale 1986). Keratins are a major group of water-insoluble structural proteins that are synthesised by keratinocytes. Keratins have a molecular weight ranging from 40-70 kD, however those between 56.5 and 67 kD are associated with more differentiated cells above the BM (keratinised epidermis) (Woodcockmitchell *et al,* 1982; Sun *et al,* 1983). Therefore, the expression of different types of keratins correlates with the extent to which a cell has differentiated (Tseng *et al,* 1982; Sun *et al,* 1983).

The predominant cell type within the germinative layer is keratinocytes, however there are others including melanocytes and Merkel cells. Up to 10 % of the cells in the SG are melanocytes, which are specialised dendritic cells that form a complex with approximately

36 keratinocytes and one Langerhans cell to form a 'melanin unit' (Fitzpatrick and Breathnach 1963; Montagna and Carlisle 1991). The function of melanocytes is to synthesise the dark, UV absorbing, pigment melanin in their melanosomes and transfer them to keratinocytes. Once inside keratinocytes, the melanosomes are degraded by lysosomal enzymes to release melanin, which accumulates as a nuclear 'cap' that is thought to shield the keratinocytes from the harmful effects of UV radiation, which may induce DNA damage (Montagna and Carlisle 1991). Hence, prolonged exposure to UV radiation darkens skin giving it a 'tanned' appearance due to increased production and transfer of melanin granules to the keratinocytes. Merkel cells are neuroendocrine cells that are normally located in the touch-sensitive areas of skin, such as the whisker follicles of the face, specialised epithelial structures of the hairy skin called touch domes, rete ridges and glabrous (hair-less) skin surfaces (Halata *et al,* 2003). The precise function of Merkel cells remains unknown, however they are suggested to be essential for mechanosensation (Borghi and Nelson 2009; Maricich *et al,* 2009).

Startum Spinosum

Once basal cells begin to migrate towards the surface, they encounter the spinosus layer. This layer is characterised by polyhedral-shaped cells that contain large nuclei with prominent nucleoli, indicative of active protein synthesis. These cells begin to produce large amounts of the intermediate filament cytokeratin. These cytokeratin filaments then become bundled together to form tonofibrils that converge into desmosomes, and form tight junctions between the keratinocytes. Due to the ‘spikey’ appearance of the tonofibrils, they are sometimes referred to as ‘prickles’; hence the stratum spinosum is often referred to as the ‘prickle cell layer’. It is also within this layer that membrane-bounded vacuoles (Odland bodies), which contain the precursors to the epidermal lipids, become evident. The prickle cell layer also contains Langerhans cells. These star-shaped immune cells serve to uptake antigens that have entered the epidermis and present them to the immunocompetent T-cells of the regional lymph nodes (Romani *et al,* 2010).

Stratum Granulosum

The stratum granulosum is comprised of three to five layers of keratinocytes that are in the late stages of differentiation, and it is here that migrating keratinocytes lose their polyhedral morphology, becoming more flattened, and begin producing proteins required for cornification such as K1 and K10 keratin filaments. Additionally, dense basophilic granules of keratohyline begin to appear within the cells of this layer, and it is the presence of these granules from which the layer derives its name. These keratohyaline granules are rich in profilagrin, a 400-kDa precursor protein which is cleaved to form the 37-kDa peptides of filaggrin which aggregates keratin filaments into tight bundles, leading to the cells becoming flattened squames (Candi *et al,* 2005; Palmer *et al,* 2006). Together, filaggrin and keratin

constitute the greatest portion of epidermal proteins, comprising between 80-90 % (by mass) of the epidermal proteins (Candi *et al,* 2005).

Cells within this region also synthesise the structural proteins, loricrin, involucrin, trichohyalin and small proline-rich proteins (SPRPs), which are all elements of the cornified envelope (Rinnerthaler *et al,* 2013). Lamellated granules that contain water-repellant polar lipids, glycosphingolipids, and free sterols, which are transferred to the extracellular space via exocytosis triggered by the increased calcium concentration in the region, also accumulate in the granular cells (Downing *et al,* 1987; Oren *et al,* 2003). These lipids are then modified and arranged into intercellular lamellae, which lay parallel to the cell surfaces.

Stratum Corneum

The outer most part of the epidermis is the stratum corneum (SC). It is composed from a continuous sheet of 20-30 layers of corneocytes, and it accounts for up to 3/4 of the thickness of the epithelium (Marieb and Hoehn, 2007). Corneocytes are fattened, anuclear epithelial cells, that are encased by a cornified envelope of cross-linked proteins, and embedded in an intracellular matrix of hydrophobic non-polar lipids, which are organised as lamellar layers. The cornified envelope (CE) is a tough polymeric structure, consisting of a lipid envelope and a protein envelope that forms above and below the cytoplasmic membrane respectively (Candi *et al,* 2005). The protein element of the CE is derived from a range of proteins including: involucrin, loricrin, trichohyalin (Nemes and Steinert 1999), which become cross-linked via transglutaminases to form both disulphide and N-epsilon-(gamma-gluramul)lysine isopeptide bonds; thus proteins impart mechanical strength to the epidermis (Koch *et al,* 2000; Segre 2006). For example, the dermis of loricrin-deficient mice was found to be more susceptible to mechanical stress (Koch *et al,* 2000), and mutations in some of the genes encoding CE proteins have been implicated in a number of keratodermas (skin disorders characterised by horny-like structures) (Ishida-Yamamoto and Iizuka 1998).

The lipid envelope is a specialised membrane that replaces the outer membrane layer of the bi-layered plasma membrane (Swartzendruber *et al,* 1987), and it is built from lipids that are extruded into the extracellular space from lamellar granules where they are synthesised (Kalinin *et al,* 2002). The proteins involucrin, envoplakin and peroplakin then form covalent linkages with the lipid envelope to integrate the cells with the intercellular lipid lamellae (Marekov and Steinert 1998), and together they reinforce the epidermal barrier. In addition corneodesmosomes, specialised desmosomes that connect adjacent corneocytes, form tight junctions which are important for SC cohesion and thus barrier function (Descargues *et al,* 2005). On the basal side of the cells, adhesion junctions serve to maintain epithelial integrity under shear stress. Thus, the SC is the principle barrier to the penetration of damaging agents such as chemicals and microbes, and it is capable of

withstanding mechanical forces and providing water impermeability to the skin (Madison 2003).

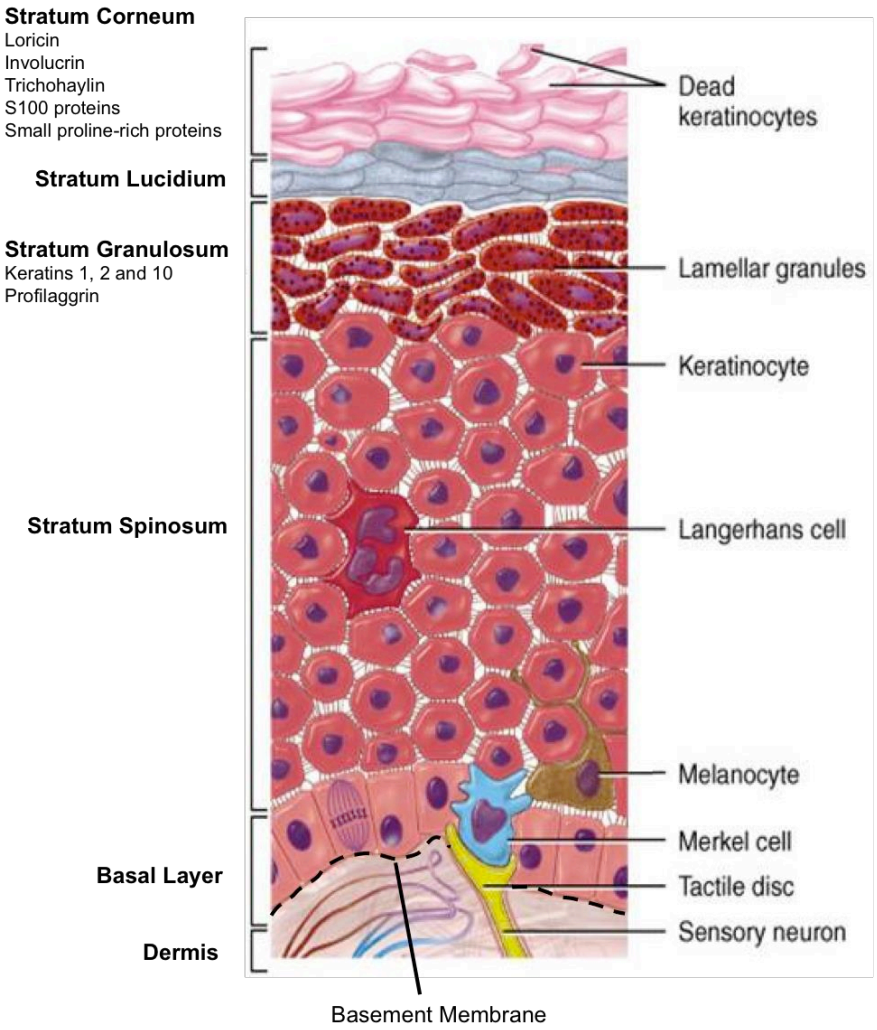

***Figure 1.3**. Composition of the Epidermis. Note- The **stratum lucidium** is a thin translucent layer of dead keratinocytes that is only present in areas of thick skin where it helps to reduce friction and shear forces between the stratum corneum and the stratum granulosum. (Image adapted from jessicamilleratomy.com).*

Structure of the Dermis

The dermis is a dense layer of specialised connective tissue that primarily functions to support the epidermis, however it also provides substantial mechanical protection to the body and binds together all superficial structures. It is comprised of an extracellular matrix (ECM) consisting of GAGs, elastins and collagen fibres. Collagen and GAGs can associate with large volumes of water and give the dermis its gel-like properties that are considered to impart the intrinsic tension of skin and act as a barrier to foreign particles (Marieb and Hoehn 2007). Collagen also gives the dermis its structural integrity due to the protein's fibrous nature, whilst elastin confers elasticity to the skin. The principle cell type resident in the dermis is the fibroblast and these cells produce and maintain the ECM through the synthesis of elastin and collagen. There are 28 different types of collagens within the collagen family, however the main collagen in dermis is type I, which accounts for approximately 75-80 % of the collagen content in the tissue (Epstein and Munderloh 1978).

The deepest region of the dermis is the reticular layer, and in this region sweat (ecrrine) glands, mechanoreceptors and blood vessels can be found (Figure 1). Superior to the reticular dermis is the papillary dermis, which is characterised by finger-like projections, called papillae, that interdigitate with the overlaying epidermis; in between the dermal papillae are rete ridges which contain pockets of basal keratinocytes. Together the papillae and ridges increase the surface area (SA) between the dermis and the epidermis. These structures are important for two reasons. Firstly, small blood vessels run through the dermal papillae that supply oxygen and nutrients to hair follicles and the cells of the lower epidermis; a high SA greatly increases exchange of nutrients and waste products. Secondly, it helps prevent the epidermis from separating from the dermis by providing a greater area for sites of anchorage between these two layers.

1.2. Wound Healing

Because skin serves as a protective barrier, any breach in its integrity must be rapidly and efficiently repaired. To this end, skin has a remarkable capacity to heal itself following tissue damage from insult and injury. It is a complex phenomenon that can be broadly characterised into four distinct but overlapping phases, which proceed over the time course described in Figure 1.4.

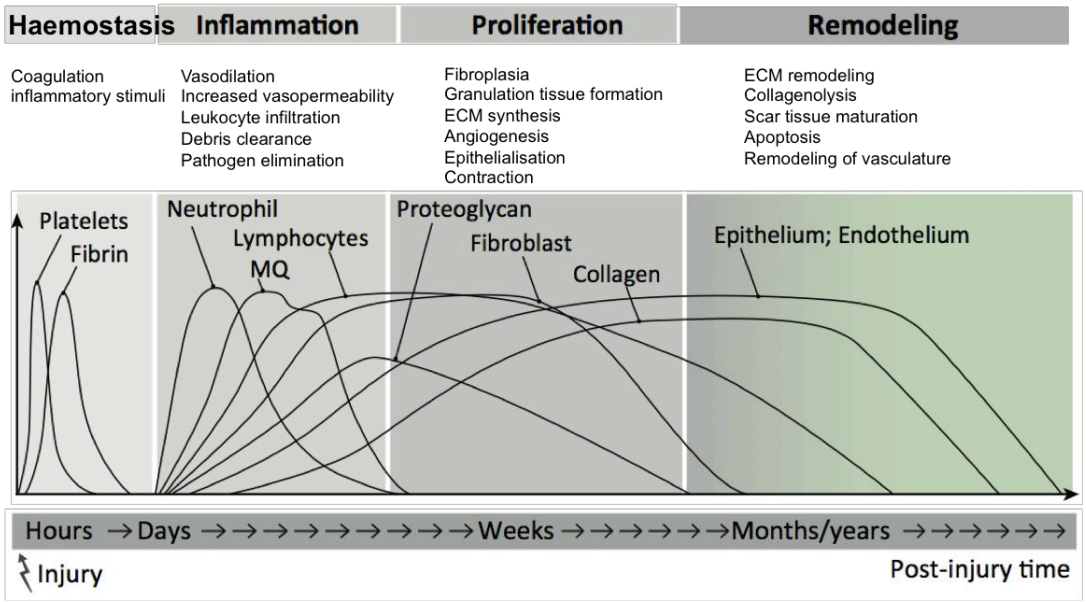

Figure 1.4*. Phases of wound healing. (Figure adapted from Shechter and Schwartz 2013).*

Haemostasis

Skin wounds cause disruption to the blood vessels, leading to blood loss. Immediately following endothelial cell injury, prevention of local haemorrhage is achieved through blood platelet activation and the initiation of the coagulation cascade. The resulting blood clot serves to form a plug to terminate bleeding, and acts as a temporary barrier to the external environment. It also functions to provide a provisional matrix for the invasion of new capillaries (this happens around 4 days post-injury), which endows the neostroma with a granular appearance; hence it is named granulation tissue.

The clot consists of platelets embedded in a mesh of cross-linked fibres derived from the plasma proteins fibrinogen, fibronectin, vitronectin and thrombospondin, which are cleaved by the enzyme thrombin (Clark 2001). This fibrin mesh serves to stabilise the platelet plug because activated platelets express the integrins ($\alpha_{IIb}\beta_3$), which allows them to interface with fibrin (Fang *et al,* 2005). In addition activated platelets secrete a number of growth factors such as platelet-derived growth factor (PDGF) and epidermal growth factor

(EGF); these factors stimulate activation of fibroblasts to produce collagen, GAGs and proteoglycans (Bauer *et al,* 1985; Brissett and Hom 2003).

Inflammatory Phase

Inflammation is a controlled vascular and cellular response to injury that sets the stage for tissue regeneration by clearing dead tissue and foreign materials. The inflammatory response is characterised by an increase in vasopermeability, vessel dilation, and leukocyte infiltration (Stadelmann *et al,* 1998). The infiltration of granulocytes and monocytes are regulated by a diverse range of chemo-attractants such as the cleavage products of blood derived fibrinogen and fibrin (Richardson *et al,* 1976; Gross *et al,* 1997), but also ECM components including collagen (Postlethwaite and Kang 1976), elastin (Senior et al, 1980) and fibronectin (Clark *et al,* 1998). Additionally, transforming growth factor beta (TGF-β) also acts as a chemo-attractant (Barshavit *et al,* 1990).

Post-injury monocytes attach to the endothelium of blood vessels at the site of injury and migrate through the vessel wall into the ECM (Diegelmann *et al,* 1981); and they eliminate contaminating bacteria via phagocytosis. Granulocytes are a collection of polymorphonuclear leukocytes (PMN), which include neutrophils. Neutrophils are the first leukocyte cells to populate the wound. They protect the wound from infection by killing bacteria through the production and release of toxic reactive oxygen species (ROS). They also release lysosomal enzymes together with neutral proteases that debride the wound (Segal 2005). However, ROS cause minor collateral damage to cells in their vicinity which further stimulates inflammation.

Following the acute phase of inflammation, macrophages become the predominant cell type within the leukocyte population at the wound site. Macrophages have multiple roles in wound healing. For instance, macrophages promote further recruitment and activation of leukocytes to the wound thus, promoting inflammation. However, they also induce apoptosis in irreparable cells and clear the wound of apoptotic cells (including neutrophils), which paves the way for the resolution of inflammation. In addition, macrophages undergo a phenotypic transition to a reparative state, whereby they stimulate both fibroblast and keratinocyte migration and activation, and angiogenesis through secreting a plethora of macrophage-derived growth factors (Table 1.1). Thus, they promote tissue regeneration and the proliferative phase of healing (Meszaros *et al,* 2000; Mosser and Edwards 2008; Guo and DiPietro 2010).

Lymphocytes are the last leukocyte population to enter the wound, and their numbers increase during the late proliferative phase/ early remodeling phase. The role of lymphocytes however is less clear and is the subject of much research (Guo and DiPietro

2010). For example, a delayed T-lymphocyte infiltration, in combination with a decreased T-lymphocyte count in the wound site, has been associated with impaired wound healing (Swift *et al,* 2001). However, others have reported that lymphocyte-deficient mice showed lesser scar formation (Gawronska-Kozak *et al,* 2006). Dendritic epidermal T-cells (DETCs) are thought to regulate many aspects of wound healing including inflammation resolution and pathogen defense. They are activated by stressed or damaged keratinocytes, and in response they produce fibroblast growth factor-7 (FGF-7), keratinocyte growth factors, and insulin-like growth factor 1 (IGF-1), to support keratinocyte proliferation and survival; and mice deficient in DETCs exhibit delayed wound closure and decreased peri-wound keratinocyte proliferation (Jameson and Havran 2007; Mills *et al,* 2008).

Proliferative Phase

Fibroblasts appear in the wound 2-3 days post-wounding, and dominate the wound cell population. They are sourced from fibrocytes in connective tissue and perivascular region, and there is also evidence that bone marrow stem cells contribute to the wound fibroblast population (Opalenik and Davidson 2005). Fibroblasts form an amorphous gel composed of GAGs and proteoglycans called 'ground substance', and it plays an important role in the deposition and aggregation of collagen fibres. Initially, fibroblast activity is devoted to proliferation and migration; thereafter they are dedicated to the synthesis of extracellular collagen. The tensile strength of the reforming tissue correlates with collagen content, and during the proliferative phase, collagen production from fibroblasts continually increases for approximately 3 weeks until homeostasis is achieved (i.e. the rate of collagen synthesis and degradation becomes equal) (Stadelmann *et al,* 1998). Approximately one week into wound healing, a proportion of wound fibroblasts are stimulated to transform into a contractile phenotype, becoming myofibroblasts characterised by the expression of smooth muscle actin (Gabbiani *et al,* 1971). Myofibroblasts adhere to one another as well as the wound margins via secure intercellular attachments, and they generate strong contractile forces at the wound margins, drawing the wound edges closer together (Montandon *et al,* 1977). The fibroblast-myofibroblast transformation is largely as a result of TGF-β (Desmouliere *et al,* 1993) and mechanical tension generated from forces resisting wound contraction (Grinnell 1994).

Angiogenesis occurs throughout the proliferative phase to meet the increased metabolic demands from the tissue, and support the provisional matrix, which is rich in fibroblasts, leucocytes, endothelial cells and myofibroblasts. Angiogenesis results from the migration and proliferation of endothelial cells, and it is initiated by tissue destruction and hypoxia. Subsequently, angiogenesis is stimulated by growth factors such as, basic fibroblast growth factor (also known as FGF-2), vascular endothelial growth factor (VEGF), TGF-β, which are secreted by macrophages, keratinocytes and endothelial cells (Martin

1997). Additionally, angiogenesis is dependent on proteolytic activity of plasmin and matrix metalloproteinases (MMPs) (Singer and Clark, 1999). Both MMP-2 and MMP-9 are expressed in endothelial cells (Mirastschijski *et al,* 2002; Hieta *et al,* 2003); and these gelatinases are essential for digesting constituents of the vascular BM, which is a key factor for new blood vessel generation in both physiologic and tumorigenic states (Itoh *et al,* 1998; Bergers *et al,* 2000; Kato *et al,* 2001).

Wound re-epithelialisation is established by a sequence of mobilisation, mitosis, and differentiation of epidermal cells, and it begins within hours after injury. Wounding disrupts the BM to which keratinocytes are attached via their integrins (α6β4) to laminin. This triggers cells at the leading edge to express new integrins for fibronectin (α5β1, α5β6) and vitronectin (α5β5), as well as relocalise collagen receptors (α2β1), so that they can 'grasp' and migrate across the provisional wound matrix (Cavani *et al,* 1993; Breuss *et al,* 1995). Subsequently, keratinocytes at the wound edge lose their basal polarity and extend pseudopodia from their baso-lateral sides into the wound. Keratinocytes then dissect through the clot along the interface between the clot and the healthy dermis to discard the eschar from the viable tissue (Clark *et al,* 1982). In order to do this, the leading-edge keratinocytes must dissolve the fibrin via a variety of proteases. The main fibrinolytic enzyme plasmin, derived from the clot itself, is only activated in the presence of tissue-type plasminogen activator (tPA) or urokinase-type plasminogen activator (uPA); the production of both activators is up-regulated in migrating keratinocytes (Grondahlhansen *et al,* 1988; Romer *et al,* 1994). Once the wound gap is closed, the BM and the cellular contacts are re-established, and keratinocytes differentiate thus reconstituting the multi-layered epidermis (Figure 1.5.).

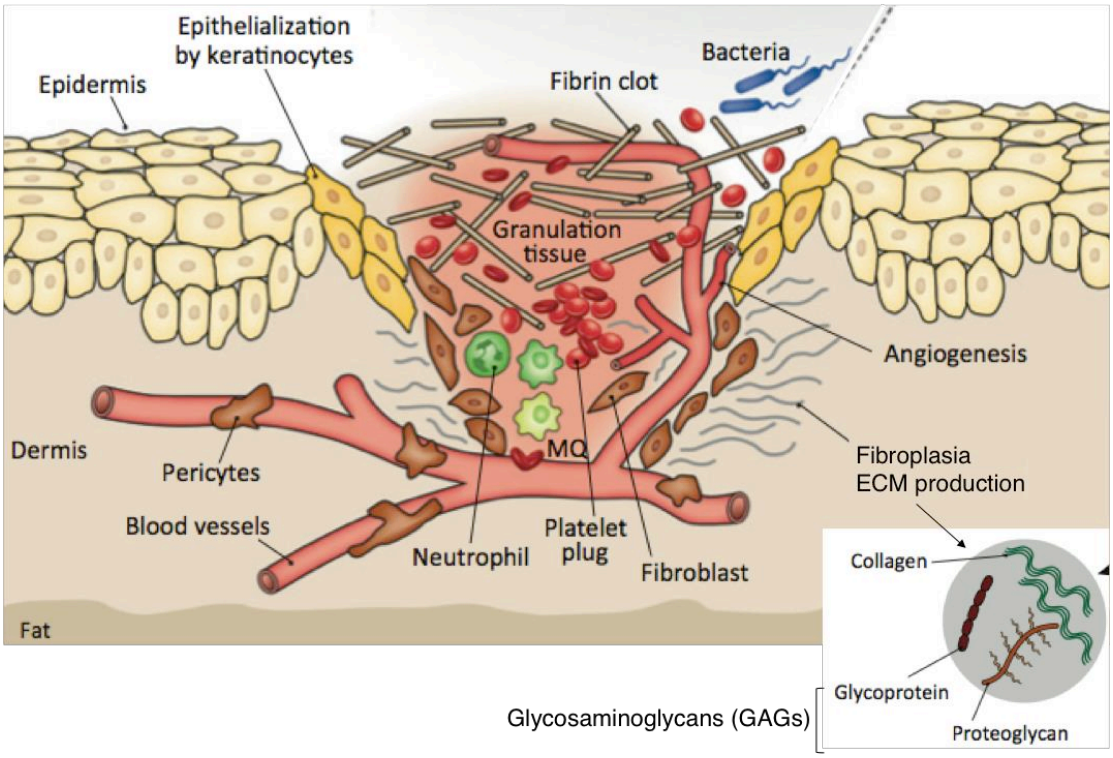

Figure 1.5. *The late inflammatory/ early proliferative phase of wound healing. The granulation tissue is rich in newly sprouted blood vessels, and fibroblasts begin to proliferate and synthesise collagen and ECM components. Keratinocytes of the leading-edge (shown in yellow), begin to re-epithelialise by firstly migrating underneath the eschar to separate it from the underlying regenerating tissue. Figure adapted from (Shechter and Schwartz 2013)*

Maturation Phase

Remodeling or maturation is the process by which collagen fibres are reorganised into a more defined lattice structure by mechanical forces. Remodeling begins approximately 3 weeks after injury and continues for up to two years, during this time the wound continues to increase in tensile strength. The majority of the collagen laid down early in the healing process is type III which is gradually replaced by type I collagen until the normal 4:1 ratio of collagen I to III is re-established, while the GAGs are steadily degraded until they reach normal concentrations. After a period of four weeks wounds typically reached 70 % of the strength of undamaged tissue, thereafter a plateau is gradually reached and the new tissue never exceeds 80 % of the strength of normal skin (Madden and Peacock 1968). In the final stages of remodeling, the high density of new blood vessels regresses via endothelial cell apoptosis, while myofibroblasts and fibroblasts also withdraw from the wound in a similar fashion. Lastly, the hypertrophic epidermal layer that was produced becomes progressively thinner.

In summary, wound healing is a highly coordinated programme that requires the participation of different cell types and it is mediated not only by cell-ECM contacts,

intracellular contacts and changes in mechanical stress, but also by a plethora of growth factors and cytokines that regulate cell behavior. By raising antibodies against specific growth factors, or by knocking out growth factors using genetically modified animals, many authors have demonstrated how crucial growth factors and cytokines are to wound healing. For example, experimental depletion of FGF-2 almost completely blocks angiogenesis (Broadley *et al,* 1989; Chmielowiec *et al,* 2007), and mice lacking receptors for hepatocyte growth factor fail to re-epithelialise (Chmielowiec *et al*, 2007). For a comprehensive overview of such studies I refer the reader to reviews by Werner and Grose, and Baum and Arpey (Werner and Grose 2003; Baum and Arpey 2005). Tables 1 and 2 list the most extensively characterised growth factors and cytokines essential to wound healing, and the cells from which they originate and their function.

Table 1.1. *Growth factors in wound healing.*

Growth Factor	Major Source	Biological Activity
CTGF	Platelets Fibroblasts Endothelial cells	Fibroplasia ECM production Angiogenesis Mediates action of TGF-B on collagen synthesis
EGF	Platelets	Keratinocyte proliferation and migration Endothelial cell proliferation ECM deposition
FGF-1	Keratinocytes	Pleiotropic mitogen ECM production
FGF-2 (bFGF)	Keratinocytes Fibroblasts Macrophages Endothelial cells	Pleiotropic mitogen Angiogenesis ECM production
HB-EGF	Keratinocytes Macrophages	Keratinocyte proliferation and migration Fibroblast proliferation
HGF/SF	Fibroblasts, Keratinocytes	Epithelialisation Angiogenesis Leukocyte recruitment
IGF-1	Platelets Fibroblasts Keratinocytes	Epithelialisation ECM Production
KGF	Dermal Fibroblasts	Keratinocyte proliferation and differentiation
PDGF	Platelets Macrophages Keratinocytes	Chemoattractant for macrophages & fibroblasts Macrophage activation Fibroplasia ECM production Contraction
TGF-α	Macrophages Neutrophils Keratinocytes	Similar to EGF but more potent angiogenic action
TGF-β	Platelets Macrophages Keratinocytes Fibroblasts	Fibroplasia ECM production Reduced scaring Collagen synthesis Contraction Macrophage recruitment
VEGF	Keratinocytes Macrophages	Angiogenesis Vascular permeability

Table 1.2. *Cytokines in wound healing.*

Cytokine	Major Source	Biological Activity
Proinflammatory		
TNF-α	Macrophages Keratinocytes	Neutrophil migration and cytotoxicity ECM degradation Expression of growth factors
IL-1	Macrophages Keratinocytes	Fibroblast and keratinocyte chemotaxis Collagen synthesis Expression of growth factors
IL-2	T-cells	Increases fibroblast infiltration and metabolism
IL-6	Macrophages Neutrophils Fibroblasts	Fibroblast proliferation and hepatic acute-phase protein synthesis
IL-8	Macrophages Fibroblasts	Macrophage and Neutrophil chemotaxis Keratinocyte maturation
γ-interferon	T-cells Macrophages	Macrophage and nuetrophil activation Retards collagen synthesis and cross-linking, and stimulates collagenase activity
Anti-inflammatory		
IL-4	T-cells	Inhibition of TNF, IL-1, and IL-6 production; fibroblast proliferation; and collagen synthesis
IL-10	T-cells Macrophages Keratinocytes	Inhibition of TNF, IL-1, and IL-6 production and inhibits macrophage and PMN activation

Key

CTGF, connective tissue growth factor; ECM, extracellular matrix; FGF, fibroblast growth factor; HB-EGF, heparin binding epidermal growth factor; HGF/SF, Hepatocyte growth factor/ scatter factor; IL, Interleukins; IGF, Insulin-like growth factor; KGF, keratinocyte growth factor; PDGF, Platelet-derived growth factor, TGF, transforming growth factor; TNF, Tumour necrosis factor; VEGF, vascular endothelial growth factor.

(The information within table 1 and 2 are adapted from reviews by (Martin 1997; Stadelmann et al, 1998; Lobmann et al, 2005; Toriseva and Kahari 2009) references within).

1.3. Chronic Wounds

The Problem of Chronic Wounds

Chronic wounds (CWs) are by definition 'wounds that have failed to progress through the normal stages of wound healing and therefore enter a pathological state of inflammation. As a result, the healing process is delayed, or incomplete, and does not proceed in a coordinated manner, subsequently resulting in a poor anatomical and functional outcome' (Lazarus *et al,* 1994). CWs are a major cause of disability and often relapse following treatment. The aetiology of non-healing wounds is varied, however the majority (70 %) are caused by ischemia secondary to diabetes, venous stasis, and pressure (Nwomeh *et al,* 1998). Common problems caused by CW include: chronic pain extrudate and odour which dispose people to loss of sleep; loss of mobility, which may limit work capacity and lead to social isolation; and the psychological wellbeing of the person can be negatively affected (Herber *et al,* 2007). Additional complications such as wound infections may lead to the development of abscesses, cellulitis, gangrene, osteomyelitis and sepsis and even malignant transformation (Eltorai *et al,* 2002).

With respect to diabetes, patients with the disease have a 12-25 % lifetime risk of developing a diabetic foot ulcer (DFU) (Abbott *et al,* 2005; Singh *et al,* 2005), and 5-8 % require amputation within 1 year (Jonasson *et al,* 2008; Prompers *et al,* 2008). In fact complications of DFUs are the primary cause of non-traumatic lower extremity amputations with DFUs preceding approximately 85 % of such amputations (Larsson *et al,* 1998; Miyajima *et al,* 2006). Furthermore amputation secondary to DFUs is associated with a high morbidity and mortality rate, with a survival rate as low as 31 % for major limb amputees.

At present 4.6 % of the UK's population are diagnosed with diabetes, and approximately 200,000 of those patients present with DFUs annually. This amounts to an annual cost of 2.3-3.1 billion pounds in treatments (at 2005-6 costs), which represents around 3 % of the NHS healthcare expenditure budget (Posnett 2007). However this is set to rise as obesity is becoming more prevalent in the UK population, and diabetes onset is associated with obesity (Guo and DiPietro 2010). Globally, the incidence of diabetes mellitus is 347 million, however it is predicted that diabetes will affect 439 million people (7.7 % of the global population) by 2030 (Shaw *et al,* 2010; Danaei *et al,* 2011). The risk of developing DFUs is also age related, with 85 % of diabetics presenting with DFUs of these cases occurring in individuals aged over 65 (Guo and Dipietro, 2010). Therefore with the UK's ageing population and the rising incidence of diabetes, the burden of chronic wounds is a mounting issue facing health care.

Summary of the Diabetic Wound Environment

The pathogenesis of DFU is complicated and multi-factorial, resulting from the combined effects of both local and systemic abnormalities. In summary, the main factors to consider are sustained hypoxia, cellular dysfunction, impaired angiogenesis and neovascularisation, elevated levels of MMPs, oxidative damage, decreased host immune resistance, and neuropathy (Figure 1.6.).

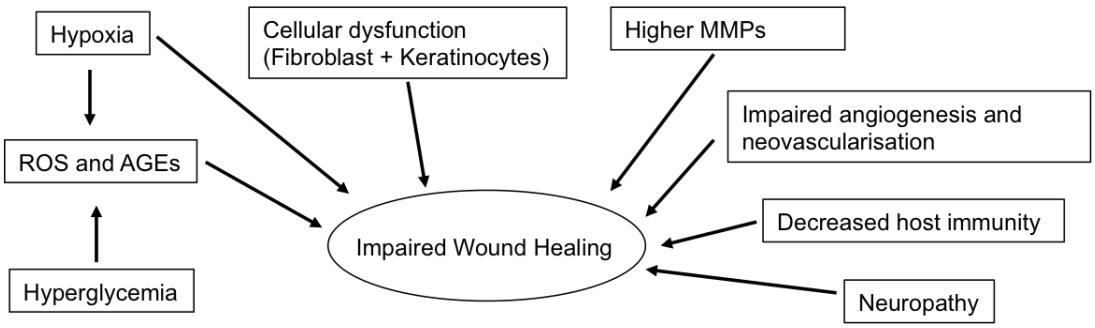

Figure1.6. *Factors impairing wound healing. ROS- reactive oxygen species; AGEs- advanced glycation end products (Figure adapted from Gou et al, 2010).*

Hypoxia

In common with venous stasis disease and pressure-related chronic wounds DFUs are notably hypoxic, and as a result ischemia may contribute to 30-40 % of DFUs. (Jiang *et al,* 2012). Tissue oxygen tensions in CWs for example have been measured to lie between 5 and 20 mm Hg, which is far lower than the typical oxygen tension from normoxic tissue, which lies in the region of 30 to 50 mm Hg (Tandara and Mustoe 2004). Diabetes is characterised by endothelial dysfunction attributed to defects in nitric oxide synthase 3 (eNOS3), and it is thought to promote vascular disease leading to micro and macrovascular defects resulting in impaired vascular blood flow and hypoxia (Calles-Escandon and Cipolla 2001; Versari *et al,* 2009). Recently, Wei et al provided evidence that diabetes-related vascular defects are linked to the absence of fatty acid synthase (FAS), of which levels are substantially reduced in diabetics (Wei *et al,* 2011).

Temporary hypoxia following tissue injury plays an essential role in stimulating the early phase of tissue repair by amplifying the inflammatory response, and stimulating macrophages, fibroblasts and keratinocytes to produce cytokines and GFs (PDGF, TFG-β, VEGF, TNF-α and endothelin-1), which promote angiogenesis, cell proliferation, migration and chemotaxis (Bishop 2008; Rodriguez *et al,* 2008). Transient hypoxia also increases the production of reactive oxygen species (ROS), which are understood to act as cellular messengers to stimulate wound healing. However, chronic hypoxia delays wound healing because sustained ROS elevation causes additional tissue damage and, more importantly, without adequate tissue oxygenation the increased metabolic demands of a tissue in a state

of reparation cannot be met, thus wound healing is impaired (Bishop, 2008; Rodriguez *et al*, 2008).

Angiogenesis in DFUs is also impaired which perpetuates wound hypoxia. Insufficient angiogenesis is thought to result from endothelial cell progenitor cell (EPC) mobilisation from bone marrow and, homing to the wound site being impaired in diabetics. Additionally, the primary angiogenic factor VEGF is released in decreased amounts in individuals with diabetes (Brem and Tomic-Canic 2007; Gallagher *et al,* 2007; Quattrini *et al,* 2008). In light of this, preclinical studies have shown that administration of exogenous VEGF improves repair outcomes (Kirchner *et al,* 2003; Galiano *et al,* 2004b). In light of the above, it is not surprising that diabetic patients with ischemic foot ulcers have the worst prognosis of all chronic skin wound patients (Jiang *et al,* 2012).

Hyperglycaemia

Hyperglycaemia accelerates the formation of advanced glycation end-products (AGEs), and with their receptors is associated with impaired wound healing (Huijberts *et al,* 2008). Hyperglycaemia also affects the stability and activation of the transcription factor hypoxia inducible factor-1α (HIF-1α). HIF-1α up-regulates the transcription of multiple genes required for successful wound healing, and when its action is suppressed the production of PDGF, VEGF and TGF-β, which are essential to angiogenesis, are reduced (Botusan *et al,* 2008).

Dysfunctional Cell Types

Diabetes impairs the function of immune cells and skin-derived cells at the wound site. The combined effect of defective T-cell immunity, leukocyte chemotaxis, phagocytosis, reduced bactericidal capacity, and impaired cytokine production leads to poor bacterial clearance, which can often result in infection which complicates wound healing by prolonging inflammation (via TNF-α and IL-1) and consequently elevating MMP activation. (Loots *et al,* 1998; Geerlings and Hoepelman 1999). Bacteria that survive in infected wounds form biofilms, which are 'complex communities of bacteria embedded in a self-secreted extracellular polysaccharide matrix' (Edwards and Harding 2004); and such biofilms provide a microenvironment that is more resistant to conventional antibiotics. Thus, the bacterial burden plays an important role in the chronicity of ulcers. Furthermore, keratinocytes and fibroblasts from diabetic wounds show a reduced migratory capability, diminished response to growth factors, and increased apoptosis (Loots *et al,* 1999).

Abnormal Cytokine Profile

Inflammation in acute wounds serves to prepare the wound for healing by clearing

cell debris, destroying pathogens and activating fibroblasts, and in normal wounds it is a self-limiting process. In contrast, diabetic wounds are associated with a chronic inflammatory environment (Pradhan *et al,* 2009). The inflammatory response in such wounds is exacerbated by factors such as tissue trauma from pressure, bacterial overgrowth, leukocyte trapping or ischemic-reperfusion injury, which perpetuates inflammation leading to what is described as 'pathologic inflammation' (Menke *et al,* 2007b). Unlike acute wounds, factors such as TNF-α, which stimulate inflammation by enhancing neutrophil migration, tend to predominate (Mast and Schultz 1996), thus neutrophils remain present within CWs for the duration of healing (Armstrong and Lavery 1998; Apelqvist *et al,* 2008). Large numbers of activated neutrophils results in the accumulation of excessive amounts of MMPs in the wound fluid (Nwomeh *et al,* 1998); for instance, neutrophil elastase is present in CWs at a concentration 10-fold higher than that of acute surgical wounds (Yager *et al,* 1997). In turn this leads to ECM degradation being favoured since MMP activity is not balanced by 'tissue inhibitors of MMPs' (TIMPs) unlike normal wounds (Yager *et al,* 1996; Lobmann *et al,* 2002)(. Thus, DFUs are environments where proteolysis is both elevated and disregulated. Elevated expression of MMPs further compounds wound healing by degrading growth factors and their receptors, thus suppressing the mitogenic potential of the wound environment (Lobmann *et al*, 2002; Nwoweh et *al*, 1998). This effect may contribute to the observation that factors stimulatory to cell proliferation and matrix deposition such as PDGF, EGF, FGF2 and TGF-β, are much reduced in concentration compared to acute wound fluid (Cooper *et al,* 1994)**.** In accordance with this, it has been demonstrated that wound fluid from CWs interferes with cell proliferation, and fails to stimulate DNA synthesis in fibroblast cultures (Bennett and Schultz 1993), suggesting that the activity of the above growth factors is essential to normal wound healing. Furthermore, not only is the inflammatory cytokine profile altered within CWs, but fibroblast function is also altered. For example, fibroblasts isolated from CWs are reported to undergo premature senescence and display an impaired migratory capacity in response to GFs (Brem and Tomic-Canic 2007). Conversely, a subset of fibroblasts in the CW has been found to enter a hyper-synthetic mode, whereby collagen is produced and deposited en mass, however due to excess MMPs it is degraded faster than it is produced (Menke *et al,* 2007b).

Neuropathy

Diabetes causes neurovascular defects, and over time this causes neuronal damage. Damaged nociceptive fibres which may result, can lead to the inability of such fibres to generate an electrical stimulus in response to micro injury/ trauma, therefore resulting in decreased pain perception. As a consequence, diabetic patients may be unaware sustaining of minor injuries to the foot, such as splinters and blisters, and therefore they may not pay minor wounds attention which increases the likelihood of them becoming worsened through additional trauma or infection (Zou *et al,* 2012). Furthermore, sensory

nerves can modulate the wound milieu by releasing neuropeptides (nerve growth factor, substance P and calcitonin gene-related peptide), which stimulate chemotaxis, cell proliferation, and growth factor production. Sensory nerves also exhibit a level of control over leukocyte infiltration, with denervated skin showing reduced levels of leukocyte infiltration and rates of healing (Galkowska *et al,* 2006)..

Other Contributory Factors

There are many other systemic factors besides diabetes that can affect how wounds heal, these include: age, stress, smoking, alcohol consumption, nutrition obesity and medication. All of which have been recently reviewed by Guo and Dipietro, and I refer the reader to their article for further information regarding these additional (Guo and Dipietro, 2010).

Treatments for Chronic Wounds

Although the type of treatment that is opted for depends on the type of chronic wound, there are basic procedures that are common to all, such as regular wound debridement and pressure off-loading. Compression bandages form an essential and effective part of the treatment of venous ulcers, whereas DFUs often require glycemic control, antibiotics and even skin grafting (Werdin *et al,* 2008). Recent advances in understanding CW pathology and developments in bio/nanotechnology have accelerated the production of novel therapies (Dissemond 2006; Jiang *et al,* 2011).

Wound Dressings

Typical wound dressings include alginates, hyaluronic acid, hydrogels, hydrocolloids, collagen, semi-impermeable membranes, and silver dressings (Dissemond, 2006). However bioactive dressings and tissue-engineered (TE) skin substitutes also show promise. Bioactive dressings combine cells, matrices or growth factors, and they are able to modulate the process of wound healing via tissue interactions, and examples include keratin dressings (Pechter *et al,* 2012; Tang *et al,* 2012) and Promogran (Systagenix Wound Management, Inc). TE substitutes include Dermagraft (Advanced BioHealing, Inc), Apligraf (Organogenesis Corp), which are FDA approved for the treatment of venous leg ulcers and DFUs (Sussman *et al*, 2003; (Zaulyanov and Kirsner 2007). However, a single type of dressing is not sufficient for the management of all types CWs, and few are suited to intervention at any stage in wound healing (Sussman *et al*, 2003).

Negative Pressure Therapy

Negative pressure therapy (NPT) is a therapeutic technique whereby a vacuum is used to remove wound exudates (Evans and Land 2001), helping to improve interstitial fluid control, restore blood flow and reduce bacterial load (Armstrong *et al,* 2005). A recent systematic review by Xie *et al* (2010), reported that NPT is beneficial for in the treatment of DFUs is consistent, however the same could not be said for other types of chronic wounds. The review also found NPT not to cause any significant complications (Xie *et al,* 2010). However, side effects such as pain and fluid loss, and the risk of bleeding, limit its use to small wounds (Fan *et al*, 2010). In relation to pressure treatments, Piaggesi *et al* demonstrated pressure casts to be effective at reducing wound size (Piaggesi *et al,* 2003). Ten patients were fitted with casts to provide pressure off-loading to the areas surrounding their DFUs, and compared to patients without such casts and with comparable lesions, wounds were found to have significantly reduced in size after 20 days. In addition, they discovered histopathological differences between the two groups. Compared to ulcers from patients without the casts, ulcers from cast-treated patients showed fibroblast and newly formed capillaries to be prevalent as opposed to inflammatory elements. Thus changes in the wound environment were associated with the increase in wound healing (Piaggesi *et al*, 2003).

Hyperbaric Oxygen Therapy

Hyperbaric oxygen therapy (HBOT) is a treatment designed to increase the supply of oxygen to wounds that are not responding to conventional treatments. HBOT involves the patient breathing in pure oxygen in a room that is pressurised up to three times that of atmospheric pressure. Under these conditions the partial pressure for oxygen in tissues is increased since the blood plasma can transport significant amounts of oxygen in addition to oxygen transport via heamoglobin. This may mobilise stem/progenitor cells from the bone marrow, via nitric oxide-dependent mechanism, which can aid wound healing and may account for patient cases which suggest recovery of damaged tissues by HBOT (Thom *et al,* 2006). A recent systematic review concluded, that in relation to DFUs, HBOT only provides an initial benefit to wound healing, because after long term follow-up HBOT did not reduce the amputation rates. Furthermore, no evidence was found to suggest HBOT was effective to treat venous and pressure ulcers and its use is restricted by the requirement of specialist equipment and expertise.(Kranke *et al,* 2012).

Growth Factors

Since cytokines/ GFs orchestrate wound healing events such as cellular proliferation, differentiation, migration, and metabolism, and given there is an inherent lack of theses factors in CWs, much investigation has been conducted into the use of exogenous

cytokines and growth factors to ameliorate wound healing. Numerous animal studies have demonstrated that local application of growth factors (PDGF, FGF2, TGF-β, VEGF) can accelerate wound healing in both normal and healing-impaired models (Lynch *et al,* 1989; Puolakkainen *et al,* 1995; Davidson *et al,* 1997; Loots *et al,* 2002; Galiano *et al,* 2004b). In 1986 Knightington *et al* conducted one of the first clinical trials whereby an autologous mixture of platelet-derived releasates (PDGF, TGF-β, PDAF, PDEGF and other unknown factors) was applied to chronic wounds. The authors reported the addition of these factors increased wound healing over the control group (Knighton *et al,* 1986). Pressure ulcers and venous stasis ulcers have also been treated similarly and yielded positive effects (Robson 1997). Currently, human recombinant PDGF is the only efficacious preparation that is approved for clinical use in diabetic foot ulcers by the US Food and Drug Administration (FDA) (Steed *et al,* 1995; Smiell *et al,* 1999). Despite this it has not found widespread use because many CWs fail to respond (Menke *et al,* 2007a); this may be due to the presence of proteases capable of degrading PDGF and TGF-β and patient variability in the protease activity in the wound environment (Yager *et al,* 1997).

GFs alone however will not work in the long-term if the underlying pathology is not addressed; GFs only serve as local stimulators for healing by aiding the wound to surmount an otherwise hostile and inhibitory environment (Greenhalgh 1996; Stadelmann *et al,* 1998). Therefore, in addition to treating the immediate wound environment, efforts must also be made to abate systemic contributing factors such as arterial insufficiency, venous hypertension, vasculitis, edema, diabetes and infection, prior to GF treatment (Lobmann *et al,* 2005). However, not all CWs respond to GFs even if the underlying pathology is managed. This could be due to the inherent heterogeneity within the CW population, which makes conducting randomised controlled trials difficult, and therefore can make clinical data hard to evaluate (Lobmann *et al,* 2005).

MMP Inhibitors

Given that elevated protease activity is a characteristic of CWs, the deleterious effects of excessive MMPs may be dampened through the local application of protease inhibitors (Menke *et al,* 2007a). One such inhibitor doxycycline, which competitively blocks MMPs and the TNF-α converting enzyme, has been shown in a randomised controlled clinical trial to improve wound healing in DFUs (Chin *et al,* 2003). Concomitantly, doxycycline also reduces inflammation by decreasing nitric oxide synthesis (Lamparter *et al,* 2002). An alternative approach is to apply a dressing to the wound that is composed of protease substrates such as gelatin or collagen (Veves *et al,* 2002; Vin *et al,* 2002). Such dressings outcompete the endogenous collagens for their degradative enzymes, thus shielding them in a concentration-dependent manner from them.

Stem Cells

Mesenchymal stem cells (MSCs) resident in the bone marrow have been shown to positively interact with the cells of the wound environment, and produce a wealth of beneficial growth factors and cytokines to stimulate wound healing through angiogenesis, fibroblast proliferation and keratinocyte migration and by calming wound inflammation. A review of the role of MSCs in wound therapy is presented in section 1.4.

1.4. Mesenchymal Stem Cells

MSCs hold great promise in regenerative medicine and in the treatment of cutaneous wounds because, in addition to their multipotent differentiative capacity, they can stimulate the wound environment via paracrine actions, through the release of trophic and Immunomodulatory factors (Hocking and Gibran 2010; Sorrell and Caplan 2010; O'Loughlin *et al,* 2011; Chen *et al,* 2012; Jiang *et al,* 2012; Mulder *et al,* 2012). Importantly, these cells can be sourced and easily extracted from a variety of tissues (both autologous and allogeneic) and remain stable when expanded in culture. The minimum criteria, established in 2006 by the International Cell Society (Dominici *et al,* 2006), to qualify cells as MSCs *in vitr*o is as follows:

1) The cells must be adherent to tissue culture plastic when maintained in standard conditions.
2) The cells must express CD105, CD73 and CD90, and lack the expression of CD45, CD43, CD14 and human leukocyte antigen (HLA)-DR surface molecules.
3) The cells must be multipotent and differentiate to osteoblasts, adipocytes, and chondrocytes in vitro.

The first evidence for the existence of mesenchymal progenitor cells arose during the late 1960's and early 1970's when Friedenstien and colleagues identified a small fraction of fibroblast-like bone marrow (BM) cells that adhered to and proliferated on tissue culture substrates (Friedens.Aj *et al,* 1968; Friedens.Aj *et al,* 1974). Such cells readily generated single cell derived colonies and were originally referred to as colony forming unit fibroblasts (CFU-F), subsequently CFU-Fs were demonstrated to be a heterogeneous population of non-heamatopoietic stem cells that reside in the marrow stoma. Hence, these cells are referred to as mesenchymal stem, progenitor, or stromal cells (Horwitz *et al,* 2005). These cells were later shown to differentiate *in vitro* into multiple cell types of the mesenchymal lineage, such as adipocytes, oesteoblasts, and chrondrocytes, hence these cells are described as mesenchymal stromal/progenitor cells (Pittenger *et al,* 1999) (Figure 1.7.).

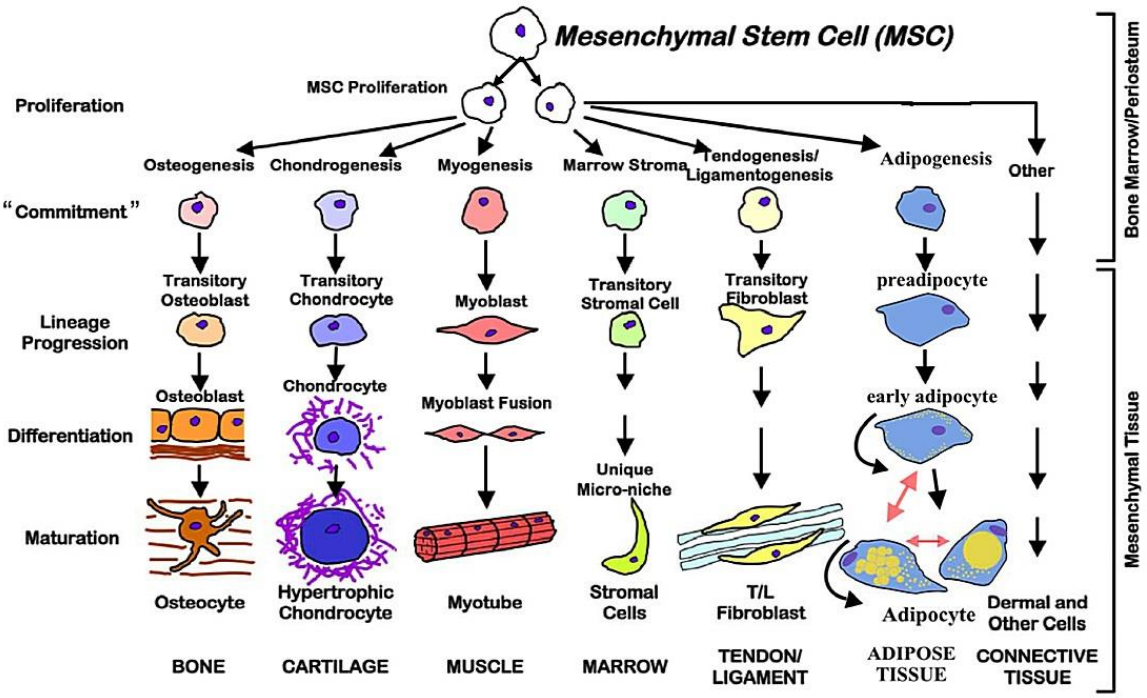

***Figure 1.7**. Differentiative capacity of BM-MSCs, (Figure reproduced from Caplan et al, 2005).*

However their differentiative capacity is not restricted solely to the mesenchymal lineage; they show a propensity to become a variety of other unrelated cell types including: retinal cells, neural cells, astrocytes, hepatocytes, and pancreatic cells (Pountos and Giannoudis 2005). Additionally, it is now widely accepted that most postnatal organs and tissues in the body have a resident population of multipotent MSC-like cells including, adipose tissue, synovial membranes, bone, skin, pancreas, blood, fetal liver, lung and umbilical cord blood, pericytes synovial fluid, muscle, dermis, deciduous teeth, trabecular bone, infrapatella fat pad, articular cartilage, periosteum (Si *et al,* 2011). However BM-derived MSCs are the best characterised MSCs and were used in the experimental sections of this thesis, therefore they will be the subject of this review.

MSCs in Wound Healing

Pre-clinical Studies

Much pre-clinical work has been undertaken over the last 20 years using animal models to investigate the effects of bone marrow MSCs in cutaneous wound healing. A notable pre-clinical study performed by Wu *et al* found MSCs to enhance wound healing in both normal and healing-impaired genetically diabetic mice (db/db mice). Full-thickness dermal excisional wounds were made in both groups of mice and allogeneic GFP-labeled murine MSCs were injected around the wound bed. As controls, either allogeneic neonatal

dermal fibroblasts or vehicle medium were added to wounds. Their results demonstrated that the MSC-treated wounds exhibited accelerated wound closure, with increased re-epithelialization, cellularity, and angiogenesis vs. the controls (Wu *et al,* 2007). Table 1.3 highlights noteworthy pre-clinical studies in relation to CWs to date and summarises their outcomes.

In addition, several studies have found that MSCs not only accelerate wound healing, but they also improve the quality of repair of incisional wounds, resulting in healed tissue with notably reduced scaring, and an enhanced wound tensile strength (Stoff *et al,* 2009) and wound breaking strength (McFarlin *et al,* 2006; Kwon *et al,* 2008). For example, it is reported that following incisional injury, a rabbit's skin only achieves 40 % of the tensile strength of uninjured tissue after 120 days. However, Stoff *et al* showed that after treating rabbit incisional wounds with human MSCs, the skin regained 52 % of the tensile strength of uninjured skin at day 80 after surgery and treatment, while untreated wounds regained only 31 % of their original strength by this time (Stoff *et al*, 2008). Although the authors did not state why this result occurred, others have associated an immediate increase in collagen in the wound bed with the increase in wound breaking strength (McFarlin *et a*l, 2006; Kwon *et al*, 2008). The mechanism by which collagen secretion is increased by the presence of MSCs is currently under investigation (Zou *et al*, 2012).

Importantly, there have also been studies evaluating the use of whole bone marrow aspirate (BMA) to ameliorate poor wound healing (Tateishi-Yuyama *et al,* 2002; Badiavas and Falanga 2003; Yamaguchi *et al,* 2005). However BMA is a heterogeneous population of cells consisting of both mesenchymal and haematopoietic progenitor cells, therefore it is not clear from these studies which population is the contributing party. To test the hypothesis that MSCs from BM are the major contributors to wound healing, Javazon *et al* (2007) compared the effects of BMA to a purified population of MSCs from the BMA on wound healing in mice. Their results showed MSCs significantly accelerated wound closure, enhanced re-epithelialisation, granulation tissue formation, and increased blood vessel density at the wound site compared with control wounds treated with BMA or PBS alone. They also showed that 7 days after treating the wounds, higher frequencies of MSCs remained in the wound compared to BMA cells, demonstrating that MSCs engraft to the wound site (Javazon *et al,* 2007).

Murine models have been crucial for advancing the understating of wound healing, however there are fundamental physiological and anatomical differences between mouse and human skin. Murine skin is similar to human skin in that it consists of three layers (epidermis, dermis and hypodermis), however the chief difference in regard to wound healing, is that murine skin contains a unique thin layer of muscle called the panniculosus layer which produces rapid wound contraction following injury. By contrast, human wounds

heal primarily via granulation tissue and re-epitheialisation, with limited contracture. However, splints can be sutured to excisional murine wounds to prevent the contraction of the panniculosus carnosus, thus allowing healing to proceed in a fashion that better recapitulates healing in man (Galiano *et al,* 2004a). An additional difference is that rete ridges are absent from murine skin, although similar structures often become apparent during wound healing (pseudoepitheliomatous/ pseudocarcinomatous hyperplasia) (Sundberg *et al*, 2004). There are also gender differences between male and female murine skin. For example, the dermis of male skin is much thicker than female skin, and exhibits a thicker epidermis and hypodermis, consequently male skin is 40% stronger than female skin (Azzi *et al,* 2005). These differences are important to consider when assessing the translational relevance of mouse studies. Therefore to truly evaluate the potential of MSCs in wound healing, clinical studies are essential.

Table 1.3. The use of MSCs in pre-clinical studies.

Wound	Cell type	Delivery	Outcome	Reference
FTDW (1.5 x 1.5 cm) F344/JCl nude rats	Human BM MSCs (Allogeneic)	Dermal substitute, soaked in bFGF (5×10^6 cells)	Accelerated wound healing. Human pancytokeratin was detected- possible trans-differentiation.	(Nakagawa *et al,* 2005)
Incisional wounds (5 cm) Rat (Sprague-Dawley)	Rat BM MSC (Allegeneic)	IV injection (5×10^6 cells) and local injection along wound margins (6×10^6 cells)	Both methods of administration increased Wound breaking strength (WBS). Increased collagen production and neovascularisation	(McFarlin *et al,* 2006)
FTDW (1 x 1.5 cm) Diabetic mice	Murine BM MSCs (Allogeneic)	Topical Fibrin spray	Accelerated wound healing	(Falanga *et al,* 2007)
FTDW (8 mm) Diabetic mice (Lepr $^{db/db}$)	Tested BMA vs. BM MSCs (Allogeneic- murine)	Injection into wound bed (7.5×10^5 cells)	Enhanced epithelial gap closure/ accelerated reepitheilalisation. Increased granulation tissue area Increased blood vessel density (CD31+) at wound site	(Javazon *et al*, 2007)
FTDW (6 mm) (C57BL/6, BALB/c db/db mice	Murine BM MSCs (Allogenenic)	1×10^6 cells (70 % injected intradermally at 4 sites, 30 % in growth factor reduced matrigel).	Accelerated wound closure, with increased re-epithelialization, cellularity, and angiogenesis in both models. MSCs, colocalised with keratin and formed glandular structures, suggesting epithelial transdifferentiation Ang 1, VEGF found in higher levels *in vivo*	(Wu *et al*, 2007)
FTDW (1.5 x 1.5 cm) New Zealand White Rabbit	Rabbit BM MSCs (Autologous and Allogeneic)	Human amniotic membrane seeded with (HAM) ($2x10^5$ cells) vs. injection (6.6×10^6 cells).	HAM +MSCs showed improved healing over injected MSCs -Thinner epidermis mature differentiation, plus recovered skin appenagages in dermal layer. Cell origin made no difference.	(Kim *et al,* 2009)
TFDW (10 mm) C57BL/6 mice	BM MSCs	IV injection (1×10^6 cells)	Reduced wound area. Local injection of chemoattractant increased the number of MSCs engrafted into the wound form IV administration and accelerated wound closure all the more. GFP MSCs co-localized with endotheial and pericyte markers.	(Sasaki *et al,* 2008)

Full-thickness incisional wounds (3cm long) and sutured. **New Zealand White Rabbit**	Human BM MCSs (Allogeneic)	Intradermal injection around wound site- 1.5 x 10^6 cells	Inhibited scar formation and increased tensile strength of the wounds above controls	(Stoff *et al*, 2008)
Incisional wounds (5 cm) Strptozotocin-induced diabetic Sprague-Dawley rats	Rat BM MSCs (Allogeneic)	Systemic IV injection (1.5 x 10^6 cells each day for 4 days after injury) and local injection (6 x 10^6 cells)	Systemic and local delivery improved wound breaking strength; this was associated with an increase in collagen. Wounds improved with respect to inflammatory cell infiltration, + evidence of neovascularisation Increased the expression of growth factors critical to proper repair at wound (TGF-β, KGF, (EGF, VEGF, PDGF-BB)	(Kwon *et al,* 2009)
Full-thickness excisional wound **New Zealand White Rabbit.**	Rabbit BMA (Autologous)	Intradermal injection at wound margins	Granulation tissue appeared significantly faster. At 21 days better epithelisation more wound contraction. Healing tissue showed early disappearance of inflammatory reaction, significantly more neovascularisation, and more fibroplasias and early lay down and histological maturation of collagen (via histological analysis/ scoring).	(Borena *et al,* 2010)
FTDW (20 mm) **Sprague-Dawley Rat**	Rat BM MSC (Autologous)	Type I collagen Matrix (2 x 10^6 cells)	Accelerated early phase healing. Earlier expression of MMP-9 which correlated with maximal VEGF expression and enhanced neovascularisation	(Kim *et al,* 2011a)
FTDW (10x10 mm) **Sprague-Dawley Rat**	Human BM MNCs (Allogeneic)	Nanofibrous scaffold (elecrospun collagen PLGA surface functionalised with CD29 to improve cell attachment (produced in mouse) (3 x 10^6 cells)	Accelerated wound healing/closure. Faster re-epithelialisation and healed skin contained differentiated epithelium Increased Collagen production.	(Ma *et al,* 2011)
FTDW (Rabbit model)	Rabbit BM MNC (Autologous)	Intradermal injection at wound margins (2 x 10^6 cells)	Increased neovasularisation; thicker granulation tissue; thicker and better arranged collagen I fibres, increased reticulin and elastin fibres.	(Akela *et al,* 2012; Argolo Neto *et al,* 2012)

FTDW (Streptozotocin-induced diabetic mice)	Murine BM MSCs (Autologous)	Saline (3.3 x 10^7 cells), and covered with a polyeurothatne semipermeable membrane	Increase rate of wound closure. Increased collagen I Decreased scarring.	(Argolo Neto *et al,* 2012)
FTDW Geneticaly diabetic mice (Lepr $^{db/db}$)	Murine BM MNCs (Allogeneic)	Subcutaneous injection	Promoted wound healing, neovascularization, and EPC recruitment	(Castilla *et al,* 2012)
FTDW (5x6 cm). Streptozotocin-induced diabetic Wistar Rat	Rat BM MSCs (Allogenic)	Intradermal injection (1 x 10^7 cells), 8 sites around wound margin	Accelerated wound healing time, rats that received a second dose of MSCs healed faster compared to rats treated once Enhanced wound epithelialization and neovascularization, increased expression EGF and VEGF. Reduced CD45 inflammatory cells	(Kuo *et al,* 2011)
FTDW (10x10 mm) (C57BL/6 mice)	Murine BM MSCs (Autologous)	8 % Methlycelulose containing cells (1 x 10^4) overlyn with dermal substitute.	Increased vascular density (CD31+ cells) with in the dermal substitute.	(Leonardi *et al,* 2012)

Key: *BALB/c mice= Defective T-cell immunity; C57BL/6 mice= Immunocompetent; Db/db mice= diabetic- healing incompetent; FTDW= Full-thickness dermal wound (excisional); IV= intravenous administration. Note- All results reported are statistically significant unless otherwise stated.*

Clinical Studies

However, despite promising findings in animal studies, few clinical trials have taken place. There have been but a handful of case studies examining the effects of autologous BM-derived cells on chronic wounds involving fewer than 20 patients (Mulder *et al,* 2012). Although many authors refer to the cells investigated in these studies as 'MSCs', they were applying BMA or bone marrow mononuclear cells (BM MNC) to chronic wounds. Few authors have actually extracted and characterised the population of MSCs from the bone marrow and used them therapeutically (Falanga *et al,* 2007; Dash *et al,* 2009; Lu *et al,* 2011; Xu *et al,* 2012) Therefore the term 'MSC' is implied in the loosest sense in studies involving BMA, since BM is a heterogeneous mix of cell types that contains a small sub-population of MSCs.

Ichioka *et el* demonstrated that after administering autologous BMA to a patient with a wound which was unresponsive to conventional wound therapies, healing was achieved. Two weeks following treatment vascularised granulation tissue was apparent which facilitated the successful take of a split thickness skin graft, and the patient remained free of complications thereafter (Ichioka *et al,* 2005). Other reports presented similar findings and are summarised in Table 1.4**.** In common with all reports, authors admit that a case study alone is not a basis for sound conclusions, and they recommend a wider number of patients to be recruited for future trails, however they demonstrate the success of BMA cell-therapy where conventional treatments have failed and provide insight into the effects of BM-derived cells. Recently Yoshikawa and associates treated 20 patients with various untraceable dermatopathies, (including burns, skin ulcers and DFUs), using artificial dermis implanted with autologous bone marrow-derived cells. The authors reported this treatment to be successful because 18 out of the 20 wounds had mostly healed (13 completely and 5 partially), and even in the wounds that showed the least improvement, the outcomes were still improved (Yoshikawa *et al,* 2008).

One critique of the use of BMA lies in the inability to quantify the number of viable MSCs applied to the wound in these studies. This is important because a correlation exists between the number of MSCs per surface area and reduction in ulcer size (Falanga et al, 2007), and the cellular faction obtained from BMA varies between individuals (Sarasua *et al,* 2011). Therefore purifying the MSCs population from BMA in accordance with good manufacturing practice (GMP) may enhance the clinical efficacy cell therapies.

Lu *et al* recently compared the use of BMA vs. MSCs isolated from BMA, in a double bind randomised controlled trial, to treat patients with bilateral chronic wounds arising from diabetic critical limb ischemia. The ulcer-healing rate from the MSC group was significantly higher than that of the BMA group 6 weeks after intramuscular injection, and complete

healing was achieved 4 weeks earlier than with the BMA group. Furthermore, both treatments provided a better outcome than treating the wound with saline (control). Upon follow-up at 24 weeks, the MSC group presented with improvements in limb perfusion over the BMA group (assessed by painless walking time, ankle brachial index, transcutaneous oxygen pressure and magnetic resonance angiography analysis). Additionally, cell treatments lowered the incidence of amputation over the follow-up period, however there was no difference in limb salvage between the treatment groups (BMA vs. MSCs). The authors recommended that larger sample-sizes and longer-term follow-ups are necessary to determine statistically significant differences. In summary they demonstrated MSCs to be more effective than BM (Lu *et al*, 2011).

Falanga *et al* (2007) applied autologous culture-expanded BM-MSCs to both acute wounds, secondary to excision of skin lesions, and DFUs using a topical fibrin spray. They reported that MSCs did not significantly help acute wounds heal. Of the four patients assessed, only two presented control sites with wounds of similar size, and no difference was observed between the control and treatment sites on these individuals. However one patient who presented with an initial wound area of 20 cm^2, which was more than twice the average area of the other participants, showed accelerated healing. Of the six patients that presented with DFUs, one incidence of complete healing was reported, one did not respond, while the remaining four exhibited a mean wound area reduction of 40 % over 20 weeks (Falanga et al, 2007).

To date there is only one published report where a randomised controlled clinical trial has been conducted. Dash *et al* (2009) used culture-expanded BM-MSCs to treat a total of 24 patients with chronic non-healing lower extremity ulcers resulting from either diabetes or Buergers disease. The treatment group received autologous BM-derived MSCs via intramuscular injection around the wound margins, whereas the control group only received standard wound dressings. After a 12 week follow-up the authors reported a significant reduction in ulcer sizes of both treatment groups. With respect to the DFU MSC-treated group, the mean ulcer size decreased by 72 %, while those who received the standard treatment had ulcers which only decreased by 23 %. In addition, MSC injections showed no adverse effects as assessed by hepatic and renal functional tests, and the MSCs injections increased the patient's pain free walking distance. Furthermore, wound biopsies revealed an increased number of mature immune cells and fibroblasts in the dermis of MSC-treated wounds, suggesting an augmented immune response (Dash *et al*, 2009).

Table 1.4. The use of BM cells for the treatment of non-healing wounds in the clinic.

Wound type	Therapy type	Delivery Method	Controls	Summary of Findings	Reference
Chronic wounds (n = 3)	BMA (Autologous)	Subcutaneous injection and 1-3 topical applications	None	Complete closure of wounds. Increased inflammatory response and angiogenesis	(Badiavas and Falanga 2003)
Chronic leg ulcer (unknown aetiology) (n=1)	BMA (Autologous)	Collagen matrix impregnated with cells	None	Improved vascularization and granulation tissue developed (2 weeks), which facilitated split-thickness skin grafted to completely close the wound. Patient remained complication free (18 month follow-up).	(Ichioka *et al,* 2005)
1) Acute wounds (n=4) 2) DFUs (n=6)	BM MSCs (Autologous)	Topical fibrin spray	Acute: 2 patients had untreated wounds DFU: None	Acute wounds: No difference in healing rate. Noted pain relief. DFUs: 1 completely healed, 1 no difference, and 4 mean wound area reduction 40 %. Dose dependent effect.	(Falanga *et a*l, 2007)
DFU (n=1) (CLI-induced)	BM-MNC (Autologous)	Intramuscular injection multiple sites	None	Compete wound healing (20 weeks) Improved angiogenesis and perfusion in foot stump	(Kirana *et al,* 2007)
Chronic wounds (HIV-neuropathic, n=1) (Venus insufficiency, n=1) (DFU- neuropathic, n=1)	BMA (Autologous)	Injected directly into wound.	None	Improved granulation tissue production in all 3 patients, which facilitated the take of STGSs leading to complete healing. Reduced scaring also observed.	(Rogers *et al,* 2008)
20 patients with irretraceable dermatopathies (serve burns, (n=2); skin ulcers, (n=7); traumatic skin necrosis, (n=1) and decubitus ulcers, (n=10)).	BMA (Autologous)	Artificial dermis soaked with BMA	None	Wounds mostly healed in 18 of the 20 patients. In all patience autologous cell transplantation was shown to be effective.	(Yoshikawa *et a*l, 2008)
Chronic wounds (DFUs and Buergers Disease) (n = 24)	BM-MSC (Autologous)	Intramuscular and subcutaneous injection of $> 1 \times 10^6$ cells/cm^2 ulcer.	Standard wound care	Decreased wound sizes. Increased pain-free walking distance	(Dash *et al*, 2009)
DFU (n=41)	BM MNC	Intramuscular injection	Bilateral ulcers (n	Ulcer healing rate of the BM-MSC group was	(Lu *et al*,

(CLI- induced)	(n=21), BM MSC (n=20) (Autologous)	multiple sites wound margins	=41), saline injection	faster than BM-MNCs group, healing 4 weeks earlier (week 6). Controls failed to heal after 24 weeks. BM-MSCs improved limb perfusion over controls.	2011)
DFUs (n=8) (Neuropathic)	BM MNC (Autologous)	Direct Injection into wound bed various sites, followed by platelets and fibrin glue mixed with BM-MNCs, and covered by collagen matrix seeded with BM-MNC	None	Wounds completely healed in 3 patients, and were significantly reduced in the remaining 5 after 4 weeks.	(Ravari *et al,* 2011)
Pressure ulcers (Type IV) > 4 months in duration (n=22)	BM MNC (Autologous)	Injection in wound site	None	Pressure ulcers fully healed in 19 patients, after a mean time of 21 days. None of the resolved ulcers recurred after 19 months. The number of MNCs isolated was patient dependent, although similar clinical outcomes were observed in each case. Compared to conventional surgical treatment, mean intra-hospital stay was reduced from 85.16 to 43.06 days.	(Sarasua *et a*l, 2011)

Key
BMA= Bone marrow aspirate; BM-MNC= Bone marrow mononuclear cells; BM-MSC= Bone marrow mesenchymal stem cells; CLI= Critical limb ischemia; DFU= Diabetic foot ulcer. Where indicated in the source literature, the number of cells administer is given.

MSC's Mechanisms of Action in Wound Healing

Differentiation

There is evidence to suggest that MSCs can mobilise from the bone marrow stroma, and translocate or 'home' to sites of ischemic tissue in a cytokine-dependent manner (Chen *et al,* 2011). It is also hypothesised that mechanical stresses in the skin triggers the release of various cytokines, which recruit blood-circulating MSCs (Rochefort *et al,* 2006).

Once at the site of injury, MSCs may contribute to wound healing via differentiation into dermal and epidermal cell types. In vitro MSCs have been shown to transdifferentiate into keratinocytes and endothelial cells both *in vitro* and *in vivo* (Oswald *et al,* 2004; Paunescu *et al,* 2007; Wu *et al,* 2007). For example, Sasaki *et al* demonstrated that MSCs in vitro, in the presence of bone morphogenetic protein-4, could induce the expression of Keratin 14 (Sasaki *et al,* 2008), which is considered a biochemical marker of stratified squamous epithelia (Coulombe *et al*, 1989). In addition, Sasaki et al provided evidence that MSCs may transdifferentiate to vascular-type cells in vivo. The authors showed GFP-labeled BM-MSCs, in wounded murine tissue, to be co-localised with the expression of markers for endothelial cells (CD31) and pericytes (smooth muscle actin). Cell-fusion was ruled out as a possibility by in-situ hybridisation for X-Y chromosomes, since sex mismatched MSCs were donated to the recipient mouse, thus suggesting that these cells may directly contribute to angiogenesis through differentiation (Sasaki *et al*, 2008). However, the extent to which MSCs contribute to wound healing via differentiation is a subject of debate, especially concerning their contribution to skin cells (Prockop 2007). For example, there are studies that report MSCs can engraft to the epidermis (Badiavas and Falanga 2003; Fathke *et al,* 2004), however engraftment has not been shown to be a long-term phenomena (Wu et al, 2007).

Paracrine Mechanisms

1) Angiogenic and Trophic Factors

There is growing evidence to suggest paracrine signaling is the predominant mechanism by which MSCs mediate their therapeutic benefits, and a wide range of cytokines produced by MSCs are thought to be involved in acceleration of wound healing. So-called 'conditioned medium' (CM) (culture medium collected after cells have been sustained by it for a defined period of time under hypoxic conditions), from BM-MSCs has been shown to be rich in mitogens secreted by the cells. Furthermore, MSC-CM has been shown *in vitro* to enhance the migration and proliferation of numerous cell types important to wound healing and it has also been shown to accelerate wound healing (Kinnaird *et al,*

2004; Volk *et al,* 2007; Chen *et al,* 2008; Kwon *et al,* 2008; Walter *et al,* 2010). In 2008, Chen and associates published a seminal work in which they extensively characterised the effects and composition of MSC-CM upon wound healing (Chen *et al*, 2008); a summary of their key findings will be presented.

Compared to human dermal fibroblasts, the authors found CM originating from human BM-MSCs to contain a distinctly different profile of cytokines. Enzyme-linked immunosorbent assay (ELISA) and protein array analysis revealed MSC-CM to contain much greater amounts factors such as: VEGF-α, IGF-1, EGF, KGF, angiopoietin-1, HGF, macrophage inflammatory protein-1 alpha and beta, stromal derived factor-1 and erythropoietin, compared to dermal fibroblast CM; all of which are essential to productive wound healing (Chen *et al*, 2008).

The authors subsequently demonstrated the ability of MSC-CM to enhance the migration of CD24+ monocytes, keratinocytes and HUVECs (human umbilical vein endothelial cells) across a transwell in a concentration-dependent manner (i.e. with serial dilutions of CM diminished the cells migratory capacity). Additionally, MSC-CM was found to support the proliferation of both keratinocytes and HUVECs in a similar fashion compared to their standard growth media, and in both instances MSC-CM was more effective than fibroblast-CM at stimulating cell proliferation (Chen *et al*, 2008). Accordingly other authors have shown paracrine factors in MSC-CM to: accelerate fibroblast and keratinocyte migration in scratch assays (Walter et al, 2010); promote tubule formation from endothelial cells (Wu *et al,* 2007); and enhance endothelial cell and smooth muscle cell migration and proliferation in vitro in a concentration dependent manner (Kinniard *et al*, 2004). Thus, MSC-released cytokines positively affect cell types involved in wound healing *in vitro*.

Furthermore, Chen et al proved MSC-CM could accelerate wound healing in a full-thickness excisional mouse model. Compared to vehicle medium or fibroblast-CM, MSC-CM exerted potent chemoattractive and mitogenic effects *in vivo*. Wounds treated with MSC-BM showed higher proportions of cells positive for endothelial-lineage cell markers (CD34, C-kit and Flk-1), and also an increased presence of macrophages. These results were consistent with the cytokine profile from MSC-BM whereby chemoattractants for the aforementioned cells types were found to be in abundance; their results were also consistent with those of others (Kinnarid *et al*, 2004; Wu *et al*, 2007; Volk *et al*, 2008).

In addition an association has recently been made between MSC-derived pro-angiogenic factors and improved healing outcomes for DFU-patients in the clinic. Lu *et al* showed that culture medium collected from autologous BM-MSCs under hypoxic conditions contained high levels of angiogenic factors (VEGF, FGF-2 and Angiopoietin-1). CWs are by their very nature hypoxic environments therefore, the authors attributed, in part, the

improvement in limb perfusion experienced by patients following treatment with MSCs to their ability to create an angiogenic drive (Lu *et al*, 2011). Together these findings provide strong evidence to support the hypothesis that MSCs mediate their wound healing benefits in a paracrine fashion, since MSC-produced paracrine factors alone can accelerate wound healing. For this reason, Caplan (2007) has suggested renaming MSCs as "medicinal signaling cells." Figure 1.8, summarises MSC paracrine action (Caplan 2007).

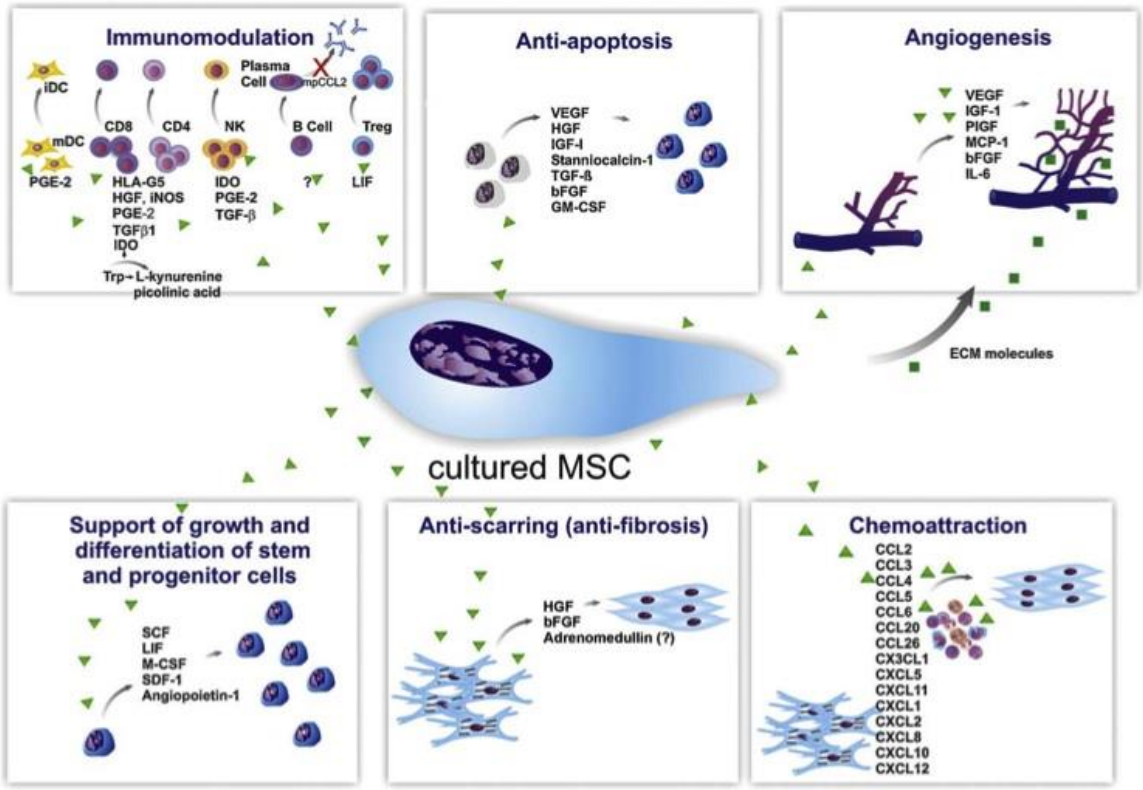

Figure 1.8. *Paracrine mechanisms of MSCs. (Figure reproduced from (Meirelles et al, 2009).*

2) Immunomodulatory properties

As previously described, chronic wounds fail to progress through the normal phases of wound healing and enter a state of pathological inflammation. Therefore, reducing inflammation may improve wound healing (Ishida *et al,* 2004). An important property of MSCs, which has been demonstrated both *in vitro* and *in vivo*, is their immunosuppressive effect. MSCs are able to influence the activities of macrophages, dendritic cells and T-cells (Djouad *et al,* 2007; Selmani *et al,* 2008; Nemeth *et al,* 2009; Cutler *et al,* 2010) by the release of bioactive molecules which are produced either constitutively, or as a result of cross-talk with target cells (Tu *et al,* 2010). One such constitutively expressed molecule is hepatocyte growth factor (HGF), which has been shown to suppress CD4 and CD8 positive T-cells (Di Nicola *et al,* 2002). MSCs also alter the cytokine profiles of dendritic cells,

effector T-cells, and natural killer cells to more anti-inflammatory phenotypes (Aggarwal and Pittenger 2005), and this phenomenon is thought to be the basis for the use of MSCs to treat graft rejection and graft versus host disease (Bartholomew *et al,* 2002; Le Blanc *et al,* 2004). Indeed, some authors have hypothesised that the resolution of chronic wounds after treatment with MSCs may be partly attributed to their immunosuppressive effect, however this has yet to be fully investigated (Chen *et al*, 2012).

1.5. Optical Coherence Tomography (OCT)

OCT is an interferometric imaging technique that maps depth-wise reflections of near-infrared (NIR) light from tissue in real-time to form cross-sectional images of morphological features at the micrometer scale (Zysk *et al,* 2007). Therefore, OCT is often described as the 'optical analogue' of ultrasound (Marschall *et al,* 2011). However unlike ultrasound, it is able to resolve features laterally in the order of 10 μm and with a depth (axial) resolution of 1 μm or greater (Povazay *et al,* 2002; Drexler 2004). Thus, OCT fills the gap, in terms of resolution and depth penetration, between that of ultrasound and confocal microscopy (Figure 1.9). In addition, unlike ultrasound, OCT holds the advantage of being a non-contact technique because no inductively coupling gel is required, and direct contact of the transducer with the sample is not necessary.

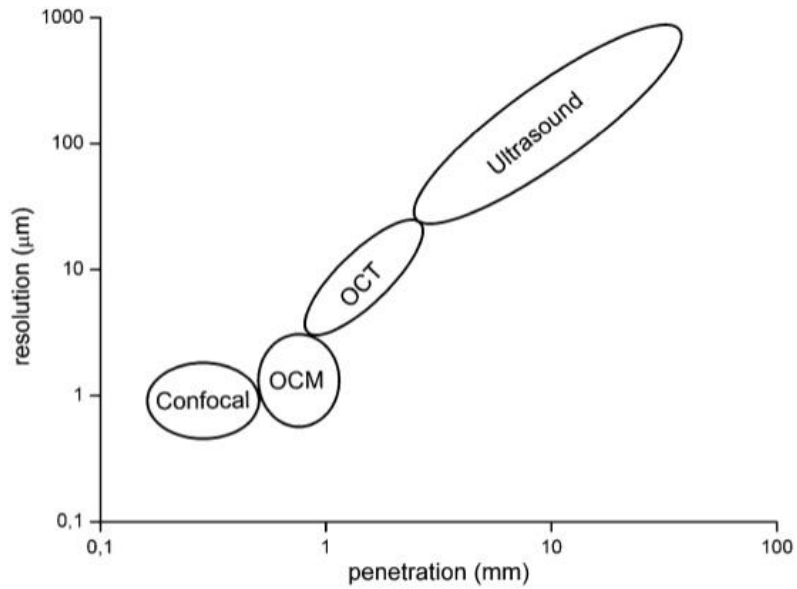

Figure1.9. *Comparison of depth/axial resolution vs. depth penetration of OCT compared to other imaging modalities (OCM= optical coherence microscopy). (Figure reproduced from Marshcall et al, 2011).*

Figure 1.10. is a cross sectional image of human skin and illustrates the unique capabilities of OCT. Within a depth of 700 μm, back-scattering structures, such as the stratum corneum and epidermis, are clearly resolved and displayed. OCT therefore can provide information regarding the structure and morphology of tissue that would otherwise only be obtainable via histology. Indeed, OCT is often referred to as an 'optical biopsy' method because OCT images of skin tissue correlate to the tissues histology (Brezinski *et al,* 1997).

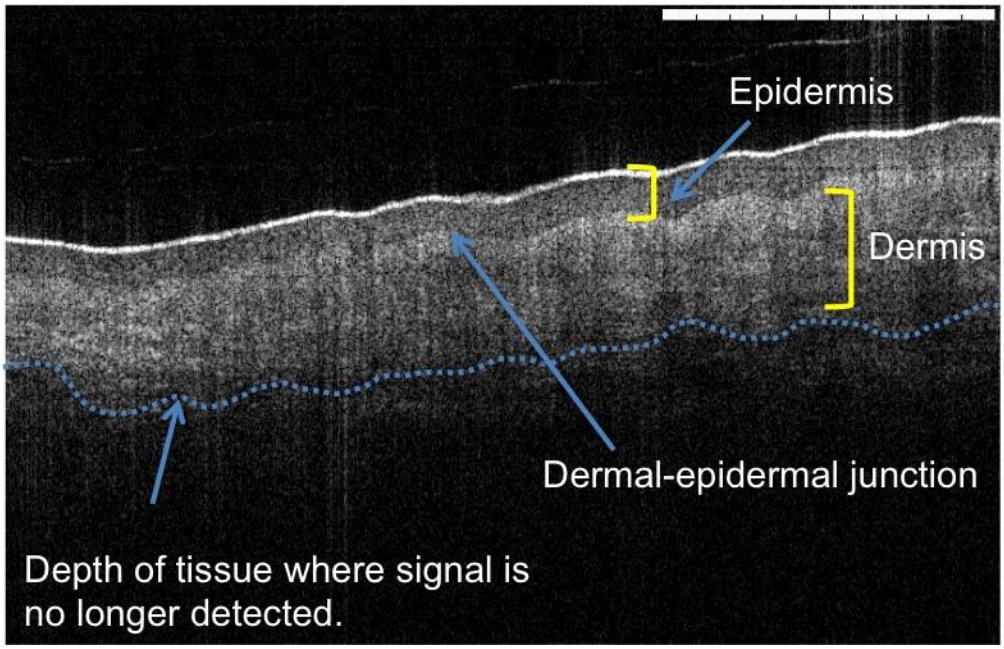

Figure 1.10. *OCT image from palmar skin. Scale bar= 1 mm.*

The principles of various OCT systems are discussed below, however a detailed discussion of the theoretical aspects and physics related to OCT is beyond the scope of the thesis. For a more comprehensive overview I refer the reader to articles written by Fretcher, Ponoleanu,Smidt and Tomlins and Wang (Schmitt 1999; Podoleanu 2005; Tomlins and Wang 2005; Fercher 2010) .

Optical interference is at the core of OCT methods. In its most basic form, an OCT instrument consists of a Michelson-type interferometer with a focused sample arm and a lateral-scanning mechanism. Using a Michelson interferometer, a beam of light from the optical source is simultaneously split into two beams of nearly equal intensity using a half-transparent mirror oriented at a 45-degree angle (plate beam-splitter). One beam, the internal or reference beam is directed on to a flat fixed 'reference mirror', and the second beam is directed onto the sample. Reflected light from both optical paths is then recombined at the beam-splitter and a pattern of optical interference is produced and detected. The resulting one-dimensional depth scan produced from a single plane through the sample is called an A-scan (1D depth resolved point scans). Many adjacent A-scans can be made in succession by lateral scanning to produce a B scan (2D slices through a volume) (see Figure 1.11.), and C scans can also be made to produce 3D volume images.

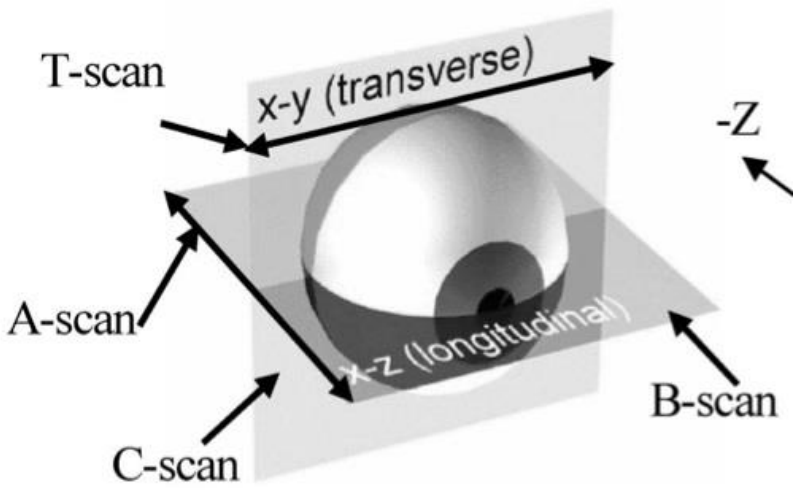

Figure 1.11. *Imaging planes. (Figure reproduced from Podolenau et al, 2005).*

Types of OCT System

A-scans can be generated by two methods: time domain (TD) or frequency domain (FD). TD-OCT systems were the first to be implemented (Huang *et al,* 1991) and composed the majority of systems between 1991 and 2003, but since then most of systems that have arisen have been FD OCT. This is because the SNR (signal: noise ratio) has been shown to be 100 times better than TD systems (Leitgeb *et al,* 2003), thus paving the way for real-time B-mode imaging.

Time Domain OCT

OCT uses low coherence light. All light has a finite coherence length, which is defined as the distance over which trains of light remain in phase or synchrony. Coherence is inversely proportional to the bandwidth of a light-source; therefore light sources simultaneously producing a wide range of wavelengths provide light with lesser coherence than light which is produced from a single wavelength source (Figure 1.12.) (Chen and Lee 2007). By using light with a broad spectral bandwidth, and thus a short coherence length, only backscattered light from the sample that has a path-length difference that is within one coherence length of the light-source, can interfere with the reference beam to create interference fringes. This condition creates a spatial and temporal gate whereby light can only be interrogated from a certain depth within the tissue; signal detected from shallower and deeper structures are rejected. This so-called 'coherence gate' can be shifted along the probing beam's axis through changing the length of the reference path by translating the reference mirror along the axial direction (Figure 1.13.). Analysis of the detected optical interference pattern provides information regarding the echo time of the sample that

corresponds to a depth within the sample. Together with the magnitude of the interference, this information is used to create a grey-scale cross-sectional image of the tissue.

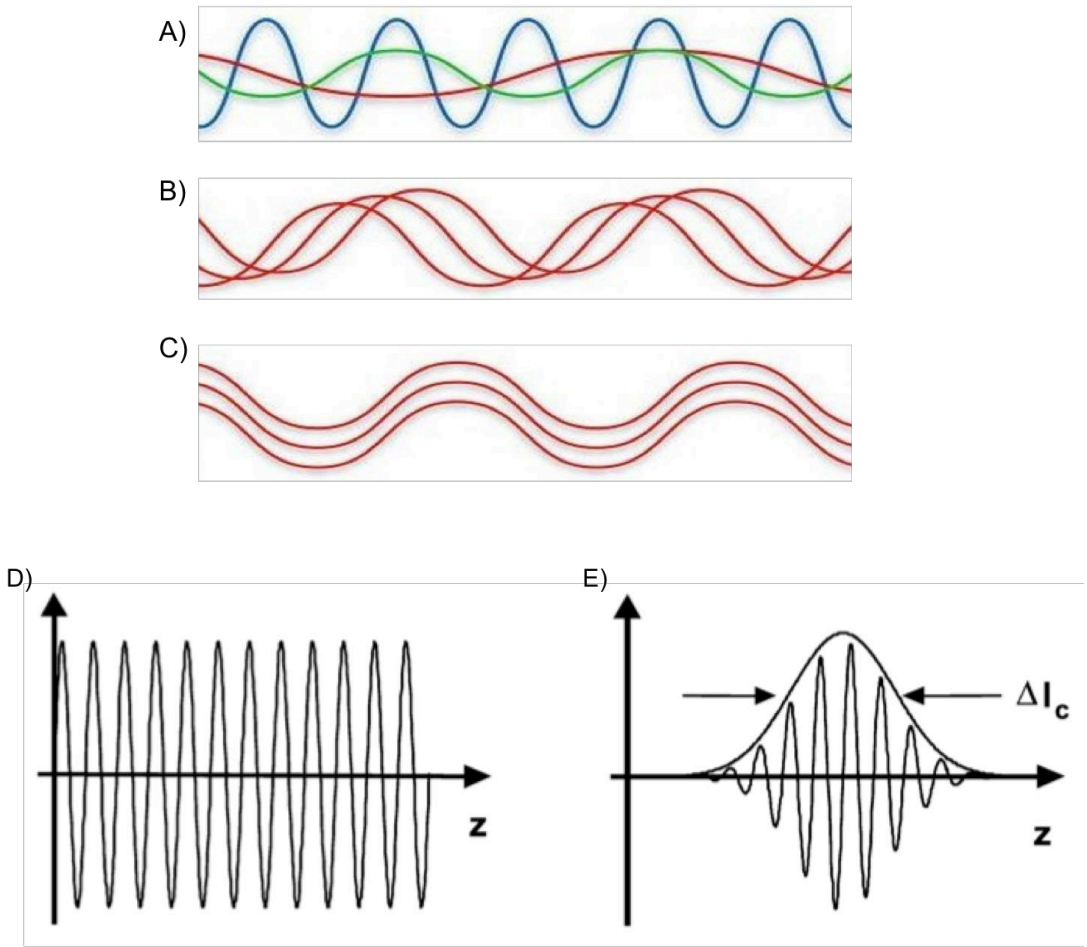

Figure 1.12. *Coherent and non-coherent light. A) Broad band light consisting of spectrum of colours (wavelengths). The light is incoherent. B) Monochromatic light such as LED light. Waves are not in phase (non-coherent). C) Laser light where waves are in phase (coherent). D) Light with a long coherence length. E) Light with a short coherence length.*

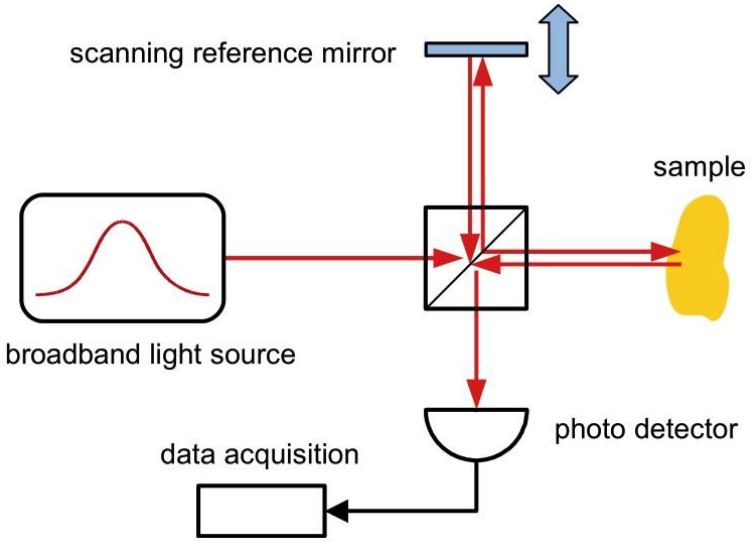

Figure 1.13. *A typical TD-OCT system set-up (Figure reproduced from Marshcall et al 2011).*

Frequency/ Fourier Domain OCT (FD-OCT)

In TD-OCT, the speed at which the path length can be changed is the rate-limiting factor in image acquisition speed, i.e. the faster the reference mirror can move the faster imaging can proceed (Tomlins and Wang 2005). Frequency domain (FD) systems hold the advantage of being able to acquire A-scan images much more rapidly because they do not require a moving reference arm that limits the image acquisition rate. FD systems acquire A-scans using a fixed reference path, and the sum of all the reflections from the tissue are detected, and the phase of the reflected light at certain frequencies is compared to the signal source, hence the name frequency domain (Fercher *et al,* 1995). Information regarding signal depth can be extracted using Fourier transform algorithms to reveal the sample's reflectivity profile; the term Fourier domain OCT therefore can be used interchangeably with frequency domain.

There are two ways in which FD-OCT image acquisition can be achieved. One can illuminate the interferometer with a broadband light source and then separate the reflected light originating from the sample into desecrate spectral components by placing a spectrometer at the output. This method is called 'spectral domain OCT (SD-OCT) (Bail *et al,* 1998) (Figure 1.14 a). Alternatively, 'swept source OCT' (SS-OCT) can be performed by probing a sample sequentially with different optical frequencies using a tunable narrowband light source that is able to sweep across a broad range of optical frequencies (Figure 1.14 b). The strength of the reflected signals at each wavelength is recorded using a single balanced detector which subtracts the reference and sample signals, and the remaining signal emanating from a location within the sample is then amplified; this method is quoted

more economical than using an array detectors as found in SD-OCT systems (Tomlins and Wang, 2005). SS-OCT systems contain spectrometers comprised from very fast read-out 1D linesman cameras that can offer up to several 100,000 readouts per second, and SS-OCT lasers are capable of rapidly sweeping through their spectrum (Matcher, 2010).

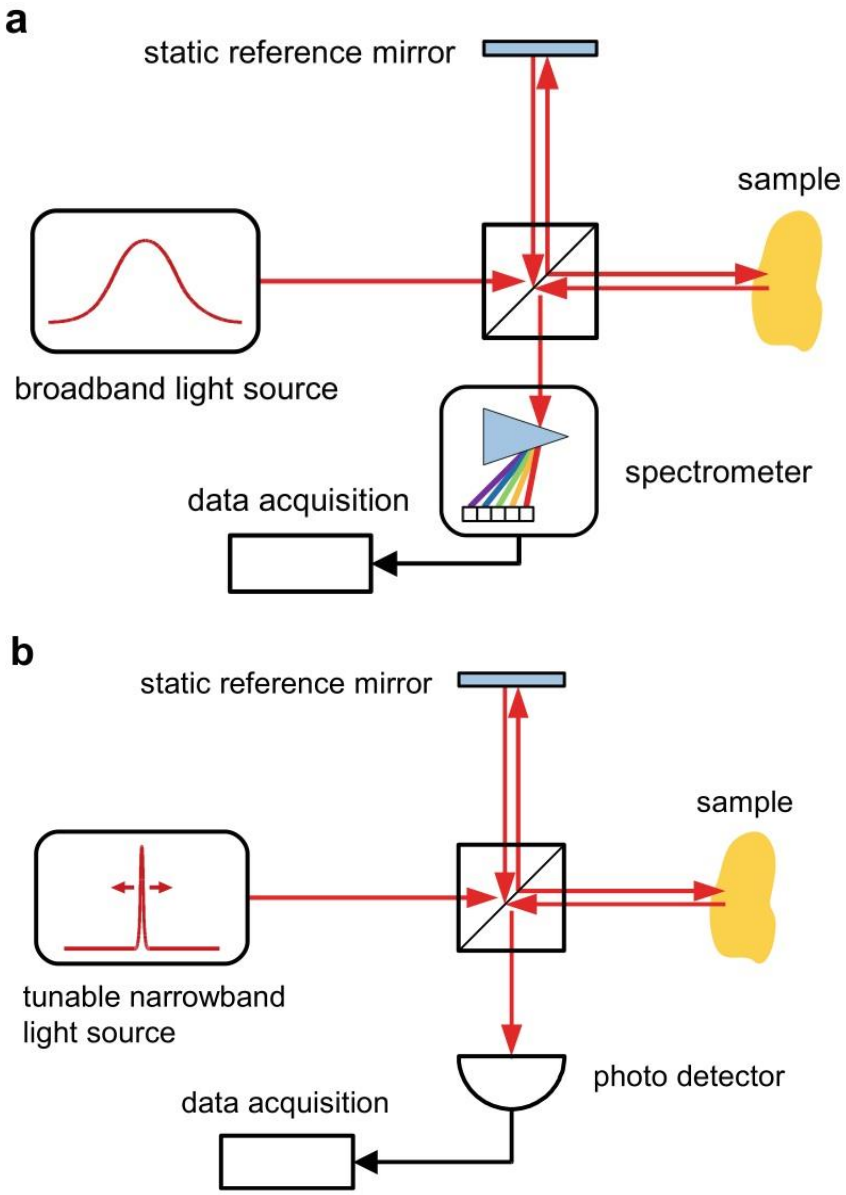

Figure 14. *FD-OCT systems. A) Spectral Domain OCT. B) Swept-Source OCT. In both cases the reference mirror remains in a fixed position, and sampling the interference pattern by optical frequency provides a depth scan. If a broad band light source is used as in A), a spectrometer is used to separate the reflected light into discreet bands for analysis. Alternatively a tunable narrowband light source that can rapidly sweep through a range of optical frequencies can be used (b). (Figure reproduced from Marshcall et al, 2011).*

Fundamentals

OCT Vs. Confocal Microscopy

Confocal microscopes (CM) can achieve high axial and lateral resolutions because they use objective lenses with high numerical apertures (NA). However, because OCT achieves axial resolution using coherence gating, low NA lenses are selected because they provide a depth of focus that is able to cover the entire imaging depth range. This is one of the ways in which OCT can image deeper structures than CM, however it comes at the expense of losing some lateral resolution, leading it to be several tens of μm rather than several microns (Marschall *et al,* 2011). This problem can be in part alleviated by using TD-OCT because dynamic focusing can be performed, i.e. the focus can be shifted through the sample in synchrony with the coherence gate. Thus higher NA lens can be used whilst maintaining a good imaging depth (Holmes *et al,* 2008); this allows TD-OCT to collect 'en-face' (parallel to the surface). This technique is often termed optical coherence microscopy (Yang *et al,* 2006), and it is often performed when the most relevant information is contained within the en-face plane and where high-speed image acquisition is not a priority (Matcher 2010).

In addition, due to the low NA of OCT lenses, working distances can be over several cm compared to less than 1 mm for high-NA objectives used for confocal. Several more points for comparison are listed below:

- By its very nature OCT is insensitive to fluorescence emission, therefore fluorescence labeling is of little value. OCT can however be made indirectly sensitive to fluorophores using a functional method called 'pump probe' OCT (Jacob *et a*l, 2010).

- OCT images contain an inherent form of noise called 'speckle' which is absent in confocal images.

- OCT produces 2D depth-resolved slices, whereas confocal microscopy produces 2D 'en-face' transverse slices. In both instances, software can be used to convert between these formats.

Light Source/ Wavelength Selection

The light source is the most important component of an OCT device because it is the primary determinant of imaging depth and resolution. Only broadband light sources that are

of short coherence length make it possible to accurately measure the depth of the backscattered signal from tissue. Such light can be generated from femtosecond mode locked pulsed lasers, super-luminescent diodes of fiber amplifiers. NIR light is most commonly used, because as a general rule, the longer the wavelength the less scattering the light experiences, leading to deeper penetration of the tissue, and such wavelengths are not absorbed by haemoglobin (Matcher, 2010).

Original OCT systems operated in the region of 800 nm, and this remains the most widely used wavelength in ophthalmology because it has excellent penetration through water, however 1060 nm is emerging as the new preferred wave length because of its increased depth penetration and higher resolution due to a reduced sensitivity to blurring from water dispersion (Sharma *et al,* 2008). Light with a wavelength of 1300 nm has proven to be the most popular non-ophthalmic application because it has the advantage of achieving greater depth penetration into biological tissues than 800 and 1060 nm sources. There are a wide choice of sources available that operate in this range, however they are not suitable for imaging though aqueous environments due to high adsorption in water (Matcher, 2010).

Resolution

Resolution is a measure of the ability of an optical system to distinguish detail. It can be defined as the minimum distance over which two distinct points can be separated for them to be identified or 'resolved' as two single points. For example, if two points have a proximity to each other that is within the resolution limit of the imaging system, they will be resolved as two desecrate points/pixels. If however they are closer to each other than the resolution limit, they will not be resolved and the two points will appear as a single point. The greater the resolving power of the system, the finer the detail that can be differentiated in an image. One of the advantages of OCT is that the axial resolution (the depth) and lateral resolution (transverse) are independent of each other (Mason *et al,* 2004). The axial resolution is inversely proportional to the bandwidth (Fujimoto 2001), therefore low coherent light sources provide greater axial resolutions compared to sources with a smaller bandwidth. Typical OCT systems provide axial resolutions of approximately 10 μm which is up to 100 times that of ultrasound, thus making it suited to imaging morphological changes in smaller biological structures such as epithelia (Gambichler et al, 2006). In addition, novel ultra high-resolution OCT systems with laser light sources have achieved resolutions as high as 1 μm (Morgner *et al,* 2000). The transverse/lateral resolution is dependent on the optical properties of the system, such as NA and focal spot size on the lens. The lateral resolution typically achieved in OCT is between 10-25 μm (Gambichler at al, 2006). The lateral resolution can be improved upon by imaging with a high NA lens and focusing the beam to a smaller spot size, however a compromise must be made because imaging with a high NA lens sacrifices the depth of field (Fujimoto, 2001).

Optical Properties of Skin

The optical properties of the tissue greatly influence the performance of OCT in terms of depth penetration and SNR. The extent to which light is able to penetrate into tissue is determined by several factors, which include the absorption and scattering coefficient (the sum of which constitutes the attenuation coefficient); all of which are dependent on the make-up of the tissue. Understanding the structure of skin aids in understanding the factors governing its optical properties, which will be described below.

1) Absorption

Absorption describes a reduction in light energy. Within skin, haemoglobin and melanin dominate the absorption of visible light. The dermis is the primary absorber of visible light due to the presence of haemoglobin contained within the erythrocyte-laden dermal vasculature (Bashkatov *et al,* 2005). In the IR range, light absorption is dominated by its interactions with water, which is estimated to comprise between 65.1 and 75.8 % of the volume fraction in the dermis (Reinoso *et al,* 1997). However despite waters' abundance in tissue it is not a substantial absorber of light in the visible region (Meglinski and Matcher 2002). Melanins contained within the epidermis absorb light most strongly in the UV region, with the degree of absorption curtailing toward the IR end of the spectrum. Further absorption can be attributed to lipids (Prahl and Jacques, 2009), cell nuclei and filamentous proteins (Dawson *et al,* 1980).

2) Scattering

When light changes direction, polarisation or phase, it is said to have been 'scattered'. Light can be scattered from surfaces by way of reflection, or most commonly refraction, or as a of result interactions with regions of a material whose optical properties differ from its surroundings (particulate scatter) (Lister *et al,* 2012). Between 4 and 7 % of all visible light is estimated to be reflected from the surface of skin irrespective of skin colour; remaining light is refracted into the skin as it passes from air to tissue (refractive indices of 1 and 1.36 respectively) (Anderson and Parrish 1981; Takiwaki 1998). Filamentous proteins present the principle source of scattering within skin. In the epidermis, keratins are the greatest filamentous protein constituent, whereas collagens are the most abundant filamentous component of the dermis, comprising 18-30 % of its volume (McGrath and Uitto, 2004).

Using a Mie solution to Maxwell's equations, it has been shown, using data from *in vitro* skin, that the scattering probability increases with the diameter of fibrous proteins and decreasing wavelengths (Graaff *et al,* 1992) Taken together, the dependence of scattering upon fiber diameter, and the fact that protein structures in the dermis may be up to 10 times

as large as those of the epidermis (McGrath and Uitto, 2004), suggests the dermis produces a greater scattering cross-section despite the dermis containing a lesser density of filamentous proteins compared to the epidermis. In relation to collagen, scattering has been shown to occur at both the level of individual fibers and bundles (Bashkatov *et al,* 2011), and the reticular and papillary dermis, which differ principally in collagen fiber diameter have been shown to have a differential effect on the backscattering of light. For instance, the papillary dermis is highly backscattering because the collagen fibres are an order of magnitude lower than that of visible light, whilst the larger diameter collagen fibers of the reticular dermis cause a high degree of forward scattering (Claridge *et al,* 2003).

OCT is only able to detect light that is backscattered since it is only the backscattered light that escapes the tissue and reaches the detector. By considering skin a composite material composed of layers of different materials, one can understand how the grey-scale cross-sectional image is produced. The areas of the material which scatter light to the greatest degree have their pixels assigned a high white colour-intensity. Equally, pixels that originate from depths whereby there is a lesser degree scattering are represented in a relatively lesser intensity when the image is composed. Absorption of light does not directly contribute to image production. In order to maximise the optical inhomogeneity of the tissue, OCT systems must be optimised to reduce absorption (Welzel 2001). As discussed above, long wavelengths of light (between 750 and 1400 nm) are used because they experience less scattering than shorter wavelengths, thus allowing greater depth of penetration. Transparent tissues such as the eye allow the greatest depth of imaging, and depths of tissue-engineered structures (Georgakoudi *et al,* 2008) can be seen up to 2-3 mm, which is the limit for many tissues (Fujimoto 2003).

Applications of OCT

Ophthalmology

OCT has made its most significant contribution to the field of ophthalmology, and it has been adopted as a standard diagnostic tool in the study of many retinal and vitroretinal diseases such as glaucoma (Medeiros *et al,* 2005), vitreous separation (Uchino *et al,* 2001), macular edema (Antcliff *et al,* 2000) and macular degeneration (Jumper *et al,* 2000). OCT has also been used to evaluate disease treatment protocols because it can capture treatment-induced retinal changes on the μm scale (Costa *et al,* 2006).

Compared to other imaging methods such as fluorescein angiography and ophthalmic ultrasound, retinal OCT is able to provide high resolution images of subsurface retinal features that were previously undetectable. Because of the different structure and reflectivity of the layers comprising the retina, each layer (retinal nerve fibber, nuclear layers, plexiform layers, external limiting membrane, retinal pigment layers and choriocapilliaris can be identified by this modality. Areas of the retina that contain cells which are aligned horizontally for example are correlated with high reflectivity, while layers that contain vertical structures and nuclei exhibit low reflectivity; and it is the differences in the optical properties of the retinal layers that allow each layer to be delineated (Zysk *et al,* 2007).

Cardiology

Key to OCTs advancement in cardiology has been the miniaturization and the accommodation of the technology into rotational catheter-based probes (Zysk et al, 2007). OCT therefore has been used to examine the structure and integrity of the coronary artery. Compared with intravascular ultrasound (IVS), which is the current standard for imaging, OCT provides a greater resolution by approximately an order of magnitude, and is able to image 1-3 mm into the tissue with good correlation to IVS (Brezinski *et al,* 1997; Jang *et al,* 2002). Applied to atherosclerosis, OCT can monitor the development of vulnerable atherosclerotic plaques in the coronary or carotid arteries to evaluate their potential for progression or rapture. When it comes to treating chronic total occlusions via stenting, OCT can be used to navigate the guide wire (Yabushita *et al,* 2002; Tearney *et al,* 2003; Chau *et al,* 2004); an inability to do so is the most common cause of procedural failure. It is also being evaluated as a tool to decrease the chances of guide wire perforation and dissection of the intima (Tanigawa *et al,* 2007). Also in relation to stenting, OCT imaging can be performed before and after balloon inflation (angioplasty), thus giving surgeons real-time information regarding stent apposition and re-expansion of the vascular walls (MacNeill *et al,* 2004), stent overexpansion (Bouma *et al,* 2003), and vessel injuries acquired post-stenting (Surmely 2007). In addition, due to OCT's superior resolution over IVS, it has also enabled the visualisation of stent integrity, neointimal proliferation, and neovascularization

(Kume *et al,* 2005a; Kume *et al,* 2005b; Regar *et al,* 2005). Recent efforts to develop functional modalities of OCT have allowed cardiovascular imaging to progress beyond morphological sensitivity alone, and thus has helped bridge the gap between structural and the underlying physiological information (Zysk, 2007). For example, fibrous calcified plaques have unique birefringence properties that can be visualised with polarization sensitive OCT (PS-OCT), and changes in these properties are thought to indicate changes in tissue structure. For instance, since the concentration of collagen dominates the birefringent signal in the image, it has been hypothesised that decreases in collagen, associated with vulnerable plaques, can be detected by PS-OCT (Giattina *et al,* 2006). Other functional techniques like optical coherence elastography are also being used to evaluate the mechanical properties of arterial walls (Rogowska *et al,* 2006).

OCT in Dermatology

From the outset, OCT has been investigated as a tool for dermatology because skin presents the most readily accessible part of the human body. Over the past decade OCT has proven to provide optical biopsies with good homology to the histopathologies of a number of different skin diseases (Gambichler *et al,* 2011). Therefore, OCT is proving a useful tool in examining skin abnormalities that are difficult to assess by visual inspection alone. In particular, its use in assessing non-melanoma skin cancers has been the subject of much research, however OCT has also been used to study photo damage, burns and inflammatory diseases such as psoriasis and contact dermatitis and skin infections such as onychomycosis and scabies (Steiner *et al,* 2003; Mogensen *et al,* 2009b).

In spite of the many applications of OCT, it has yet to be adopted into the mainstay of clinical dermatology. OCT images are able to clearly differentiate layers of the skin's structure such as the stratum corneum, proliferative epidermis and dermis because each layer backscatters light to different extents, underpinned by their compositional make-up (Mogensen *et al,* 2008b). However, OCT cannot resolve individual cells; therefore it can only determine the presence of a skin disease if it causes the scattering properties the tissue to become significantly altered from the norm due to disease-related gross tissue morphological abnormalities. For example, OCT can detect the presence or absence of types of skin lesions, however it lacks the resolution to distinguish between cancer subtypes (Marschall *et al,* 2011); thus making it a tool most useful for screening but not for determining a differential diagnosis.

1) Psoriasis

OCT is able to detect psoriatic patches by observing a strong entrance signal comprised from several parallel layers; with the layers resulting from the poorly backscattering region of poorly differentiated cells amongst mature highly backscattering

keratinocytes (Welzel *et al,* 2004). In hyperkeratotic conditions, due to the increased production of keratins, backscattering is increased from the superficial layers of the epidermis. Psoriatic pustules can also be identified; these appear as intraepithelial holes that are strong in signal intensity due to their backscatter (Welzel et al, 2004). Acanthotic epidermis (diffuse hyperplasia) can also be evaluated by tacking thickness measurements of the epidermis by means of A-scans averaging from B-scan images. A study by Morsely et al showed that OCT measurements of epidermal thickness from psoriatic skin correlates with other parameters of disease severity; thus OCT assessment of psoriatic plaques may prove a non-invasive method for following the development of psoriatic lesions in vivo (Morsy *et al,* 2010). However, OCT is not yet sensitive enough to differentiate between inflammatory skin conditions (Gambichler *et al,* 2007a). Additionally, OCT has also been applied in our lab to image inflammation in a model of psoriasis using cytokine-induced chronic inflammation in tissue engineered skin. Here, OCT was able to detect a hyperkeratotic thickening in the keratinised epidermis, and the images have also shown a good comparison to their histology (Bullock *et al*, 2011- shortly to be prepared for submission).

2) Blistering Diseases

Both intradermal and subdermal blistering can be seen by OCT (Gambichler *et al,* 2007), and it presents as large gaps between the dermis and the epidermis. In addition to the position of the blister, the nature of its content can also be deciphered via OCT *in vivo*. For example, serous infilling of the blister can be noted if the blister appears to be highly transparent, due to the area containing few scattering cellular components, whereas those that contain pus are perceived as brighter (more highly scattering) blisters because they contain a much greater volume of cells (Mogensen *et al,* 2008a) Again, however, due to the limits of OCT's sensitivity, it cannot distinguish between blistering diseases because the variations are too subtle; an enhanced resolution of OCT may overcome this shortcoming (Mogensen *et al,* 2008b)

3) Skin Cancers

Actinic keratosis is an intraepitheilal neoplasm, of which 10 % progress to squamous cell carcinomas (Glogau 2000), and it can be identified by OCT, with an 83 % specificity (Korde *et al,* 2007) versus non-diseased skin, as white dots and streaks corresponding to hyperkeratosis. It has been suggested therefore that OCT can characterise and monitor the response of such neoplasms to chemotherapeutic agents (Jorgensen *et al,* 2008). Additionally, features of basal cell carcinomas (BCC) can be identified by OCT with excellent correlation with histology (Olmedo *et al,* 2006). Solid tumors for example can be discriminated by their homogeneous signal distribution (Forsea *et al,* 2010), whereas tumour cell nests present as sub-dermal hypereflective zones with a similar size and locality

to that which is observed via histology (Olmedo et al, 2006). Multiple smaller tumour cell nests may also be observed deeper in to the dermis as poorly backscattering spots (Bechara *et al,* 2004). In malignant melanomas, large vertical, oval-shaped structures are the most striking OCT feature, which are absent from benign naevi, and these distinct features correlate to histopathological findings (Gambichler *et al,* 2007b). Signal intensity profiles can also be used to evaluate if a melanoma has become invasive. There is usually a second intensity peak from the backscattered light that represents the boundary between the epidermis and the dermis, however this peak may disappear, signifying that epidermal cells have invaded the dermis, although the extent of invasion can only be determined up to 1 mm into the tissue due to the limitation of depth of light penetration into the tissue (Welzel *et al*, 2004).

Additionally, through the use of functional OCT methods extra information can be gained regarding the nature of the tumour, allowing it to be characterised more thoroughly than by visualisation alone. Using polarisation sensitive OCT (PS-OCT, the birefringent signal, originating from the highly organised collagen fibers, can be measured from the tissue; this signal becomes much attenuated when skin lesions are present. Therefore, it may be possible to use PS-OCT in addition to SS-OCT to identify basal cell carcinomas (Bredfeldt *et al,* 2005).

Interestingly, OCT has also proven to be less biased and more precise than 20-MHz high frequency ultrasound for measuring the thicknesses of BCC lesions (Mogensen *et al,* 2009c). However one cannot differentiate between subtypes of BCC by OCT alone; histopathology is required (Gambichler et al, 2011). Despite OCT's inadequacy to diagnose BCC type, it has a relatively high accuracy when it comes to determining the presence of tumorous lesions from normal skin and identifying their boarders (Mogensen *et al,* 2009a) . Therefore, because of its non-invasive nature and ability to quickly acquire images over large areas of skin, it is a valuable tool for BCC tumor detection and screening. OCT can also be applied in surgery where cancer removal is concerned. Following the excision of diseased skin, the surgical wound margins can be examined to determine if any lesions that are not visible upon gross examination remain. The advantage over typical procedures for pathological assessment of excised tissue for cancerous remnants, such as light microscopy of paraffin embedded or frozen sections, is that it is far less time consuming and labor intensive and it does not suffer from limited spatial sampling over the mass, or artifacts produced from radiographic protocols (Vo-Dinh 2003). Therefore due to its ability to non-invasively image to a depth of 1-2 mm, an entire tissue area can be immediately scanned in a timely manner to determine if tissue resection is required by the surgeon. For example, Hamdoon *et al*, demonstrated that OCT can be used to guide photodynamic therapy; by discriminating between healthy and tumor-involved tissue, the therapy could be better targeted to tumor sites thus reducing necrosis of healthy tissue (Hamdoon *et al,* 2011).

4) Evaluation of Therapeutics

The effects of a variety of therapeutics, including moisturisers, ointments, and biochemical agents such as glucocorticoids can be studied via OCT (Pagnoni *et al*, 1999; Welzel, 2001). Skin hydration for example can be monitored by determining changes in the tissue's refractive index (RI) and scattering indices, and it has been demonstrated that an inverse relationship exists between the hydration state of the skin and its refractive index (i.e. the more hydrated skin, the lower the RI (Knuttel *et al,* 2004). Interestingly, it has been shown that the application of topical agents such as glycerol can transiently change the optical properties of skin tissue, by either decreasing reflectivity of the surface (Welzel *et al,* 2004) or increasing transmittance (Vargas *et al,* 1999); thus allowing light to penetrate deeper into the tissue enabling greater depth of visibility form the tissue.

Because OCT can be used to quantify epidermal thickness, it has proven useful in the early detection and monitoring of the side effects of topical creams. Pagnoni *et al* studied glucocorticoid steroid (GCS) induced skin atrophy by OCT and reported a 21 % reduction in epidermal thickness over a 3 week period following the application of 0.05 % clobetasol propionate cream (Pagnoni *et al*, 1999). The authors additionally investigated experimentally induced acute inflammation via stimulating the skin with Dimethyl Sulfoxide (DMSO), and revealed morphological changes in the epidermis and a small attenuation of light in the dermis. Similar findings were reported by inducing inflammation with histamine and nicotinic acid (Welzel *et al*, 2004). Recently, Ashcoff investigated the effects of 1 % hydrocortisone cream on uninvolved skin in patients with atopic dermatitis, and found that after 2 weeks of application of the cream a 6 % reduction in epidermal thickness resulted (Aschoff *et al,* 2011).

5) Wound Healing

OCT can be applied to study the mechanical properties of wounds. Using a novel TD-OCT based air-jet indentation system, which probes the wound by subjecting it to temporal waves of pressure leading to deformations at the level of microns (Huang *et al*, 2009), Chao et al were able to characterise the mechanical properties of diabetic wounds in a non-invasive manner (Chao *et al,* 2011). After gathering data from eight subjects with diabetic foot ulcers (10 in total), the authors reported the average stiffness coefficients from the peri-wound area were significantly higher than that of the central wound bed (0.47 N/mm vs. 0.35 N/mm respectively), with high test/retest reliability (Chao *et al*, 2012). Since the biomechanical properties of connective tissues are dependent on the arrangement of their collagen and elastic fibers (Culav *et al,* 1999), it is thought that knowing the mechanical properties may provide insight into the extent to which the collagens are cross-linked and the degree of degradation of the elastic fiber network (Culav *et al*, 1999). Therefore this

technique offers a novel method to objectively monitor wound healing of diabetic wounds which may help shed more light on wound pathogenesis. However a limitation of the system is that it cannot measure tissue thickness, therefore it may be used in conjunction with other OCT methods to more comprehensively characterise the wounds.

Ferraq et al used OCT to evaluate the use of lasers to create area and depth-defined skin wounds *in vivo* for the purpose of creating local environments in which wound healing could be studied. OCT was able to provide information regarding the depth and size of the wounds created via Er:YAG laser tissue ablation, and they found that laser created wounds were much more even in depth and size in comparison to those achieved via the established blister suction method (Ferraq *et al,* 2012). Therefore OCT has found use in developing protocols for creating experimental wound sites *in vivo*.

In addition, because OCT can perform optical biopsies, it can also be used to monitor wound healing both *in vivo* using animal models (Oh *et al,* 2006; Singer *et al,* 2007; Todorovic *et al,* 2008; Sahu *et al,* 2010) and *in vitro* using tissue-engineered skin (Yeh *et al,* 2004; Smith *et al,* 2010). It has also been used to evaluate novel wound dressings (Yeh *et al,* 2004; Wang *et al,* 2008). Recently Barui *et al* (2011) conducted a clinical pilot study using SS-OCT to monitor wound healing under honey dressing in patients with traumatic leg wounds and found that the OCT image could be correlated with the immunohistochemistry findings. The authors observed a characteristic transition from a uniform hypolucid (poorly backscattering) region, which was present below the early reformed stratum corneum, to a highly lucid region in the OCT image, which corresponded to the maturation of the epidermis as confirmed by histology. They also reported that the aforementioned change in optical properties of the tissue in the epidermal region corresponded to the time point when E-cadherin, a key cell-cell epidermal adhesion protein involved in wound healing (Jakob *et al,* 1999) was maximally expressed. Therefore Barui *et al* propose that OCT can indirectly provide information as to the extent of maturation and integrity of the reformed epidermis during wound healing (Barui *et al,* 2011).

There is particular interest in using OCT to elevate the severity of burns because early determination of wound depth is vital to informing clinicians as to how to treat the wound, which in turn is a key determinant of the prognosis (Monstrey *et al*, 2009). While the standard for burn assessment is visual, the accuracy of evaluation is largely dependent on the surgeon's experience; OCT however offers a more objective way to non-invasively evaluate the wound (Kim *et al,* 2012). Collagen, in its native state, is capable of polarising light into two perpendicular rays; a phenomenon known as birefringence. Upon thermal injury however the collagens become denatured and their birefringencey (BF) is lost (Thomsen *et al,* 1989). PS-OCT is able to determine the state of polarisation of backscattered light from tissue, in terms of birefringence amplitude orientation and

attenuation, therefore PS-OCT can quantify tissue damage by monitoring differences in phase retardance between burn and healthy tissue. A reduction in collagen's BF is thought to be related to burn depth, as well as collagen unraveling during healing, and animal studies have shown that PS-OCT measurements hold good correlation to histology with regards to burn depth (Park *et al,* 2001; Srinivas *et al,* 2004). Although most studies on OCT and its application to burns have been conducted on animals or *ex vivo* skin (Pierce *et al,* 2004), Kim *et al* recently reported the use of OCT to evaluate burns in the clinic. The authors examined two paediatric patients, both superficial and deep burns, by both conventional and PS-OCT, and observed that superficial burns presented with a similar layered structure to their contralateral control but with increased visibility of dermal vasculature and a reduced BF. In contrast, deeply burned skin presented a loss of its layered structure, almost absent vasculature, and a much reduced BF. In both instances the burned tissue had significantly reduced levels of BF throughout the depth of imaging compared to the controls (Kim *et al*, 2012).

OCT can also be used to determine the state of scaring following burn injury. In more than 60 % of patients, scars often become hypertrophic, which may lead to complications such as skin contraction over joints (Li-Tsang *et al,* 2005; Engrav *et al,* 2007). Hypertrophic scars are characterised by a high degree of angiogenesis, which presents as redness and an over-production of collagen at the wound margin; the higher the degree of redness, the higher the risk of scar hypertrophy. Visual assessment of scars based on the Vancouver scar scale for example are open to subjectivity, therefore more objective assessments of scar characterisation are required. OCT can create vascular maps of tissues by speckle de-correlation techniques based on determining fluctuations in the intensity of reflected light due to moving blood's endogenous scattering properties (Enfield *et al,* 2011). Liew *et al* (2013) recently demonstrated that OCT was capable of visualising wound vasculature to a depth of 600 μm in patients presenting with hypertrophic scars at various stages. They reported that hypertrophic scars contained much more vasculature compared to contralateral tissue as observed by the OCT images (Liew *et al,* 2013). In addition, they derived a methodology for the automatic quantification of vessel parameters such that median vessel diameter and total vessel area density data could be extracted from the OCT images. Accordingly, both parameters were found to be much increased in hypertrophic scars vs. healthy tissue (Liew *et al*, 2013). Therefore OCT can provide both qualitative and quantitative information regarding scar formation; this may aid the identification of wounds that are likely to become hypertrophic and assist in the evaluation of scar treatments though observing vessel reduction.

Aims and Objectives

Aims

This project aimed to develop an MSC delivery method derived from synthetic materials, and evaluate the healing potential of MSCs in *in vitro* wound models, derived from TE skin, using OCT.

Objectives

1) To evaluate to ability of medical grade silicone modified with plasma polymerised acrylic acid to deliver MSCs to model wound beds. The suitability of the delivery method was assessed by determining the efficiency of MSC delivery along with viability, and effects on cell phenotype and function.

2) To develop a reproducible 3D wound model based TE skin that could be used to study the effect of MSCs in an in *in vitro* wound environment.

4) To adapt the use of OCT so that it was optimised for use in making non-invasive assessments of wounded TE skin. As part of this objective, the most appropriate way to sample wound volumes and extract quantitative information from the images was determined.

5) To apply OCT to evaluate the wound healing of TE skin in the presence or absence of MSCs. As part of this evaluation, histology and immunohistochemistry was performed to complement the OCT images.

6) To screen wound models, in the presence of absence of MSCs, for several key soluble factors (HGF, IL-8, bFGF), by ELISA to determine if an association could be made between wound healing outcomes and the relative levels of these factors.

Chapter Two:

Materials and Methods

2.1 Materials

Cell Culture

1) Dulbecco's Modified Eagle's Medium (DMEM), GlutaMAX™- (Gibco/Invitrogen, UK)
2) Nutrient Mixture F12 (Ham's F12)- (Biosera, UK)
3) MSCGM™- Mesenchymal Stem Cell Growth Medium- (Lonza Biologics, UK)
4) Fungizone® Amphotericin B- (Invitrogen, UK)
5) L-Glutamine- (Sigma Aldrich, UK)
6) Fetal Calf Serum- (Biosera, UK)
7) Penicillin/ Streptomycin- (Sigma Aldrich, UK)

8) Adenine- (Sigma Aldrich, UK)

   0.5 g adenine powder was added to 70 ml distilled water (dH_2O) and acidified by adding 1 M Hydrochloric acid (HCl) until the power dissolved. The solution was brought to a final volume of 80 ml by adding a further 10 ml dH_2O to give a final concentration of 6.25 μg/ml. After filter sterilisation the adenine solution was aliquoted and stored frozen at -20°C.

9) Insulin from bovine pancreas- (Sigma Aldrich, UK)

   10 mg of insulin powder was dissolved in 1 ml 0.01 M HCl, to which 9 ml dH_2O was added to give a final concentration of 1 mg/ml. The stock solution was stored at 4°C.

10) Apo-Transferrin, Human minimum 98 % (3,3'5-Triiodo-L-thyronine Sodium salt) (T3)- (Sigma Aldrich, UK)

11) T3/Transferrin Solution

    13.6 mg of T3 was dissolved in a minimum of 0.02 M Sodium Hydroxide (NaOH) and made up to a volume of 100 ml in dH_2O. 250 mg of apo-transferin was dissolved in 30 ml phosphate buffered saline (PBS) to which 0.5 ml T3 solution was added. The volume was made up to 50 ml with PBS and the stock solution was aliquoted and stored at -20°C. The final concentrations were (1.36 μg/ml T3) & (5 mg/ml apo-transferrin) respectively. The stock solutions were stored at -

20°C.

12) Hydrocortisone- (Sigma Aldrich, UK)

25 mg of hydrocortisone power was dissolved in 1 ml dH_2O, and the final volume was made up to 10 ml with PBS to produce a stock concentration of 2.5 mg/ml. The stock was stored at 4°C.

13) Epidermal Growth Factor (Human Recombinant from E. Coli)- (Sigma Aldrich, UK)

14) Cholera Toxin- (Sigma Aldrich, UK).

1 mg of cholera toxin (extracted from Vibrio Cholera) was dissolved in 1.18 ml dH_2O and stored at 4°C. 100 µl of this stock was diluted in 10 ml serum free medium to give a concentration of 8.47 µg/ml.

15) Phosphate buffered saline (PBS)- (Oxoid Ltd, UK).

One PBS tablet (Dulbecco A) was added to every 100 ml of dH_2O prepared in a glass bottle suitable for the autoclave. PBS was autoclaved for 10 min at 115°C and stored at room temperature. The final concentration was 100 mM.

16) Trypsin EDTA -(Sigma Aldrich, UK).

0.25 % (v/v) trypsin and 0.02 % (w/v) ethylenediaminete- traacetic acid (EDTA) solution in PBS (pH 7.4).

17) Trypan Blue- (Sigma Aldrich ,UK).

18) Difco-Trypsin- (DIFCO Laboratories, USA).

Difco-Trypsin was prepared at a concentration of 0.1 % (w/v), with added D-glucose 0.1 % (w/v). To 100 ml of PBS, 0.1 g of trypsin and 0.1 g of D-glucose were added, along with 100 µl phenol red. The pH of the solution was adjusted to 7.45 by the addition of 2 M NaOH. Difco-trypsin was filter sterilised, divided into 10 ml aliquots, and stored at -20°C. Prior to use the Difco-Trypsin was supplemented with 100 IU/ml penicillin, 100 mg/ml streptomycin and 0.625 µg/ml amphotericin B.

19) Collagenase A (from *Chlostridium Histolyticum*)- (Roache Diagnositics, USA)

A 0.05 % solution (w/v) of collagenase A was made by dissolving 0.05 g collagenase A in 10 ml DMEM supplemented with 10 % FCS. The volume was filter sterilised, divided into 10 ml aliquots and stored at -20°C.

Immunohistochemistry

1) Rabbit Anti-Human RFP- (Abcam, UK)
2) Mouse Anti-Human Pan-Cytokeratin- (GeneTex, USA)
3) Biotinylated Goat Anti-Rabbit IgG- (Vector Labs, USA)
4) Texas Red Goat Anti-Rabbit IgG- (Vetor Labs, USA).
5) FITC Horse Anti-Mouse IgG- (Vetor Labs, USA).

6) Sodium Citrate Buffer

   2.94 g of sodium citrate were dissolved in 1 L of dH_2O to make a 10 mM solution. 1 M HCl was added slowly to adjust the pH to 6.0, and 0.5 ml of Tween-20 was added (0.05 %, v/v). The buffer was stored at RT for 3 months or at 4°C for long-term storage.

7) Tris/EDTA

   A 1 M stock of Tris (mw 121.4) was made by adding 12.1 g Tris to 100 ml of dH_2O. A 0.5 M EDTA (Mw 292.24) stock was madly adding 1.46 g EDTA in 7 ml dH_2O and adding 5 M NaCl until the EDTA dissolved and the volume was then topped up to 10 ml by adding additional dH_2O. A 10/1mM working solution of Tris/EDTA was prepared by adding 10 ml of a 1 M Tris Base stock solution to 2 ml of a 0.5 M EDTA stock and making the final volume up to 1 L by adding 988 mL dH_2O. 0.1 % Tween-20 (v/v) was then added, and the pH was adjusted to 9.0 by adding 1 M NaCl. Once made, it was stored at RT and used within three months.

8) Trypsin- for enzymatic antigen retrieval.

   A 0.5 % solution of trypsin (Sigma Aldrich, UK) was made by adding 1 ml of a 0.5 % trypsin (w/v) stock solution (50 mg in 10 ml dH_20), to 1ml of 1 % calcium chloride (w/v) stock solution (0.1 g $CaCl_2$ in 10 ml dH_2O), and adding 8 ml dH_2O to make the final volume 10 ml. The solution was mixed well and pH adjusted to 7.8 through the addition of 1M NaOH. The working solution was stored at 4°C for one month of at -20°C for long-term storage.

9) DAPI 4', 6-diamidino-2-phenylindole- (Invitrogen, UK)

   A 5 mg/ml stock solution was prepared my dissolving 10 mg in 2 mL of dH_20 or dimethylformamide (DMF). For long-term storage the stock solution was aliquoted and stored at -20°C and protected from light. For use, aliquots were diluted 1:1000 by adding 10 µl to 10 ml of PBS. The final concentration was 300 nM.

10) Vectastain Elite® ABC Reagent- Avidin and Biotinylated horseradish peroxidase macromolecular Complex (ABC), (Vector labs, USA)

11) 3,3'-diaminobenzidine (DAB), (Vector Labs, USA)

12) Hydrogen Peroxide (H_2O_2) (Invitrogen, UK)
    A 0.3 % (v/v) solution of H_2O_2 was prepared by diluting a 3 % stock solution 1:10 in dH_20

ELISA

1) Human IL-8 ELISA Development Kit- (PeproTech, Germany).
2) Human bFGF ELISA Development Kit- (PeproTech, Germany).
3) Human HGF Quantikine ELISA Kit- (R&D Systems, USA).

Note- each kit came complete with capture and detection antibodies, cytokine standards and Avidin-HRP conjugate.

4) ABTS Liquid Substrate (2,2′-Azino-bis(3-ethylbenzothiazoline-6-sulfonic acid)- (Sigma Aldrich, UK).

5) Substrate Reagent Pack (Stabilised hydrogen peroxide and stabilised tetramethylbenzidine)- (R&D Systems, USA).

6) Stop Solution (2N Sulphuric Acid)- (R&D Systems, USA).

Others

1) Mounting Medium DPX- (VWR International, UK)
2) (3-(4,5-dimethylthiazol-2-yl)-2,5-diphenylltetrazolium bromide (MTT)- (Sigma Aldrich, UK)
3) Stainless steel metal grids
4) Stainless steel rings (8 mm diameter)
5) All solvents were purchased from Fisher Scientific UK Ltd.
6) Tween-20- (Sigma-Aldrich)
7) Sodium Citrate- (Tri-sodium citrate (dehydrate) (Invitrogen, UK)
8) Calcium Chloride- (Sigma-Aldrich, UK)
9) Trizma- (Sigma-Aldrich, UK)
10) Parafilm M- (Alcan Packing, UK)
11) Cylindrical glass vessel- (QVF Process Systems, UK).
12) Two-stage rotary vane pump- (Vacuum Research, USA)
13) Pirani gauge -(Edwards Crawley, UK)
14) Anhydrous Acrylic acid 99 %- (Sigma Aldrich, UK)
15) RBS 35 Detergent Concentrate- (Thermo Fisher Scientific, UK)
16) Medical Grade Silicone- (Polymer Systems Technology, UK)
17) Paraffin Wax- (Sigma-Aldrich, UK)
18) Fragrance free exfoliating facial sponge (Boots, UK)
19) Ramer sponge- (Boots, UK)
20) Ear plugs- (Boots, UK)
21) Washing up sponge- (Wilkinsons, UK)

2.2. Methods

Cell Culture

All cell culture was carried out in Class II laminar flow hoods (Walker Safety Cabinets, UK). Any equipment or materials used within the hoods were sterilised prior to use by 70 % (v/v) industrial methylated sprits (IMS) (Fisher Scientific, UK) or by autoclave. Sterile plastic wear used for cell culture was purchased from Costar, UK and Greiner Bio-one, UK. Any liquids used for cell culture were purchased sterile from the supplier or sterilised prior to use by passing them through a 0.2 μm filter (Millipore, USA). All cells were maintained in their appropriate growth medium and incubated at 37°C in a humidified environment containing 5 % CO_2. Medium was changed every 2-3 days.

Culture of Epidermal Keratinocytes

Freshly isolated keratinocytes were cultured in Greens medium, composed according to Table 2.1. in the presence of a feeder layer of lethally irradiated 3T3 murine fibroblasts (i3T3) (XCELLentis, Belgium). Keratinocytes were not used after passage 3.

Component	Stock Concentration/Volume	Final Concentration
DMEM GlutaMAX	330 ml	66 %
Hams F12	108 ml	21.6 %
FCS	50 ml	10 %
Penicillin/ Streptomycin	5 ml containing 10,000 IU/ml penicillin & 10,000 μg/ml streptomycin	100 IU penicillin 100 μg streptomycin
Amphotericin B	1.25 ml of 250 μg/ml	0.625 μg/ml
Adenine	2 ml of 6.25 μg/ml	0.025 μg/ml
Insulin	2.5 ml of 1 mg/ml	5 μg/ml
T3/transferrin	0.5 ml containing 1.36 μg/ml T3 & 5 mg/ml transferrin	1.36 ng/ml T3 5 μg/ml transferrin
Hydrocortisone	80 μl of 2.5 mg/ml	4 μg/ml
EGF	25 μl of 100 μg/ml	5 ng/ml
Cholera toxin	500 μl of 8.47 μg/ml	8.47 ng/ml

***Table 2.1**. Composition of Green's Medium.*

Culture of Dermal Fibroblasts

Dermal fibroblasts were cultured in DMEM supplemented with additional components (Table 2.2.). Fibroblasts were used between passages 3 and 8.

Component	Stock Concentration/Volume	Final Concentration
DMEM	438.75 ml	87.75 %
FCS	50 ml	10 %
Penicillin/ Streptomycin	5 ml containing 10,000 IU/ml penicillin & 10,000 μg/ml streptomycin	100 IU penicillin 100 μg streptomycin
Amphotericin B	1.25 ml of 250 μg/ml	0.625 μg/ml
L-Glutamine	5 ml of 200 mM	2 mM

Table 2.2*. Composition of fibroblast medium.*

Culture of Mesenchymal Stem Cells (MSCs)

Human bone marrow MSCs (passage 2), were purchased from Lonza Biologics, England, and expanded in complete mesenchymal stem cell growth medium (MSCBM) supplemented with L-glutamine, gentamicin sulfate, amphotericin B, and mesenchymal cell growth supplement (Lonza Biologics). MSCs were used between passages 3 and 8.

Passaging of cells

When cultured cells had reached 80 % confluence in their culture flasks, the medium was decanted from the flask. The surface of the flask was rinsed twice with 10 ml of PBS to remove any remaining medium; medium contains serum proteins that will hinder the action of the trypsin in the subsequent step. To detach the cells, 5 ml of trypsin/EDTA, pre-warmed to 37°C in a water bath, was added to the flask, and the flask was incubated at 37°C for a minimum of 5 min with the trypsin/EDTA. The incubation time varied depending on the cell type. Trypsin was neutralised by the addition of medium which contains aprotinin, the bovine equivalent of human basic pancreatic trypsin inhibitor (BPTI). Cells were centrifuged at 1200 revolutions per minute (rpm) for 5 min using a bench top centrifuge. The supernatant was discarded from the resulting cellular pellet, and the pellet was re-suspended in a desired volume of medium. The cells were 'split' by seeding them at lower cell densities into additional culture flasks.

Counting Cells

Cells were counted using a Neubauer hemocytometer (Weber Scientific International, UK). A glass coverslip was slid over the top of the hemocytometer and 10 μl of cell suspension was pipetted under the coverslip on both sides of the glass, so that the counting grids of the hemocytometer were filled. The hemocytometer was placed under a light microscope and the number of cells was counted in each grid. Each 1 mm^2 grid had a

volume of 1 x 10^{-4} ml. Therefore, by knowing the cell count and the volume they occupied, the cell concentration was calculated as follows:

Average number of cells/1 mm^2 grid x Dilution factor= Cells/ml
Volume counted (1 x 10^{-4}ml)

e.g. An average cell count of 100 with no dilution = 1 million cells/ ml

Trypan blue which permeates damaged membranes was used to identify dead cells so that they could be excluded from the cell count. Trypan blue was diluted 1:1 with cell suspension (usually 10 μl of each) and then a small volume was introduced to the hemocytometer.

Freezing cells for Cryo-preservation

For long-term cell storage; cells were kept frozen in liquid nitrogen; this required the use of a preserving agent. Cells were trypsinised as above and re-suspended in cryo-preservation medium (90 % FCS, 10 % DMSO v/v). The cells were counted, and cell concentrations between 1 and 3 x 10^6 cells/ml, depending on cell type, were pipetted to fill a set of cryovials (Cellstar cryovials, Greiner Bio-one, UK). The cryovials were placed in a Nalgene™ Cryo 1°C freezing container (Nalgene Co, USA), which contained 250 ml isopropanol. This allowed the cryopreservation medium, and thus the cells, to cool at a rate of 1°C/ min in a -80°C freezer; thus avoiding cell lysis caused by rapid freezing. Cells were kept in a -80°C freezer for a minimum of 4 h before they were transferred to a liquid nitrogen Dewar (temperature of -196°C). The described method was performed quickly because at room temperature DMSO is toxic to cells. Cells were stored for no longer than 3 years.

Thawing Cells

Cryovials containing the desired cell types were removed from storage in liquid nitrogen and immediately placed in a water bath (37°C) to thaw. Once thawed the cell suspension was added to 10 ml of the cell appropriate pre-warmed medium and centrifuged at 1200 rpm for 5 min. The supernatant was discarded form the cellular pellet, and the cells were re-suspended in culture medium and counted. Resulting cells were divided into T-75 flasks and cultured until a passage was required. The medium was changed after 24 h of being put into culture, to remove any dead cells, and then replaced every 2-3 days thereafter. Cells were used for up 10 passages; stocks of low passage cells were kept in storage. Cells were periodically tested for mycoplasma infection and any infected cells were discarded.

Cell Isolation from Human Skin

Skin, from which fibroblasts and keratinocytes were extracted, was kindly donated for research purposes by patients undergoing plastic surgery (breast reductions and abdominoplasties) at the Royal Hallamshire Hospital (Sheffield). Informed consent from patients and full ethical approval was sought through the Sheffield Hospitals Ethical Committee. All research using this skin took place in the Kroto Research Institute under the Research Tissue Bank License No. 12179.

Keratinocyte isolation

Skin was removed from its collection pot, placed into a petri dish containing a small volume of PBS, and the skin was unfolded so that it lay flat in the petri dish. Using a scalpel, the biopsy was cut into small pieces of approximately 0.75 - 1 cm^2. The pieces were transferred to a sterile plastic tube containing 15 ml of 0.1 % w/v Difco-Trypsin (plus 0.1 % w/v D-glucose in PBS, pH 7.45), and incubated overnight at 4°C for a minimum of 12 h, but no more than 20 h. The following day, pieces of skin were removed from the Difco-Trypsin and placed dermal side down into a petri dish where they were washed with PBS. Using forceps, the epidermis was gently peeled from the dermis to expose the underside of the epidermis and the papillary dermis. Using a scalpel, the undersides of pieces of epidermis and the papillary dermis were gently scraped to remove cells into suspension. The cell suspension was removed from the petri dish and pipetted into a 30 ml universal tube containing 10-15 ml of Green's medium and spun at 200 x gravity for 10 min in a centrifuge. The supernatant was discarded and the resulting pellet was re-suspended in Green's medium and counted. Additional medium was added to the cell suspension to produce a keratinocyte concentration no less than 1.5 x 10^6 cells/ml, and cells were placed into a T-75 flask containing a feeder layer of i3T3 cells. These primary cultures once established are termed P0.

Fibroblast Isolation

After removal of the epidermis from skin during the keratinocyte isolation procedure, the dermis was kept aside in PBS for fibroblast isolation. The pieces of dermis were cut even smaller with a scalpel and placed into a universal containing collagenase A for an overnight incubation at 37°C. The following day the collagenase appeared cloudy indicating the presence of cells in suspension, the pieces of dermis were removed and the collagenase was centrifuged for 10 min at 2000 rpm. The supernatant was discarded and the resulting cell pellet was resuspended in DMEM. The cells were counted and, if necessary, additional medium was added to make the final concentration 1 million cells/ml. Between 0.5 and 1x10^6 cells were seeded in each T-75 flask.

Preparation of de-epithelialised Dermal Substrates

De-epithelialised dermal (DED) substrate was prepared from two sources. Firstly 'fresh' skin that was not used for the extraction of keratinocytes and fibroblasts provided a source of dermis, and secondly when this was not available, Euroskin (glycerol-preserved split thickness cadaveric skin) was used (Euro Tissue Bank, Beverwijk, The Netherlands). Prior to the use of Euroskin, the preserving glycerol was thoroughly removed by extensive washing with PBS. Both fresh skin and Euroskin, following glycerol removal, were then treated similarly. Skin was incubated in sterile 1 M Sodium Chloride (NaCl) for 18 h at 37°C. Subsequently, the epidermis was separated from the dermis to leave behind DED (bare dermis). 'Fresh' skin requires only a pair of sterile forceps to peel a continuous sheet of epidermis from the dermis, whereas for Euroskin, because of glycerol preservation, a scalpel blade had to be used to gently scrape the epidermis from the dermis. DED from either source was incubated at 37°C and 5 % CO_2 in Green's medium for 48 h as a means to test sterility of the preparation; the medium containing phenol red would rapidly change colour, from red to orange, in the presence of any contamination. The two skin sources were used interchangeably between experiments.

Making Tissue Engineered Skin

DED prepared from 'fresh' skin from surgery was cut into approximately 2 cm^2 pieces using a scalpel and placed into individual wells of a 6-well plate. Sterile stainless steel chamfered-edge rings (0.8 mm in diameter) were placed on top of each piece of DED and pressure was applied to the top of the ring using forceps, so that the edges of the ring impressed into the DED. To the center of the ring, $3x10^5$ keratinocytes at passage 2 or 3, and 1 x 10^5 fibroblasts were added in suspension. These new so-called 'composites' were placed in an incubator (37ºC and 5 % CO_2) for 24 h. The following day the rings were removed from the composite and medium was replaced so that the composite was submerged in medium. Composites were kept in submerged culture for two days before being lifted to an air liquid interface (ALI). ALI was achieved by placing the composites onto stainless steel grids, which raised the composites approximately 0.5 cm from the base of the well plate. Green's medium was pipetted into the wells up to the point just below where the medium would break over the surface of the composite. This allowed the composite to be perfused with medium from the underside of the tissue, whilst the top surface was kept as dry as possible. This differential in environment was essential to the development of a good stratum corneum by promoting differentiation by the basal keratinocytes. Once at ALI the medium was changed every 2-3 days, and the composites could be maintained at ALI for up to 14 days.

Plasma Polymerisation

Plasma Polymerisation of Acrylic Acid

Polymerisation was carried out in a 6.2 L cylindrical glass vessel which was sealed by stainless steel flanges with PTFE gaskets at both ends (Figure 2.1). A vacuum was obtained within the vessel using a two-stage rotary vane pump, and liquid nitrogen cold trap. A Pirani gauge, which was placed downstream from the vessel, measured the pressure in the rig. The base pressure in the reactor was less than $3x10^{-3}$ mbar. Monomeric anhydrous acrylic acid (AA) (CH_2=$CHCO_2$) was used for plasma polymerisation without any prior pre-treatment, except for degassing by several freeze-thaw cycles. AA contained within a round-bottomed glass flask was connected to the reactor through one of the flanges via the needle inlet valve. The needle valves were used to control the flow rate of the monomer through the reactor due to AA's high vapour pressure at room temperature. Flow rates of 4.8-5.2 cm^3 (STP) min^{-1} (sccm, standard cubic centimeter per minute) were established and maintained using methods first described by Yasuda (Yasuda 1985). To measure flow rate, the stop-valve was closed for 30 sec, while the monomer was allowed to continually flow into the reactor. The resulting increase in the pressure within the system was noted, and the flow rate was calculated using the following equation:

$$\text{Flow rate (sccm)} = \Delta P\ (Pf - Pi) \times V$$

P= pressure, Pf= final pressure in the system (30 seconds after stop-valve closure), Pi= initial pressure of the system (before stop-valve closure), V= volume of the reactor (6.2 L).

Typically, an initial pressure of 7.5 $x10^{-2}$ mbar was sufficient to produce a flow rate between the desired ranges (4.8- 5.2 sccm). The flow rate was calculated several times to be certain the flow rate was stable. A plasma was initiated and sustained via a radio frequency (RF) source (13.56 MHz, 2 W), which was inductively coupled to the reactor by copper wiring which was coiled around the outer surface of the glass chamber. An impedance matching unit was then fine-tuned to minimise power loss from reflectance to < 0.1 W.

Sheets of medical-grade silicone were cut to fit neatly into Petri dishes and placed in the 'glow' region of the reactor; up to three petri dishes could be placed into the reactor at any one time. The plasma was sustained for 20 min to ensure it produced a polymer thickness sufficient to obscure the signal from the substrate in XPS analysis; a thickness was taken to be greater than 5-10 nm (Beamson and Briggs 1998). After the allotted deposition time, the power was switched off and the monomer flow rate was measured to ensure that there had been no change in the flow rate during the deposition cycle. Before opening the reactor, monomer was allowed to continue to flow through the reactor for a

further 10 min to terminate any reactive free radical species that remained on the surfaces of the samples, and to reduce the uptake of atmospheric oxygen by the surface. The flow of monomer into the reactor was finally terminated by fully closing the needle valve, and monomer that remained in the chamber was drawn out by the vacuum for a further 5 min before the reactor was opened. Once removed from the reactor, samples were stored at room temperature and wrapped in Parafilm (Alcan Packing, UK) to prevent them from accumulating moisture from the atmosphere. After the silicone had been plasma treated with acrylic acid they were termed 'carriers', and they were used for the later culture and delivery of MSCs within 60 days of production. No sterilisation step was performed prior to the use of the materials in cell culture because it is assumed that the harsh environment, which is rich in free radicals and UV radiation, of the plasma kills bacteria thus sterilizing the surface (Moisan *et al,* 2002).

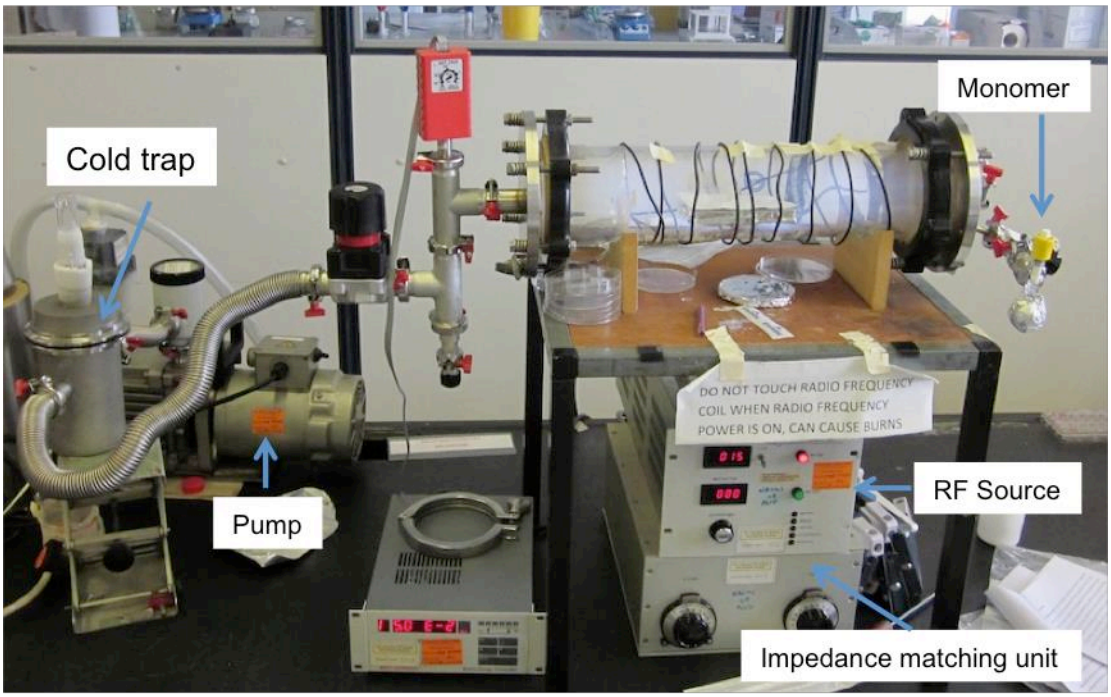

Figure 2.1. *A photograph of the plasma polymerisation rig.*

Degassing the Monomer

Under vacuum, vaporised acrylic acid may not be the only gas that enters the reactor from the monomer flask - atmospheric gases that became trapped in the aqueous acid during storage may also be released into the system. If not removed, additional gases will contribute to the pressure of the system and the flow rate of monomer will be overestimated. A process of degasification by cycles of freeze thawing, which achieves the removal of gases from liquids, was therefore performed prior to calculating the flow rate of the acid into the reactor. The flask containing AA monomer was rapidly frozen by partially submerging it

in a container of liquid nitrogen. Once frozen, the monomer was thawed at RT under vacuum. The needle valve was opened allowing any bubbles of gas eluted from the acid to be released into the vacuum. Once the acid had thawed, the process was repeated a minimum of three times or until no more evolution of gas was observed during thawing.

Cleaning the Monomer Flask

The monomer flask was routinely cleaned after the monomer in the flask had expired, and before fresh monomer was added. To this end, a 10 % (v/v) solution of RBS detergent in acetone was poured into the flask and the flask was placed into a sonicator for 5 min. This removed any impurities and contaminants from the flask. Monomer was replaced in the flask every 2 weeks, and the flask was stored at 4°C. The flask was wrapped in foil when it was used at the reactor to protect the acid from the light, and thus slow the rate of spontaneous polymerisation.

Cleaning the Rig using an Oxygen Plasma

Before any reaction took place, the reactor was exposed to a high-energy oxygen plasma. This buffeted any material that had previously been used in the reactor and had polymerised from the wall of the reactor, thus preventing contamination of samples when a new deposition cycle was run. The chamber was evacuated to a base pressure between 6-8 x 10^{-2} mbar, and O_2 was let into the reactor into the reactor until the pressure became 1.5-1.7 x 10^{-1} mbar. 50 W of RF energy was put into the system and the reflected energy was minimised by fine-tuning the impedance matching unit. A blue plasma was ignited as cleaning began as a result of exciting the pre-deposited polymer from the reactor walls. Once the reactor was clean, the blue plasma disappeared indicating the residual polymer had been successfully removed. This took between 20-30 min depending on the amount of residual polymer that was coating the walls of the reactor.

Contact Angles

Samples were placed onto the stage of a RemeHeart goniometer (RameHart, USA) (Figure 2.2.a), and a 2 μl drop of dH_2O was dispensed onto the surface of interest using a Hamilton Syringe (Hamilton, Switzerland). The droplet formed was backlit using a lamp, and the sample was viewed through an eyepiece. The angle between the stage and the drop profile, with the origin at the three-phase line, was noted. Two points on each sample were measured from three replicate preparations. Surfaces that create droplets with contact angles exceeding 90° are described as hydrophobic with poor wetting, poor adhesiveness and a low solid surface free energy. Hydrophilic surfaces create contact angles lower than 90° and have the opposite characteristics of hydrophobic surfaces (Figure 2.2.b).

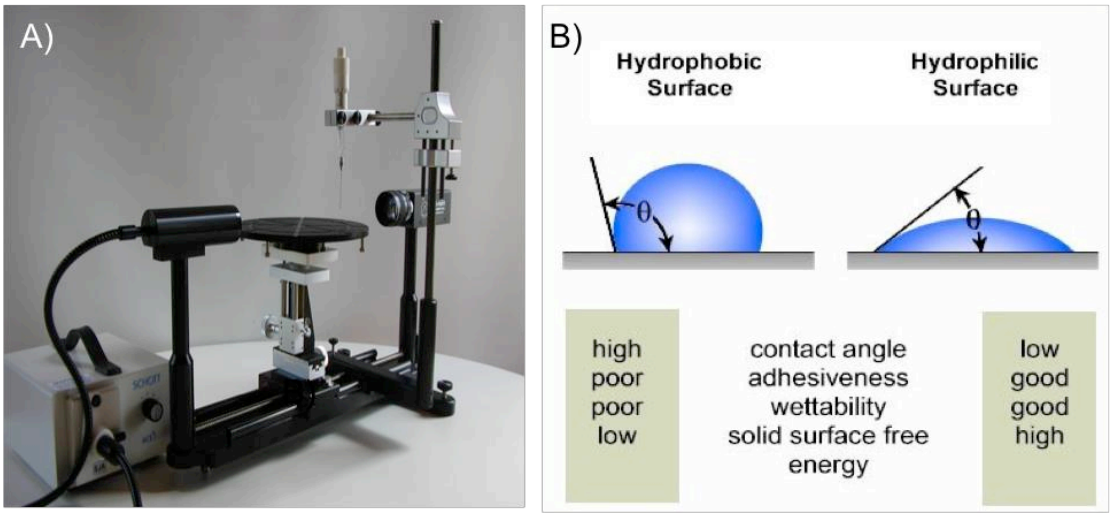

Figure 2.2. *Measurement of contact angles. A) RameHart Gioniometer. B) Hydrophilic vs. hydrophobic surfaces. (Images from RameHart.com).*

X-Ray Photoelectron Spectroscopy (XPS)

XPS was carried out using a Kratos Axis Ultra X-ray photoelectron spectrometer (Kratos Analytical Ltd, Manchester, UK). All samples where maintained under a vacuum of 1 x 10^{-8} mbar for 2 hours prior to XPS analysis, and all data were collected at 90° relative to the sample plane. A minimum of two survey scans and two narrow scans were performed on each sample, with pass energies of 160 eV and 20 eV respectively, to obtain O1s and C1s peaks. Charge neutralisation was applied to all samples.

CasaXPS software (www.CasaXPS.com, UK) was used to determine the elemental composition of individual peak areas. C1s peaks where fitted using combinations of Gaussian (30 %) and Lorentzian (70 %) curves against a linear background. The full width half maximum of all components was constrained to be equal to that of the aliphatic carbon, but all other parameters where left to free to vary during fitting, optimizing parameters taken from spectra of similarly prepared surfaces in the literature (Alexander and Duc 1998; Haddow *et al,* 2003)

Seeding Cells onto Carrier Surfaces

2 cm^2 (2 x 2 cm) pieces of silicone treated with acrylic acid (carriers) were placed acid side up into wells of a six well plate. 8 mm diameter stainless steel rings were placed on top of each carrier, and 5 x 10^5 cells were seeded into the volume of the ring; thus providing a cell density of 38,000 cells/cm^2. Rings were used to confine the cells to the carrier's surface. Prior to the introduction of cells, the quality of the seal provided by the rings on the surfaces was tested in two ways: firstly, each carrier was wetted with medium

and placed on top of the rings. Each ring was then inverted and held upside-down using forceps; the carrier should have remained stuck to the underside of the ring. If the carrier adhered to the underside of the ring it was placed into the well plate and gentle pressure was applied to the top of the ring with forceps. Secondly, a test volume of 800 μl of medium was pipetted into the ring to completely fill it, and 10 min later the rings were observed to see if any leakage of medium had occurred. If leakage was evident the carrier was resealed to the ring and retested for further leakage. Once cells were seeded, additional medium was added to top-up the total volume of medium in the ring to 800 μl, and the volume outside of the ring was filled with medium (Figure 2.3.). Well plates containing the carriers were placed into an incubator (37°C, 5 % CO_2, humidified environment) for 24 h before the medium was discarded. The rings were carefully lifted from the carriers using forceps and the carriers were submerged in fresh medium and cultured on the carrier for up to 7 days, with medium changes every 2-3 days.

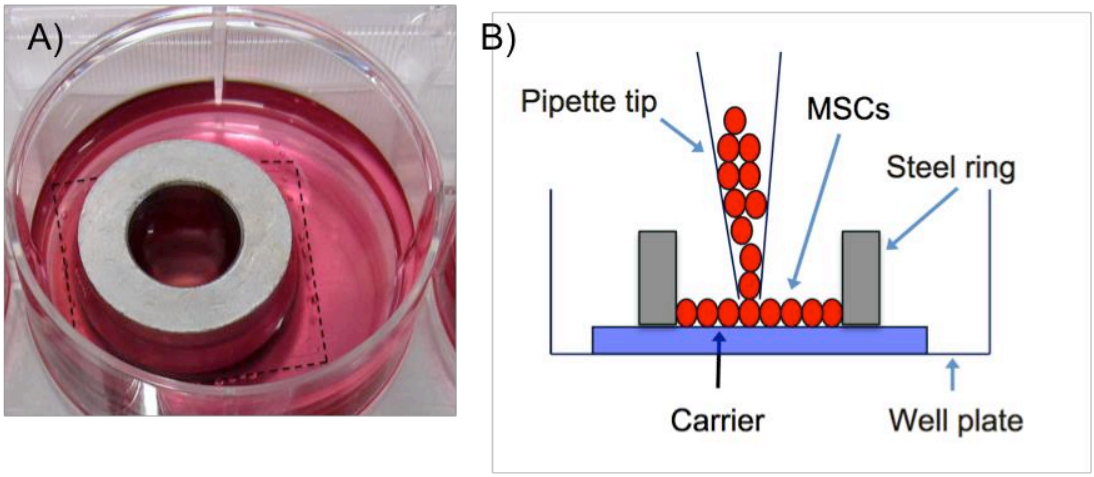

Figure 2.3. *Seeding cells onto the carrier. A) photograph of a well that contained a carrier seeded with cells. Dotted line indicates the carrier. B) a labeled diagram of A).*

Cell Transfer from Carriers to DED

Cells were transferred from the carriers to 1.5 cm^2 pieces of de-epithelialised dermis (DED), after being in culture for 24 or 72 h on the carriers. DED was placed papillary side up in a separate 6-well plate. Medium was removed from a well containing a carrier, and the carrier was plucked from the well by its corners using forceps. The carrier was then placed cell-side down onto the dermis (Figure 2.4.). To achieve this, one edge of the carrier was carefully aligned along one edge of DED, from this point of contact the rest of the carrier was brought down to meet the DED's surface by a rolling action (similar to the action of peeling but in reverse). Fresh medium, enough to submerge the carrier, was pipetted into the well. Stainless steel grids were placed on top of the carriers to provide a light weight to keep the carrier from sliding over the surface of the DED when medium was added. Carriers were left in contact with the DED for 24 h before the carriers were removed from the DED using forceps.

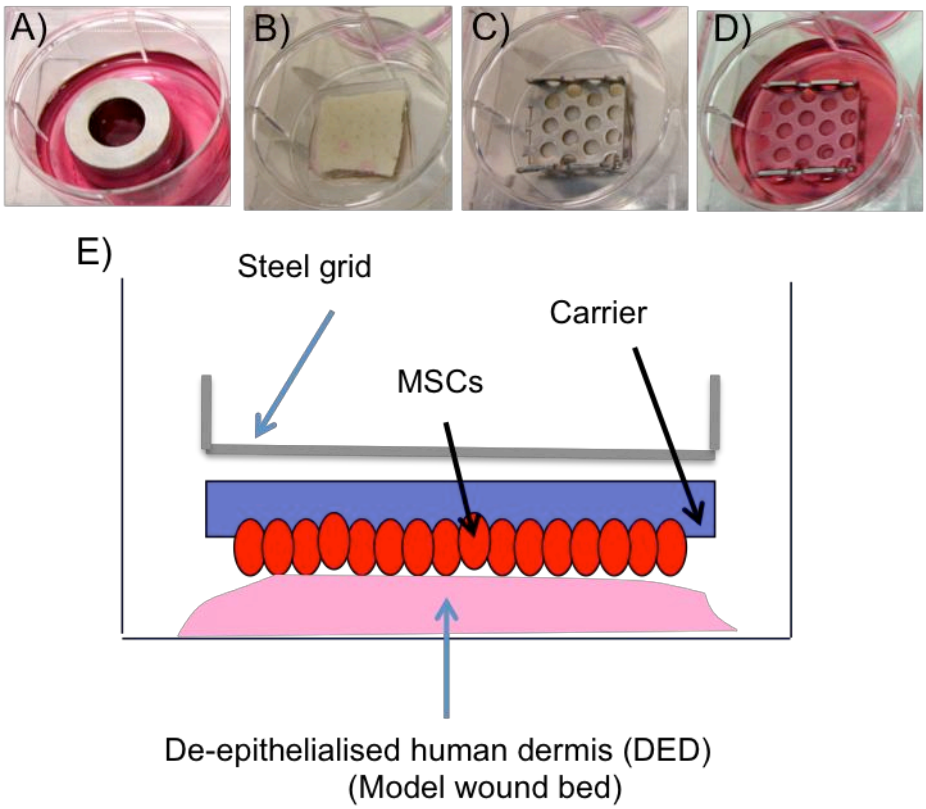

Figure 2.4. *Cell transfer regime. A-D sequence of events in the method. A) Carrier during culture. B) Carrier placed on top of DED. C) Steel grid placed on top of the carrier. D) Well filled with medium. E) Schematic representation of C.*

Assaying Metabolic Activity Via MTT

The metabolic activity of the cells was assayed by 3-[4,5-di- methylthiazol-2-yl]-2,5-diphenyltetrazolium bromide (MTT), and it was used as a crude indicator for cell viability (Mosmann 1983). MTT is a tetrazolium dye that when up taken by cells, becomes reduced by their mitochondria producing an insoluble formazan salt. The salt, which is dark blue/purple in colour, can be eluted from the cells using an inorganic solvent, and the optical absorbance/density of the solubilised salt can be measured to give a semi-quantitative measure of the metabolic activity of the cell population. The absorbance is directly related to the amount of formazan salt formed, which in turn is related to the metabolic activity of the cells.

After 24 h of contact with the DED, carriers were separated from the dermis using forceps, and the metabolic activity of the cells that had been transferred to the dermis was assayed by MTT at 24 h, 72 h, or 7 days following transfer. The dermis and the carriers were washed twice with PBS to remove remaining medium. MTT (0.5 mg/ml in PBS) was

added to each well and the samples were incubated at 37°C with 5 % CO_2 for 40 min. Formazan salt was eluted by adding 500 μl of 2-hydroxy ethanol (Sigma-Aldrich, UK), or acidified isopropanol (125 μl 10 M HCl in 100 ml isopropanol, final concentration 12.5 M). The elutant was mixed by pipetting, and 200 μl were transferred twice from each sample to a 96-well plate to provide readings in duplicate. The optical density (OD) of the solution was read at 540 nm and a reference wavelength of 630 nm was used on a spectrophotometer. In addition, the MTT assay was also performed on blank DED (DED without any transferred cells); the average OD from the blank, served as a baseline that was subtracted from the experimental values. In this way, any contribution to the reduction of formazan from the DED alone was accounted for.

Vascular Tubule Assay

Endothelial colony forming cells (ECFCs) were derived from umbilical cord blood (sourced from the John Radcliffe Hospital, Oxford, England, with ethical approval from the Oxford and Berkshire Ethics Committees, and with fully informed and written consent), and cultured in complete endothelial growth medium-2 (EGM-2) (Lonza Biologics, UK), before being phenotyped or labeled with eGFP previously described (Zhang *et al,* 2009; Khoo *et al,* 2011). Approximately 1 x 10^5 hBM-MSCs were seeded into the wells of six-well TCP plates (5000 cells/ cm^2), that either contained or did not contain ppAAc carriers. hBM-MSCs were cultured for 24 or 72 h before 4 x 10^4 they were reseeded into collagen-coated 48-well plates (BD Biosciences, UK). Cells were allowed to adhere for 2 h, before 2-8 x 10^3 (passage 4-5) eGFP-labeled ECFCs were added to the culture in EGM-2. Medium was changed every 2-3 days for 14 days and the cultures were periodically photographed. Image analysis was performed using the semi-automated AngioSys software program (TCS Cellworks, England), and the number of junctions and tubules, and total tubule lengths per field (8.4 mm^2) were calculated similarly to Khoo *et al* (2011).

Flow Cytometry

Adherent cells were detached from tissue-culture flasks by treatment with accutase (PAA Laboratories, Austria) for 5 min at 37°C, and washed twice with PBS with 1% BSA. Cells were incubated with FcR blocking reagent (Miltenyi Biotec, Germany), followed by relevant conjugated Mabs or isotype-matched negative-controls at 4°C for 30 min. The following test antibodies were used: CD44-FITC, CD90-FITC, CD106-FITC, CD14-PE-Cy7, CD45-PE-Cy7, CD73-PE, CD117-PE (Becton Dickinson (BD) Biosciences, USA), CD146-FITC (Millipore Ltd, UK), CD34-APC (Miltenyi Biotec, Germany), CD29-FITC (Immunotech, USA), and CD105-FITC (R&D Systems, USA). The corresponding isotype-matched antibodies used included: mIgG2a-FITC (Serotec, Germany), mIgG1-FITC, mIgG1-PE (R&D systems, USA), mIgG2a-APC (Miltenyi Biotec, Germany), mIgG2a-PECy7, mIgG1-PE-Cy7

(BD) Biosciences, USA). The final concentration was the same for the isotype control and test antibodies. Cells were resuspended in PBS with 1% BSA before running them through an LSR II flow cytometer (BD Biosciences, USA), A minimum of 20,000 events were collected, and analysis was performed using FACS DIVA software (BD Biosciences, USA).

Cytotoxicity of Sponges

Five different sponge materials (listed in materials) were placed in medium and placed in an incubator (37°C, 5 % CO_2) for 24 h. The presence of leachates from the material into the medium was observed by eye after the incubation period. Of the materials that did not produce leachates, 1 cm^2 blocks were cut form them using a scalpel and, they were sterilised with 70 % IMS for 24 h at RT. The foams were thoroughly washed with PBS to remove the IMS. The sponges were placed into a transwell insert (Gibco, UK), and each insert was placed into a single well of a TCP 12-well plate. Each well of the 12 well plate contained 3 x 10^5 (cell density= 7,893 cells/cm^2) human dermal fibroblasts (passage 4-7) which had been seeded 24 h prior to the introduction of the transwell inserts. Immediately before the transwells were inserted the medium was changed and the sponges remained in contact with the culture medium for 24 h before the transwells were removed and an MTT assay performed on the cultures. Fibroblasts cultured in the absence of indirect contact with sponges served as positive controls.

Histology

Processing

Samples were washed twice with PBS and then directly placed into 3.7 % formaldehyde (Sigma-Aldrich, UK) (diluted stock 1:10 in PBS), for 24 h at 4°C. Post fixation, the samples were infiltrated with wax to offer support to the tissue during microtomy. Paraffin is hydrophobic and immiscible with the formalin fixative, therefore dehydration of the tissue to dispel it of water was required before paraffin infiltration could occur. To achieve this, the samples were run through a graded series of alcohols of increasing concentration in order to remove the fixative. Following this, the alcohol was replaced by a 'clearing' solution, such as xylene, that was miscible with the embedding medium (paraffin wax). The wax was then allowed to replace the clearing medium. The above sequence of tissue dehydration, clearing, and wax infiltration was automated by a bench-top tissue processor (Leica TP1020, Leica microsystems, UK). Samples were placed into the processor overnight, and the processor followed the regimen in Table 2.3.

Solution	Exposure Time (hours)
10 % Formalin	1 h
70 % Ethanol (1)	1 h
70 % Ethanol (2)	1 h

80 % Ethanol	1h 30 min
90 % Ethanol	1h 30 min
95 % Ethanol (1)	1h 30 min
100 % Ethanol (2)	1h 30 min
Xylene (1)	1h 30 min
Xylene (2)	1h 30 min
Paraffin Wax (1)	2 h
Paraffin Wax (2)	2h

Table 2.3. *Histological Processing Schedule.*

Once the processing cycle had finished, the samples were promptly removed from the molten paraffin; too long a time in the paraffin can make the specimen hard and brittle, which becomes evident during tissue sectioning. Long exposure times to the high temperatures sufficient to melt the wax (50-60°C) can have deleterious effects on the staining of some antigens (Bancroft and Stevens, 1996).

Embedding

Samples were embedded in blocks of paraffin wax so that they could be mounted onto a microtome for sectioning. Embedding took place in a Leica EG1160 embedding center, dispenser and hot plate (Leica microsystems, UK). A small amount of molten paraffin was dispensed from the reservoir of the embedder into a metal mould, and the mould was placed on the hot plate to prevent the wax from setting. In turn, each sample of tissue was removed from its cassette and bisected (through the middle), using a scalpel. The partially wax-filled mould was then moved to a cold plate, and forceps were used to place the newly exposed edges of the tissue, revealed after bisection, into the center of the setting wax. The halves of the tissue were placed parallel to each other and perpendicular to the bottom surface of the mould, so that the samples could be cut in the required orientation. The wax-filled mould was left on the cold plate to complete setting, and as the wax cooled and solidified it held the tissue firmly in place. Once the wax set and hardened (about 30 min), the paraffin block was removed from the mound leaving a block of wax attached to a cassette base. Tissue blocks were stored at RT.

Sectioning

Tissues were sectioned using a Leica RM2235 microtome (Leica microsystems) fitted with a S35 type blade (Feather, Japan). Wax blocks were initially 'trimmed', making serial cuttings 10 μm thick, until both halves of the tissue were fully exposed on the surface of the wax block. Slices 5-6 μm thick were then cut, producing a string or a ‘ribbon’ of serial slices joined together. Ribbons of tissue were transferred to a water bath (40°C), which allowed the wax sections to warm slightly. Glass slides were placed under the tissue sections and

they were lifted out of the water and onto the surface of the glass slide. Residual water was dried from the slides on a hot plate (37°C) overnight (Leica). 2-3 cuttings were mounted onto each standard glass slide, if H&E was to be performed, or to SuperFrost® Plus slides (VWR, International, UK), if immunohistochemistry was to be performed.

Haematoxylin and Eosin Staining

Wax was removed from the slides using xylene, and then the tissue was gradually rehydrated by placing the slides through a graded series of alcohols, from high to low concentration: absolute ethanol (5 min); 95 % ethanol (5 min); 70 % ethanol (5 min), and then into distilled tap water for 5 min. Regressive H&E staining was then performed. Slides were transferred to Harris haematoxylin solution for 4 min to deliberately over-stain the samples, after which they were removed and placed under running tap water for 5 min to perform 'blueing'; a process that removes excess stain from the tissue so that a blue color was differentiated. Slides were stained with eosin-Y solution of 5 min and subsequently washed briefly in water, cleared and mounted. Slides were quickly dehydrated by dipping them through a series of graded alcohols low to high concentration: 70 % alcohol (30 sec); 95 % ethanol (30 sec); 100 % ethanol (1 min) and then into xylene for clearing for 1 min. It was important that dehydration was performed quickly because eosin is dissolved in 95 % ethanol; if it is left too long in ethanol the stain will be eluted from the slide leading to decolouration. 7-10 rinses in 95 % ethanol was sufficient to remove excess stain but minimise losses. The samples were then mounted in xylene-based DPX medium and dried at RT, before they were observed under a light microscope and photographed.

Immunohistochemistry (IHC)

Wax Removal and Rehydration

5-6 μm thick sections were made from paraffin wax embedded samples, using a microtome, and mounted on to SuperFrost® slides. Wax was removed from the tissue by placing the slides in xylene for 5 min at RT. The tissues were rehydrated using a graded series of alcohols from high to low concentration: 100 % ethanol (5 min); 95 % ethanol (5 min); 70 % ethanol (5 min); dH_2O (15 min).

Quenching Endogenous Peroxidase Activity

Where antigen detection was performed using an avidin-biotin system that contained the enzyme Horseradish peroxidase (HRP) to develop a coloured precipitate, blocking of endogenous peroxidase activity in the tissue was required. Samples were incubated with 0.3 % H_2O_2 (15 min), followed by washing in PBS (5 min).

Antigen Retrieval

Heat-mediated antigen retrieval was performed by placing the slides into a glass beaker filled with either TRIS/EDTA (pH 9) or sodium citrate buffer (pH 6), and heating the buffer close to its boiling point on a hot plate for 20 min. After which, the slides were cooled to RT in water. Enzymatic antigen retrieval (Typsin) was performed for 20 min at RT when detecting antigens in the presence of eGFP, since heat-mediated methods strongly diminished eGFP's fluorescence.

Blocking

'Normal serum' from the species in which the secondary antibody was raised was used in the blocking buffer. Blocking was performed using 10 % normal serum in PBS containing 0.1 % Tween-20. Enough volume of blocking buffer was dropped to cover the surface tissue from a pipette, and it was incubated with the samples for 2 h. The area containing tissue on each slide was ringed with a hydrophobic barrier pen (Dako pen) to confine the blocking buffer to the tissue; this greatly reduced the quantity of reagents that were in contact with the slides.

Endogenous biotin was also blocked to prevent the Avidin in the ABC reagent from binding non-specifically. Blocking was performed using an Avidin/ Biotin blocking kit (Vector Labs) after blocking with normal serum; biotin blocker was dispensed from the drop-bottle onto the tissue and incubated for 15 min at RT. Following this it was washed off in PBS for 5 min and Avidin blocking solution was added to the samples and incubated at RT for 15 min.

Addition of Primary Antibodies

Primary antibodies (1° Abs) were added to the tissue, in 1 % Goat serum with 0.1 % Tween-20 at the following dilutions: Collagen IV (1:500); RFP (1:1000); Pancytokeratin (1:50). The optimum dilution was determined by performing an antibody titer. 1° Abs were incubated with the tissue overnight at 4°C in a humidified chamber.

Addition of Secondary Antibodies

After incubation with the 1° Abs the slides were washed with PBST (x 3) for 10 min to remove residual antibodies. Biotinylated 2° Abs (Vector Labs, USA) were added to the tissue at a dilution of 1:500 in PBS containing 0.1 % Tween-20 and 1 % Goats serum, and incubated for 45 min at RT. The tissue was washed extensively in PBST (three 15 min washes) to remove unbound 2° Abs.

Detection

Slides were incubated with Vectastain® Elite ABC reagent for 30 min and washed for 5 min in PBS. The chromogen 3,3'-diaminobenzidine (DAB) was added to the samples (one at a time), and colour development was monitored under a light microscope. DAB produced dark brown staining at the site of the HRP, and sufficient staining intensity was produced between 3-5 min. The reaction was terminated by placing the slides in dH_20 to elute the DAB from the tissue.

Counterstaining and Mounting

Slides were counter-stained with haematoxylin by placing them in contact with the solution until the desired staining intensity was produced, about 30 seconds provided a good balance between obtaining nuclear detail without masking the chromogen. The slides were then dehydrated, cleared and mounted by placing them through a graded series of alcohols (low to high concentration), and then into xylene for 1 min each. DPX mounting medium was used to seal the coverslips to the slides. The slides were left at RT for the mounting medium to harden, and the samples were viewed the following day.

Immunofluorescence

For immunoflourence protocols, the IHC procedure was performed up to the addition to the 2° Abs. The 2° Abs applied in step 6 were fluorophore-conjugated (FITC, Texas Red). They were applied at a dilution of 1:100 in 1 % goat serum, 0.1 % Tween-20 in PBS, and incubated for 45 min at RT. The sides were then washed in PBS for 15 min (x3) and counter stained by incubating the samples with DAPI for 30 min at RT. The slides were washed in PBS for 5 min before mounting coverslips on the slides using aqueous mounting medium.

ELISA (Enzyme-linked immunosorbent assay)

All capture antibodies were diluted with PBS to the concentration specified by the manufacturer. 100 µl of the capture Abs were added to each well of the ELISA plates (NUNC, Maxisrop), and incubated over night at RT; the plates were sealed with parafilm. 300 µl blocking buffer (1 % BSA in PBS) was added to each well and incubated at RT for 2 h. Cytokine standard solutions were prepared according to the manufactures instructions, and serially diluted eight-fold in PBS (+ 0.05 % Tween-20, 0.1 % BSA). 100 µl of the standards and samples were added to the ELISA plates in duplicate and the plates were incubated at RT for 2 h. 100 µl of biotinylated anti-cytokine primary antibodies were then incubated for 2 h at RT with the samples and standards. Avidin-HRP conjugate was

prepared according to the manufacturer's instructions and 100 µl was added to each well in the plates and incubated at RT for 30 min. 100 µl of ABTS substrate was added to the IL-8 and bFGF ELISA, and the colourimetric signal was detected on a plate reader at 405 nm with the wavelength correction set to 650 nm. The readings were used to construct a standard curve from which the concentrations of the samples could be calculated. For the HGF plates, 100 µl of TMB substrate solution was used instead of ABTS, and incubated for 25 min at RT before 50 µl stop solution was added to each well. The plates were then read at 450 nm and referenced at 560 nm. Before new reagent/solution was added to each ELISA plate, the plate was aspirated and washed with wash buffer (0.05 % Tween-20 in PBS).

Wound Healing Study

Full-thickness incisional wounds were made (10 mm in length) in TE skin, which had been raised to ALI for 5 days, using a 15A blade scalpel. Wounded TE skin samples were divided equally into two groups. Both groups of samples had 100 µl of fibrin glue inserted into their wound cavities. The concentrations of fibrinogen and thrombin were 6 mg/ml and 25 IU respectively. One group however also contained 1x 10^5 RFP-labeled MSCs within the fibrin glue.

MSCs were pelleted via centrifugation (5 min, 1500 rpm), after being removed from culture, and the supernatant was discarded. Following this, PBS was added to the MSC pellet and they were resuspended by gentle pipetting and centrifuged for a second time; this was performed to remove residual culture medium, since it caused premature clotting when cells were added to the fibrinogen. MSCs (passage 5-8) were kindly donated by Prof. Suzanne Watt's Group.

At days 1, 3, 7, 10 and 14 after wounds were created, medium was collected from the samples and frozen (-20°C) before an ELISAs for HGF, IL-6 and bFGF were performed (see ELISA methods for details). At each of the above time points, samples were imaged via OCT. At days 1 and 7 one sample form each experimental condition was removed and histology and IHC was performed. RFP-labeled MSCs and pan-cytokeratin were detected in IHC using I° Ab concentrations of 1:1000 (rabbit polyclonal) and 1:50 (mouse monoclonal) respectively. All IHC sections were counterstained with DAPI (see IHC section for details). At day 14, the final time point, histology and IHC were performed on all remaining samples. Figure 2.5 outlines the experimental plan for the above.

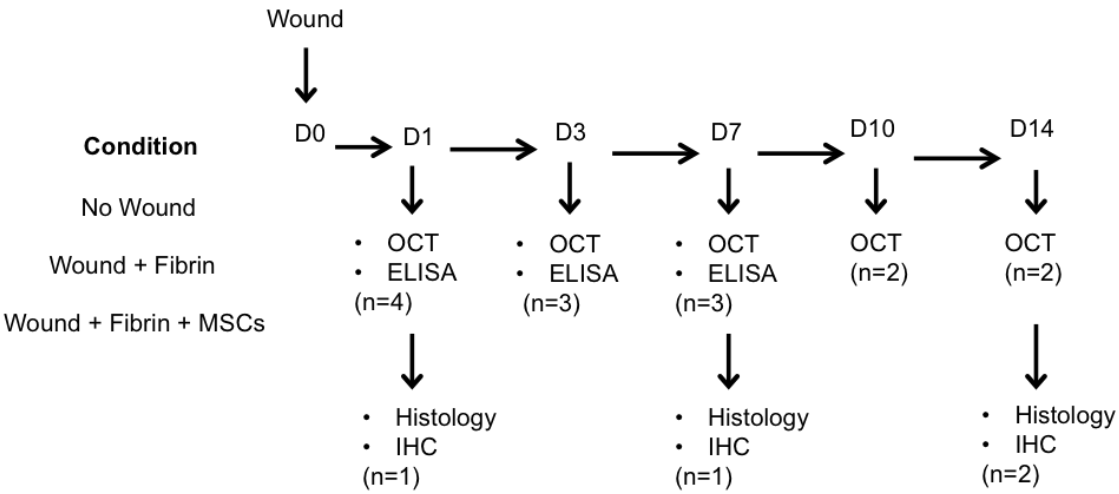

Figure 2.5. *Experimental overview. (IHC= Immunohistochemistry; ELISA= Enzyme-linked immunosorbent assay; D= day; n= number of samples/experimental condition)*

Fluorescence Imaging

Wide-Field Fluorescence Microscopy

Fluorescence microscopy using an ImageExpress® imaging system (Molecular Devices, USA). DAPI was excited using a wavelength of 340 nm, and a 400 nm filter was used to detect its emission. TRIC/Texas Red was excited at 543 nm, and 560 nm long pass filter was used in fluorescence detection. GFP/FITC was visualised by exciting at 405 nm and filtering at 488 nm. All images were obtained from samples using the same exposure settings.

Confocal Microscopy

All images were collected using a Zeiss LSM 510 META Upright Laser Scanning Confocal Microscope using either a x 10 or x 40 objective lens (Carl Zeiss, England). eGFP-labeled cells were excited with a 488 nm argon laser. Fluorescent light was collected through a 505 nm long-pass emission filter. Z-series compositions were acquired by photographing sections at 2 µm intervals. All cells were imaged at RT in pre-warmed (37°C) phenol red free alpha minimum essential medium. Images were analysed using the corresponding LSM 510 META Software (Carl Zeiss, England).

OCT Imaging of Tissue Engineered Skin

Imaging of TE skin was performed using a swept-source optical coherence tomography system (SS-OCT) (Figure 2.6). The system was comprised from a commercially available OCT apparatus (Michelson Diagnostics Ltd, EX1301), which contained a swept-source laser, and an in-house fibre optic Michelson interferometer. The laser operated at a sweep rate of 10 KHz, and had a central wavelength of 1315 nm, a bandwidth of 128 nm, a wavelength range of 157 nm, and an output of 10 mW. The spectral characteristics of the source provided an axial resolution of 10 μm in air, and the optics of the system provided a lateral resolution of 25 μm, according to the focused spot size from the Thorlabs LSM03 OCT telecentric scanning lens in the sample arm. The SS-OCT system employed balanced photodetection to improve signal to noise ratio (SNR).

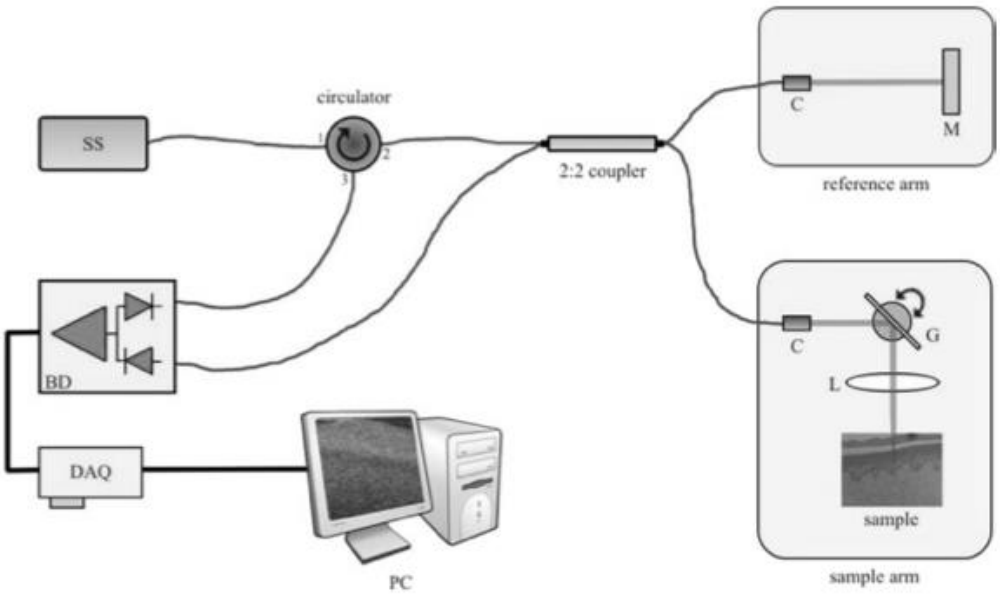

Figure 2.6. *SS-OCT set-up. SS, swept-source; C, collimator; BD, balanced photodetection and signal conditioning; DAQ, data acquisition card; L, focusing lens; G, galvanometer; M, mirror. Figure reproduced from Smith et al, 2010.*

Statistical Analysis

Statistical differences were determined using a two-tailed, unpaired Student's t-test where two different experimental groups were compared. Paired t-tests where performed to determine differences between the same experimental group. One-way analysis of variance (ANOVA), in conjunction with Tukey's test post-hoc, was performed where three data sets were compared. Test p-values < 0.05 were regarded as statistically significant. Origin 8 software was used to conduct all statistical analysis.

Chapter Three:

Delivery of MSCs to Model Wound Beds

3.1. Aim

The aim of this work was to evaluate the use of cell-carriers derived entirely from synthetic materials, by preparing surfaces of medical-grade silicone elastomers with acrylic acid via plasma polymerisation, to deliver human bone marrow-derived mesenchymal stem cells to model human skin wound beds. Parts of this chapter have been published in Tissue Engineering. Part C: Methods, 18 (2): 143-155, (2012).

3.2. Introduction

Wounds arising as a result of age or diabetes-related vascular problems, pressure sores or chronic limb ischemia can lead to chronic non-healing wounds. Current methods for treating these wounds are often met with limited success, and as such they cause significant morbidity and disability (Calles-Escandon and Cipolla 2001). Therefore there is a need for more active therapies for the treatment of complicated wounds. Cell therapy may offer a feasible and beneficial alternative. In recent years, mesenchymal stem cells (MSCs) have been shown to positively affect wound healing outcomes in both the pre-clinical and clinical setting (Reviewed in Chapter 1). MSC can accelerate re-epithelialisation and epithelial differentiation, increase angiogenesis and collagen production, reduce scaring, and modulate the inflammatory response to injury.

Currently, the main procedure for administering MSCs to wounds in patients is via subcutaneous injection around the wound margins, or intramuscular injection; and these are favored because they are minimally invasive (Jiang *et al,* 2012). However, poor cell viabilities are often attained post injection (Zhang *et al,* 2001; Aguado *et al,* 2011), and this may limit their therapeutic potential, especially considering that chronic wounds present difficult microenvironments to cells, because they are sites that display high levels of enzymatic activity and inflammation (Lobmann *et al,* 2005; Brem and Tomic-Canic 2007). Therefore, increasing the percentage of live cells delivered to wounds may be key to the success of MSC therapies.

Alternatively, MSCs may be delivered to wounds in the clinic using natural materials such as, animal-derived collagen in the form of matrices (Vojtassak *et al,* 2006; Ravari *et al,* 2011) or as a component of artificial dermis (Yoshikawa *et al,* 2008). However, it is desirable to avoid the use of xenogeneic materials due to concerns surrounding the transmission of bovine spongiform encephalitis (BSE), and the risk that an immune

response could be mounted (Keenan *et al,* 2006) Additionally, fibrin glues can be used to entrap MSCs at the wound site (Falanga *et al,* 2007), however these delivery methods are disadvantaged by their complex preparation requirements and short working times and the potential to negatively affect cell proliferation (Ho *et al,* 2006). Therefore developing a cell delivery method derived from synthetic materials, which is a lower risk to patients and is convenient for the clinician to use, would be advantageous.

Silicone elastomers are synthetic materials that have many rarely-combined physical properties which include: thermal stability, flexibility, transparency, low chemical reactively and toxicity, excellent gas permeability (over 400 times that of a typical rubber at RT) and good electrical insulation (Owen 1990). Chiefly however, the material is considered 'biocompatible'. Williams, as part of the European Society for Biomaterials in 1986, defined biocompatibility as ‘‘the ability of a material to perform with an appropriate host response in a specific application’’ (Ratner 2004). Therefore, silicone elastomers are well tolerated by tissues, and they do not provoke an inflammatory reaction upon contact with the body or its fluids. Because of these traits, silicone elastomers are biomaterials that have become widely used in the medical industry since their introduction in the 1960s. They can be found in devices such as: artificial limbs, breast implants, catheters (both urinary tract and intravenous), contact lenses, external feeding tubes, hearing aids heart valves, oxygenators and voice prostheses (Yoda 1998).

Therefore silicone elastomers possess many desirable characteristics that would make them a preferred material in the development of a cell-delivery vehicle. However, silicone elastomers are very hydrophobic, with surfaces energies equal to or below 23 nN/m (Jones, 1988), as such, cell attachment via protein adsorption to its surface, is more often than not, reported to be poor (Harris *et al,* 1980). To devise a cell-carrier therefore, it is important that the material possesses not only the desired bulk properties, but also favorable surface chemical properties that promote cell attachment. There are many methods that have been used to improve cell anchorage to silicone by altering its surface chemistry including non-covalent methods (physioabsorption of fibronectin) (Grey et al, 2003), however the adsorption of matrix proteins to silicone elastomers has since been shown to be inefficient and often not reproducible (Cunningham *et al,* 2002). Additionally, surface oxidation via plasma treatment (Prichard *et al,* 2007), gelatine glutaraldehyde cross-linking (Ai *et al,* 2002); layer-by-layer polyelectrolyte coatings (Ai *et al,* 2003); and plasma treatment of materials to create hydrophilic groups or radicals at the surface to which pre-formed polymers can subsequently be grafted (Hsiue *et al,* 1994), have also been explored, although these surfaces have been shown to degrade when stored in air to their original chemistry (Lee et al, 2004).

Plasma polymerisation is a well-established, one-step technique that can be used to provide a defined surface chemistry to almost any substrate with little or no pretreatment, and without detriment to the bulk properties of the material (Desmet *et al,* 2009). Plasma polymerised deposits of acrylic acid (ppAAc) have been shown to support the attachment and spreading of a variety of cell types including keratinocytes (France *et al,* 1998; Higham *et al,* 2003), melanocytes (Eves *et al,* 2005), and corneal epithelial cells (Deshpande *et al,* 2009), on surfaces previously unfavorable to cell-surface interactions. It has also been demonstrated that delivery of keratinocytes, in isolation or in co-culture with melanocytes, can be achieved from ppAAc-coated medical-grade silicone elastomers to model wound beds *in vitro* (Haddow *et al,* 2003; Bullock *et al,* 2006; Eves *et al,* 2008) These so-called 'carriers' have been used successfully in the clinic to deliver autologous keratinocytes to challenging wound environments in patients presenting with extensive skin loss resulting from diabetic foot ulcers, or flowing trauma from burn injuries (Moustafa *et al,* 2004; Zhu *et al,* 2005; Hernon *et al,* 2006; Moustafa *et al,* 2007). Recently, ppAAc surfaces have been shown to enhance cell attachment and spreading of MSCs (Colley *et al,* 2009; Filova *et al,* 2009). In this study, medical-grade silicone elastomers were surface-functionalised with acrylic acid, via plasma polymerisation, for the purpose of supporting cell attachment of MSCs to the substrate, and their potential as a cell-delivery vehicle for these cells, to model wound beds, was evaluated *in vitro*.

3.3 Results

Surface Characterisation

Cell carriers were derived from silicone elastomers that were coated with a thin layer of ppAAc that was deposited from a low-power (2 W) radio frequency sustained plasma. After the surfaces had been prepared and removed from the reactor, their static water contact angles (WCA) were recorded, and further characterisation by X-ray photoelectron spectroscopy (XPS) was performed to analyse their surface elemental and functional composition.

Hydrophobicity

To observe if the plasma deposition cycle had altered the hydrophobic character of the silicone elastomers, their WCAs were measured and compared with untreated silicone. Untreated surfaces created a water droplet with a 'balled' profile, whereas ppAAc coated surfaces allowed water to spread more freely over the surface. These observations were reflected by their respective WCA's; ppAAc surfaces exhibited a much reduced WCA compared to un-functionalised silicon (25° ± 3° vs. 99° +/- 2°) (Figure 3.1).

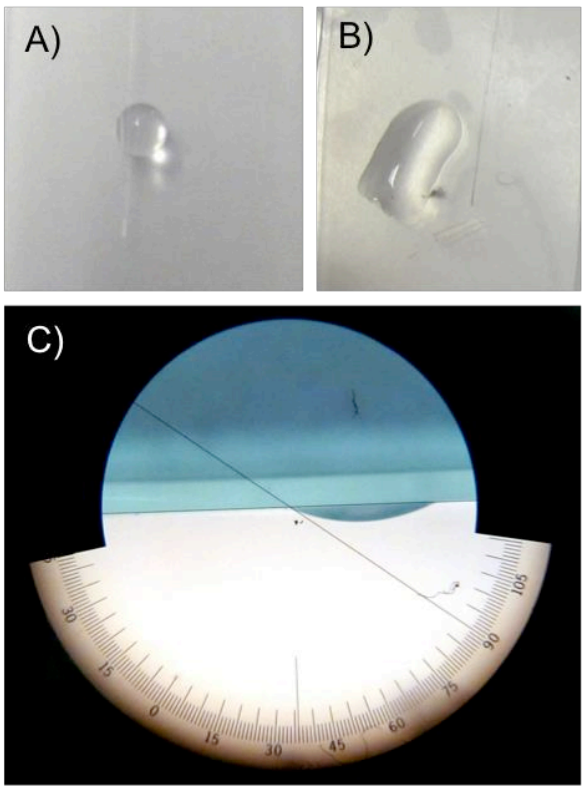

Figure 3.1. *Hydrophobicity of ppAAc silicone surfaces. A and B, Silicone without and with plasma treatment respectively. C, A typical contact angle measurement for the samples depicted in B.*

X-Ray Photoelectron Spectroscopy (XPS)

Wide scans revealed, in order of abundance, the presence of the following superficial elements: oxygen, silicone and carbon. The proportion of silicone that was detected indicated that the silicone substrate was covered with an acid layer with a thickness less than the depth of X-ray penetration (8 nm for Si 2p photoelectrons) (Figure 3.2). Narrow scans (high-resolution scans) of the C1s region revealed the high binding energy peak pertaining to C(=O)OX's, and its associated beta-shifted carbon C-C(= O)OX. Where 'X' could represent a diversity of functional groups such as carboxyl groups (where X=R) and/or ester (where X=R) and/or anhydrides (where X=H). Collectively, C(=O)OX's and C-C(= O)OX comprised 43.5 % of the C1s peak area (8.1 % and 35.4 % respectively).

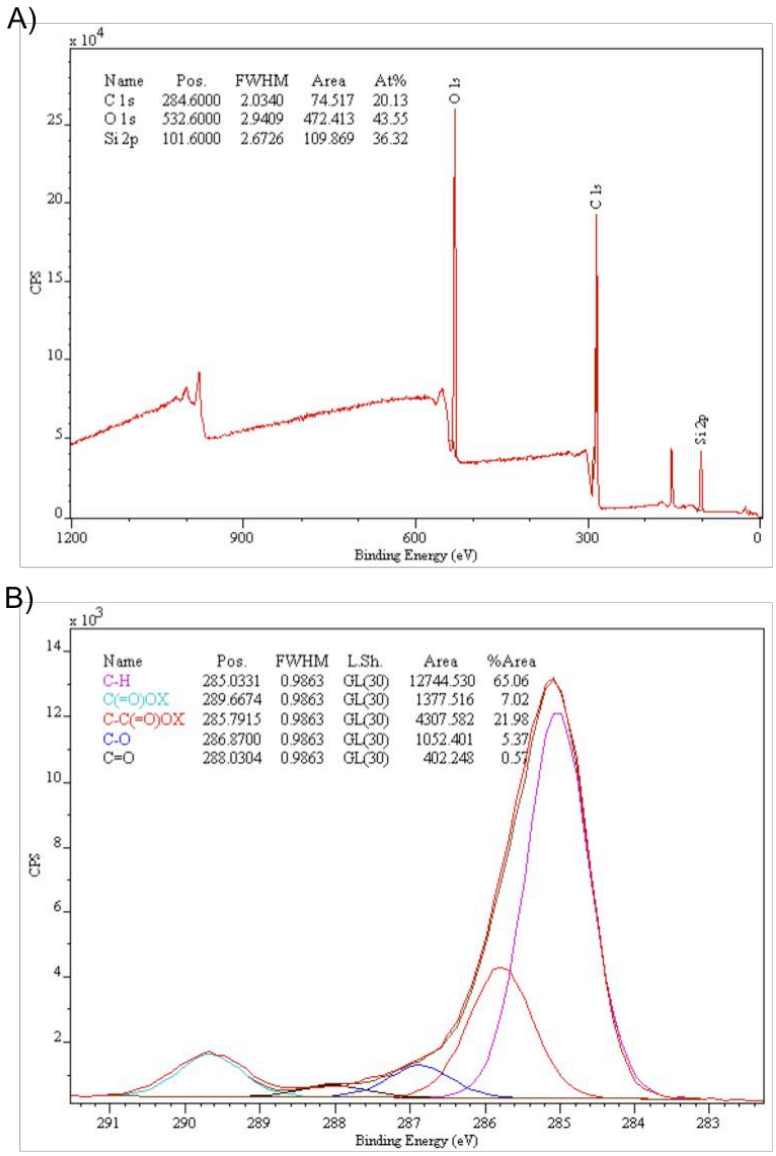

Figure 3.2. *XPS. A) wide scan of the ppAAc coated silicone. B) narrow scan of the C1s peak present in A)..*

MSC Phenotype

The cells used in this study were provided through collaboration with Prof Suzanne Watt's Group. The cells were purchased from Lonza Biologics UK and phenotyped using flow cytometry by the Watt Group to confirm that the cell population possessed an antigen profile characteristic of MSCs. Figure 3.3 shows the cells to be negative for CD14, CD34, and CD45, and positive for CD73, CD90 and CD105; this expression profile meets the minimum requirements as specified by the International Society of Cellular Therapy (Dominici *et al,* 2006) for classifying MSCs, because there is no single-cell marker that uniquely identifies them. The cells were also tested by Prof Suzanne Watt's lab, at passages 4-5 for their tri-lineage potential to generate adipogenic, chondrogenic, and osteogenic cell-types. In addition, they also had the capacity to support neovascularization in vitro (Martin-Rendon *et al,* 2008). Taken together, the cells most certainly had the properties of MSCs.

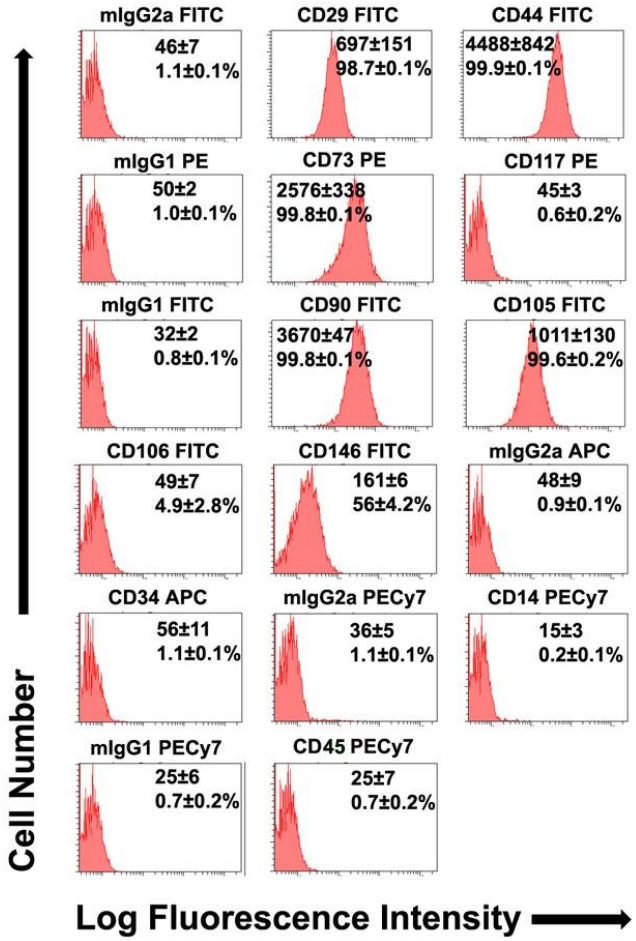

Figure 3.3. *Immunophenotype of cultured MSCs. Representative flow cytometry histograms are shown displaying the median fluorescence intensity for three independent batches of MSCs. (Data courtesy of Gigorious Tsaknakis).*

Coated Vs. Uncoated Carrier (Cell Behaviour)

Cell Attachment to ppAAc Surfaces

To assess cell attachment to the carriers, cells were seeded on to either ppAAc surfaces or untreated silicone for 24 h, before an MTT assay was performed to identify the presence of cells on their respective surfaces by their metabolism of the yellow MTT dye to a purple formazan salt. Cells attached well to the ppAAc surfaces, whereas few cells adhered to uncoated silicone (Figure 3.4A). Cells could be seen as a circular and densely stained purple patch on the center of the ppAAc surfaces thus, indicating where the cells had been seeded at high density within the confines of the stainless steel rings. In contrast, only a faint amount of formazan could be seen by eye on untreated surfaces because the majority of cells failed to adhere to these surfaces. These observations were reflected by the optical density (OD) values from the cells following formazan salt elution as measured by spectrophotometry (Figure 3.4B.. The uncoated carriers recorded significantly lower OD values than that which was obtained from the ppAAc surfaces (0.02 vs. 0.15 a.u. respectively, $p<0.001$).

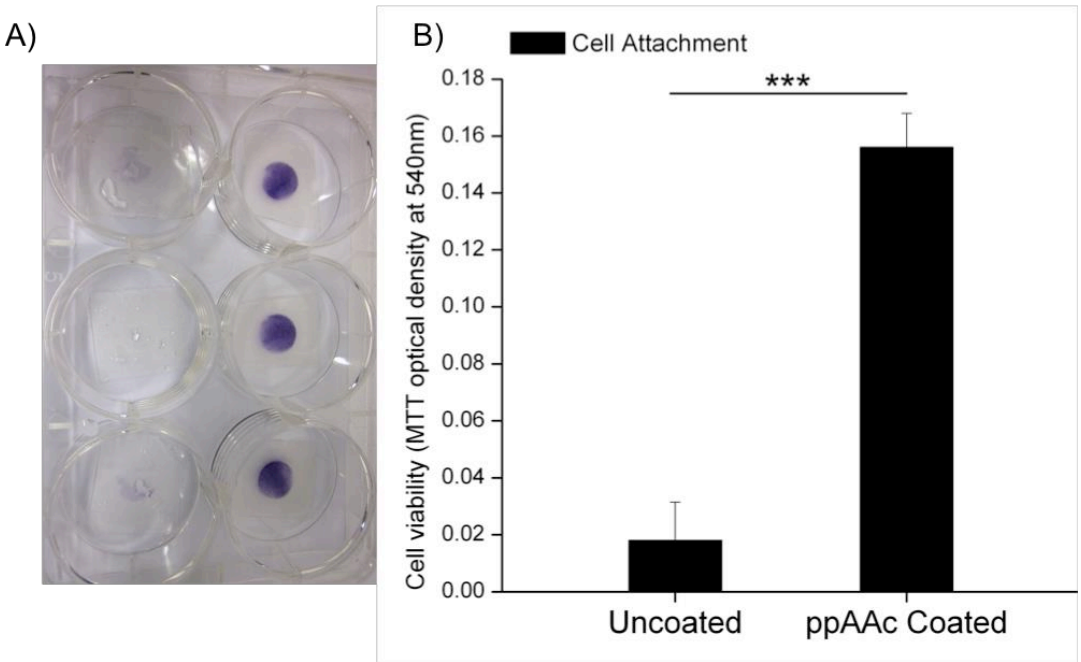

Figure 3.4. *Cell attachment to surfaces (ppAAc Coated Vs. Uncoated). A) Representative photograph displaying cells attached to uncoated (left wells) and ppAAc coated surfaces (right wells) after incubation with MTT, B) Mean optical density values of formazan salt eluted from cells on their respective surfaces following incubation with MTT (± SEM). (N=3, n-3). (***p < 0.001).*

Cell Viability on ppAAc Surfaces

72 h after seeding MSCs onto tissue culture plastic (TCP) or ppAAc carriers, their viability was assessed by TO-PRO®-3 staining followed by flow cytometry. TO-PRO®-3 is a fluorescent live/dead stain, that is only permeable to cells that are dead or dying because of their lack membrane integrity. The dye cannot permeate live cells. MSCs cultured on the carriers showed no difference in cell viability vs. those cultured on TCP. The majority of the cell counts from both surfaces (TCP and ppAAc) were in the lowest region of fluorescence intensity (< 10^3 a.u.), thus showing that there was mass exclusion of TO-PRO 3 uptake by the cell population, and therefore indicated that the cells had high viability on both surfaces. Indeed, the fluorescence intensity histograms had similar profiles, with 85.3 % (TCP) vs. 83.7 % (carrier) of the total cell counts from each surface lying to the left of an arbitrarily set gate (Figure 3.5), showing that the ppAAc surfaces did not significantly affect cell viability relative to TCP surfaces. If there were a large subset of dead cells within the population cultured on the ppAAc carriers, a secondary peak would be observed much higher in fluorescence intensity.

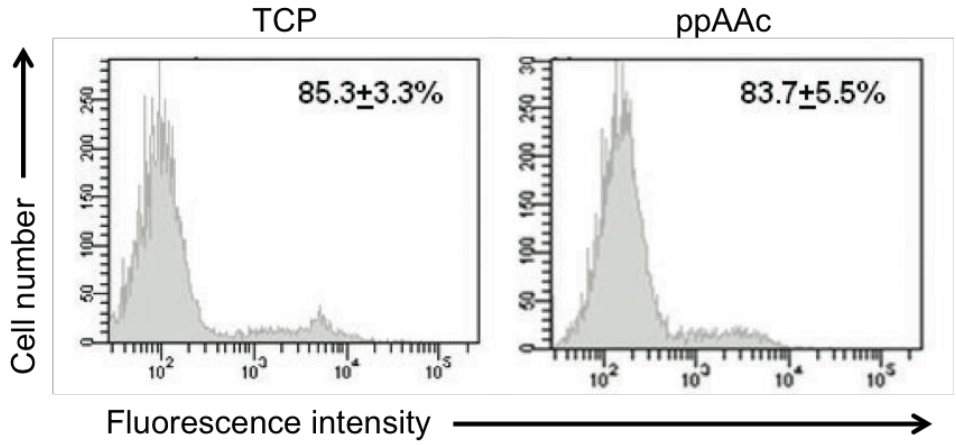

Figure 3.5. *Cell viability by TO-PRO®-3 staining. Viability of MSCs cultured on TCP or ppAAc carriers (left and right panel respectively) via TO-PRO-3 staining. Flow cytometry histograms are representative of three independent batches of MSCs. (Data courtesy of Anita R Mistry).*

Optimal Cell Seeding Density on Carrier

To determine the optimal cell seeding density, cells were seeded onto carriers at a range of cell densities (1 x 10^4 - 6 x 10^4 cells/ carrier) and cultured for 7 days with AlamarBlue assays carried out on the first and last day of the experiment. The increase in percentage AlamarBlue reduction between the two time points served as an indicator for cell proliferation on the carrier. The results showed that the MSCs attached to the ppAAc surfaces and proliferated over the course of 7 days regardless of their initial seeding density, in a similar fashion to those cultured on TCP (Figure 3.6). However, successive doublings in cell densities above 4 x 10^4 cells/ carrier did not significantly increase viabilities

at day 7 as compared with those obtained, at the same time point, from 4 x 10^4 cells/ carrier; this is likely due to the phenomena of contact inhibition (Abercrombie 1967; Abercrom.M 1970). Accordingly, for the subsequent cell transfer experiments, cells were seeded on to carriers at a density of 5 x 10^4 cells/ carrier.

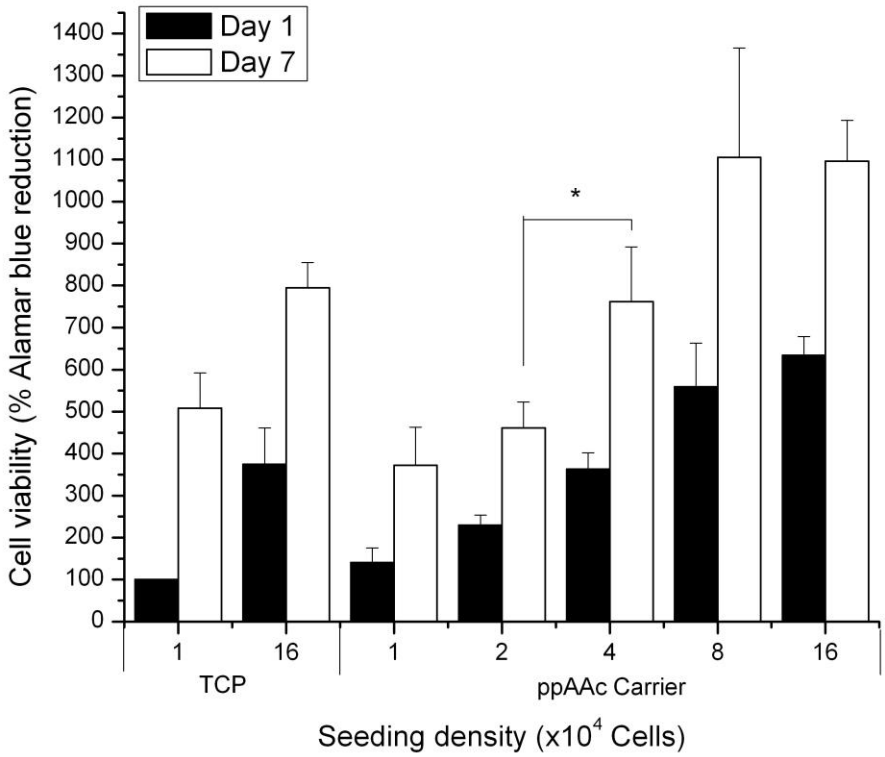

Figure 3.6. *Cell seeding density. Cell viability over 7 days on either TCP or carriers as determined by AlamarBlue. The percentage reduction of AlamarBlue is shown normalised to 1 x 10^4 cells on TCP. Error bars indicate the SEM for three independent experiments performed in triplicate. (* $p < 0.05$, ** $p < 0.01$, *** $p < 0.001$). (Data courtesy of Louise E Smith).*

MSC Phenotype After Contacting Carriers

To evaluate if MSC culture on ppAAc surfaces affected their phenotype, cells were cultured on TCP or ppAAc surfaces for 72 h before they were detached and phenotyped by flow cytometry. Analysis revealed no significant changes in the cell surface expression for key markers including: CD90, CD105, CD73, CD34, CD14, CD45, HLA-ABC and HLA-DR (Figure 3.7).

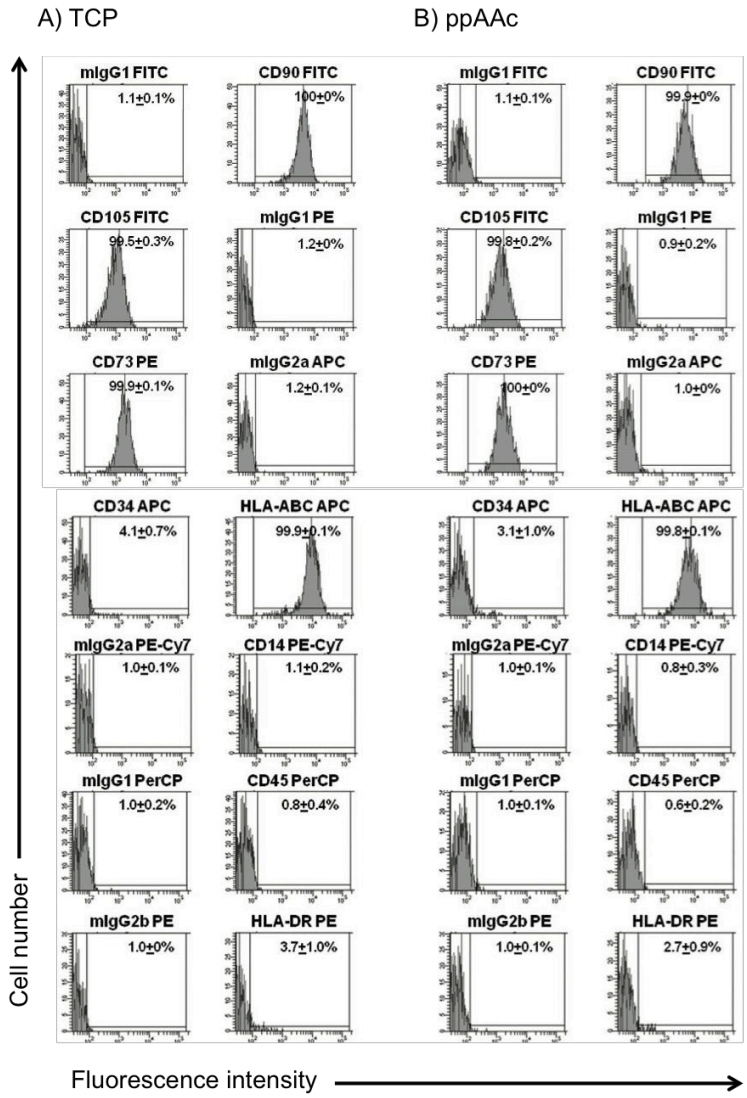

Figure 3.7. *Cell phenotype analysis following culture on ppAAc surfaces. Immunophenotyping for the antigens CD90-FITC, CD105-FITC, CD73-PE, CD34-APC, anti-HLA-ABC-APC, CD14- PE-Cy7, CD45-PerCP, and anti-HLA-DR-PE antibodies or appropriate isotype controls. Flow cytometry histograms are representative of three independent batches of MSCs. The mean % positive ± SEM above an arbitrary gate set for the isotype control is indicated for each histogram by two intersecting* lines, one in the horizontal and the other in the vertical plane. (Data courtesy of Anita R Mistry).

MSC Tubule Formation Capacity

MSCs were cultured on both the carriers and TCP for 24 and 72 h, and their ability to support vascular tubule formation from umbilical cord blood derived endothelial cell colony forming cells (ECFCs) *in vitro* was assessed and quantified. The results showed that contact with ppAAc surfaces for up 72 h did not affect the functional capacity of the MSCs to form tubules from ECFCs (Figure 3.8 and 3.9). Qualitatively, MSCs cultured for 24 or 72 h on either TCP or ppAAc surfaces prior to ECFC co-culture were capable of stimulating tubule formation from the ECFCs, as evidenced by the similar density of vascular-like

structures that were derived (Figure 3.8 B). By contrast, in the absence of MSCs, ECFCs did not form tubules in culture regardless of their seeding density; neither a cell seeding density of $4x10^3$ or $8x10^3$ cells/ 48-well plate (4210 cells/cm^2 or 8420 cells/cm^2 respectively) could derive tubules (Figure 9 A). Following imaging, image analysis was performed to quantify tubule formation from the ECFCs in co-culture with the MSCs. The results demonstrated that there were no significant differences in the numbers of junctions, tubules, or the total tubule lengths that were formed from ECFCs cultured with MSCs that were cultured on either surface (TCP or ppAAc carriers) for 24 h (p= 0.77, p= 0.90, p= 0.80, respectively) or 72 h (p= 0.37, p= 0.88, p= 0.69, respectively) prior to commensuration of the co-culture (Figure 9 B). There were also no significant differences between the numbers of junctions, tubules, or the total tubule length that could be formed after MSCs were cultured for 24 h versus 72 h on their respective surfaces; TCP (p= 0.96, p= 0.99, p= 0.55) or on the ppAAc carriers (p= 0.14, p= 0.72, p= 0.14).

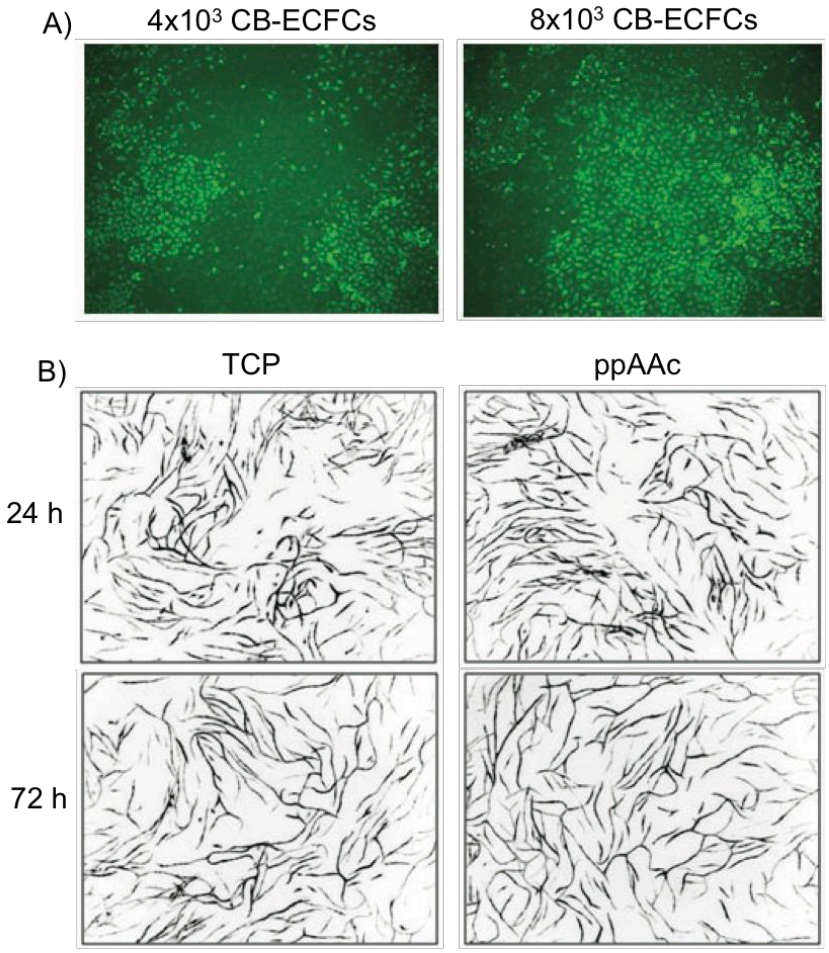

Figure 3.8. *Tubule formation. A) Umbilical cord derived ECFCs seeded at either 4 or 8 x 10^4 cells/well in a collagen coated 48-well plate and cultured in the absence of MSCs. B) Representative photographs of MSC in co-culture with ECFCs after 14 days (magnification x 4, field area 8.4 mm^2). MSCs were cultured on TCP or ppAAc surfaces for 24 or 72 h before co-culture began. Vascular tubule formation assays were carried out for three independent batches of MSCs. (Data courtesy of Anita R Mistry).*

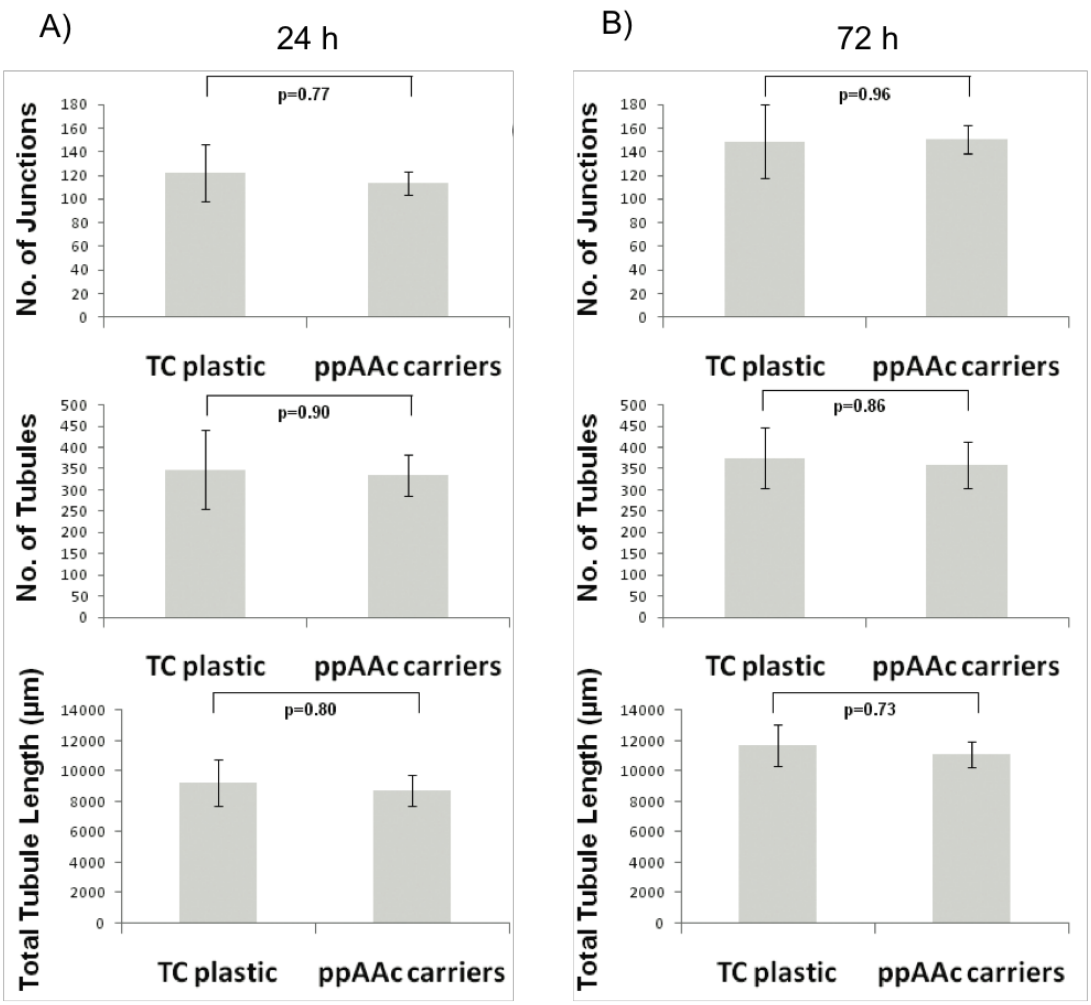

Figure 3.9. *Quantitation of tubule formation. The numbers of tubules and junctions formed, and total tubule lengths per field area (8.4 mm^2) at day 14 of MSC-ECFC co-culture are tabulated. MSCs were cultured on TCP or ppAAc surfaces for 24 h A) or 72 h B) before commencing co-culture. Vascular tubule formation assays were carried out on three independent batches of MSCs. Bar charts represent the mean ± SEM..(Data courtesy of Anita R Mistry).*

Assessment of Cell Transfer

Verification that DED was Decellularised

Before attempting to transfer cells to dermis from ppAAc carriers, it was important to ensure that the dermis was successfully decellularised by the NaCl protocol, so that it could be said that the presence of cells on the DED's surface were externally derived following cell transfer. Histological analysis verified that the dense layer of keratinocytes comprising the epidermis was completely removed and the dermal fibroblasts contained within the dermis were also removed (Figure 3.10 A and B). Collagen IV staining revealed that the decellularisation protocol did not remove the basement membrane (Figure 3.10 C).

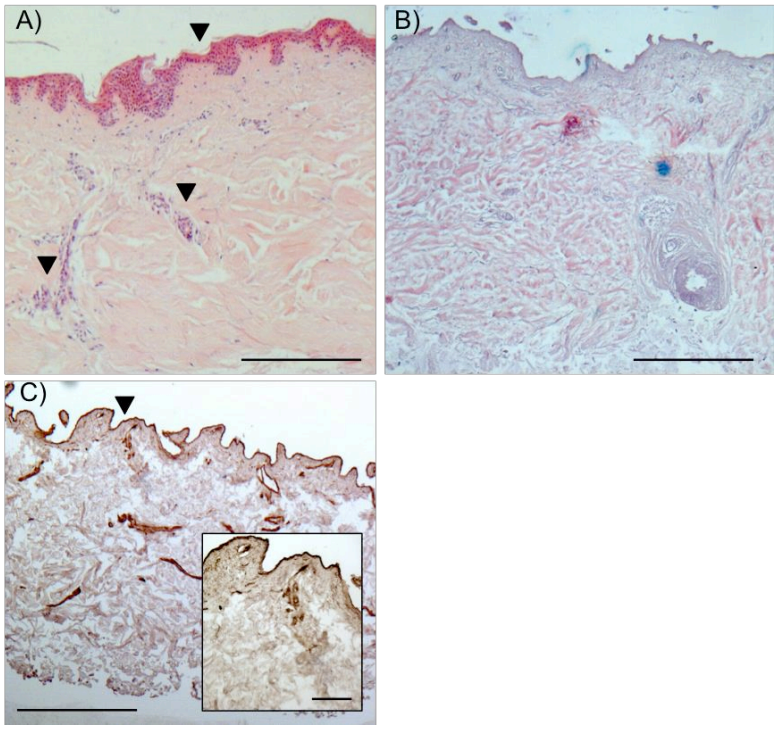

Figure 3.10. Decellularisation of dermis. A) and B) Cellular composition of skin before and after NaCl decellularisation, (arrows indicate cells). C) Basement membrane indicated via collagen IV detection. All photos were taken at x 10 magnification, and x 40 inset, with scale bars representing 200 and 100 µm respectively.

Uncoated Vs. ppAAc Coated Silicone

Cell delivery from the ppAAc surfaces to model wound beds, composed from DED, was assessed by culturing MSCs for 24 h on either unmodified silicone substrates or ppAAc surfaces, and placing them in contact cell-side down with the DED. After 24 h in contact with the DED the substrates were separated from the DED, and both the substrates and the DED were incubated with MTT to visualise and describe semi-quantitatively the extent of cell delivery to the DED from the substrates. ppAAc-functionalised surfaces were capable of delivering far more cells than un-functionalised silicone. Initially, a large number of cells were attached to the ppAAc carrier, and after contact with DED, few cells remained present on the carrier because the cells had transferred to the DEDs' surface (Figure 3.11 A and B). In contrast, far fewer cells could be transferred from the unmodified surfaces to DED, however far fewer cells attached to these surfaces in the first instance. These observations were confirmed by their respective MTT OD values (Figure 3.11 C). After contacting ppAAc surfaces, the OD vales obtained from the DED were significantly higher ($p < 0.001$) than those obtained from DED following contact with unmodified surfaces (OD values of 0.075 and 0.015 respectively). The OD values from the carriers or unmodified surfaces after transfer were very similar (0.005 and 0.007 respectively) and bordered on the threshold of detection by the spectrophotometer.

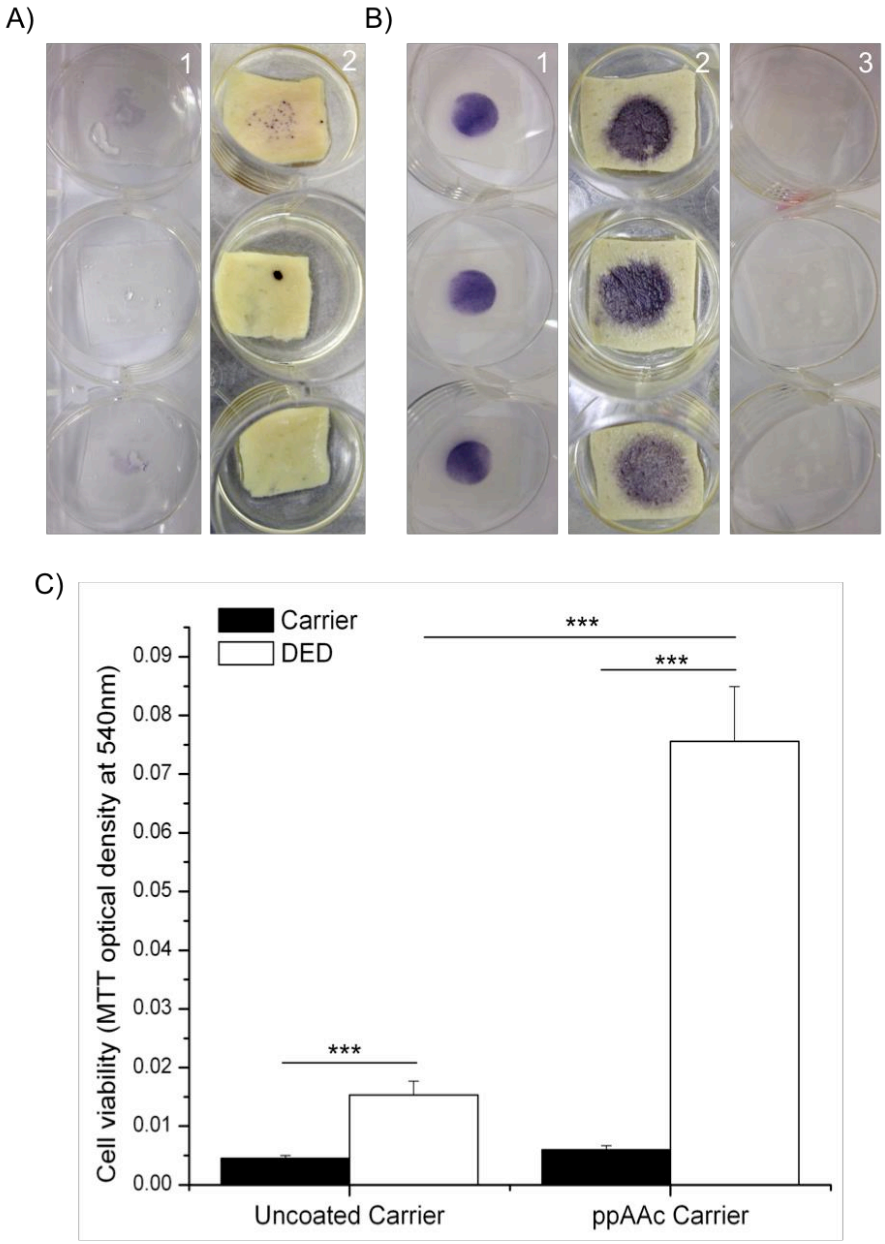

Figure 3.11. *Assessment of cell transfer (ppAAc-coated vs. uncoated carriers). A) Photographs of MTT-stained MSCs before and after transfer from uncoated silicone, A^1 and A^2 respectively. B) Photographs of MTT-stained MSCs before and after transfer from ppAAc carriers. B^1) MSCs on carrier prior to contact with DED, B^2) MSCs present on DED after contact with the carriers, B^3) MTT stained ppAAc carrier after transfer. C) Elution of the stain from the DED. Mean ± SEM, (N=3, n=3), (*** $p < 0.001$).*

Cell Viability Post Transfer

The viability of the cells following their transfer to DED was assessed over a period of 7 days. An MTT assay was performed on the DED 24 h, 72 h and 7 days after cell transfer.

Figure 12 shows that the cells remained viable post-transfer to the DED for at least 7 days, and by day 7 the metabolic activity of the cell population had significantly increased ($p < 0.05$), suggesting that the cells had begun to proliferate on the DED after transfer.

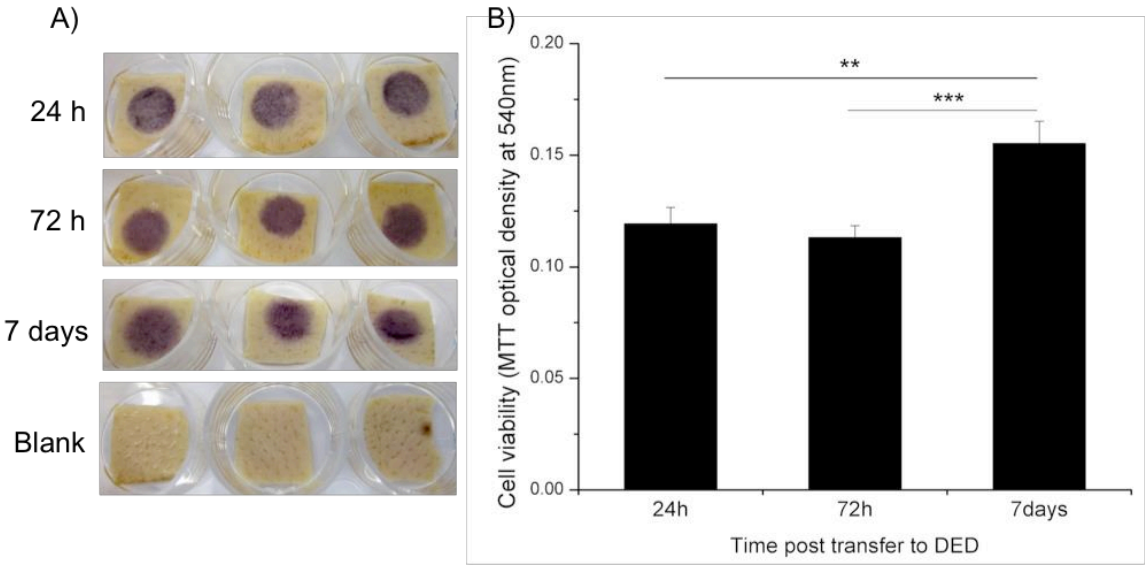

Figure 3.12. *Cell viability 7 days following transfer. A) Representative photographs of MTT-stained cells 24 h, 72 h, and 7 days after transfer. B) MTT O.D. values following stain elution. Mean ± SEM from three independent experiments performed in triplicate. (** $p < 0.01$, *** $p < 0.001$).*

Cell Transfer After 72 h on Carrier

MSCs were cultured on ppAAc carriers for 72 h before they were placed in contact with DED, and cell viability of cells on the DED was measured by MTT at the following time points: 24 h, 72 h and 7 days. Similarly to 24 h pre-culture prior to transfer, the cells remained viable post-transfer to DED (Figure 3.13). However, there was a slight difference in the degree of cell transfer to the DED after an extended period of culture on the carrier prior to transfer. After 24 h of pre-culture on the carrier, few cells remained after transfer (OD values from the carrier were just above the threshold of detection by the plate reader). In contrast, following 72 h of pre-culture more cells remained on the carrier after transfer to the DED; the OD values from the carriers were 0.006 vs. 0.012 for 24 h and 72 h pre-culture respectively ($p < 0.05$). The differences obtained were perhaps due to an increased amount of extracellular matrix produced from the MSCs during a longer residence on the carrier prior to transfer, which may have enhanced cell adhesion to the carriers making them more 'reluctant' to transfer. Despite this, approximately 80–90% of the cells transferred to the DED. While there is a significant difference ($p < 0.05$) between the MTT values obtained for cell viabilities on the DED between the experiments performed in Figure 3.12 and 3.13, at 72 h and 7 days, this may be due to a difference in the metabolic activity of cells from different donors (Sittichokechaiwut et al, 2012).

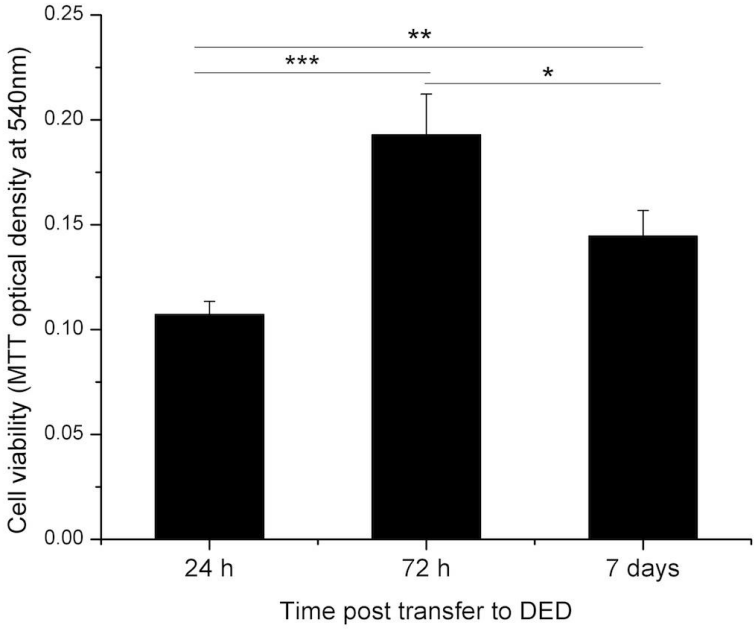

Figure 3.13. *Cell viability post transfer (72 h Pre-culture). Mean ± SEM (N=3, n=3), (* $p < 0.05$, ** $p < 0.01$, *** $p < 0.001$). All experiments were conducted on split thickness skin.*

Cell Transfer to Gelatin Coated Surfaces

To investigate if the presence of basement membrane collagen on the surface of DED (as earlier identified, Figure 3.10) was a factor facilitating cell transfer, the cell transfer regime was performed on gelatin-coated surfaces. Gelatin surfaces were prepared at concentrations of 5 %, 1 % and 0.1 % (w/v) in dH_2O and dispensed to cover the surface of wells in TCP 6-well plates. Cells were then seeded on the carriers as previously described, and after 24 h culture on the carriers they were placed cell-side down on to the gelatin surfaces for 24 h, before an MTT assay was performed on both the gelatin-coated surfaces and the carriers to determine the extent of cell transfer. Sirius red staining, which associates with collagen, was performed to determine if the gelatin had successfully coated the well plates. Staining clearly confirmed the presence of a thin layer of gelatin from the 5 % gelatin preparation, however staining was much weaker for the 1 % and 0.1 % gelatin concentrations (Figure 3.14 A). Following the removal of excess Sirius red, by washing with PBS, much gelatin was removed from the wells coated with the 1 % and 0.1 % gelatin concentrations. As a result much lower levels of Sirius red staining was visible after the samples had dried (Figure 3.14 B). Nonetheless gelatin was present on the surfaces of wells from each of the gelatin concentrations tested. MTT staining showed that cell transfer was possible from the carriers to the gelatin surfaces. Cells could be seen (by retention of the formazan salt from MTT) on the surfaces for each of the gelatin preparations, with the greatest extent of transfer achieved to the 0.1 % gelatin surfaces, although in all instances a considerable number of cells remained on the carriers (Figure 3.14). Cell transfer was most consistent to the 0.1 % gelatin surfaces, and as a result it was the only gelatin concentration

for which there was a statistically significant difference between the number of cells on the gelatin compared to the number on the carrier ($p < 0.01$).

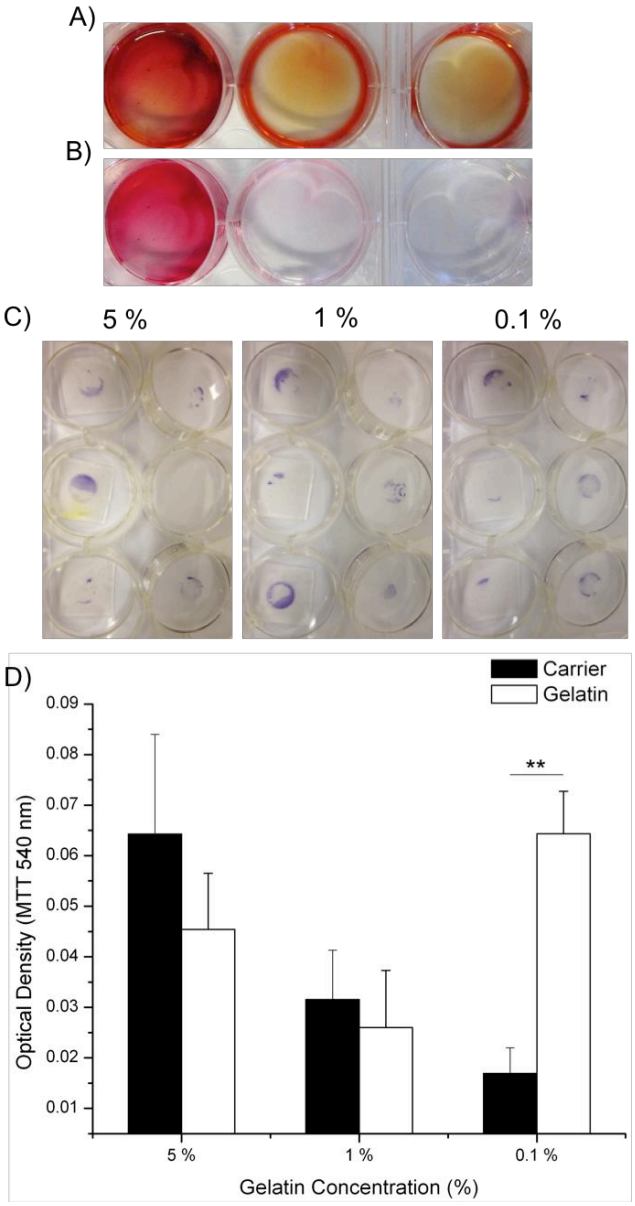

Figure 3.14. *Cell transfer to gelatin surfaces. A and B) Sirius red staining before and after washing of excess stain (5%, 1% and 0.1% from left to right). B) Representative photographs of MTT stained cells on the carriers (left) and the gelatin surfaces (right). C) Optical density of the stain eluted from the cells. Error bars represent the SEM of three independent experiments performed in triplicate. (**p < 0.01).*

MSCs Post-Delivery to DED

Enhanced green fluorescent protein (eGFP) labeled MSCS were used to visualise the cells post transfer to the DED by confocal microscopy, chosen for its ability to conduct optical slicing, to investigate if cells were able to migrate into the dermis. Firstly however, cell transfer experiments were conducted, using the regime described earlier, to determine

that the eGFP-labeled cells could behave similarly to the untransfected cells (i.e. transfer was possible and the cells remained viable). Figure 3.15 shows that the eGFP-labeled cells were able to successfully transfer to the DED from the carriers, and proliferate over the course of 7 days. Transfer of non-transfected cells to DED was efficient because very few cells remained on the carriers as indicated by the very low OD value (0.013) (data not shown) and the higher OD reading from the DED (0.072) ($p < 0.05$). At each successive time point, the cells on the DED showed significant increases in their metabolic activity, as indicated by the OD values.

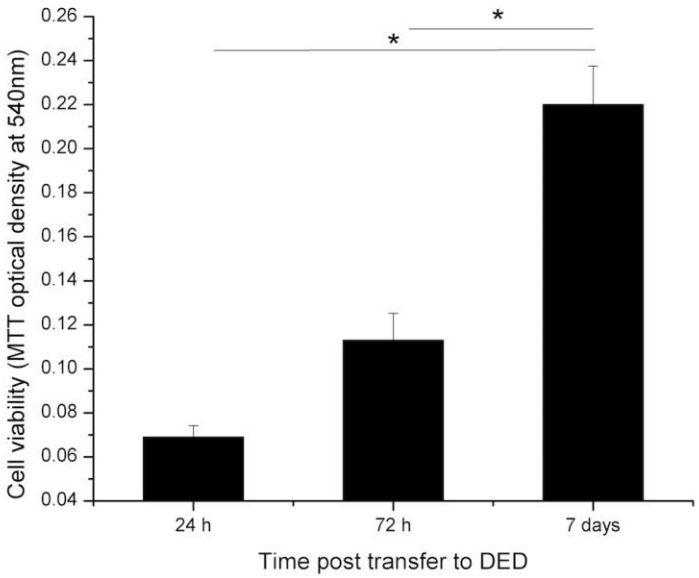

Figure 15. *eGFP-MSC viability post-transfer to DED via MTT. (*p < 0.05) Mean ± SEM for three independent experiments performed in triplicate.*

Confocal microscopy was conducted to image cells cultured on the ppAAc carriers for 7 days or 7 days following cell transfer to DED, and showed that cells could be clearly identified on their respective surfaces (Figure 3.16). Cells cultured on the ppAAc carriers had a flattened morphology, similar to that found in culture on TCP surfaces, whereas those that were transferred to the DED possessed a more spindle-like appearance. Z-stack images of the DED acquired 7 days after transfer showed cells to be present to a depth of up to 80 μm (Figure 3.17).

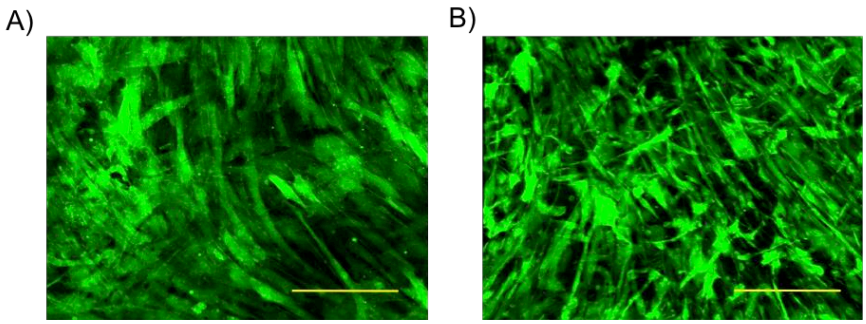

Figure 3.16. *MSC morphology on ppAAc surface and DED after extended culture. Representative confocal images of MSCs either cultured on the carrier for 7 days A), or on the DED 7 days after transfer to DED from the carrier B). (Scale bars= 200 μm).*

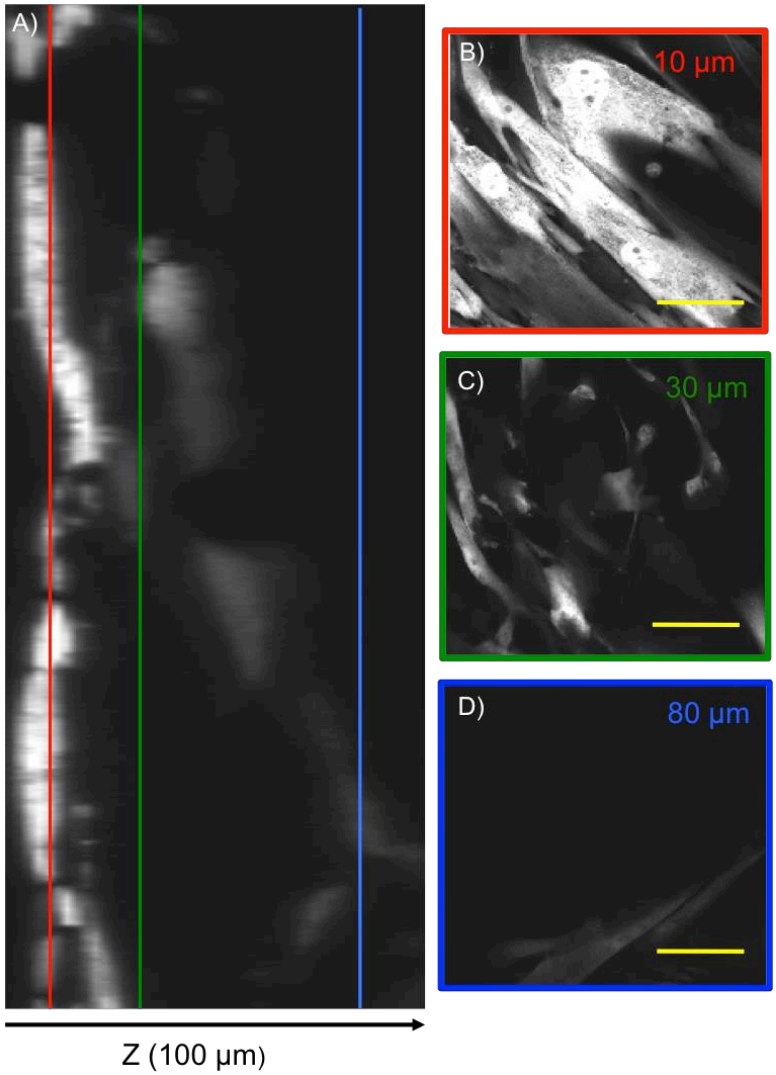

Figure 3.17. *Confocal microscopy of eGFP-MSCs. A) an y/z composition derived from serial sections (2 µm/ slice, 50 slices) through the DED 7 days after cell transfer from the carrier. TB)-D) are x/y images that correspond to the red, green, and blue transects in the z-plane in A). (Scale bar B- D)= 40 µm).*

Histology Post Cell Transfer to DED

Histology was performed on the DED as an additional means to determine if the cells were able to migrate into the dermis following transfer. Histology confirmed the presence of cells on the surface of the DED as a superficial layer (Figure 18). Previous testing of DED preparations showed the effective removal of intrinsic cells, therefore the cells on the DED's surface came from the carriers and were transferred MSCs and not cell remnants from insufficient cell removal during DED preparation.

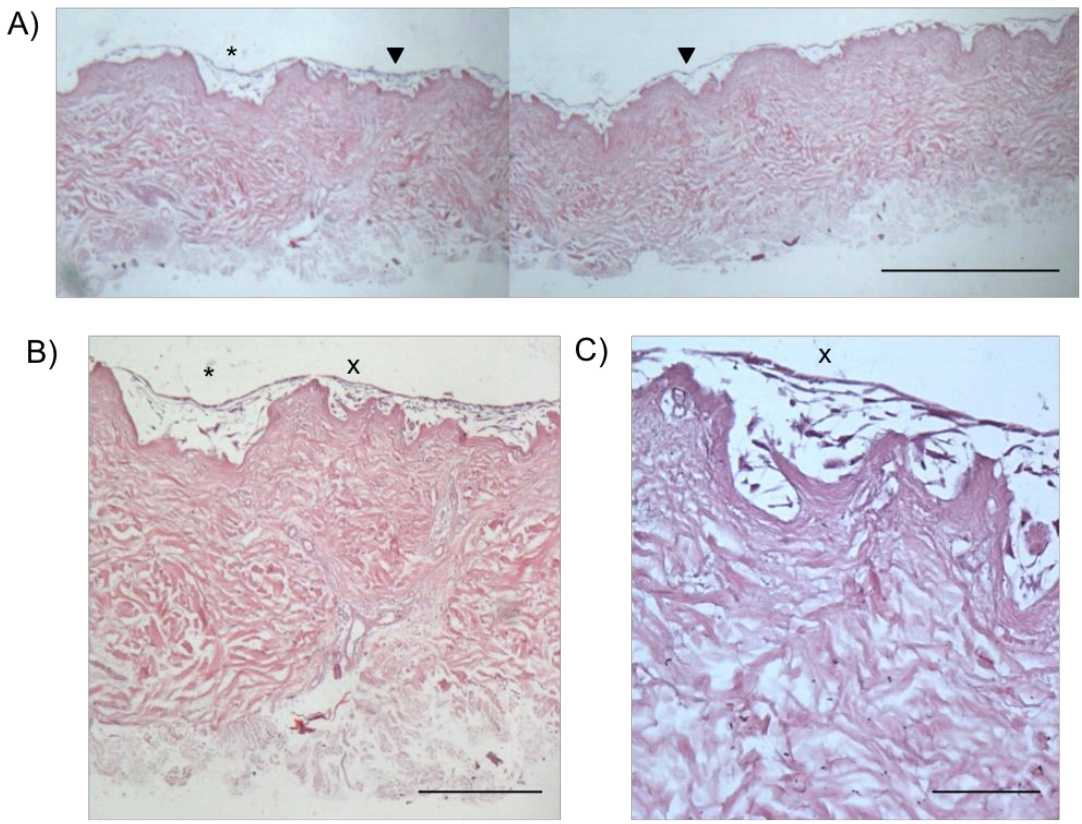

Figure 3.18. *Histology post cell transfer to DED from ppAAc carriers. A) Representative image of H & E stained DED 7 days after MSCs delivery from the ppAAc carrier. B) An enlarged image from the stared region in A). C) an enlarged image of the region marked 'x' in B). The arrowheads indicate the presence of MSCs, which can be identified as a superficial layer even at the lowest magnification (x 4).* Scale bars: 1 mm, 250 µm and 50 µm in A-C respectively.

Transfer Vs. Direct Seeding

To investigate if the cells were prohibited from migrating into the dermis because the carrier had affected them in some way, cells that were transferred from the ppAAc carriers were compared to cells that were seeded directly onto the DED and evaluated histologically after 7 days (Figure 3.19). Upon comparison of results, no difference between the two methods could be observed, and in both cases the MSCs could be seen on the DED's surface as a superficial layer and migrated into the dermis.

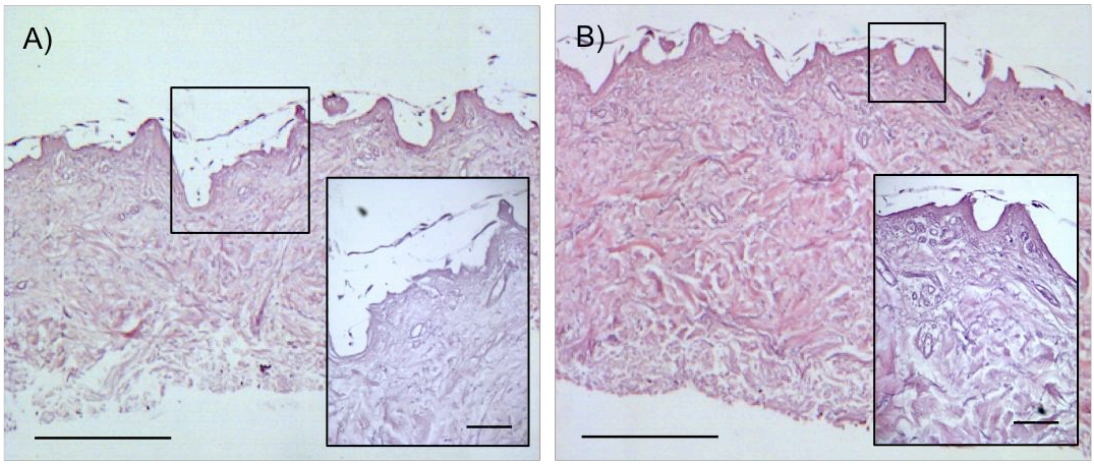

Figure 3.19. *Transfer Vs. direct seeding. H&E stained DED 7 days after direct seeding or 7 days after transfer form carriers (A and B respectively). Representative photographs are show from three independent experiments performed in triplicate. Images are shown at x 10 and x 40 magnification inset with scale bars representing 200 µm and 100 µm inset.*

eGFP-MSC and Keratinocyte Co-cultures on DED

Keratinocytes were co-cultured with eGFP MSCs on the DED to determine if the presence of keratinocytes could encourage the MSCs to migrate into the dermis. After 7 days of co-culture on the DED, fluorescent microscopy was performed to identify the MSCs, via their GFP label. The basement membrane (BM), which was stained by immunofluorescence using a TRIC-labeled secondary antibody raised to the anti-collagen IV primary antibodies. Cell nuclei were stained by DAPI, and this stain predominantly indicated the presence of keratinocytes. In the presence of keratinocytes, MSCs were capable of migrating across the BM and they could be identified in the dermis to a depth of up to 907 µm, and very few MSCs remained above the BM, which was heavily populated by keratinocytes. By contrast, MSCs cultured on DED's surface in isolation were not capable of entering the dermis and they remained as a layer above the BM (Figure 3.20). Following counting of the MSCs, it was revealed that their migration across the BM and into the dermis increased 2.06 fold ($p < 0.001$) in the presence of keratinocytes; 30.31 % of MSCs penetrated the BM vs. 62.51 % (MSCs alone vs. co-culture with keratinocytes) (Figure 3.21).

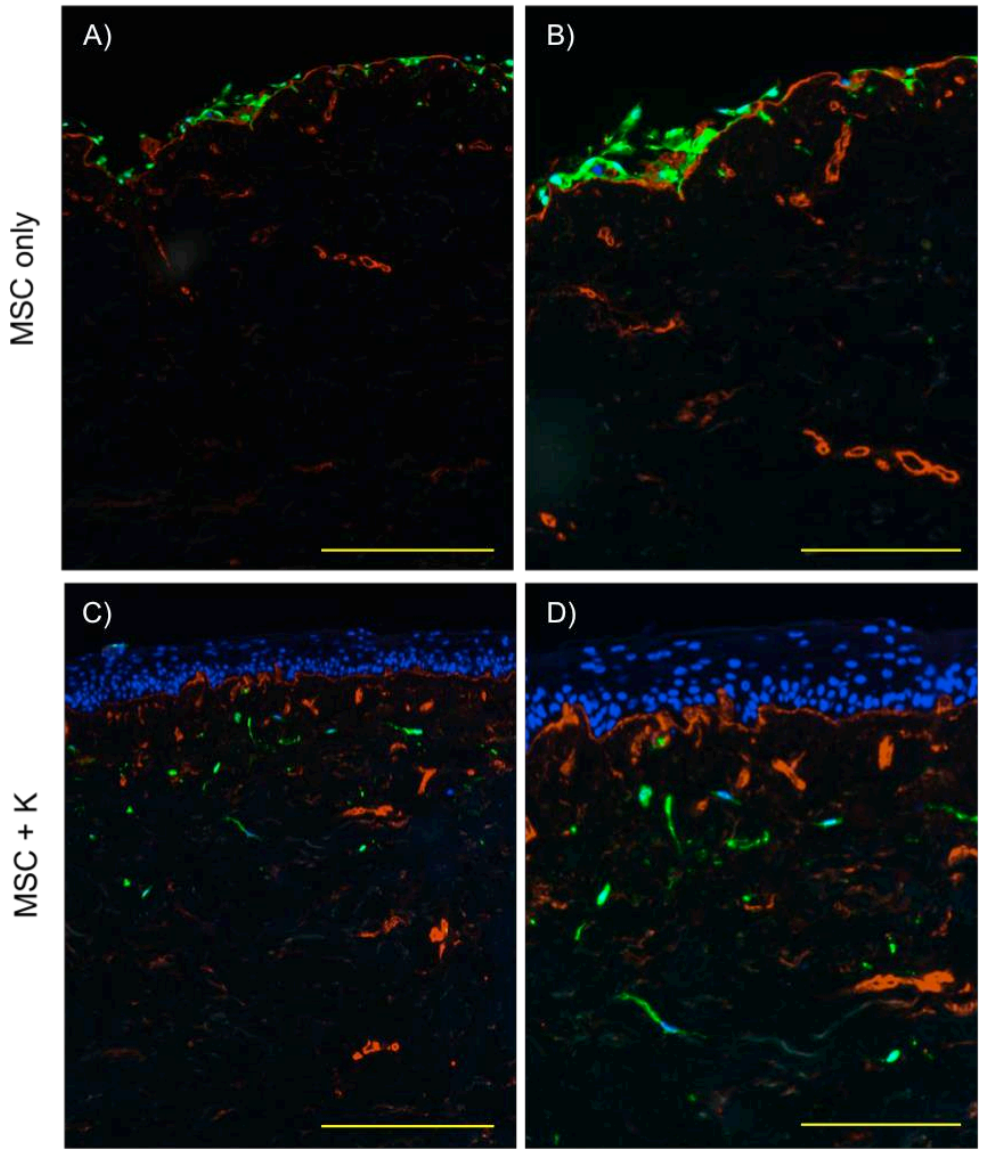

Figure 3.20. *MSC and keratinocyte co-culture on DED. A) and B) fluorescent micrographs of DED seeded with 5 x 10^5 MSCs after 7 days of culture on DED. C) and D) fluorescent micrographs of DED seeded with 5 x 10^5 MSCs and 1 x 10^6 keratinocytes (K) after 7 days co-culture on DED. Images in A) and C) were taken at x 10 magnification, the scale bars represent 200 µm. Images in B) and D) were taken at x 20 magnification, with scale bars representing 100 µm. Blue= DAPI, Green= eGFP-MSCs, Red= Collagen IV. A & B) Representative images from three independent experiments performed in triplicate are shown.*

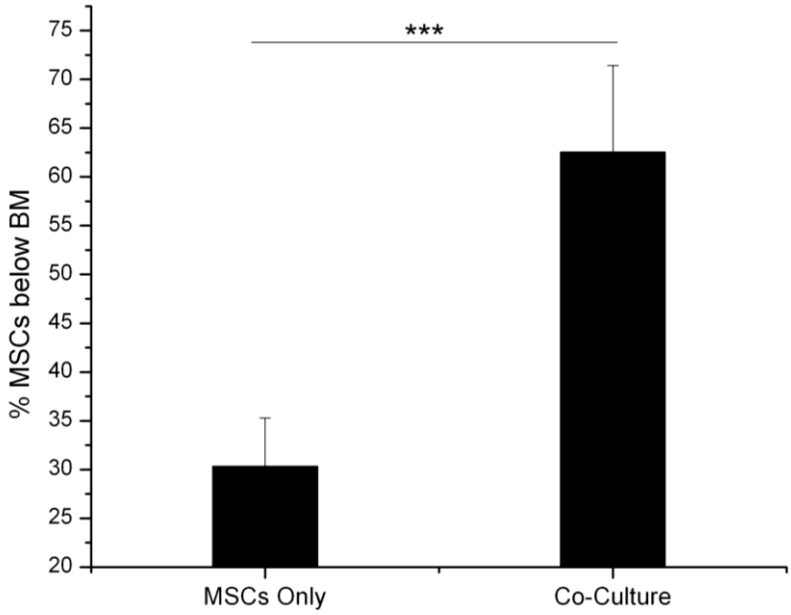

Figure 3.21. *Percentage of MSCs present below the basement membrane (BM) of DED in the presence (Co-culture) or absence of keratinocytes (MSCs Only). MSCs that were situated above or below the BM, identified by their eGFP-label, were manually counted using the 'cell count' plugin in image J. Approximately 50 cells were counted/field of view obtained with using x 10 objective and approximately 200 cells were counted/ sample. The bar chart represents the mean percentage of MSCs that were found below the BM, +/- the SEM from three independent experiments performed in triplicate. (***p < 0.001).*

3.4. Discussion

The aim of this work was to evaluate the use of a synthetic cell carrier dressing, prepared from ppAAc-coated medical-grade silicone, for the delivery of MSCs to a skin wound model.

Surface Characterisation

It is known that significant fragmentation of the monomer occurs in glow discharges, and as a result, a wide range of functional groups appear in the coating (Kelly *et al,* 2003). As can be seen from the C1s trace, a range of surface functionalities are produced including: carboxylic acid/ester (COOH/R), carbonyl, alcohol/ester, and hydroxyl, resulting from the break down of the acrylic acid as it is induced into a plasma. A limitation of XPS is that it cannot distinguish between carboxylic acid and ester groups, which collectively generate the carboxylate (COOH/R) peak. O'Toole et al demonstrated, by grazing angle infrared (IR) spectroscopy, that the entire carboxylate peak in the XPS spectra from plasma deposits of acrylic acid generated under low energy conditions (5 W), related to the presence of carboxylic acid rather than to esters; whereas under higher power conditions (10 W), plasma deposits contained a greater proportion of ester vs. acid groups (Otoole *et al,* 1996) (O'Toole et al, 1996). In addition, Alexander and Dunc demonstrated that at low power: flow ratios, approximately 30 % of the carboxylate peak can be assigned to acid groups (Alexander and Duc 1998).

In relation to the C-OH/R group, it is thought to consist predominantly of hydroxyl groups resulting from a reaction between the plasma deposit and water desorbed from the walls of the reactor during polymerisation, and atmospheric oxygen and water post polymerisation (Haddow *et al,* 2003). On the basis of these studies, it must be acknowledged that the entire COOH/R peak obtained in this work does not pertain wholly to acid, however because low power conditions (2 W) were employed in this study, it can reasonably be assumed that a significant proportion of the carboxylates are acids.

The degree of fragmentation can be minimized by carefully tuning parameters such as power, input and duty cycle to obtain a high degree of monomer structural retention in the deposited film. Alexander and Dunc demonstrated under an 'energy-deficient' regime (where incident power into the reactor is very low), films of acrylic acid could be produced with an elemental and functional composition similar to that of conventional acrylic acid. Using similar conditions used in the experimental set-up herein (flow rate of 5 sccm and lowest power used of 2 W), they showed that both the functional and elemental composition of the surfaces changed as a function of power. By incrementally increasing the power above 2 W to 20 W, a successive decrease in the surface oxygen content, and an increase

in the C-C content were noted, as well as a decrease in (COOH/R) content. In addition, the authors indicated, by secondary ion mass spectrometry (SIMS), the presence of linear structures containing up to five acrylic acid units, which bared close resemblance to the spectrum from pure polyacrylic acid (Alexander and Dunc, 1998). Therefore in light of this study, it can be said with confidence that the deposits of acrylic acid on our silicone substrates possess good functional retention of acid groups.

The presence of surface acid groups increases the number of oxygen-containing species available on the surface, and surface oxygen content has been shown to positively correlate with surface wettability, and in most cases cell adhesion (Parhi *et al,* 2010). ppAAc was capable of producing surfaces that could convert the properties of the silicone from hydrophobic to hydrophilic. Water that was dispensed to the surface of the uncoated silicone presented a 'balled-up' appearance, presumably because on such hydrophobic materials water interacting with itself proved more energetically favorable than interacting with the surface, thus limiting the spreading of water. By contrast, water spread rapidly over the ppAAc surfaces. These observations were reflected by their respective contact angles. The presence of ppAAc reduced the contact angle from over 100 degrees to 25.03 +/- 3 degrees; this finding is in agreement with other studies (Colley *at al*, 2009; Flivova *et al*, 2009).

Cell Attachment to ppAAc and Un-functionalised Surfaces

Protein adsorption plays a vital role in affecting how cells respond to a material. When a material is placed in contact with cell culture medium containing serum, adsorption of proteins to its surface from the serum happens almost instantaneously (Baier and Dutton 1969). Cells, which later come into close proximity to the substrate's surface recognise the adsorbed proteins because they act as ligands for cell surface receptors such as integrins; a family of heterodimeric transmembrane receptors that connect the extra cellular matrix (ECM) to the cytoskeleton (Roskelley *et al,* 1995). Integrins are not only involved in anchoring cells to the ECM; they also support cell spreading (Reddy *et al,* 2001), motility (Vicente-Manzanares *et al,* 2009) and trigger intracellular signals that regulate survival, proliferation and differentiation (Chastain *et al,* 2006; Tan *et al,* 2010; Du *et al,* 2011) Therefore, cellular responses on substrates are affected by the biological activity and composition of adsorbed protein layer, which is underpinned by the surface chemical properties of the material. Thus, cells do not interact directly with the surface chemistry, rather they interact indirectly with the surface via an adsorbed protein layer; the composition of which is governed by the surface chemistry. Although the exact mechanisms are poorly understood, parameters such as surface free energy, roughness, and chemical composition have a significant influence (Wilson *et al,* 2005).

The surface chemistry of a material is reflected, in part, by its wettability, and it is widely accepted, although there are exceptions, that hydrophilic polymers generally enhance cell adhesion and spreading (Guo *et al,* 2008; Dowling *et al,* 2011) (Dowling et al, 2011). The general observation that wettable surfaces display enhanced cell adhesion to polymeric surfaces, was reflected by the fact that cell attachment to ppAAc coated surfaces was considerably greater than to un-functionalised surfaces, which were hydrophilic and hydrophobic respectively. In relation to MSCs, both conventional acrylic acid, and plasma-polymerised acrylic acid containing surfaces have been shown to support cell attachment, spreading and differentiation (Guo *et al,* 2008; Colley *et al,* 2009; Filova *et al,* 2009). With respect to ppAAc, Filova et al prepared micro-patterned surfaces by coating silicone wafers with ppAAc followed by the deposition of a 1,7 Octadiene (OD) through a mask to investigate the spatial distribution of various cell types. Their results showed that a range of cell types including rat vascular smooth muscle cells, bovine endothelial cells, porcine mesenchymal stem cells (MSCs) and human skeletal muscle cells, grew preferentially on the ppAAc strip domains; with 90 % of the MSCs favoring the ppAAc surface. This was expected because OD is a hydrocarbon containing polymer that is known to be inhibitory to the adhesion of a numerous cell types (Daw *et al,* 1998; France *et al,* 1998), and it has been used as both a negative control to investigate plasma polymers, and as a diluent in acrylic acid plasmas to control the percentage of COOH functional groups on a surface. However they showed for the first time that MSCs cultured on ppAAc possessed more organised actin cytoskeletons and more pronounced tallin staining, indicating the presence of better developed focal adhesion plaques, as compared to the small proportion of MSCs found on the OD surfaces (Filova et al, 2009). Colley et al (2009) studied cell attachment and morphology of MSCs on ppAAc coated polydimethylsiloxane (PDMS) substrates of varying stiffness to determine the effect on differentiation. They found that cell attachment to ppAAc PDMS was markedly improved over untreated PDMS, and provided a similar level of attachment to tissue culture plastic (TCP). In addition they showed ppAAc did not affect MSC proliferation over 7 days and showed, similar to Filova, that cells on ppAAc surfaces contained a more defined actin cytoskeleton. Interestingly, they also demonstrated MSCs had reduced capacity for osteogenic differentiation on ppAAc surfaces, the cells retained their 'stemness'. Although a differentiation study on ppAAc surfaces was not conducted as part of my own study, the results demonstrated that brief contact (up to 72 h) with the ppAAc surface did not affect the MSCs' functional capacity; as shown by their ability to form tubules from ECFs. The physical properties of the material as opposed to the surface chemistry may have contributed to Colley *et al's* results, because MSCs only showed a reduced oesteogenic capacity on PDMS substrates with low Young's moduli (low stiffness), and substrate stiffness can alter cell phenotype (Engler *et al,* 2006).

However, none of the studies highlighted above investigated the proteins adsorbed to the ppAAc surfaces, and how they influenced MSC attachment. One candidate protein for

MSC attachment is fibronectin. Serum contains numerous proteins including albumin, immunoglobulins, fibrinogen, fibronectin (FN) and vitronectin (VN), all of which have been studied with relation to adsorption to substrates and subsequent cell responses (Yun *et al,* 1995; Tsai *et al,* 2002; Higuchi *et al,* 2003; Keselowsky *et al,* 2003). Of particular interest are the ECM proteins FN and VN; they have been shown to control cell adhesion and spreading (Steele *et al,* 1995; Garcia *et al,* 1999) cell survival, proliferation and expression of differentiated phenotypes (Menko and Boettiger 1987; Werb *et al,* 1989; Streuli *et al,* 1991). Albumin is the most abundant of all serum proteins and accounts for nearly one half of all plasma proteins (Blomback 1976), however it is not considered to be cell adhesive due to its lack of cell binding domains (Carter and Ho 1994), as such Allen et al hypothesised that the initial attachment of osteoblasts was most likely influenced by albumin adsorption. They found more albumin than FN was adsorbed from serum to pNIPAM surfaces compared to their more hydrophobic counterparts, and accordingly fewer cells were observed to attach to the hydrophilic surfaces (Allen *et al,* 2006) In contrast, Zelzer *et al* demonstrated that from a binary mixture of FN and albumin, hydrophilic surfaces of plasma polymerised allyamine (ppAAm) adsorbed more FN and provided significantly better cell adhesion than their more hydrophobic hydrocarbon containing counter parts (Zelzer *et al,* 2012). These two studies, where contradictory results are reported, highlight the scientific community's incomplete understanding of the nature surface chemistry plays on protein absorption and cell attachment to substrates. However both studies agreed that enhanced FN adsorption to surfaces is critical for achieving good cell adhesion. Therefore, in my study, since ppAAc greatly enhanced MSC attachment to silicone elastomers, it would be reasonable to assume that the surface selectively absorbed FN from serum thus mediating better attachment.

To my knowledge there are no studies on protein adsorption to plasma polymer deposits and their effect on MSCs attachment however, Danmark *et al* recently investigated human bone morrow MSC attachment to a variety of polymers (Danmark *et al,* 2012). They screened the MSCs for an array of integrins and showed the presence of a wide variety of integrin subunits, indicating that the MSCs expressed receptors for FN, VN, COL1, laminin α3β3γ2 (LM-332) and laminin α5β1γ 1 (LM-511), all of which are common ECM proteins (Plow *et al,* 2000). Danmark also found that VN from 10 % serum (same concentration used in this study) adsorbed 4-fold more than FN to polystyrene (the most hydrophilic material they tested compared to aliphatic polyesters). However, although VN was the most abundant surface protein, functional-blocking studies, where antibodies where targeted to either the subunits of the integrins to VN or the VN protein itself, revealed that preventing VN recognition had no effect on reducing MSC attachment, whereas preventing FN recognition halved MSC attachment (Danmark et al, 2012). Thus, their data showed that the main protein responsible for mediating MSC attachment was FN despite its low surface abundance. In addition, they identified the integrin subunits alpha 5 and beta 1 as

responsible for FN recognition by MSCs, and very recently other authors also identified these subunits as forming the key integrins of MSCs (Weeks *et al,* 2012). In light of the above, further investigation is clearly required to determine which proteins are available at the surface of ppAAc after adsorption from serum, and importantly, which of the proteins present are essential for MSC attachment by performing functional blocking studies.

In light of the above, I speculate that FN mediates the improved MSC attachment to ppAAc surfaces vs. un-functionalised. It is likely that albumin adsorbs first to the surface from serum, being the most abundant, smaller and more mobile protein than FN; and it is subsequently displaced from the surface by FN. It has been previously reported that FN's capacity to displace non-cell-adhesive albumin from hydrophobic surfaces is much reduced compared to hydrophilic surfaces (Koenig *et al,* 2003; Zelzer *et al,* 2008). Therefore, due to silicone's hydrophobic nature, silicone surfaces may absorb lesser amounts of FN compared ppAAc surfaces; thus non-acid-functionalised surfaces may present fewer ligands for MSC attachment. In addition, FN adsorbed to un-functionalised silicone may be structurally altered such that integrin recognition is perturbed (Steele *et al,* 1995). Figure 3.22 summarises the mechanism by which MSCs may attach to plasma-polymerised deposits of acrylic acid.

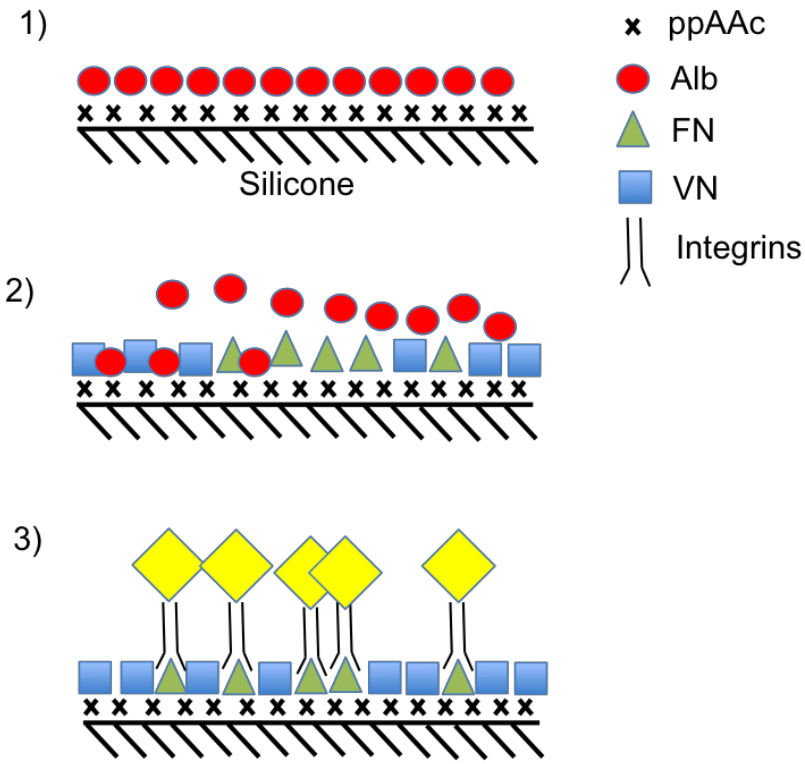

Figure 3.22. *Diagram illustrating a proposed mechanism for MSC attachment to ppAAc surfaces. 1) Albumin (Alb) absorbs first to the surface being the most abundant protein in serum. 2) Fibronectin (FN) and Vitronectin (VN) displace Albumin from the surface. 3) MSCs bind to FN via integrin α5β1.*

The results presented in this chapter also demonstrated that a very limited amount of cell attachment was attained on the non-functionalised surfaces. This could be attributed to the fact that even though the surfaces are hydrophobic, proteins for cell attachment are still adsorbed to the surface from the serum. Hydrophobic surfaces have been reported to adsorb more protein than hydrophilic surfaces (Absolom *et al,* 1987; MacDonald *et al,* 2002) , although this is not universal observation (Elwing et al, 1995; Keselowsky et al, 2002). Keselowky found that self-assembled monolayers (SAMs), which functionalised with either CH3 or COOH, producing surfaces with contact angles of 107 and 28 degrees respectively, adsorbed similar amounts of FN from serum. Therefore it is possible that the non-functionalised surfaces adsorbed much protein from serum, however those that adsorbed could have adopted a conformation that was not favorable for cell attachment. It has been shown that proteins that adsorb to hydrophobic surfaces are more susceptible to structural unfolding (Haynes *et al,* 1994; Keselowsky *et al,* 2003; Wilson *et al,* 2005), and this may alter their RGD sequences by which integrins recognise cell-anchorage proteins. In addition to the chemical surface properties, the physical properties of the material such as surface roughness may go part way in explaining why cells were adherent to the un-functionalised surfaces. Devesh et al recently attributed the attachment of MSCs to hydrophobic silicone substrates to surface roughness. They found that untreated silicone elastomers had rough surfaces, with 1.8 +/- 0.3μM ridges as determined by atomic force microscopy, and they proposed that surface roughness was able to overcome, to a limited extent, the hydrophobic nature of the silicone (Misra *et al,* 2012).

Mechanism of Transfer

With regard to the mechanism of transfer, one could speculate that the DED presents a surface more favorable to the MSCs than the ppAAc functionalised and un-functionalised surfaces. The basement membrane (BM) is a protein-rich site that provides the site of anchorage of epithelial cells and one of its chief constituents is collagen. The DED that was prepared had their BM preserved as noted by the presence of a thick band of collagen IV on the DED's apical surface. Integrins may be directed towards the collagen-containing BM where they become concentrated and produce more focal adhesions than are present on the opposing side of the cell, which is in contact with the carriers, so that the strength of cell adhesion to the DED is greater than to the carriers such that when the carriers are removed they remain in contact with the DED.

To test whether collagen mediated the transfer of cells, the transfer regimen was repeated onto wells coated with varying concentrations of gelatin (5 %, 1 %, 0.1 %). Only the lowest gelatin concentration (0.1 %) was capable of affecting significant cell transfer from the carriers ($p < 0.01$), however transfer was not as complete as compared to DED with

visibly more cells remaining on the carriers after transfer was attempted to gelatin surfaces. This could be due to gelatin being denatured collagen whereby its fibrilar structure is no longer present. It would be interesting to use BM extract such as Cultrex®, which is a soluble form of BM purified from human placenta, to investigate if collagen's fibrilar structure is necessary for effective cell transfer.

Using eGFP-labeled cells, MSCs could be identified 7 days post-transfer to DED by fluorescence microscopy to determine if the MSCs had penetrated and migrated into the DED. Confocal microscopy revealed that the MSCs could only be observed at depths up to 80 μm; this depth corresponded to that of the contours present in the DED's surface as confirmed by histology. Thus, it is possible that the cells, while well attached to the DED, did not migrate into the dermis. A comparison of cell transfer, from ppAAc carriers to direct seeding of cells to the surface of DED, revealed that the ppAAc chemistry did not influence the MSCs entry into the dermis. Therefore, it is likely that migratory/invasive cues are missing from this simple wound bed model.

A key requirement for cells to migrate into tissue is their ability to traverse the protein fibers of the ECM (Westermarck and Kahari 1999). BMs are a highly specialised, dense ECM layer that separates epithelium from the stroma, thus it may act as a barrier to MSC migration. Metalloproteinases (MMPs) are a family of zinc and calcium dependent endopeptidases that are capable of degrading most proteins of the ECM (Nagase and Woessner 1999). Of particular interest are the gelatinases MMP-2 and MMP-9, due to their ability to cleave collagen IV, laminin, aggrecan, and elastin, all of which are major BM components (Van den Steen *et al,* 2002). Cell-types of mesodermal origin, such as fibroblasts, endothelial cells, and MSCs, constitutively express MMP-2, however they only express MMP-9 upon stimulation (Nguyen *et al,* 2001; Ries *et al,* 2007; Sasaki *et al,* 2008; Ries *et al,* 2009). Dermal fibroblasts have been shown to heavily up-regulate MMP-9 upon interaction with keratinocytes, as demonstrated in both transwell systems and direct co-culture (Sawicki *et al,* 2005; Ries *et al,* 2009), thus providing evidence that communication between these two cell types are essential for modulating MMP-9 production. In addition, Gosh et al reported, whilst comparing methodologies for preparing human epidermal-dermal composites, human dermal fibroblasts could only enter the papillary dermis in the presence of keratinocytes (Ghosh *et al,* 1997); a phenomenon which Lee et al later attributed to the partial loss of the lamina densa in the presence of keratinocytes (Lee *et al,* 2004).

In light of this, and taking into account their shared embryonic lineage with fibroblasts, MSCs may behave similarly to fibroblasts with respect to their dermal migratory potential i.e. keratinocytes are required to create a permissive environment for cell migration. To investigate if the presence of keratinocytes could affect the capacity for MSCs migrate into the dermis, keratinocytes were co-seeded onto the DED with MSCs (eGFP-labeled). The

results clearly demonstrated that in the presence of keratinocytes, the majority of MSCs could traverse the BM, whereas in the absence of keratinocytes, the MSCs were restricted to the region superficial to the BM. In light of the discussion relating to MMPs, I speculate that the keratinocytes provide a permissive environment for MSC migration by way of enhancing MMP-9 production from the MSCs to a level that is sufficient to degrade the BM enough to allow their passage through it. Further investigation would be required to determine if changes in MMP-9 production were associated with the observation that MSCs could pass the BM in the vicinity of keratinocytes. Such an assessment could be made by comparing the MMP-9 content of the culture media from co-cultures on DED with the media from each cell type cultured in isolation on the DED via ELISA. If levels of MMP-9 were found to be elevated in the medium from the co-cultures, a causal link could be determined by blocking the function of MMP-9 by using specific inhibitors (Gu *et al,* 2005) to establish if MMP-9 functionality is essential to MSC migration.

On Route to the Clinic

Collagen I has been used to effectively deliver cells for skin repair in the clinic, and there are several commercially available products licensed by the food and drug administration (FDA) which include OrCell™- (Bilayered cellular matrix and composite cultured skin- 2001) and Integrea® (dermal replacement template- 2002). However, collagen is commonly bovine in origin and carries a low but inherent risk of disease transmission such as bovine spongiform encephalitis (BSE). Therefore, it is advantageous to avoid as far as possible the use of xenobiotic materials. Achieving effective cell delivery of MSCs from ppAAc carriers goes part way in achieving this goal because the materials are entirely synthetic i.e. medical grade silicone and acrylic acid. However it is also important to address the medium formulation on route to the clinic.

Fetal bovine serum (FBS) is usually added to culture medium because it provides a complex mixture of supportive agents for cell growth, including: growth factors, hormones, mitogens, transport proteins, detoxifying agents, attachment factors, protease inhibitors and vital nutrients (Freshney 2000). However, as MSCs are becoming more established in clinical settings, FBS's high content of xenogeneic proteins are a cause for concern surrounding immune reactions. In some cases, immunological reactions and anti-FBS antibodies have been observed and were considered to have affected the therapeutic outcome (Horwitz *et al,* 2002; Sundin *et al,* 2007). Despite this, most clinical data have been obtained with MSCs, expanded with FBS supplemented media, without major side effects (Bieback *et al,* 2009). In addition, FBS exhibits a high degree of batch to batch variation and carries the associated risk of transmitting infectious adventitious agents (Jung *et al,* 2012); although FBS can be obtained from clinically approved sources, originating from herds in

Australia or New Zealand where there have been no reported outbreaks of BSE, as was the case in this study. Considered together, regulators aim to minimise the use of FBS (Halme and Kessler 2006), thus creating a driving force to find alternatives.

In order to address the safety and regulatory concerns surrounding the use of FBS, human blood derived materials including human serum, platelet derivatives and cord blood serum are currently under investigation for their clinical benefit as a substitute for FBS. Autologous human serum has been reported to support MSC expansion (Stute *et al,* 2004; Kobayashi *et al,* 2005; Shahdadfar *et al,* 2005; Mizuno *et al,* 2006), although acquiring sufficient amounts to generate clinically relevant numbers of MSCs is deemed to be problematic due to the volume of blood that would be required (Sotiropoulou *et al,* 2006). Alternatively allogeneic type AB serum, which is a universal donor serum, could be pooled to provide sufficiently large quantities for large scale MSC expansion, however it has been met with mixed results. Some authors report that allogenic serum-containing medium is able to support MSC expansion over long-term culture in a similar fashion to FBS; including not altering their immunophenotype (Le Blanc *et al,* 2004) or differentiation capacity (Poloni *et al,* 2009), whilst others report growth arrest (Kuznetsov *et al,* 2000) and even cell death after the first passage (Shahdadfar et al, 2009). Other sources of allogeneic serum such as umbilical cord blood (Jung et al, 2009; Phadnis et al, 2006) and placental (Shafaei *et al,* 2011) have also been proposed as alternatives to FBS because, these primitive tissues are rich in growth factors that support the proliferation and differentiation of the resident stem cell population in fetal blood (Phadnis *et al,* 2006).

Human platelet lysate (hPL), which is prepared from the mechanical of chemical lysis of their membranes (Tekkatte *et al,* 2011), provides another growth factor-rich source that has been shown to have considerable growth promoting properties and maintenance of 'stemness' (Doucet *et al,* 2005; Capelli *et al,* 2007), however some report that hPL reduced the capacity of MSCs to differentiate down the oestoblastic and adipogenic lineage (Gruber *et al,* 2004; Lange *et al,* 2007), and also reduced their immunosuppressive capacity *in vitro* (Hartmann *et al,* 2010). Although these alternatives are promising, concerns surrounding the safety of the use of human sourced supplements still remain. There is the risk of contamination of allogeneic human growth supplements with pathogens that might pass undetected via the conventional blood screening of donors (Reinhardt *et al,* 2011) (Reinhardt et al, 2011). Also, these methods do not circumvent batch-to-batch variability similar to FBS.

Serum-free media may offer another alternative to FBS and reduce the problems associated with crude materials. By relying exclusively on the use of recombinant proteins, in replacement of those supplied by serum, serum-free media allows the precise make-up of the medium to be governed. As such, clearly defined medium formulations may be modified

in a way to enhance the expression of specific genes to promote an optimal cytokine profile for wound healing (Jung et al, 2012). StemPro MSC SFM from Invitrogen is so far the first and only commercial serum-free media that has been met with approval by the FDA (2011) as a medical device for use in clinical trials in the United States. It is therefore feasible that this media could be used in conjunction with the ppAAc carrier to provide a culture and delivery system for wound treatments that is safe for the clinic and entirely devoid of animal materials. With any change in cell culture medium formulation however, it will be important to evaluate how the MSCs respond to ppAAc surfaces under new conditions, because it has been shown that media composition can affect a cells' 'preference' for a given surface chemistry. For example, Eves et al demonstrated that under standard culture conditions melanocytes preferentially attached to ppAAc surfaces. However under serum-free conditions, this preference was reversed with the melanocytes favoring attachment to amine-containing surfaces of plasma polymerised allyamine. In a similar fashion, the authors also demonstrated that cell attachment of fibroblasts to acid or amine chemistries was influenced by the medium composition.

Colley et al reported that MSCs can attach equally well to ppAAc coated PDMS substrates in the presence or absence of serum (Colley et al, 2009), however the cells used in this study had previously been exposed to serum during their initial isolation and expansion before being switched to serum-free conditions. Therefore, it is probable that serum derived contaminants were carried over into serum-free conditions given the sticky nature of serum proteins (Jung et al, 2012). To truly assess the effect serum-free medium has on MSCs attachment to ppAAc carriers, it would be necessary to compare cells that had been isolated and expanded in both standard vs. serum-free media. This will be the subject of future investigations en route to the clinic.

To adapt the methodology further and enhance its clinical appeal, trypsin, used to detach cells from culture for seeding them onto the carriers, may be replaced by commercially available alternatives such as Accutase; a mixture of proteyolic and collagenolytic enzymes derived from an invertebrate species. In fact, Accutase was favored over trypsin by one of the collaborators that contributed to the work in this chapter, because it is thought to be a more gentle method of cell detachment (Dr Anita Mistry-personal communication, 2010). Accutase was successfully used therefore to detach MSCs and prepare them for tubule assays.

In order for off-the-shelf MSC treatments to become widely available it is important that MSCs collected from multiple tissues and donors can be stored in an accredited stem cell bank (Cavallo *et al,* 2011; Sabatino *et al,* 2012),so that they can be utilised as and when treatments are required. For example, it may not always be appropriate to use autologous MSCs from elderly patients, whereby both the proportion of MSCs in bone marrow aspirate

(BMA) and their proliferative capacity are reduced (Stolzing *et al,* 2011; Li and Pei 2012). In addition it may not be feasible to acquire BMA from patients presenting with extensive burns because maintaining bodily fluids is critical; and to perform an invasive procedure upon a patient that has suffered extensive trauma is undesirable.

An important finding in this study was that MSCs could be cultured on the carriers for periods up to 72 h whist maintaining their phenotype, viability, and functional capacity to form vascular tubules from ECFCs. In addition, cell-transfer to DED following 72 h pre-culture on the carrier was achieved to similar extents as transfer after 24 h pre-culture on the carriers. This was a key finding because this potentially provides a 3-day window, during which it may be possible for cells sourced from an accredited stem cell bank to be seeded onto the carriers and be transported anywhere in Europe. To this end, it would be useful to evaluate if the carriers could support the cells for greater durations so that MSC treatments could be provided to patients who live a considerable distance from a licensed cell therapy laboratory. In addition, performing vascular tubule assays could form part of the stem cell evaluation protocol held at a stem cell bank to assist batch screening, since stem cell quality is largely donor dependent (Pandey *et al,* 2011), and thus enhance their potential to promote wound re-vascularization and provide more effective wound healing.

Other important factors to consider, with the clinic in mind, are the cost of scaling-up of production to produce large quantities of ppAAc carriers, and evaluating the long-term stability or 'shelf-life' of the material. Whittle et al previously demonstrated that ppAAc surfaces could be prepared to be stable for up to 300 days when stored at room temperature and protected from light (Whittle *et al,* 2000). With regards to scale-up, although vacuum pressure technology is now widely used in preparing coatings in industry, the use of low-pressure plasma polymerisation techniques it is not without its limitations. Disadvantages include the high running cost of maintaining vacuums that achieve low pressures and the difficulty in developing continuous processing systems (Heyse et al, 2007). In light of this, there has been considerable interest in developing atmospheric pressure non-thermal plasma sources suitable for thin film deposition. Recently a new field of technology called atmospheric pressure dielectric barrier discharges (DBDs) has proven successful in producing polymer films of acrylic acid (Morent *et al,* 2009; Morent *et al,* 2010); achieving glow discharges and plasma deposits at low pressures makes deposition regimes much more cost effective to run because it eliminates the need for expensive vacuum equipment.

Comparison to Other Delivery Methods

The most common method for delivering of MSCs/ bone marrow mononuclear cells in the clinic for the treatment of wounds arising from chronic limb ishecmia, diabetic

ulclerations, pressure sores and acute wounds is cell injection sub-cutaneously around the wound site, or intramuscularly (for chronic limb ischemia); they are favored because they are minimally invasive (Rafii and Lyden 2003; Jiang *et al,* 2012). Table 3.1 presents a summary of the various means by which MSCs have been delivered to treat wounds. Cell injections pose several problems however; with the major obstacle being cell viabilities obtained are very poor. For example, it is reported that cell viability post injection can be as low as 1-32 % (Zhang *et al,* 2001) and it has recently been identified that it is the extensional flow that cells experience, due to the abrupt change in flow geometry which causes a dramatic change in velocity (i.e. from syringe to the needle), that is the major cause of acute cell death, although this can be much reduced by pre-encapsulating cells in alginate hydrogels to mechanically protect cells (Aguado et al, 2012). Therefore, increasing the percentage of live cells in the wound environment is critical to the success of cell therapies; this is especially important when considering cell delivery to chronic wounds because the microenvironments are harsh (hypoxic, inflammatory and display high levels of enzymatic activity) (Brem et al, 2007; Lobmann et al, 2005), and may further limit cell viability, and a positive correlation has been observed between the number of MSCs administered and the healing outcome (Flanga et al, 2007). Also, creating a suspension of cells for injection requires further cell manipulation and the use of trypsin, which can be potentially damaging to the cells.

Additionally cell-injection may not be best suited to treat large area skin defects because injection of cells around the wound margins will concentrate the cells, initially, at a single locality with the only the possibility that the cells will migrate throughout the wound. The use of carrier materials similar to those prepared in this study has previously been used clinically to deliver autologous keratinocytes to patients with chronic wounds (Moustafa et al, 2004, 2007). In particular they have also been used to expedite wound healing in patients with extensive skin loss from burns injury (Zhu et al, 2005), thus demonstrating the materials ability to cover large defects this was achieved by placing several small patches of cell containing carriers to over the wound site. Carriers containing MSCs could therefore be used to deliver cells across large skin defects.

Very recently, collaborators in Scharffetter-Kochanek's group in Germany, took the delivery method used in this study one stage further and demonstrated that MSCs could be successfully delivered from ppAAc carriers in vivo. They demonstrated in a murine diabetic mouse model, where healing is impaired, that not only could the MSCs be delivered from ppAAc carrier, but that they participated and accelerated the healing of full-thickness excisional wounds through the suppression of TNF α dependent inflammation, increasing anti-inflammatory Macrophage M2 numbers, myofibroblast differentiation and granulation tissue. In addition, the results on healing were found to be similar to those achieved via intradermal injection of MSCs, thus indicating that cell-delivery by ppAAc carriers offers a

non-invasive alternative to cell delivery to wound beds (Jiang *et al,* 2013). They also reported similar findings to this study by demonstrating that short-term culture on the ppAAc carriers did not affect MSCs functional behavior *in vitro* (as assessed by immunosuppressive assay). Although their experiments were conducted with MSCs derived from adipose tissue and not bone marrow, together it shows that the ppAAc carriers can support human MSCs from multiple tissue sources. This is advantageous because harvesting BM is an invasive procedure.

Alternatively, MSCs can be delivered from natural materials such as collagen-derived matrices (Vojtassak et al, 2006; Ravari et al, 2011), or artificial dermis (Yoshikawa et al, 2008) for the treatment of non-healing wounds in the clinic, however, for the reasons outlined above, it is desirable to avoid the use of xenogenic materials. There are many commercially available fibrin sealants (such as Tisseel ® Florseal ® Baxter healthcare; Evicel ®, Ethicon (FDA-approved homeostatic aids) that aid topical cell delivery to wounds. However these fibrin 'glues' require complex preparation; fibrinogen must be mixed with thrombin to produce a bio-polymeric hydrogel matrix that resembles a fibrin clot, and they have short working times before the clot sets (Flanga et al, 2007). In addition, the fibrinogen concentration can negatively affect cell proliferation both micro-structurally and biochemically (Ho et al, 2006), therefore the ratios of thrombin to fibrinogen must be carefully balanced so that the gel can be sufficiently cross-linked to entrap cells, whilst maintaining a window long enough to allow the glue to be manipulated and spread over the wound area before the clotting reaction is complete.

To my knowledge, there are no other cell carriers derived completely from synthetic materials used for the delivery of cells to skin. One method that may be promising though is cell-sheet technology. For example, Miyahara et al delivered sheets of MSCs to hearts following myocardial infraction using poly(N-isopropyl)acryamide (pNIPAM). This thermoresponsive polymer is able to undergo a temperature dependent hydrophilic to hydrophobic transition to release cells. However, following cell release form the pNIPAM, the authors found it necessary to transfer the cells to an elastic-plastic sheet so that the sheets could be handled, presumably because they were too difficult to handle due to their thin and fragile nature (Miyahara *et al,* 2006) (Miyahara et al, 2006). The thermoresponsive polymer therefore requires more handling on behalf of the cell culture technician than if cells are cultured directly on a carrier and then put in place. Therefore the synthetic ppAAc carriers provide a simple, efficient and non-invasive delivery method of MSCs to wounds that may be well suited to clinical applications.

Table 3.1. *Summary of delivery methods for MSCs.*

Cell Delivery Method	Cell-type	Study
Cell Injection		
Intradermal injection at wound margins	BM-MNC	(McFarlin *et al,* 2006; Volk *et al,* 2007; Wu *et al,* 2007; Kwon *et al,* 2008; Stoff *et al,* 2009; Borena *et al,* 2010; Kuo *et al,* 2011; Ravari *et al,* 2011; Akela *et al,* 2012; Castilla *et al,* 2012)
	ADSC	(Kim *et al,* 2011b)
Injection directly into wound bed	BM-MNC	(Javazon *et al,* 2007; Sarasua *et al,* 2011; Xu *et al,* 2012)
	ADCS	(Maharlooei *et al,* 2011)
Intravenous injection	BM	(Fathke *et al,* 2004; Higashiyama *et al,* 2011)
	BM-MNC	(Mansilla *et al,* 2005)
	BM-MSC	(Li *et al,* 2006; McFarlin *et al,* 2006; Kwon *et al,* 2008; Sasaki *et al,* 2008; Wang *et al,* 2012)
Intramuscular injection	BM-MSC	(Lu *et al,* 2011)
Electrospun Materials		
Chitosan/ Poly(vinyl alcohol)	UCB-MSC	(Gholipour-Kanani *et al,* 2012)
Collagen/ PLGA functionalised with CD29	BM-MSC	(Ma *et al,* 2011)
Collagen-Based Materials		
Collagen gels	ADSC	(Kim *et al,* 2007; Lee *et al,* 2011)
	BM-MSC	(Kim *et al,* 2011b; Ravari *et al,* 2011)
	BM	(Ravari *et al,* 2011)
Collagen-GAG scaffolds	BM-MSC	(Liu *et al,* 2008)
bFGF-soaked Pelnac ® (dermal substitute)	BM-MSC	(Nakagawa *et al,* 2005)
Pelnac ®	BM-MSC	(Yoshikawa *et al,* 2008)
	ADSC	(Nambu *et al,* 2007; Nambu *et al,* 2009)
Acelluar dermal matrix	ADSC	(Orbay *et al,* 2011)
Gelatin microspheres	BM-MSC	(Huang *et al,* 2012)
Collagen-chitosan scaffold	ADSC	(Shokrgozar *et al,* 2012)
Miscellaneous Natural Materials		
Amniotic membrane	BM-MSC	(Kim *et al,* 2009)
Fibrin spray	BM-MSC	(Falanga *et al,* 2007)
Fibrin gel	BM-MNC	(Mansilla *et al,* 2005)
	ADSC	(Steinberg *et al,* 2012)
Matigel (reduced growth factor)		(Wu *et al,* 2007)
Methylcellulose	BM-MSC	(Leonardi *et al,* 2012)
Synthetic Materials		
Polyurethane semi-permeable membrane	BM-MSC	(Argolo Neto *et al,* 2012)
Silicone elastomers functionalised with plasma polymerised acrylic acid	ADSC	(Jiang *et al,* 2013)

Other		
Cells in suspension	BM-MNC	(Rasulov *et al,* 2005)

Key
ADSC= Adipose tissue derived stem cells; BM=- Whole bone marrow aspirate; BM-MNC= Bone marrow mononuclear cells; BM-MSCs= Bone marrow mesenchymal stem cells; UCB-MSCs= Umbilical cord blood derived mesenchymal stem cells'

3.5. Summary

- Plasma deposited films of acrylic acid (ppAAc) supported the culture of MSCs, and facilitated the delivery of MSCs to model wound beds composed from human de-epithelialised dermis (DED).

- MSCs cultured on the ppAAc carriers for up to 72 h retained their viability, phenotype, ability to support vascular tubule formation from endothelial colony forming cells.

- MSCs remained viable and proliferated on DED for at least 7 days after delivery from ppAAc carriers. However, the basement membrane acted as a barrier to their migration. MSCs migration was observed in the presence of keratinocytes.

Chapter Four:

Developing a Wound-Healing Model Based on Human Tissue Engineered Skin

4.1. Aim

The aim of this work was to develop an *in vitro* wound model, based on tissue-engineered skin, which could be used to evaluate the healing properties of MSCs *in vitro*.

4.2. Introduction

The scratch assay is a widely used method to study factors that affect wound healing *in vitro*. The method involves creating a 'scratch' in a monolayer of keratinocytes and capturing images at regular intervals to monitor the rate of scratch closure (Liang *et al,* 2007). The scratch created is often referred to as a 'wound', hence the scratch assay in sometimes referred to as a wound-healing assay. However the scratch assay is essentially a cell migration and proliferation assay rather than a wound-healing assay, since these simple models lack epidermis-like structures, 3D cell communications and additional cell types.

So-called 'organotypic' cultures are a better alternative for studying wound healing *in vitro.* They are typically derived from collagen gels, which have been seeded with keratinocytes on the superficial side and have fibroblasts embedded within the collagen matrix. Cells in these 3-dimensional constructs form a differentiated epidermis, and thus they are a more representational model for wound healing (Maas-Szabowski *et al,* 2000)

Tissue-engineered (TE) skin, on the other hand, can be derived from *ex-vivo* decellularised human skin and isolated primary fibroblast and keratinocytes. These constructs hold the advantage of being more physiologically relevant than amorphous collagen gels. TE skin closely resembles *ex-vivo* skin and has been used extensively by our laboratory to study, melanoma invasion and bacterial invasion, skin contraction and skin pigmentation (Eves *et al,* 2000; Chakrabarty *et al,* 2001; Hedley *et al,* 2002; Harrison *et al,* 2006; Thornton *et al,* 2008; Shepherd *et al,* 2009; Shepherd *et al,* 2011).This chapter describes how a wound model was developed from TE skin, and details the problems that were faced during its development and how they were overcome.

4.3. Results

Attaining Consistent Wound Sizes

Composites, after 5 days at air liquid interface, were initially wounded using a 22-blade scalpel (Figure 4.1 A). This blade was selected because it is a good general-purpose blade that is used in the lab for a variety of applications. Chiefly, it is the blade of choice for making smaller cuttings from skin that was obtained from surgery for the purpose of making DED. However using this blade proved problematic as far as achieving consistent wound lengths were concerned. The 22-blade possessed a curved profile; it is pointed at the tip becoming rounded towards the handle. To make an incisional wound in the skin a rocking/ seesaw motion was performed by pressing the tip of the blade into the tissue and rolling the remainder of the blade across the tissue. However using this method, it was hard to create straight wounds with consistent lengths between samples (Figure 4.1 B).

After consulting a surgeon, I was informed that the 22-blade is designed for making an initial incision in tissue from which the blade could be dragged to open up a wound. Performing a dragging motion of the composite was not practical because the composites were too small. Upon surveying the full selection of blades available from Swan-Morton an alternative blade was tested. Blade 15A was chosen because it has a flat cutting surface (Figure 4.1 C). This blade could be pressed directly into the skin to create a full-thickness puncture-type wound through the skin, which resulted in making wounds with a length equivalent to that of the blade (9 mm). Upon comparing the wounds produced by each blade type, it is clear that those produced from the 15A blade are straighter and their lengths are more consistent than that which can be achieved using the 22-blade (Figure 4.1 B and D).

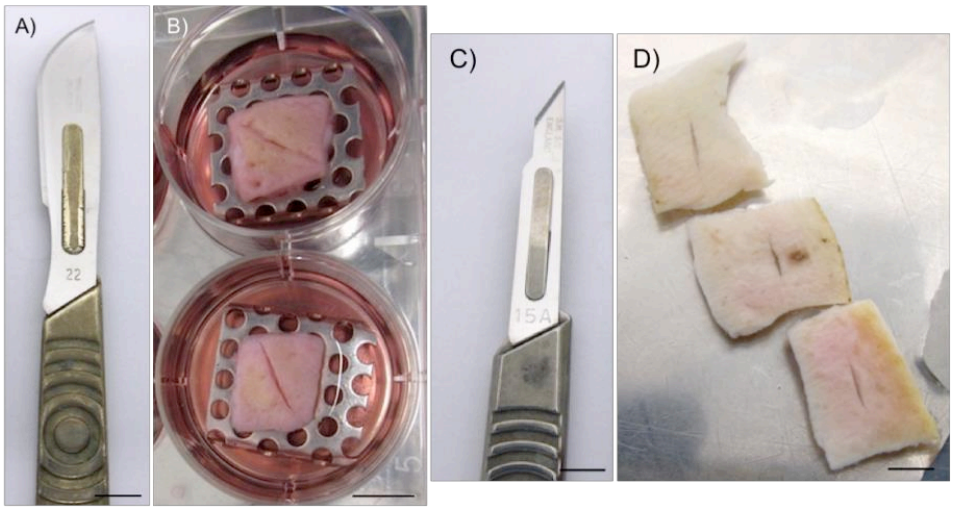

Figure 4.1. *Producing consistent wounds. A) 22-blade. B) Wounds produced in TE skin by the 22-blade. C) 15A blade. D) Wounds produced in DED by the 15A blade. Scale bar: 1 mm.*

Optimising Fibrin Clotting

Following wounding, and in accordance with the aim of the work, a suitable delivery method was sought to introduce cells into the wound. Injection of cells into the wound was not feasible, due to the small area of the tissue pieces and their thinness (< 2 mm), additionally cell injection would prove too fiddly because the tissue was difficult to handle. The carrier developed in Chapter 3 was not a suitable delivery vehicle in this application where incisional wounds are concerned. Cell delivery from ppAAc carriers is suitable for larger wounds but not for the small wounds produced in this incisional wound model.

As a result of the coagulation cascade *in vivo*, fibrin quickly forms a plug at the wound site to achieve heamostasis. As such, this naturally occurring material is frequently used as a delivery vehicle for cells for the treatment of chronic wounds (Laurens et al, 2006). Combining a mixture of thrombin with fibrinogen could make an artificial fibrin clot. Fibrinogen is a peptide that can be cleaved via the enzyme thrombin so that the fibrinogen fragments can become cross-linked to form a mesh/network structure to entrap cells. Firstly, it was important to establish the amount of thrombin to add to the fibrinogen that allowed the clots to form over a reasonable window of time. The concentrations of fibrinogen and thrombin were fixed at 6 mg/ml and 25 IU respectively and a range of volumes of thrombin was added to bijous containing 1 ml of fibrinogen. Secondly, following mixing of the two components together, the clotting time was monitored to identify the volume of thrombin that was sufficient to produce a solid clot within a 'workable' time, i.e. it was not desirable for the clot to set so rapidly that the solution could not be pipetted from the bijou to the tissue, and equally it was important that the clot was able to set after a few minutes so that cells contained within the fibrin were fixed promptly to the wound site. The optimal volume of thrombin to add to the fibrinogen was found to be 20 µl (final concentration = 10 IU) and this produced a solidified clot in less than 5 min (Figure 4.2).

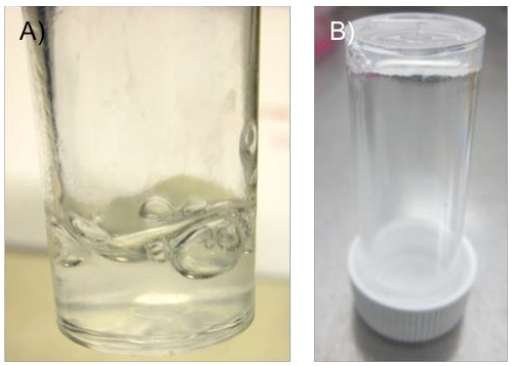

Figure 4.2. *Fibrin clot. A) 1 ml of fibrinogen (6 mg/ml) was added to 20 µl of thrombin (25 IU). Fibrin part way through the clotting reaction. B) Fibrin clot once set. The bijou has been inverted to demonstrate that the fibrin has a glue-like quality.*

Minimisng Wound Leakage

After optimising the fibrinogen and thrombin concentration and volume that produced a fibrin clot over an appropriate time, a fibrin clot was introduced into the wound site. Wounds were made in DED initially using the 15A blade as previously described. Thrombin was added to fibrinogen and mixed, and the mixture was dispensed from a pipette in to the center of the wound cavity. Leakage of fibrin, before it set, from the base of the wound was problematic. Leakages of this sort had to be prevented if cells were to be introduced in fibrin to the wound site, because leakages would substantially reduce the number of cells that could be retained in the wound. Additionally if leakage rates, or amounts from the composites differed between samples, it would likely lead to differing results in wound-healing outcomes due to differences in the number of cells that remained in the wound cavities.

Because fibrin glue is a sealant, its usefulness in preventing leakages from wounds was tested. DED was wounded through the papillary surface and then was turned over to reveal the reticular dermis. Fibrin glue was then pipetted over the reticular surface of the dermis and once it had set the DED was flipped back over. Forceps were used to push the margins of the wound wider apart than would be used in an experiment, for the purpose of creating an over-sized cavity to test fluid retention. Cell culture medium was then pipetted into the wound cavity. No medium was found to have leaked from the tissue after 30 min (Figure 4.3). Therefore this method was successful at preventing leakages.

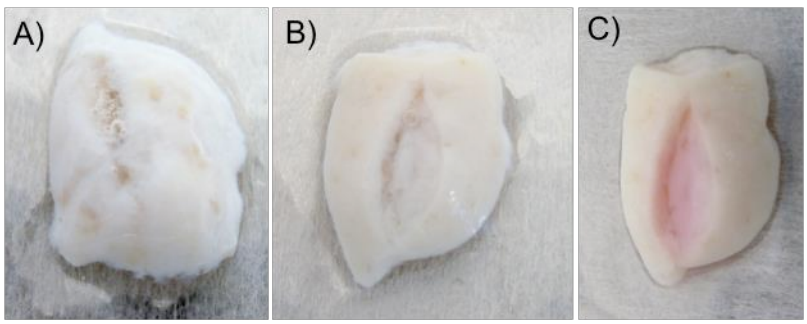

Figure 4.3. *Containing liquid to the wound site. A) Underside of a piece of DED that has been sealed with fibrin after making an incisional wound. B) Same piece flipped back over. C) Wound cavity 30 min after filling with cell culture medium.*

Consistency in Wound Diameter

The second issue to address in creating consistently sized wounds was wound diameter. After wounding either composites or DED, due to the elastic nature of skin, the wound edges would naturally lie in close proximity to each other. As such if they were left untouched, the wounds would heal too fast to measure after the introduction of fibrin; this

observation was previously reported by a former PhD student within the group (C.M.D. Marques, 2011). Therefore the wound edges needed to be prised apart slightly to create a more difficult wound to heal.

My original idea was to add some sort of 'divider' to the wound; that a short fragment of inert material might be placed in the wound to make it wider, so that when the fibrin is introduced the gap is maintained. This was decided against because the shard would remain in the wound after the fibrin had set and might prevent the course of healing at its point of introduction.

The second idea that was tried was to use a compass. As a compass contains two pins that could be set a defined distance apart, it could be used to separate the edges of the wound a set amount whilst the fibrin glue is introduced into the wound. To start with the compass was set to its narrowest position i.e. the two pins were as close together as the instrument would allow, and the pins were inserted into the wound with each pin touching opposing sides to widen the wound a fixed amount (Figure 4.4). However this approach was discarded because the narrowest distance the compass could be set (3 mm) created wounds that were too wide.

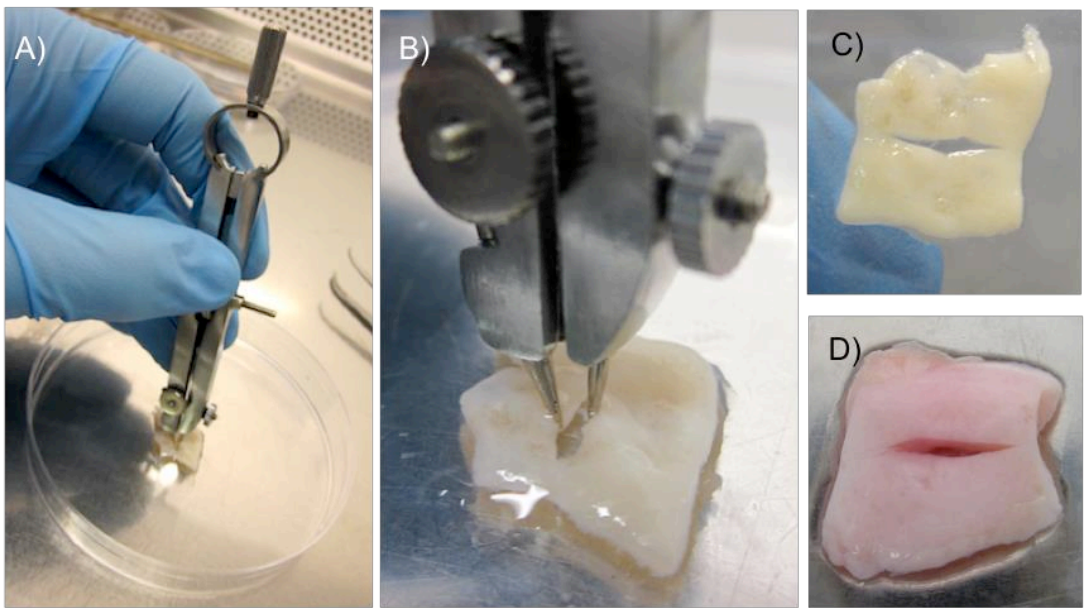

Figure 4.4. *Attempt to create a defined wound diameter. A) and B) Compass gross and close-up view. C) and D) Representative images of the wound cavities created in DED.*

A third option was to try and bend a strip of dental wire into a two-pronged fork, and use the two edges of the fork to separate the wound edges a defined distance from each other. However manipulating the wire so finely proved too difficult to reproduce.

In the end a different approach was opted for. By compressing the tips of forceps together and placing each fork of the forceps on opposite sides of the wound, the pressure from the forceps could be released just enough to reopen the wound gap (this distance was approximately 0.6-7 mm in diameter- as seen by OCT in Chapter 5). Fibrin could then be added. This method was sufficient to provide consistency in wound diameter as demonstrated by Figure 4.5.

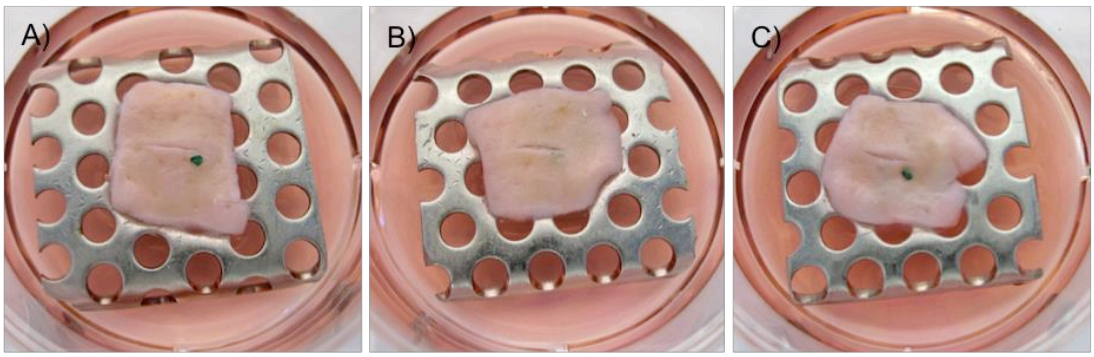

Figure 4.5. *Consistently-sized wounds. A)-C) series of wounds by the above method. Briefly, Full thickness wounds were created in TE skin, after 5 days at ALI, using a 15A scalpel blade and 100 µm of fibrin glue was inserted into the wound cavity.*

Introducing Cells to the Wound

To test whether cells could be encapsulated into a fibrin clot and delivered into the wound cavity, human dermal fibroblasts (HDFs) were tested before delivery of MSCs was attempted. This was done because the former cells are plentiful and inexpensive compared to MSCs. Cells were trypsinised, and the cell volume containing 1 x 10^5 cells were extracted and placed into a tube containing PBS. The cells were centrifuged for a second time and the cells were resuspended in fibrinogen after discarding the supernatant. The additional step of adding the cells to PBS before adding them to fibrinogen was performed to wash the cells of medium, because clotting factors within the medium, if not removed by adequate washing, caused the fibrinogen to gelate prematurely. Wounds were then made in composites that had been at ALI (for 5 days, and thrombin was added to the fibrinogen containing the desired quantity of cells and mixed by gentle pipetting. This caused the clotting reaction to begin and the solution was added to the wound site. Histology revealed that both HDFs and MSCs could be successfully delivered to the wound site in fibrin; cells could be clearly seen at the wound site contained within the fibrin clot (Figure 4.6). Furthermore, evaluation of wounds after 14 days demonstrated that fibrin was necessary for wound healing to occur; in the absence of fibrin, the wounds failed to heal (Figure 4.7).

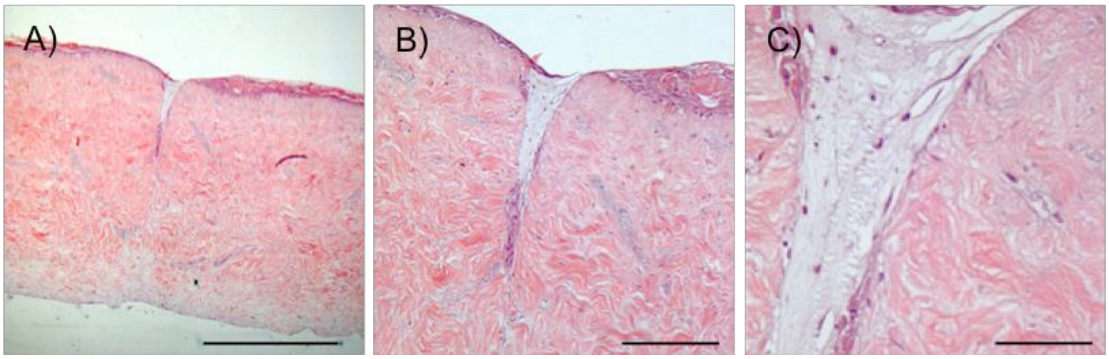

Figure 4.6. *Introducing cells at the wound site. A) - C) light micrographs showing MSCs which have been introduced into the wound via a fibrin clot, at x 4, x 10, x 40 magnification respectively, with scale bars of 100 µm, 300 µm and 500 µm respectively.*

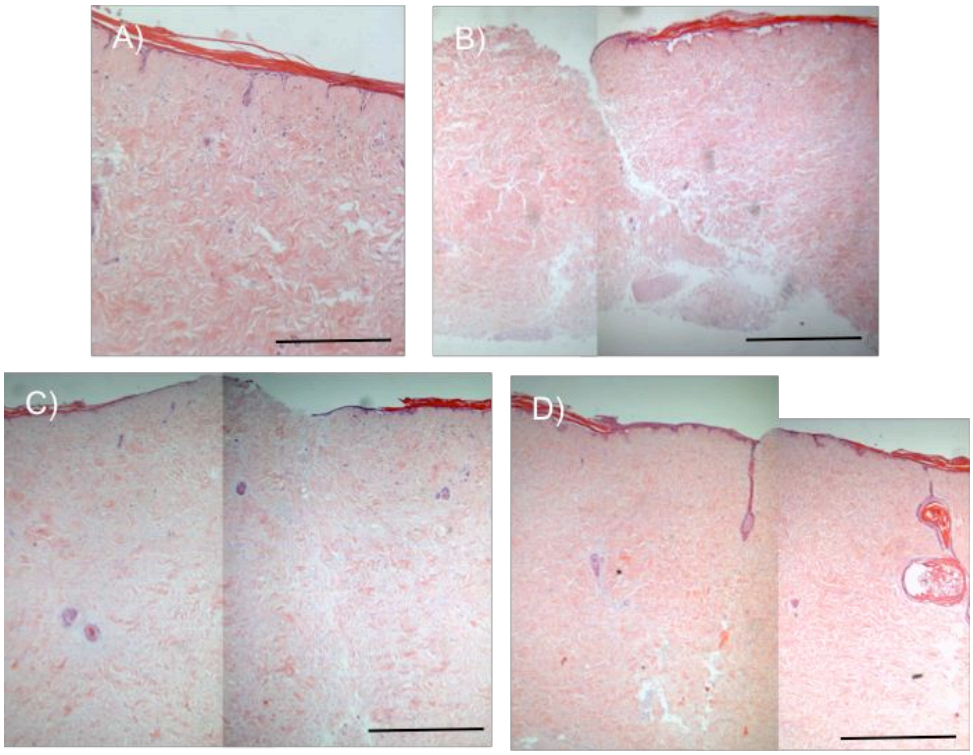

Figure 4.7. *Histology of wounded composites after 14 days. A) TE skin without an incisional wound. B) Wounded TE skin without a fibrin clot. C) Wounded TE skin plus a fibrin clot. D) Wounded TE skin plus fibrin containing fibroblasts. (x 10 magnification, scale bars: 300 µm).*

MSC Compatibility with Greens Medium

Green's medium is used to support the growth and maturation of TE skin. However if MSCs are to be introduced into the wound model, it is essential to test if this medium is capable of supporting these cells because this medium is not their standard growth medium. MSCs were cultured in either their standard medium (MSCBM) or Green's medium for 7 days, and photographs of the cultures were taken every few days to record if there were any visible proliferative or morphological changes between the MSCs cultured under each condition. At day 7 an MTT assay was performed to determine if there were differences in cell viabilities between culture conditions.

MSCs cultured in MSCBM appeared to have a more spindle-like appearance compared to Green's medium where the cells presented a more spread morphology; this difference was more pronounced at day 7 (Figure 4.8 A). There also appeared to be more cells per field of view in the MSCBM medium suggesting that this medium was more supportive of MSC proliferation, however the MTT data did not confirm this (Figure 4.8 B). The results of the MTT assay showed that there was no statistically significant difference in cell viability between the cells in the two different media ($p= 0.248$). Therefore MSCs can survive well in Green's medium.

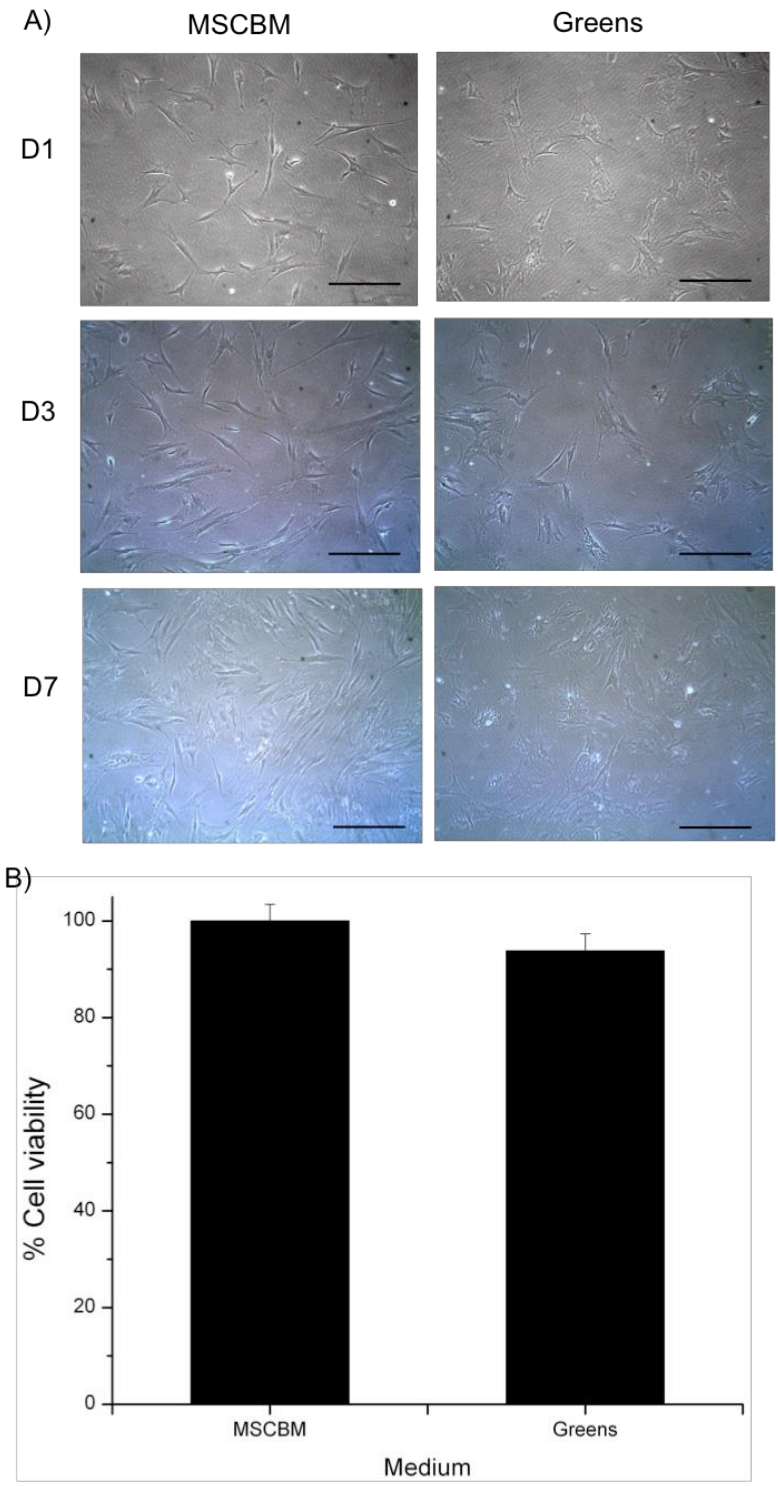

Figure 4.8. *MSC compatibility with Green's medium. A) Morphology of BM-MSCs over the course of 7 days cultured in either Greens Medium or MSCBM Medium (scale bars: 100 µm). B) Cell viability via MTT expressed as % cell viability normalised to the control medium (MSCBM). Error bars represent SEM +/- (N=3, n=3).*

4.4. Discussion

The aim of this work was to devise a wound-healing model based on tissue-engineered skin, for the purpose of evaluating the effect MSCs might have on the healing of *in vitro* wounds. The validity of the model developed in this chapter will be discussed.

The Importance of Fibrin

In the wound environment, fibrinogen is converted to fibrin, as a result of the coagulation cascade, to form an important provisional extracellular matrix for wound healing. Cells that contribute to wound healing (dermal fibroblasts, endothelial cells) are able to migrate into and degrade/remodel the fibrin and deposit neo-collagen to restore structural integrity to the skin (Laurens *et al,* 2006). TE skin has no blood supply therefore upon wounding of the TE composites there is no clotting cascade. Thus, to create a more realistic model of wound healing in TE skin, it was necessary to introduce a fibrin clot to the wound to better represent the wound environment.

An artificial fibrin clot was made by combining thrombin with fibrinogen; fibrinogen is a soluble peptide that can be cleaved by the enzyme thrombin into fibrin monomers which then cross-link with one another forming a network of insoluble fibrin polymers (Weisel *et al,* 1993). Additionally, fibrin served as a way to introduce cells into the wound site. Fibrin for example has previously been reported as an 'ideal' delivery vehicle for cells to treat chronic wounds (Ravari *et al,* 2011). Other delivery methods such as injection of cells into the wound was not feasible, due to the small area of the tissue cuttings and their thinness (< 2 mm), and cell injection would be too fiddly (the tissue would prove too difficult to handle). The carrier developed in Chapter 3 was not a suitable delivery vehicle in this application where incisional wounds were made. The carrier is suitable for the much larger wounds found in the clinic.

It is also important to mention that fibrin provides more than a provisional matrix; it mediates cell responses such as cell adhesion, migration, proliferation and tubule formation from the participating cells in wound healing (Koolwijk *et al,* 1996; Staton *et al,* 2003; Becker *et al,* 2004; Cox *et al,* 2004). Therefore, when it comes to designing an experiment to test the efficacy of a wound healing intervention such as MSCs, using the model developed herein, it will be important to assess the effect fibrin alone may have on wound healing as a control. Fibrin for example was shown to be essential for wound healing in the TE skin model because wounds failed to heal within 14 days in the absence of fibrin.

Wound Consistency

Achieving consistency in wound length and diameter was of obvious importance because, if there were differences in the sizes of the wounds between samples, it would firstly make evaluating the effect of MSCs within the wound difficult, and secondly it would hinder the reproducibility of the results. For example, MSCs introduced into the wound may have had a positive influence on the cells involved in wound healing, however an overall difference in the wound healing outcome may be masked, due to variations in wound severity between experimental conditions. Without a consistent wound size it would be very difficult to assess the wound model's response to MSCs.

The wound-healing model presented here is based on an existing model developed by a former student of Prof S. MacNeil. Claudia Marques' PhD thesis described a method for creating wounds in TE skin (Marques 2010), however I have made improvements upon her method to achieve greater consistency in wound size. For example, it is likely that Dr Marques experienced similar problems to me in that, due to the rocking action one had to perform to attain a full-thickness wound while using a rounded profile 22-blade, wound lengths could vary between samples; this difficulty was removed by opting for a 15A-blade which is a flatter blade. In addition, I added the extra step of sealing the underside of the dermis with fibrin glue before introducing cells into the wound. Therefore when cells encapsulated within fibrin were introduced into the wound cavity, no losses of cell volume were recorded. The issue of minimising leakage was important to address because leakages would reduce the number of cells retained in the wound and thus diminish their potential to ameliorate healing. Additionally, if leakage rates from the composites differed between samples, it would likely lead to differing results due to differences in the number of cells that remained in the wound cavities.

Suitability of the Method for use with MSCs

MSCs could be effectively entrapped and delivered to the wound site in fibrin glue. Although a viability study was not performed to determine if fibrin had a negative effect on MSC viability**,** and functional capacity for differentiation, other authors have previously reported fibrin not to negatively affect these properties (Catelas *et al,* 2006; Neuss *et al,* 2010; Colley *et al,* 2012). Indeed, Colley et al recently reported that MSCs expanded on fibrin substrates maintained their stem-cell like properties, thus indicating that fibrin substrates may more closely mimic the cells *in vivo* physiological microenvironment i.e. stem cell niche (Colley *at al*, 2012).

Since MSCs can home to sites of injury (Hong *et al,* 2012), it may have been important to assess if the MSCs were capable of migrating out from fibrin clots, to establish if the fibrin may prevent their relocation to the wider wound. Neuss et al demonstrated the fibrinolytic potential of MSCs to degrade fibrin clots, derived from a fibrinogen concentration

more than twice that which was used here (6 mg/ml vs. 20 mg/ml), within 24 h. The authors also reported that MSCs encapsulated in fibrin expressed both plasminogen activators (uPA and tPA) (Deng *et al,* 1996) and inhibitors (PAI) (Wei *et al,* 2001); plasminogen is a precursor to plasmin, which cleaves fibrin. Thus, they suggest MSCs exhibit control over fibrinolysis in an autocrine/paracrine manner (Neuss *et al*, 2011). Therefore, it is likely that the MSCs could behave similarly in the wound model and produce factors to facilitate their migration to the wider wound through self-regulation of fibrinolysis.

The finding that MSCs remained were found to remain viable in Green's medium was important because this medium is exclusively used to support the growth and differentiation of the keratinocytes in the TE skin, therefore MSCs must be able to tolerate the medium once at the wound site. Green's medium is supplemented with additional compounds such as adenine, insulin, T3/transferrin, hydrocortisone, EGF and cholera toxin, which are absent from standard MSC media. These factors could have affected MSC viability, which in turn would affect the outcome of a wound healing study because MSCs exert their therapeutic benefit in a dose-dependent manner (Falanga *et al*, 2007). Although at the time of writing there are no reports in the literature concerning the effects of Green's medium upon MSCs to compare the results presented with here, there are data relating to the effects of some of the components of Green's medium on MSCs. For example, hydrocortisone is an essential steroid for enhancing MSC differentiation to endothelial cells (Gang *et al,* 2006), adipose (Oishi *et al,* 2009) and neuronal cells (Mareschi *et al,* 2006) in their respective inductive media, and EGF has been used as a supplement to support MSC proliferation in serum free medium (Chieregato *et al,* 2011). In addition, Meuller *et al* recently found that insulin could promote chondrogenesis in MSCs (Müller *et al,* 2012) at similar concentrations to that of Green's medium (5 µg/ml). However, after taking into consideration that some of the additives common to Green's medium can be used in inductive media, it is unlikely that Green's medium would have exerted differentiate effects on the MSCs because each supplement alone is not capable of promoting differentiation; they must to be used in combination with many other supplements that are not present in Green's medium. For example, to achieve chondrogenic differentiation of MSCs using insulin, it is necessary to provide adequate concentrations of ascorbate 2-phosphate, dexamethasone and TGF-β1 in the inductive medium (Meuller *et al*, 2012). Taken together, Green's medium can be used to support the TE skin composites after introduction of MSCs to the wound site.

Considering Alternative Methods to Create Wounds in TE Skin

Ferraq et al recently stated: "Wound-healing studies mainly rely on mechanical methods for wound induction which are difficult to standardise" (Ferraq et al, 2007). With this in mind, the authors set out to investigate the potential of a laser-based method to create skin wounds with more control. Erbium: Yttrium-Aluminium-Garnet (Er:YAG) lasers

are capable of progressively ablating tissue a few microns at a time, without causing extensive photo-thermal induced damage; light energy (2940 nm) is selectively absorbed by water molecules which creates steam that generates an internal pressure enough to cause inorganic materials to explosively destruct before their melting points are reached (Hibst 1992; Sasaki *et al,* 2002). This so-called 'microexplosion' theory accounts for the effects of Er:YAG ablation besides thermal effects alone i.e. burning tissue. Le et al demonstrated that a relationship exists between the pulse energy of the laser and ablation depth in a murine model (Lee *et al*, 2001). Other authors have shown that the entire epidermis can be removed by exposing skin to just three pulses of light with a fluence (energy/ unit area) of 5 J/cm^2 (Alster 1999; Drnovsek-Olup *et al,* 2004). By modulating the beam energy of the Er:YAG laser, Ferraq *et al* were able to create wounds in *ex vivo* skin to varying depths, up to a mean maximum depth of 284 μm (Ferraq *et al,* 2007) Tissue, for example, could be removed from the following layers: the stratum corneum, epidermis/papillary dermis and reticular dermis using fluences of 10, 50 and 200 J/cm^2 respectively. Although at the time of writing there are no reports where lasers have been used to create full thickness wounds in skin, it is possible nonetheless since Er:YAG lasers have been used to make complete defects in the calvarial bones of mice(Cloutier *et al,* 2010). Ferraq *et al* later found that Er:YAG lasers were able to create skin wounds *in vivo* with a more uniform depth and a less variable size than those created via suction blister methods, as evaluated by OCT; they also reported the wound healing rates to be similar between the two methods (Ferraq *et al,* 2012).

The chief advantage of this method over the one developed here, is that one can generate wounds with precise dimensions very consistently. The laser for instance can be incorporated into a beam scanner so that the ablation of a defined area of the skin can be automated (Ferraq *et al*, 2012). Therefore this eliminates user-dependent variation, whereas the technique employed here, despite yielding consistent wound depth and lengths, requires skill and judgment from the researcher that only comes through careful practice. In addition, by using a scalpel, one can only produce full-thickness wounds, whereas wounds of varying depths can be produced from the laser as a function of fluence (Ferraq *et al*, 2007).

The main disadvantage of laser-based methods is the prohibitive cost of acquiring such specialist equipment; they can cost between £33,000 to £53,000 (according to emedicine.medscape.com). Additionally, although Er:YAG lasers are capable of creating wounds, the nature of the wound is very different from an incisional wound. For instance, laser ablation inevitably causes some thermal damage to the tissue, although it is very limited. Boppart et al observed that concentric rings of thermal injury were present around the site of ablation in a variety of tissues, regardless of the depth the laser penetrated, and suggested that the damage corresponded to the radial distribution of thermal energy (Boppart *et al,* 1999). Therefore, Er:YAG-created wounds are comparative to excisional

wounds, with concomitant lateral thermal injury. Whereas with the scalpel method presented here, no volume of tissue is removed; only the skin's structural integrity was compromised. This is an important distinction to note since the type of wound affects the healing response of the tissue (Monsaingeon and Molimard 1976). Burn wounds for example result in more extensive cell losses and necrosis, leading to scar formation, compared to those created via incision; thus this damage complicates the process of repair (Winter 1995). These observations were confirmed by Drapper et al after they reported consistently slower re-epithelialisation of laser-induced full-thickness wounds in murine skin compared to those which received excisional wounds (Draper *et al,* 2002). Since wound healing of TE skin happens slowly over periods of up to 14 days, and TE skin is usually only cultured *in vitro* for a maximum of 28 days under static flow conditions, it is important that the method of wounding can yield healing on a timescale compatible with the 'life' of the TE skin. Thus, incisional wounding is still the most appropriate method to wound the TE skin to study wound healing.

4.5. Summary

- TE skin can be used as an incisional wound model.
- Wound sizes could be kept consistent through appropriate blade selection.
- Fibrin was able to introduce MSCs into the wound, and cell loss from the wound cavity was minimised by sealing the base of the wound with fibrin.
- Wounds healed after 14 days and the presence of fibrin was required for wound healing.
- MSCs remained viable in Green's medium.
- The wound model was taken forward to investigate the effects of MSCs upon healing in the model.

Chapter Five:

Using Optical Coherence Tomography to Non-Invasively Image Wound Models

5.1. Aim

The aim of this work was firstly; to develop a method by which optical coherence tomography could be applied to non-invasively image wounds created in tissue-engineered skin in a consistent manner, and secondly; to develop a method of sampling wounds and determine their areas.

5.2. Introduction

There has always been a need to non-invasively image tissue especially when it comes to conducting experiments based on evaluating wound healing. *In vitro* for example, histology is the chief means by which healing can be evaluated, however it is not the most desirable method because performing a biopsy causes further trauma to the wound thus compounding wound healing. Furthermore tissue processing is time-consuming and may give rise to artifacts that can cloud microscopic evaluation. If histology is undertaken to assess an *in vitro* wound model, the sample is effectively 'sacrificed' and it is removed from the experiment. This therefore requires large numbers of samples to be used to examine tissues, particularly as they respond to injury in a time-dependent fashion.

In contrast, non-invasive imaging permits the evaluation of the same area of tissue over time. *In vivo* reflectance confocal microscopy has been applied to study wound healing in real-time with near-histological resolution, without the need to introduce fluorophores into the tissue, by detecting reflected light from endogenous chromophores. However, this technique is limited to acquiring *en face* (parallel to the surface) from the first few hundred microns into tissues, thus allowing epidermal evaluation only (Sugata *et al,* 2008; Terhorst *et al,* 2011). Alternatively non-linear confocal microscopy can be applied to image deeper into tissues and observe collagen fibre formation within a wound-bed via second harmonic generation (Zhou *et al*, 2010). Ultrasound can image much deeper into tissue, however its use in imaging skin tissue is limited due to its poor axial resolution, and fine structural features of the skin, such as the epidermis, cannot be observed (Norisugi *et al,* 2011).

Optical coherence tomography (OCT) is a relatively new platform, which bridges the gap between confocal microscopy and ultrasound in terms of axial resolution and imaging

depth. OCT can produce real-time depth-resolved 2D cross-sectional images, from up to 3 mm into tissues, in a non-invasive manner (Zysk *et al*, 2007). In OCT, near infrared light is directed into tissue, and light which is backscattered from the tissue is computationally processed to produce a grey-scale, cross-sectional, tissue map. In this respect, because OCT produces depth-resolved images, it is often described as the 'optical analogue' of ultrasound (Marcshall *et al*, 2011). OCT systems can generate images with axial resolutions of 1-15 μm, which is up to two orders of magnitude greater than can be achieved via conventional ultrasound, and lateral resolutions in the order of 10 μm (Povazay *et al,* 2002; Drexler 2004). As such, 'optical biopsies' of skin can be provided from OCT with good correspondence to histology; structures such as the stratum corneum, epidermis and dermis can all be clearly differentiated. Thus, OCT is becoming increasingly used in the field of dermatology (Gambichler *et al,* 2011) and for the evaluation of wound healing (Wang *et al,* 2008; Barui *et al,* 2011; Ferraq *et al,* 2012). In this study Swept-Source OCT (SS-OCT) was used to provide non-invasive tissue assessments of wound models constructed from TE skin.

5.3. Results

Structural Features of Skin as Observed by OCT

The ability of OCT to non-invasively image TE skin and identify its structural features was investigated. Figure 5.1 demonstrates that OCT is capable of imaging to a depth of 0.7 mm into the tissue and structures such as the epithelium can clearly be differentiated from the underlying connective tissue; in addition OCT can reveal some topographical details. The epithelium can be identified as a band comprising two layers of signals that differ in intensity and morphology. The uppermost layer is high in pixel intensity and presents as bright strip in the image. This is most likely due to the higher reflective, or greater scattering, properties of the densely organised keratin of the stratum corneum. The greater the scattering from a tissue region, the brighter the pixels from that region are portrayed. Below the keratinized layer lies a band that has a faintly distinguishable wave-like appearance, which is similar in appearance to the rete ridges that can be identified by histology. This region is also composed from pixels that are sparser and of lesser intensity than the superseding layer. Taken together, this region most likely represents the area in which the proliferative epidermal keratinocytes reside. Collectively, these two distinct bands mark the region of the epidermis, which constitutes 200-300 μm of the overall depth of the image, which is almost one third of the total depth the OCT apparatus is able to image. This thickness of the epidermis determined by OCT is similar to that which is observed by histology. Below the epidermis, the pixel intensity becomes higher again; this junction describes the epidermal/dermal junction (DEJ) below which lies the dermis. The dermis is comprised of connective tissue, mainly collagens, and because the pixels pertaining to this area are higher in intensity than the overlying epithelium, this suggests that the connective tissue is able to scatter and/or reflect more light than the adjacent epithelium.

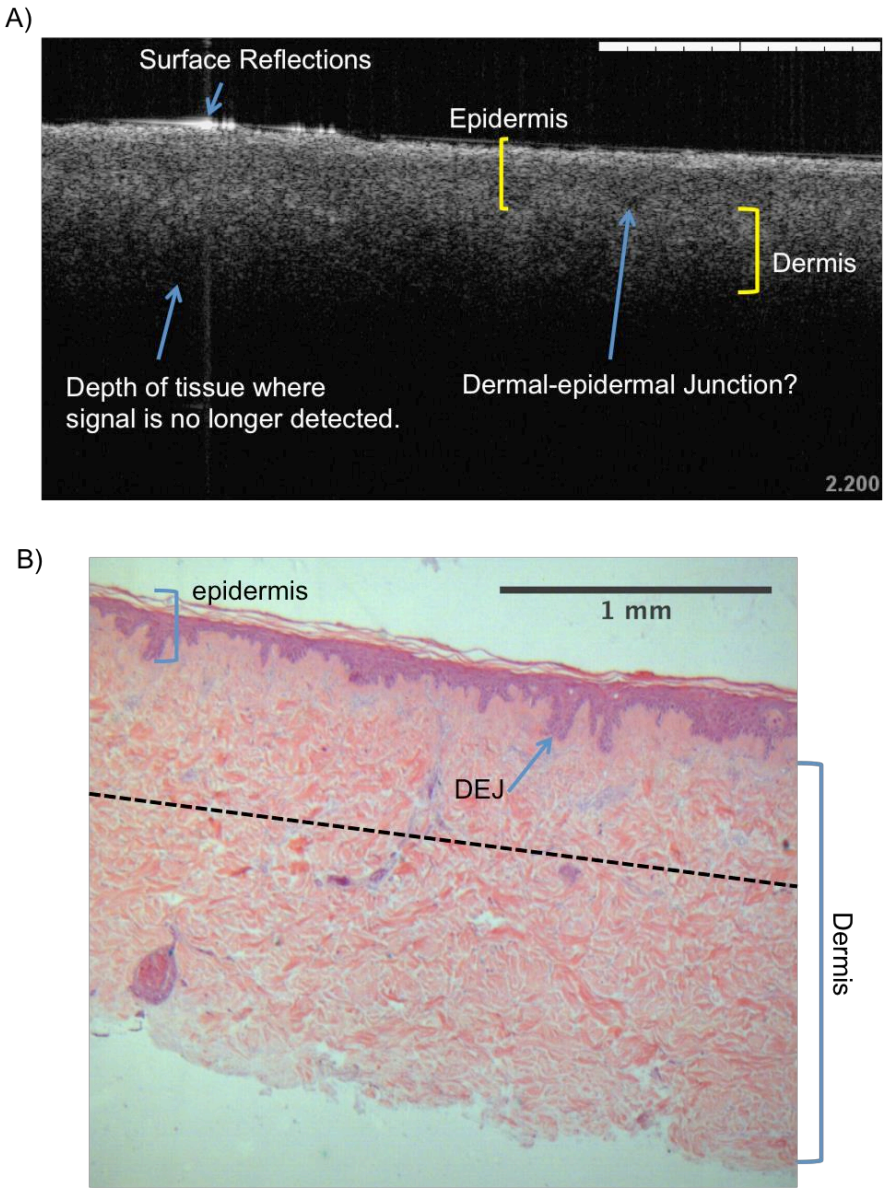

Figure 5.1. *Comparison of OCT to histology of TE skin. TE skin was maintained at air-liquid interface for 7 days and imaged by OCT A) and by light micrograph following histology B) (scale bars: 1 mm). The depth to which OCT can visualise is marked on the histological section as a dotted line for comparison.*

Imaging the Wound Model

Performing OCT on the wound model demonstrated that it was capable of clearly identifying the wound cavity and the presence of the fibrin clot within it (Figure 5.2). Figure 5.2 however, is only a single slice through the tissue. One of the advantages of OCT is that, by moving the sample through the path of the imaging laser, multiple optical sections from the tissue can be acquired, which can provide visual information from a wide area of the tissue.

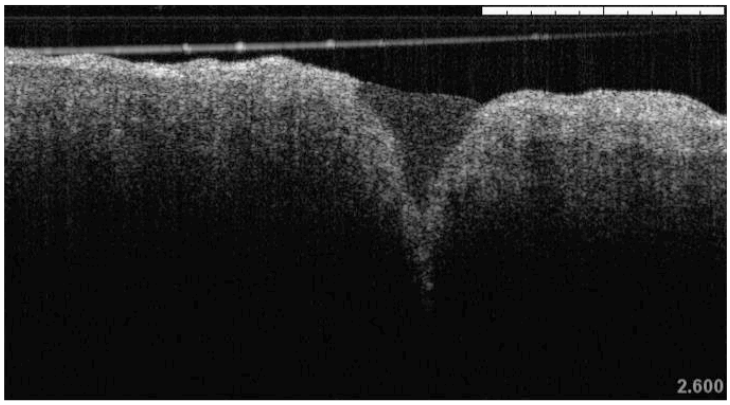

Figure 5.2. *Wounded TE skin as seen by OCT. The fibrin clot can be seen within the v-shaped wound cavity (scale bar: 1 mm).*

Consistency in Imaging

One of the main challenges in using the OCT system to image TE skin wound models over time, was ensuring that the wound area was adequately sampled, and that the same area was imaged each time. To address the issue of consistency, it was decided that a reference point needed to be marked on the surface of each sample from which the laser could be aligned before imaging commenced. However, because the laser was in the near infrared (NIR) part of the spectrum of light, the laser was invisible to the naked eye. The only way therefore to determine the position of the laser was to place a photosensitive card (Figure 5.3) underneath the lens, however the card obscured the sample. The solution to this problem was to install a visible (red) 'aiming' laser into the same optical path as the IR OCT light-source. This way the visible laser could be aligned with a reference point on the sample by manually positioning the sample on the stage, until the aiming laser was at the center of the reference point.

As for the reference point itself, it had to be a marking that did not move or fade away over the course of a 14-day experiment. Initially the idea was to stick a small pin in the surface of the composite, however this was decided against because this would cause further trauma to the composite. DED was used to try to find the best way to mark the skin. A dot of permanent ink from a marker pen was made on the surface of the DED, however the dot of ink that could be placed became diffuse due to the surface of the DED being moist. However because TE skin has a water-repellent keratinised epithelium, it could be successfully marked. In addition, this method of marking the skin was thought to be non-toxic to the composites due to the barrier action of their cornfield layer. Dark markers such as blue, black or green provided the best contrast against the red imaging laser and allowed the laser to be easily pin-pointed to the center of the reference point, which was placed adjacent to one edge of the wound margin at the head of the wound (Figure 5.4).

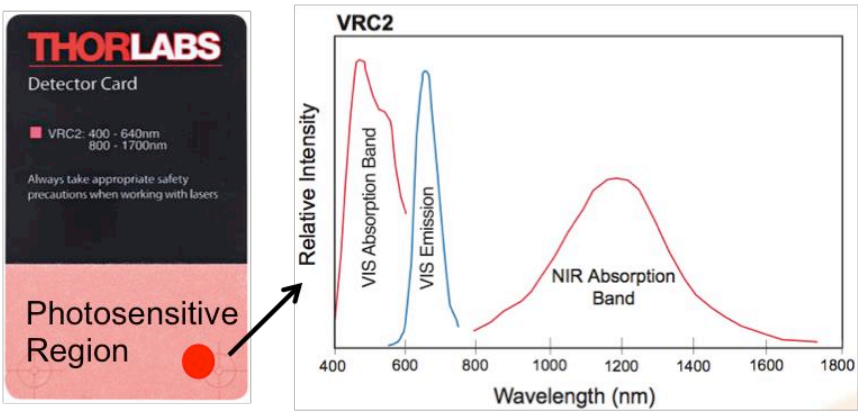

Figure 5.3. *IR detector card. The photosensitive region of the card was placed under the IR laser, and energy absorbed at the laser's focal point stimulated visible (red) fluorescence from the region of the card where the beam was aimed.*

Sampling the Wound

Next, the most appropriate way to sample the wound was determined. It was necessary to acquire images from the full length of the wound (10 mm) starting at the reference point, so that the widest portion of the wound was captured every time a wound sample was imaged. This was important because it was only from corresponding regions, within a sample imaged at different experimental time points, that measurements of wound volume could be made and compared for the purpose of evaluating wound healing.

To start with, samples placed on the stage under the lens were manually moved a fixed lateral distance (0.01 mm) by turning a dial, so that an image could be captured and then the stage moved from the reference point (a fixed amount) before another one was taken. For a wound 1 mm in length, one could take up to 100 images manually. This method was very time consuming, especially with multiple samples, and as needs progressed, an automated motorised stage (ThorLabs, PT1-Z8) was introduced into the imaging apparatus. The motorised stage was capable of moving any increment from 10 µm to 1 cm and had a maximal linear travel of 25 mm (Figure 5.4). Therefore the stage could make up to 1000 incremental movements over a 1 cm distance allowing for an equal number of images to be captured; an image could be acquired in between each movement of the stage. However in practice such a high level of sampling was neither possible nor practical. Firstly, the computer had insufficient memory to achieve this, therefore sampling volumes had to lie within the capabilities of the computer. Secondly, it would take a great deal of time to acquire such a quantity of images; OCT imaging itself is very rapid and images can be produced in a fraction of a second (A scan rate, 10,000 Hz), however the time it takes for the stage to move before each image can be captured was a rate-limiting factor.

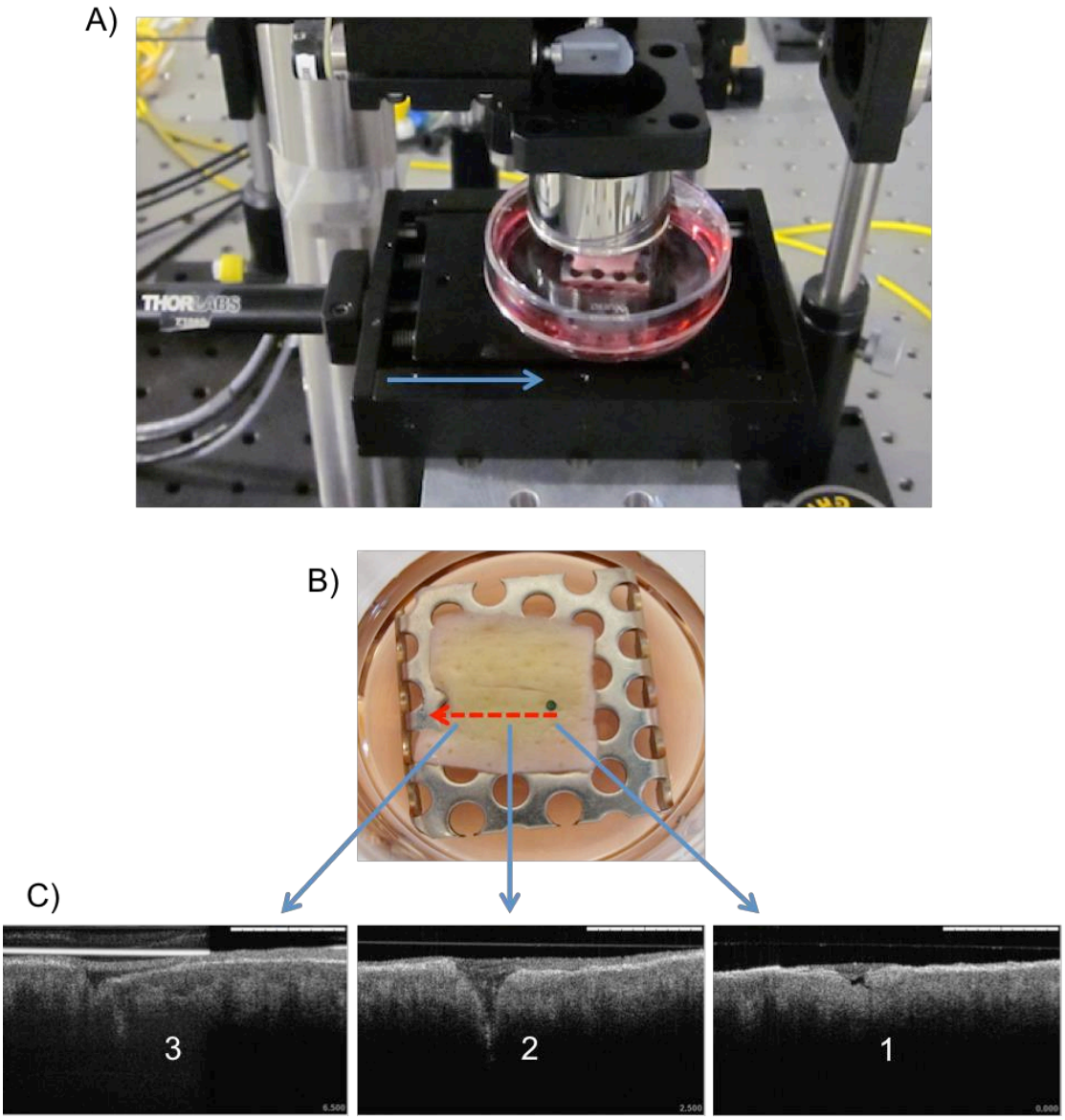

Figure 5.4. *OCT set-up. A) Photograph of a TE skin wound model resting on the motorized stage below the lens. The arrow indicates the direction the stage moved during image series acquisition. B) A close-up of the wound model. The green dot present at the wound edge is the reference point for the aiming laser. The red dotted arrow indicates the direction the sample moved relative to the imaging laser when the stage was moved. C) OCT images produced at points along the wound from the reference point; image 1 was taken closest to the reference point, and image 3 the furthest way from the reference point (scale bars: 1 mm).*

Averaging was a parameter that was taken into consideration when deciding the best way to sample the wound. Averaging was a method that was used to 'clean-up' the image by reducing the amount of noise that was present in an image. A given section of skin could be imaged a set number of times (defined as the averaging factor), and the average pixel intensities from the image series could then be calculated and displayed. The maximum averaging factor that could be achieved by the system was 5. An averaging factor of 3 was used to acquire wound images because it provided a good compromise between

image quality and time (Figure 5.5). Again, it was not the increase in the amount of images taken of a given sample of skin that was a limiting factor, because of the rapidity with which OCT can image, but rather, the lag-time it takes for the computer to do the processing required to produce an image resulting from averaging.

Finally, acquiring 200 slices (images), spaced 50 μm apart, captured with an averaging factor of 3 was settled on as the optimum sampling, because it provided a sufficient volume of images to be able to detect small changes in wound morphology between slices, and the imaging could be completed in a reasonable time scale. To image a sample took approximately 7 min, and in an experiment a minimum of three samples would be required to be imaged/ experimental condition, therefore this could take 21 min (3 samples x 7 min); it was not desirable to have the wound models out of the incubator for longer than 30 min.

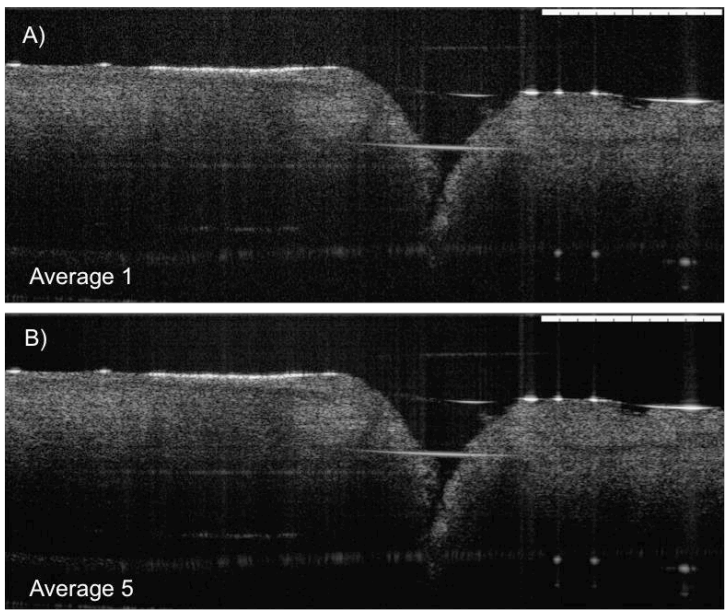

Figure 5.5. *The effect of image averaging. A) base-line image obtained from TE skin following wounding (Averaging factor 1). B) an OCT image of the area in A) acquired with an averaging of 5. The resulting image has an improved quality in terms of having a reduced level of 'speckle' particularly in the darker regions of the image.*

Measuring the Wound

Selecting the Widest Portion of the Wound

The most complete way to evaluate how wounds were healing would be to measure the total volume the wound occupied and monitor how the wound volume changes over time. This could be achieved by measuring the wound volume presented in each individual slice and adding the volume from each slice together, however this was not done for practical reasons. Since there was no way to automate image processing, each image had to be measured manually. For example, if 100 images were acquired at each time point over the course of healing (of which there were five) and there were three samples for three different experimental conditions (100 x 3 x 3 x 5 = 4500), one would have to manually measure over 4000 frames for the whole experiment which would be too time consuming.

Therefore it was decided to identify and compare the 'widest portion' of the wound that presented between time-points for any given sample (Figure 3.7), to quantify wound healing. To identify the 'widest portion', a montage was created in image J from a selection of images captured along the length of the wound, and the image that appeared by eye to contain the largest wound area was identified. Once identified, 10 additional images, 5 earlier and 5 later in the sequence were also selected (Figure 3.6). These 11 images spanning a combined distance of 550 μm through the wound, (5.5 % of the total wound length), could have their volumes measured.

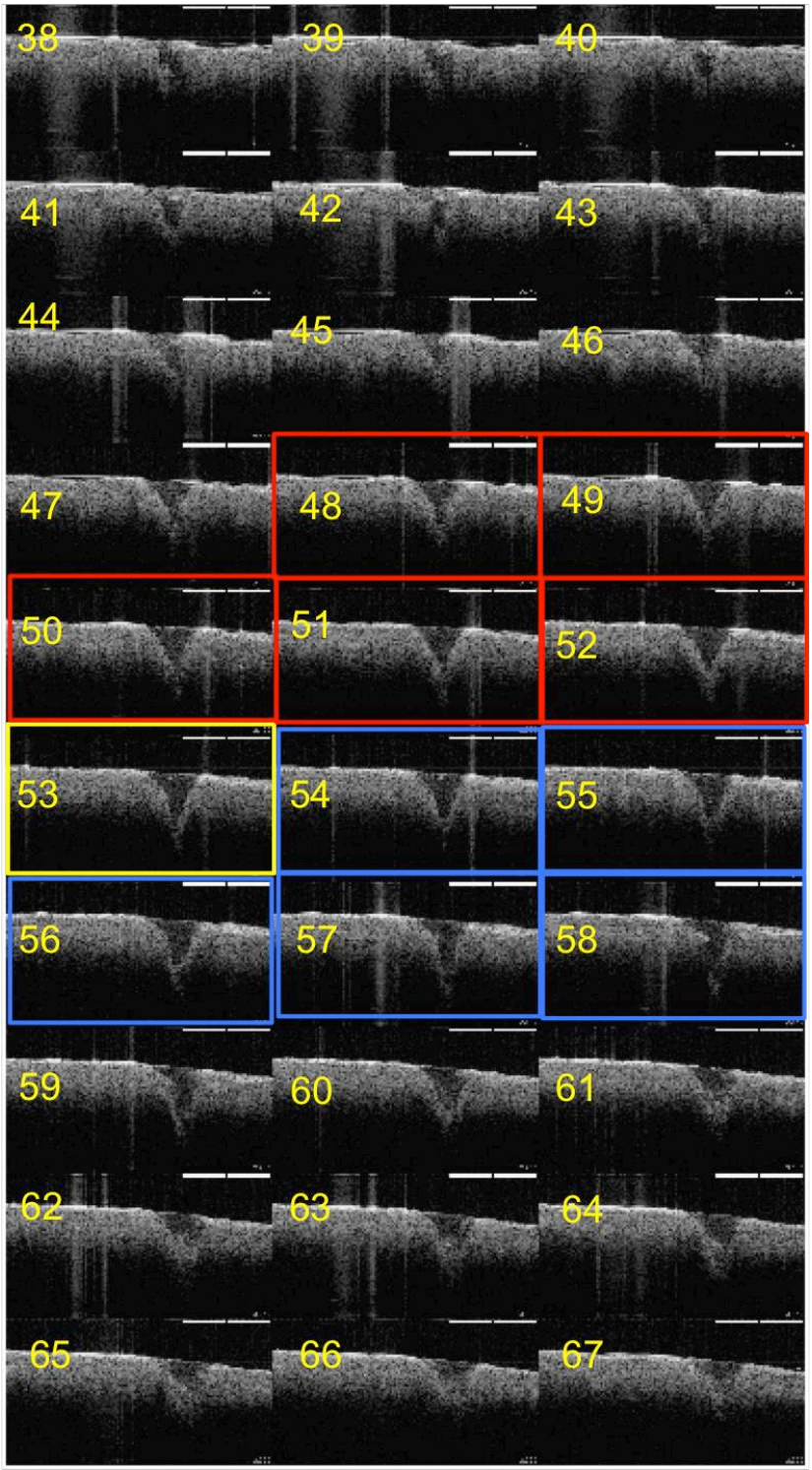

Figure 5.6. *Selecting the Widest Portion of the Wound. A montage was created in image J from series of images collected from performing OCT on a wound model. The numbers indicate the position each image was taken from the reference point. Image 53 in the yellow box shows the image in the series that hold the largest wound area. The images with the red or blue borders were also selected. Collectively these images highlight the 'widest portion' of the wound, and wound area measures were taken from this region of the sample. This method was repeated for each sample and the areas were compared.*

Achieving consistency in identifying the widest portion of the wound between time points

In order to achieve consistency in measuring the change in wound volume in a sample over time, it was important to ensure that the identical region of the wound was identified at each time point so that a direct comparison could be made. Morphological features that were clearly distinguishable and common to all the imaging sequences, gathered from a sample at different experimental time points, were used as internal reference points (Figure 5.7). These internal reference points allowed corresponding sections of the wound to be compared as time progressed.

For example, in Figure 5.7 the internal reference point identified at day one (indicated by the yellow arrow) was located 138 slices (6.85 mm) from the starting point (external marker), whereas the corresponding point could be found at slice 136 (6.75 mm) from the starting point at day 3. Therefore the starting points were different by 0.1 mm due to human error in aligning the aiming laser with the external marker on the surface of the composite between time points. Therefore this method provided accuracy and consistency in comparing like-for-like regions in wounded samples between experimental time points.

Therefore to reduce the effect this error had on identifying the ‘widest portion’ of the wound between time points, the locations of the internal reference points were noted, and the shift in the location of internal reference between time points was used to determine where the corresponding ‘widest portion’ was located. For example, in Figure 8 there was a difference of two slices between the corresponding internal reference points from the images attained at day one and day three. The reference point at day three was observed two slices earlier where it was observed at the previous time point. Therefore the corresponding 'widest portion' of the wound at day three (slice 32) was judged to lay two slices behind where it was identified at day one (slice 34).

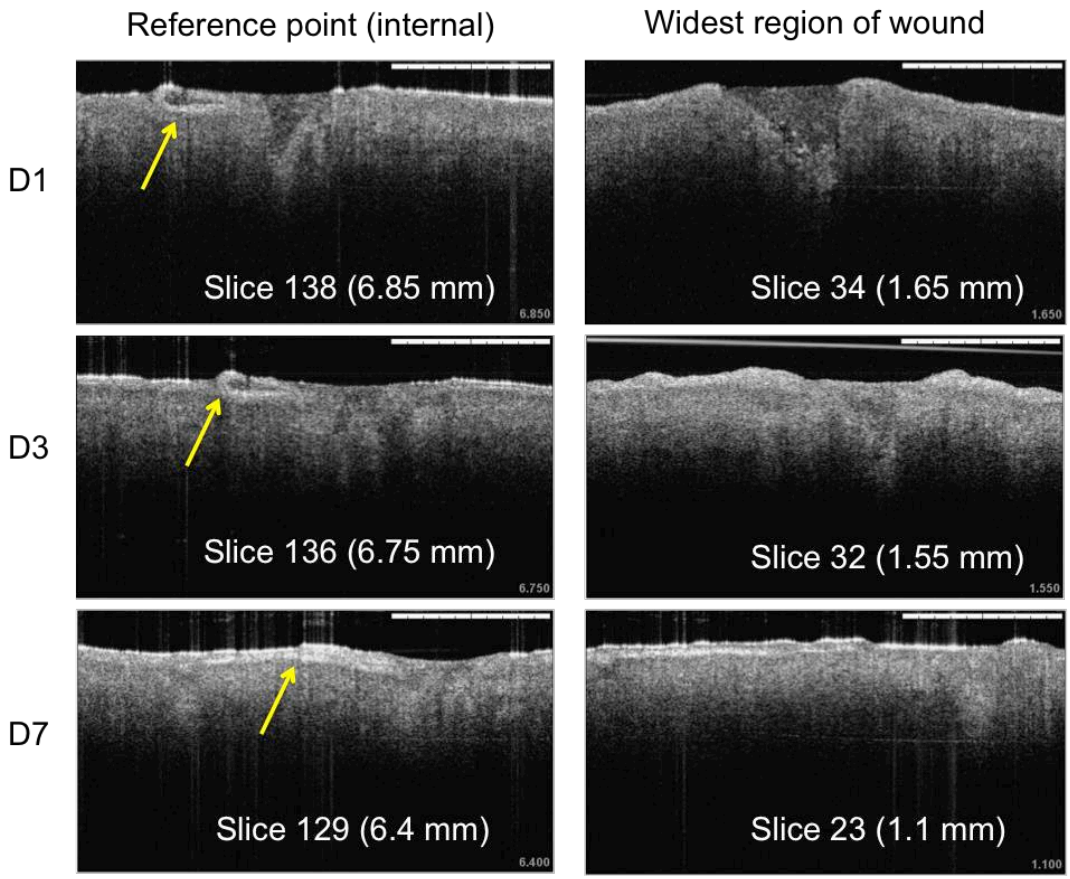

Figure 5.7. *Achieving consistency in identifying the widest portion of the wound between time points. The images in the left column show the internal reference points (yellow arrow) that were compared between time points (Day 1, 3 and 7). The images in the right hand column show slices from the widest regions of the wound. These could be identified from noting the distance the widest region lay from the internal reference point from the previous time point. The position of the slice within the series of images is shown within each image and the distance from the external reference point is indicated in brackets. Note- it was important that identifying features were located outside of the wound because the scattering in the wound becomes greater over time, which would make finding features at the wound site harder over time.(Scale bars: 1 mm)*

Measuring the Wound Area

After identifying the widest portion of the wound, the area of each of the selected slices making up the 'widest portion' was determined in Image J. The outline/ margins of the wounds were manually traced using polygonal draw tool, selected form the toolbox (Figure 8). The starting point for drawing was always the top of the keratinized epithelium (white band in the OCT image). Once the area was traced, the shape was saved as a region of interest (ROI) in the ROI manager. Once all 11 images making up the 'widest portion' had their wound margins demarcated and added to the ROI manager, the number of pixels the wound occupied in each image could be measured. Since each pixel is known to occupy an area of 1 μm^2, the number of pixels within the wound therefore was equivalent to the area of the wound in μm^2.

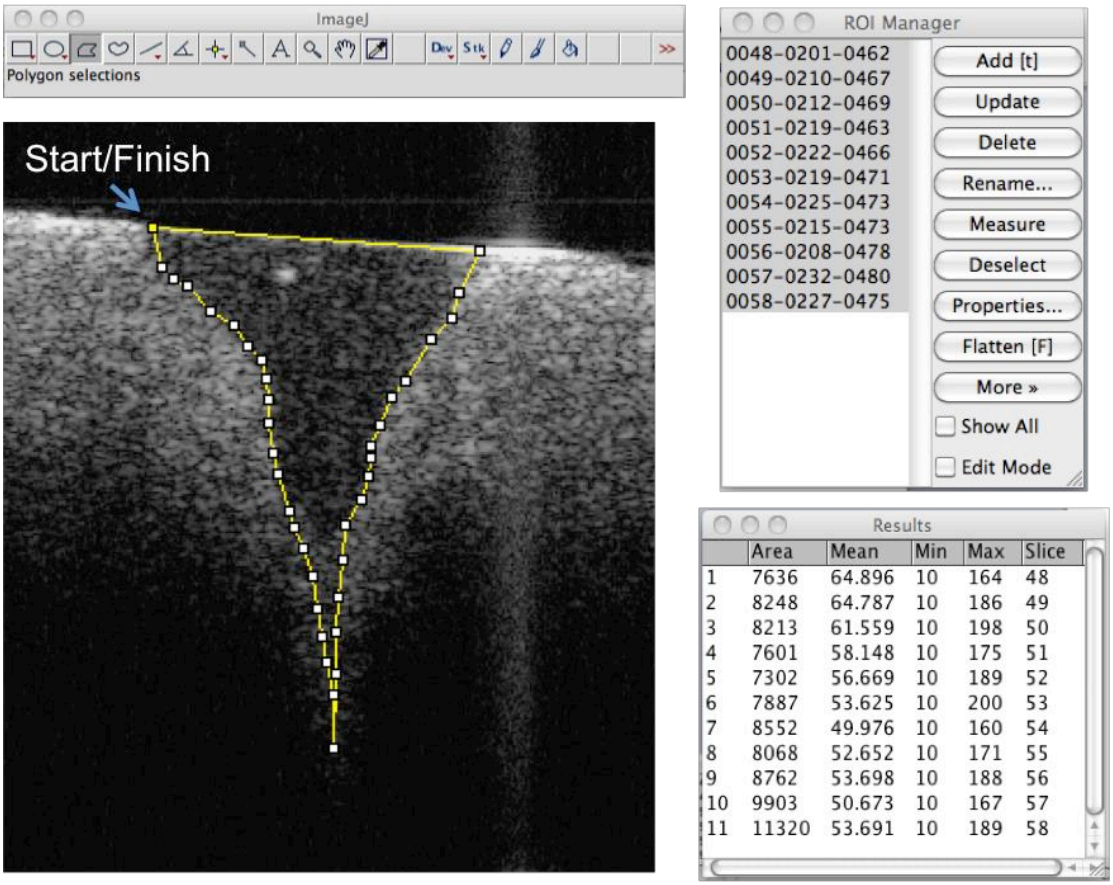

Figure 5.8. *Measuring the Wound Area. The polygonal draw tool was selected from the toolbox in Image J (top left panel). The outline of the wound was drawn by manually starting from the top of the epidermis (marked by the arrow). Once the wound had been outlined, it was added to the ROI manager (Top right panel) and when all 11 images in the selection had been added to the ROI manager, the ROIs were selected and measured by clicking the measure button in the ROI manager. A results box then appeared (Lower left panel) which displayed the number of pixels in the area of each wound as well as the mean, minimum and maximum pixel intensities.*

Other Practical Considerations

One of the things that became apparent when OCT was first performed on the TE skin was that the top surface of the composite had to sit a maximum distance of 3 mm from the underside of the lid of the petri dish; because if the samples were outside this range, the image of the lid would obscure the sample as demonstrated by Figure 5.9. Because the thickness of the skin used to make the composites could vary, due to the difficulty in preparing split-thickness skin of consistent thicknesses from different donors, or even within a donor preparation, and the height of the grids used to maintain ALI were fixed, there was a need be able to adjust the distance of the skin to within 3 mm from the lid to prevent image obstruction by the artifact of the lid.

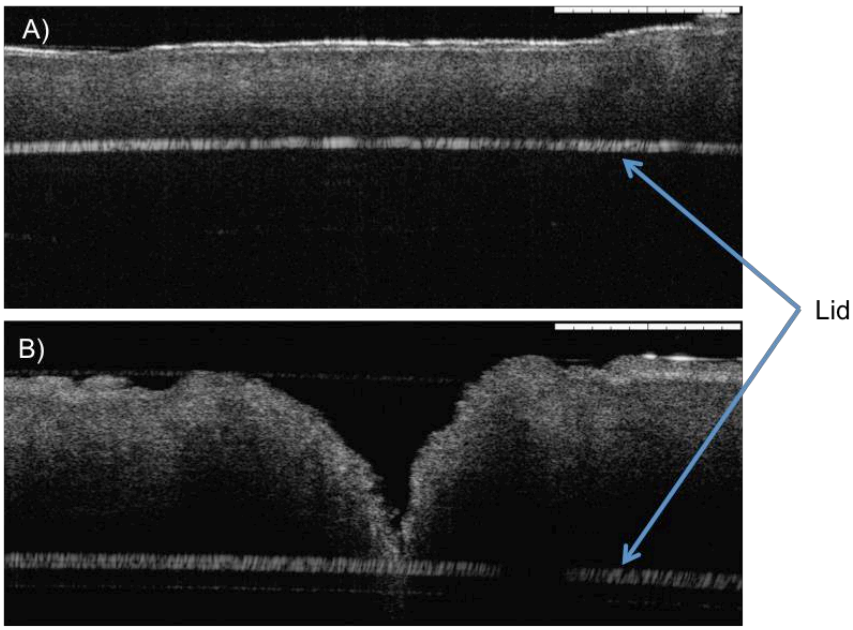

Figure 9. *Artifacts from the tissue culture lid affecting OCT imaging. A) non-wounded TE skin. B) wounded TE skin The tissue culture lid, marked by the arrows in A) and B), was able to scatterer light, and partly obstructed the samples. (Scale bars: 1 mm).*

It was thought that an alternative material that could be cut to height could be used instead of the stainless steel grids whilst OCT imaging was performed. The material had to be porous to allow an ALI (air-liquid interface) to be maintained during imaging, non-toxic to the cells, easily manipulated and be able to be sterilised. Five different foams were tested for their suitability for use, because such materials are porous and can be easily cut to size. The materials' ability to uptake medium was observed. Sponges were compressed between forceps and the foams were scored on a 1-3 basis (with 1 being poor, 2 moderate and 3 good) of their ability to uptake medium. Foams 1, 2 and 4 performed best and Figure 5.10 shows them to uptake far more than the others. However after 24 h of contact with the medium, foam 4 produced some leachates that were visible in the medium, as too did foam 5, thus suggesting that they were unstable in medium for prolonged periods. Therefore only foams 1 and 2 were taken forward to investigate if they could firstly be sterilised and maintain their integrity, and secondly not cause toxicity to fibroblasts. After 24 h in sterilising agent (70 % IMS, v/v), both appeared unchanged structurally and no visible leachates were reported. The foams were thoroughly washed from the IMS and then a toxicity study was carried out. Human dermal fibroblasts (HDFs) were cultured in 12 well-plates and transwell inserts containing foams were placed in contact with the medium surrounding the cells. After 24 h, an MTT assay for cell viability was performed. The foams were found not to affect cell viability after 24 h, indicating that there were no leachates from the foams that were harmful to the cells (Figure 5.11).

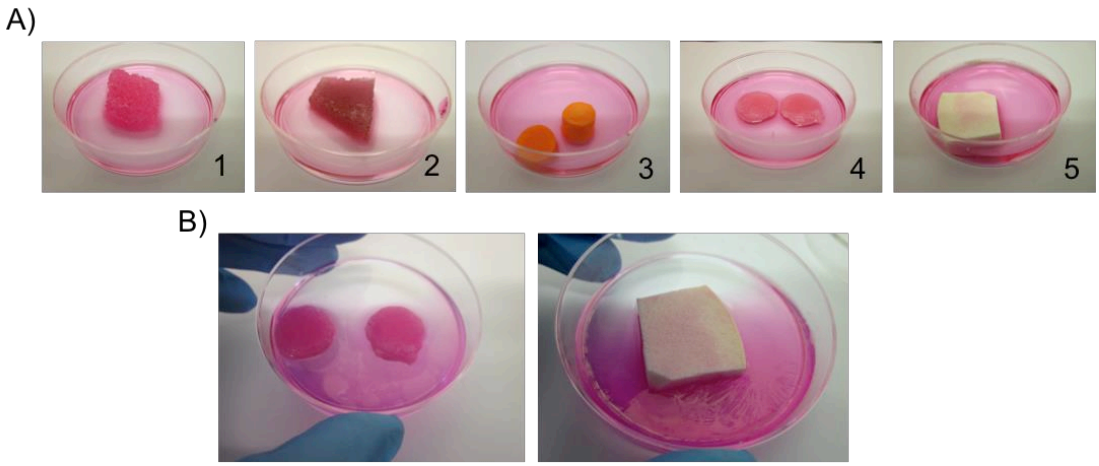

Figure 5.10. *Foams. A) The absorption of medium into each of the foams 1-5. The foams are listed as follows: 1) Boots fragrance free exfoliating facial sponge, 2)- Washing-up sponge, 3) Boots ear plugs, 4) Boots essentials sponge, 5) Boots Ramer sponge. B) Leachates from sponge 4 and 5 after 24 h in medium.*

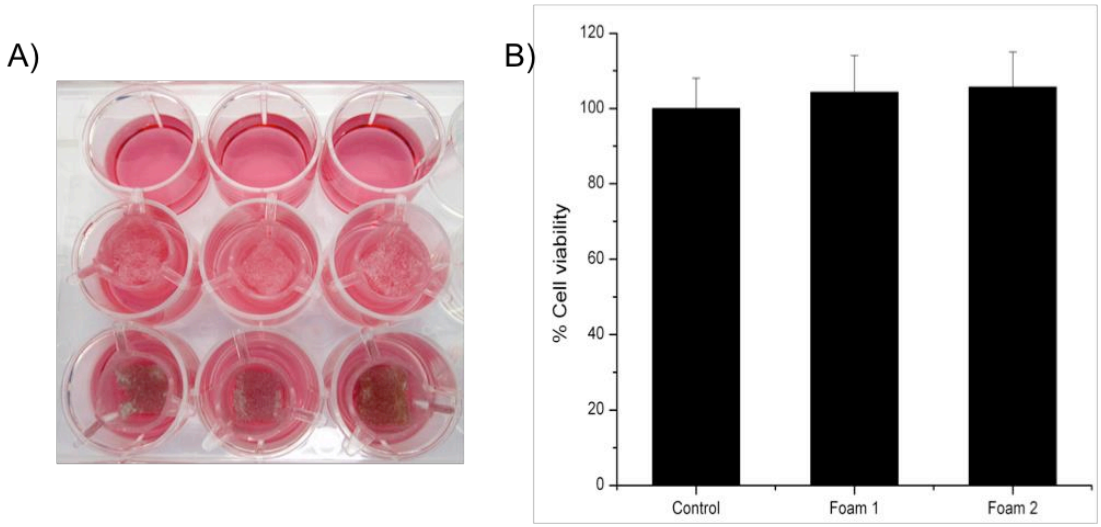

Figure 5.11. *Toxicity of Foams. A) HDFs in culture with the foams contained in Transwell inserts. B) Cell viability by MTT assay (data normalised to the control). Data represents the mean ± SEM (N=3, n=3).*

5.4. Discussion

Two types of OCT were available to our research group: TD-OCT (Time domain OCT) and SS-OCT (Swept-source OCT). For these experiments SS-OCT was chosen over TD-OCT because it had been previously demonstrated to perform better; a former member of our group found it proved more sensitive than TD-OCT and was able to distinguish between the cellular and keratinized layers of the epidermis (Hearnden, 2010). OCT was capable of delineating the wound margins and identifying the fibrin clot within the wound. Compared to *ex-vivo* skin, the quality of the images obtained from TE skin was comparatively poorer; this observation was noted by previous authors (Krstajic *et al,* 2008; Smith *et al,* 2010). However, the images were of sufficient quality to discriminate structural features of the skin. A reason for this difference could be due to the absence of 'materials' from TE skin, such as melanocytes and endothelial cells, which contribute to skin's scattering properties (Lister *et al,* 2012).

OCT was demonstrated to be a simple way of obtaining gross structural information from skin without the need for histology. A limitation of histology is that it requires a sample to be removed from the experiment. OCT however, due to its non-invasive nature, allows wound healing to be tracked over time within a sample. Histology can also produce artifacts such as foldings, especially in the wound area where tissue integrity is compromised, and during processing, differential shrinkage between the tissue and the implanted material can result in fracture or detachment of the material; together these make objectifying wound healing difficult (Yuan 2010).

In addition the OCT apparatus was capable of imaging in series through the length of the wound in an automated fashion. The advantage of this is that information can be gathered over the entirety of the wound at any given time-point. The main challenge was achieving consistency in imaging to ensure that wound measurements could be compared between time points within a sample. Consistency was achieved by adding a reference point to the surface of the samples and adding a visible laser to the imaging beam path, in this way the laser could be aligned with a fixed point on the sample, thus imaging could proceed from a fixed position. The optimal sampling was determined based on the time it takes to image the samples, of course this could be adjusted by users in the future, depending on their requirements.

Gathering as many images from the wound area as possible would be the most complete way to evaluate the wound. The imaging system had an A-scan rate of 10,000 Hz, therefore it was capable of performing imaging in a fraction of a second, and the motorised stage could move at increments of 10 um, thus 1000 images could be acquired from the 1 cm wound. Additionally the imaging processing software could perform an averaging

function from 5 B-scans which produced the clearest images. However it was neither possible nor practical to operate at this level of sampling due to limitations of time; it was important to perform imaging in a timely manner so that the samples were not out of the incubator for extended periods. Averaging took considerable time because it was very demanding on the computer's processing power, and the stage took several seconds to move each increment. Therefore a compromise was reached by sampling the wound every 50 um using an averaging factor of 3. It is possible that advancements in computer processing performance and stage movement rapidity could increase the number of images that could be acquired in a given time.

Wound areas could be determined by firstly identifying the widest region of the wound, and segmenting the wound margins from a series of images within the widest region of the wound. The sum of the wound area from the 11 slices comprising the 'widest portion' of the wound could then be compared between time points for a given sample to provide a quantitative assessment of wound closure over time. The wound area, as determined by OCT, on the day of wounding could then be normalised to 100 %, and reductions in wound size overtime could be reported as a percentage reduction from an earlier time point. Thus OCT allows wound healing to be quantified non-invasively (see Chapter 6). One limitation with this method was that manual segmentation is open to subjectivity in defining the wound margins. Manual segmentation of wound areas was opted for after automatic segmentation proved ineffective using Image J. Image segmentation is a key tool that contributes to diagnostic evaluations, however accurate segmentation of structures of interest within a tissue presents a major challenge for the following reasons. Firstly, as is the case with OCT images of skin, the target objects lack strong boundaries, and secondly, regions within a tissue often have similar intensity profiles (Song *et al,* 2013). In light of this need, Dr S.J. Matcher, Reader in Biomedical Engineering, is currently developing an automated segmentation plug-in for Image J that will work well with OCT images. The additional advantage of automatic image segmentation is that it vastly increases the speed data extraction from a series of images.

5.5. Summary

- OCT could be effectively applied to image TE-skin wound models. Structural details can clearly be identified such as the epidermis, dermis and fibrin clot.

- Wounds could be adequately sampled by OCT. The ‘largest portion’ of a wound could be identified and manually segmented to determine wound areas.

- Consistency in the identification of the 'largest portion' of a wound was achieved by identifying internal reference points within images. Thus the same region of a wound could be compared over time to evaluate wound healing.

- The OCT methodology was successfully carried forward to study the effects of MSCs in the wound model (Chapter 6).

Chapter Six:

Investigating the Effects of MSCs in Model Wounds Derived from TE skin

6.1. Aim

The aim of this work was to incorporate bone marrow-derived MSCs into TE skin wound models, and evaluate their benefit to the wound using OCT to assess wound healing in conjunction with standard histological methods.

6.2. Introduction

In vivo wound models most closely simulate human wounds in that they make use of the hosts immune and vascular systems; as such they are widely used to evaluate therapeutics. However animal models such as mouse, rat, rabbit and guinea pig are not without their limitations (Lindblad 2008). Due to distinct physiological and anatomical differences in these animals from humans, wound healing proceeds largely through wound contraction, which is brought about via the panniculus carnosus. This subcutaneous muscular layer is absent from humans, and wound healing commences by granulation tissue formation followed by epithelialization (Wong *et al,* 2011). Also, studies using animal models require large numbers of animals (replicates/ experimental condition) to be used to account for intraspecies variation, which can be costly, and stress experienced by animals in laboratories can negatively influence wound healing (Steinstraesser *et al,* 2010).

Therefore, *in vitro* experimental wound models that are convenient, easy to use and reproducible form a vital part in evaluating novel therapeutics and establish their mechanism of action. Wound closure is most commonly simulated by the 'scratch' assay, whereby a gap is created in a monolayer of cells and cell migration/proliferation is monitored as the gap is closed (Laing et al, 2007). However this model lacks aspects multi-dimensional such as three-dimensional architecture and additional cell types. There are many models that achieve 3D culture, which are better representative of wound physiology than 2D systems.

These include: co-culture systems, and collagen gels seeded with both keratinocytes and fibroblasts (Khetani and Bhatia 2006; Schindler *et al,* 2006). However, fibroblasts cultured in 3D matrices, typically composed of type I collagen or fibrin, can alter their phenotype (Gillery *et al,* 1989). Human skin equivalents such as TE skin possess a differentiated epithelium, containing a stratum corneum, which is histologically similar to *in vivo* skin. TE skin is composed from human dermis onto which primary keratinocytes and

dermal fibroblasts are seeded. The so-called 'composite' is then cultured at an air-liquid interface to stimulate keratinocyte maturation. Chapter 4 demonstrated that a wound-healing model could be developed from these TE constructs, and as such they may be used to evaluate novel therapeutics.

MSCs are biologically active therapeutics that are capable of accelerating wound healing, and they are considered to mediate their therapeutic effects via paracrine mechanisms (Hocking *et al*, 2010; Zou *et al*, 2012). Numerous studies conducted using so called MSC 'conditioned medium' have, both *in vitro* and *in vivo*, been shown to accelerate wound healing by their secreted factors (Kinnard *et al*, 2004; Chen *et al*, 2008; Volk *et a*l, 2008; Kwon *et al*, 2009; Walter *et al*, 2010;). For example, Chen et al demonstrated that MSCs produce a range of factors including: VEGF-α, IGF-1, EGF, KGF, angiopoietin-1, HGF, macrophage inflammatory protein-1alpha and beta, stromal derived factor-1 and erythropoietin, and they showed that conditioned medium could only stimulate cell migration and proliferation from keratinocytes and macrophages (Chen *et al*, 2008).

This chapter is an extension of the preceding work. Here, MSCs were incorporated into wound models derived from TE skin, as described in Chapter 4, and cell culture medium from the wound models was assessed by ELISA to detect the relative amounts of hepatocyte growth factor (HFG), Interleukin-8 (IL-8), and basic fibroblast growth factor (bFGF), all of which are essential to wound healing (Demidova-Rice *et al,* 2012), to determine if their presence could be associated with any benefit the MSC provided to wound healing in the model. OCT imaging was applied to non-invasively image wound healing outcomes in the presence or absence of MSCs. OCT had previously been shown capable of detecting the epidermis including the stratum corneum (Chapter 5).

6.3. Results

Evaluation Wound-Healing Outcomes via OCT

TE skin wound models were prepared as previously described (Chapter 4). Briefly, TE skin was maintained at an air-liquid interface for 5 days, and selected composites had 10 mm incisional full-thickness wounds made in them. The wounded composites were then divided equally into two groups; one group received fibrin alone into to the wound cavity, the other group had 1 x 10^5 MSCs incorporated into the fibrin clot, which was also inserted into the wound. As a contro, a set of TE skin composites were not wounded. The samples were then imaged by OCT, as described in Chapter 5, over the course of 14 days, with sampling every 3-4 days.

OCT revealed that unwounded samples of TE skin showed a progressive thickening of the hypolucid band from D1 to D7, and thereafter it remained similar in thickness (Figure 6.1). The hypolucid band presents as a bright white layer (high pixel intensity) in the uppermost region in the images, and results from the highly light-scattering properties of the layer. This layer was absent from decellularised dermis (DED), which contained no epithelium (Figure 6.2).

Of the TE skin samples that contained the wound, fibrin could clearly be seen within the wound as a region of lightly scattering material compared to the surrounding tissue, which was brighter due to it transmitting light less. OCT showed the cavity within the wounded TE samples to reduce in size over time, and by day 10 the cavities created by the wounds were almost indistinguishable in appearance from the surrounding tissue. In DED however there was no decrease in the size of the wound over time, thus indicating that cells were required for the clot to regress (Figure 6.2).

By day 3, wounds that contained MSCs showed the presence of an intense band over the top of the fibrin clot, which was similar in intensity to the hypolucid region either side of the wound; this was absent from the wounded samples without MSCs. This hypolucid region above the fibrin clot grew progressively thicker, and became continuous with the surrounding hypolucid material. By day 7, the MSC containing group appeared to have a scattering layer over the area of the wound/clot that was continuous with the surrounding hypolucid band. A similar band only appeared in the wound samples (no MSCs) at a later time point of 7 days.

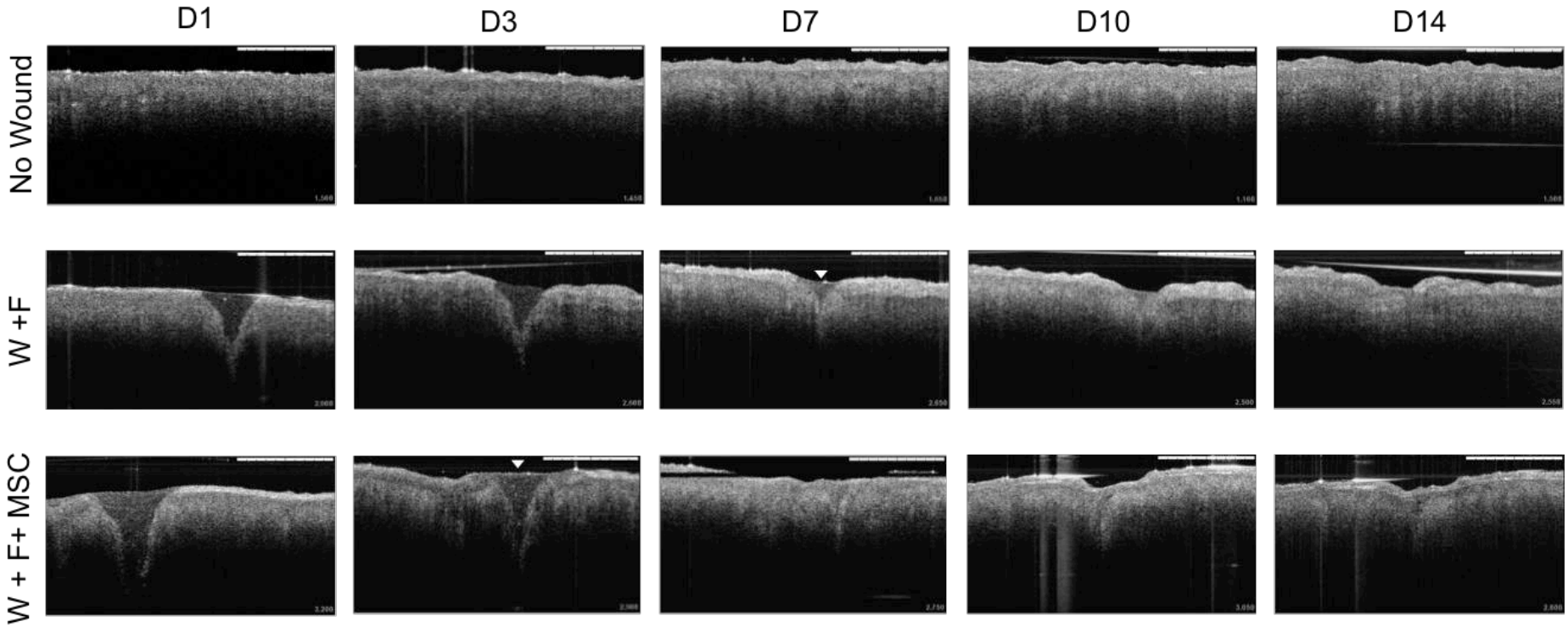

Figure 6.1. *Wound healing of TE skin imaged by OCT over 14 days (D1-D14). Images are representative of one experiment (n=4 at D1; n= 3 at D3-D7; n= 2 at D10- D14). The top row of images are controls where no wound was made. The middle row of images display wounds (W) which had fibrin (F) inserted into the wound cavity. The bottom row of images display wounds which had MSCs introduced via a fibrin clot. Images where acquired with and averaging of 3, and each image represents the 'widest' portion of the wound form a representative sample (as described in the previous chapter) (Scale bars: 1 mm). (Arrow indicates the first appearance of a hypolucid band over the top of the fibrin clot).*

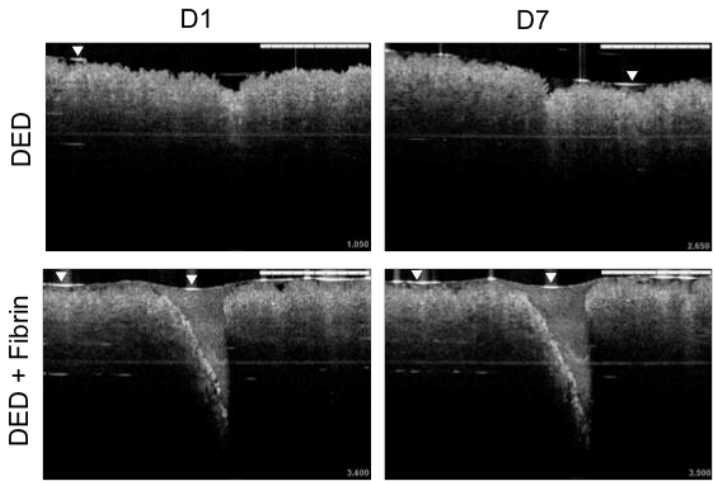

Figure 6.2. *OCT of wounded and unwounded DED. Images were acquired with an averaging of 3. Each image portraying a wound shows the 'widest' region of the wound as determined by eye (Scale bar= 1 mm). (Arrowheads indicate reflections from the surface).*

Rate of Wound Healing

Wound areas were determined from the OCT images as described in Chapter 5, and the reductions in wound areas between time points were calculated and plotted (Figure 6.3). MSCs were found not to reduce the time of wound closure. Under both wound conditions (+/- MSCs), the majority of wounds had closed by day 10. However, MSCs did accelerate the initail phase of wound healing. Over the first three days MSCs reduced the wound sizes by 18.31 % more than wounds without MSCs, but this difference was not statistically significant ($p= 0.073$) due to a low volume of samples (N=1). After day three, wound closure continued to proceed faster in the MSC group than wounds without MSCs, however this trend too was not statistically significant.

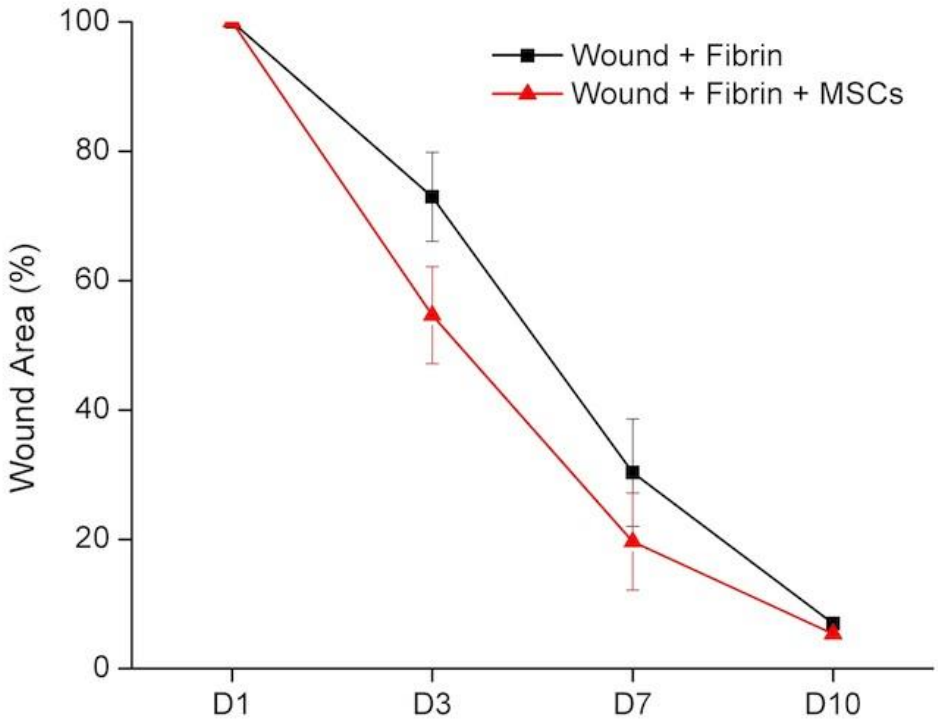

Figure 6.3. *Reduction in wound areas over 14 days. Wound areas were measured manually in image J using the method described in Chapter Five. Briefly, at each time point, the 'widest portion of the wound was identified from a series of images collected along the length of the wound, and the area this region occupied was calculated and compared the wound area of the corresponding region at subsequent time points. The wound areas at the first time point (D1) were normalized to 100 % to account for slight variations in wound sizes between samples, and the mean reduction wound sizes over time was expressed as a percentage of the original wound area (100 %). Data represent mean wound areas ± SEM (N1, n=4, 3 and 2 at days 1, 3-7 and 10 respectively as some samples were removed for histology).*

Histology of Wound Models

Both conventional histology (H&E), and immunohistochemistry (IHC) were performed to evaluate wound healing on selected samples. Over the course of the experiment, the unwounded samples showed a progressive thickening in the cornified layer of the epidermis, and this was accompanied by depletion in keratinocyte number as they gradually committed to terminal differentiation (Figure 6.4). This was seen as an increase in the thickness of the pan-cytokeratin-rich layer above the basal cells as time progressed (Figure 6.5 and 6.6).

Fibrin clots could be clearly identified in the wounded samples the day following wounding, and the area that the clot occupied within the wound cavity decreased markedly between day 1 and 7. A similar observation however could not be made of wounded acellular dermis that had fibrin introduced to the wound cavity; the fibrin clot remained at its initial size throughout the duration of the experiment (Figure 6.4) Also by day 7, a small proportion of keratinocytes had migrated into the wounds (Figure 6.4), and those that had entered the dermis produced keratins (Figure 6.6). MSCs (RFP-labeled), could be seen throughout the wound (Figure 6.5), and the MSCs resided at the wound site for the duration of the experiment (Figure 6.6).

Compared to wounds without MSCs, those with MSCs demonstrated that by day 7, keratinocytes had migrated over the top of the fibrin clot and formed an epithelium, which contained cytokeratins (Figure 6.4, and Figure 6.6). By day 14 wound healing was complete. Fibrin was no longer present in the wounded area and therefore the dermis was no longer partitioned. In addition, a keratinised epithelium had now formed over the wounded area in samples without MSCs. However, the keratinised epithelium achieved from the wounds that contained MSCs was notably thicker than that formed from the wounds without MSCs, and the typical 'basket weave' appearance of cornified layer was less pronounced (Figure 6.4 and Figure 6.6).

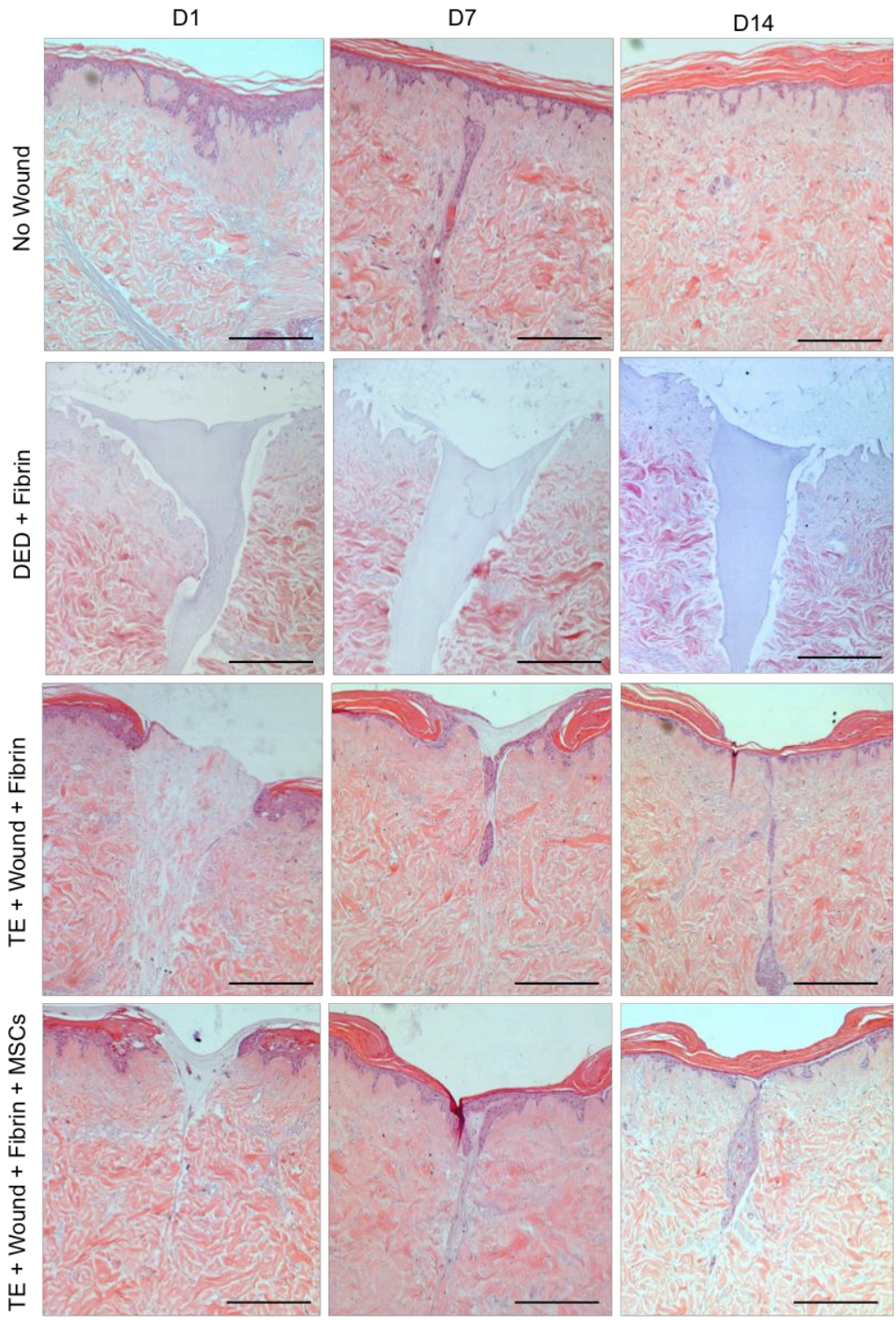

Figure 6.4 *H&E stained sections of wounded and unwounded TE skin in the presence of absence of MSCs at days 1, 7 and 14. (x 10 magnification, scale bars: 300 µm). TE skin was cultured at ALI for 5 days before 1 mm long full-thickness wounds were created, and 100 µm of fibrin glue was added which contained, where appropriate, 1 x 10^5 MSCs. In the control where no wound was made the keratinised progressively thickened over 14 days. Where wounds were made in the absence of cells (DED+Fibrin), the fibrin clot remained for the duration of the experiment. The fibrin clot regressed over time in the wounded TE skin that contained or did not contain MSCs. An epithelium had formed over the top of the fibrin clot in the MSC-containing wound by day 7; this was not apparent until later (day 14) in the wounded TE skin without MSCs.*

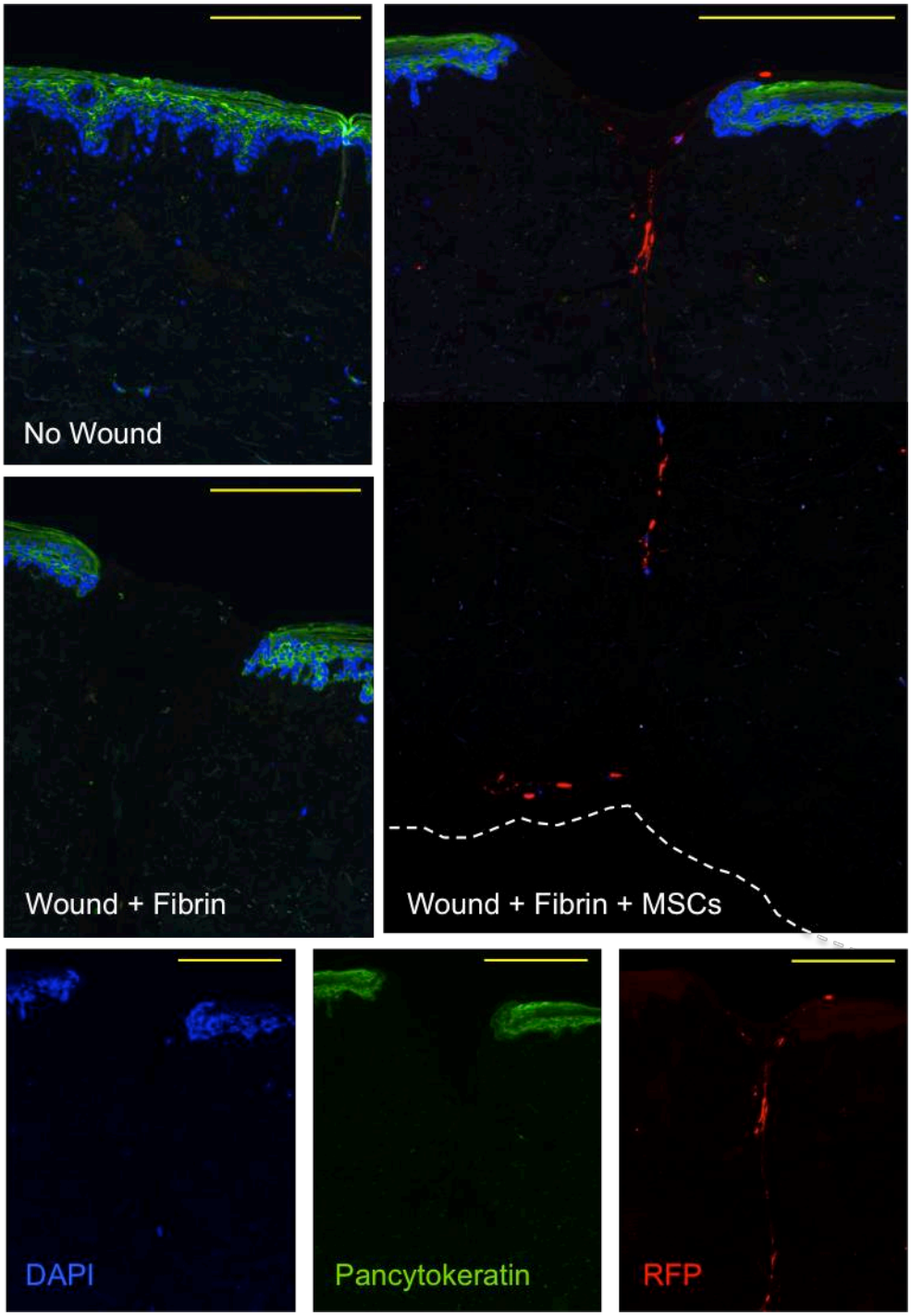

Figure 6.5. *Immunohistochemisty of wound models at day 1. Sections of TE skin were stained for pancytokeratin (green) to highlight the epidermis, and RFP to detect the so-labeled MSCs (red) (the concentration of the primary antibodies were 1: 50 and 1:100 respectively). All sections were stained DAPI (blue) to highlight cell nuclei. The dotted line in the top right image represents the bottom of the wound. (RFP= Red fluorescent protein). (x 10 magnification, Scale: 500 μm).*

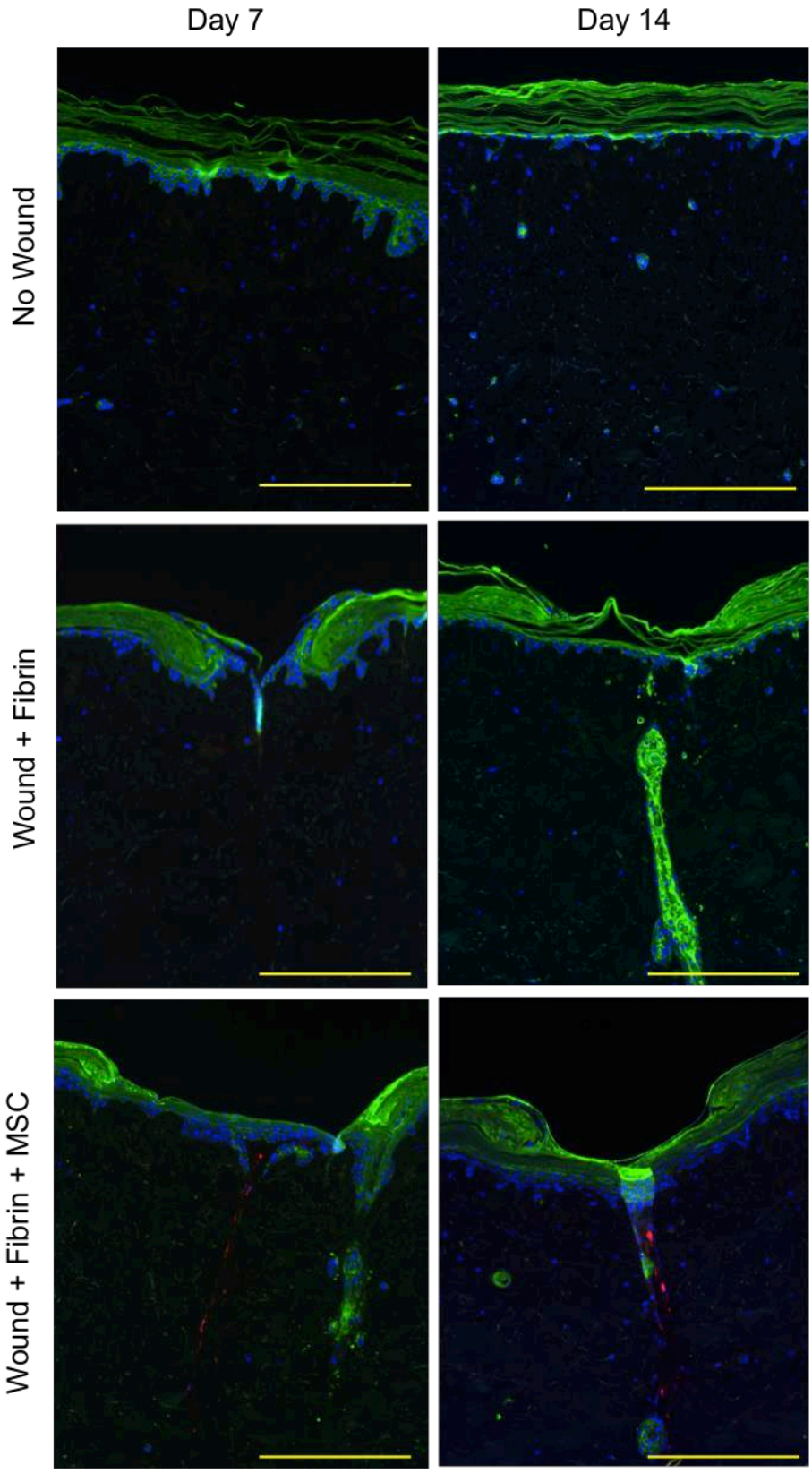

Figure 6.6. *Immunohistochemisty of wound models at days 7 and 14. As in Figure 9, sections of TE skin were stained for pancytokeratin (green) to highlight the epidermis, and RFP to detect the MSCs (red) (the concentration of the primary antibodies were 1: 50 and 1:100 respectively). All sections were stained DAPI (blue) to highlight cell nuclei. (x 10 magnification, Scale: 500 μm).*

ELISA- Cytokine Analysis from the Wound Models

During the course of wound healing, medium was collected from each sample (6, 24, 72, 168 h after wounding), and an ELISA was run for the following cytokines: HGF, bFGF, and IL-8. All data presented are representative of one independent experiment performed in triplicate.

Hepatocyte Growth Factor

6 h after wounding, approx. 25% more HGF was detected in the culture medium from wounded TE skin containing MSCs than the other conditions ($p < 0.001$). By 24 h the amount of HGF produced by MSC-containing wounds were higher still ($p < 0.001$) and remained at a similar level at all subsequent time points (Figure 6.7). In summary, HGF in medium from MSC-containing wounds remained elevated above the other conditions throughout the first 7 days of wound healing.

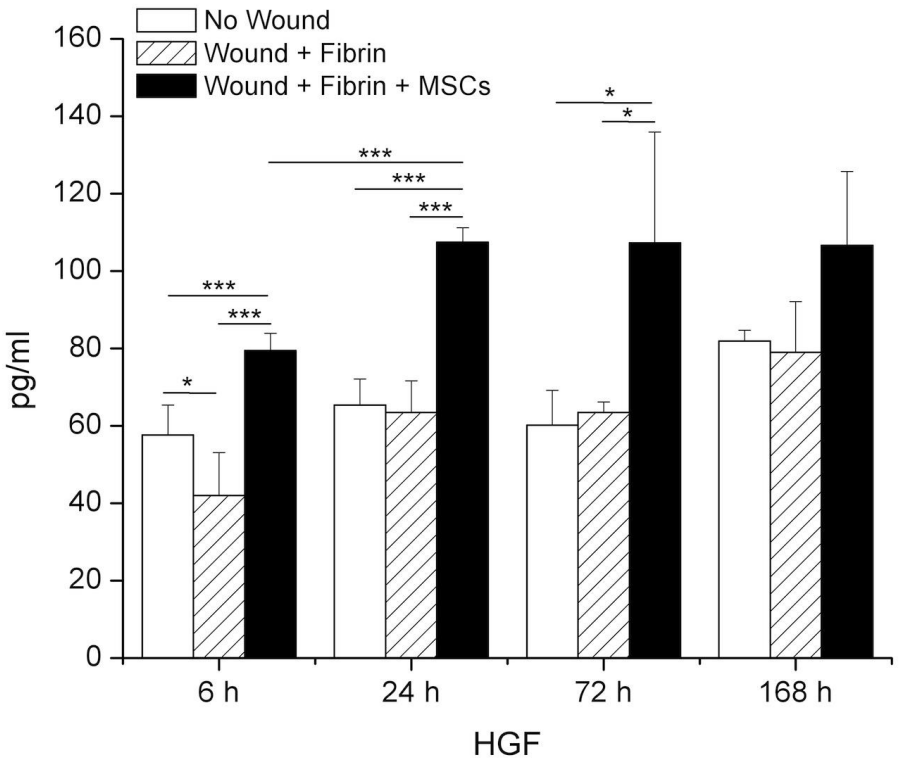

Figure 6.7. *ELISA measurement for HFG. Data are expressed as means ± SD (n=3, *p < 0.1, **p < 0.01, ***p < 0.001, after one-way ANOVA and post-hoc Tukey's tests).*

Fibroblast Growth Factor- basic

The amount of bFGF secreted into the culture medium did not vary significantly between conditions at each time point, and the levels of bFGF did not change significantly between time points over the course of wound healing (Figure 6.8).

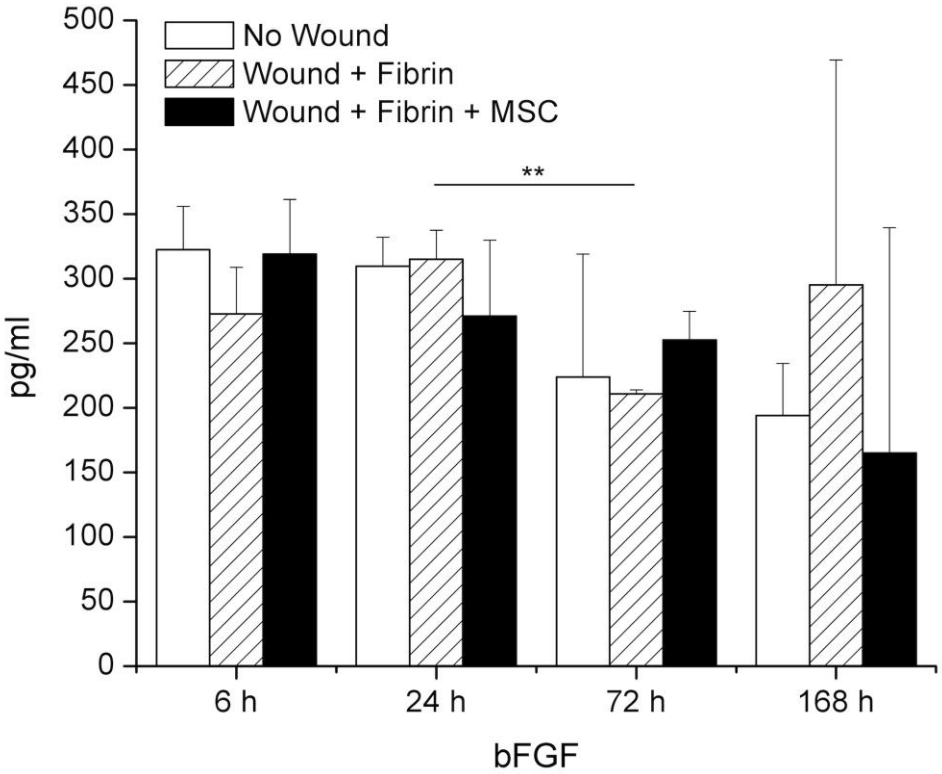

Figure 6.8. *ELISA measurement for bFGF. Data are expressed as means ± SD (n=3, *p < 0.05, after one-way ANOVA and post-hoc Tukey's tests).*

Interleukin- 8

After 6 h, the amount of IL-8 detected from MSC-containing wounds was slightly higher than wounds alone ($p < 0.01$), By 24 h, IL-8 levels had risen under all conditions; however only the rise detected in the medium from MSC-containing wounds was significantly different from 6 h ($p < 0.01$) At this time IL-8 was also detected at a concentration 3.6 fold higher than the other conditions. By 72 h, the amounts of IL-8 detected remained no different from 24 h, apart from unwounded samples where the concentration had risen 2.1 fold ($p < 0.01$). The concentrations of IL-8 detected were highest by 168 h under all conditions, and the medium collected from each condition contained more than the previous time point (Figure 6.9). In summary, IL-8 was secreted by MSC-containing wounds in greater amounts than the other conditions following wounding up to 168 h, by which time similar levels of IL-8 between the unwounded samples and the MSC-containing samples were detected.

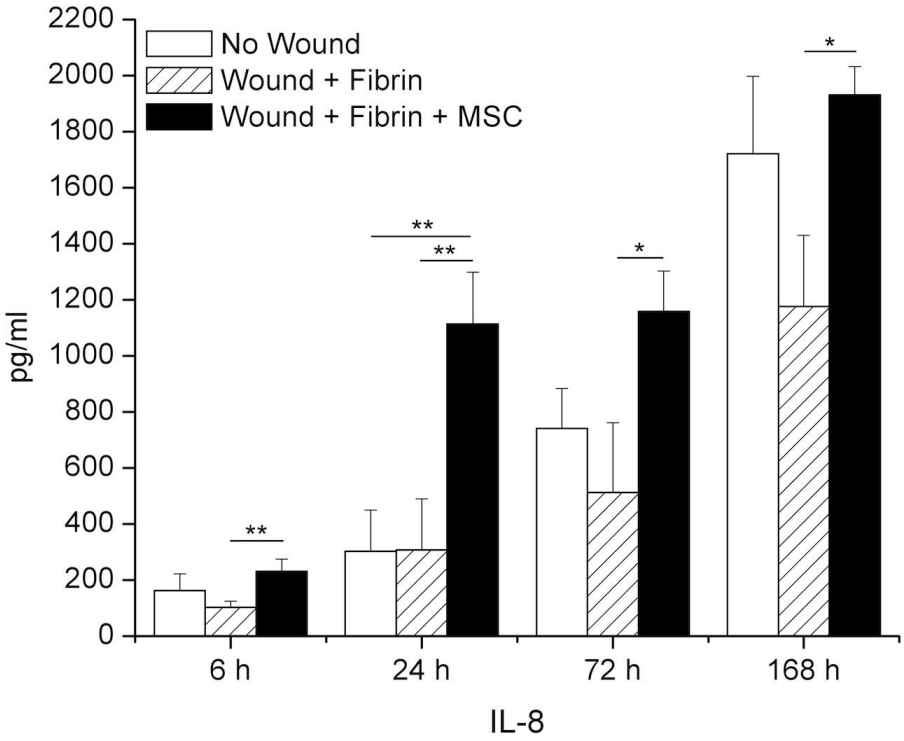

Figure 6.9. *ELISA measurement for IL-8. Data are expressed as means ± SD (n=3, *p < 0.05, **p < 0.01, after one-way ANOVA and post-hoc Tukey's tests).*

MSC Migration into the Wound

To test whether MSCs could home to the site of injury, MSCs (1 x 10^5) were seeded in fibrin onto the reticular surface of the TE skin and their location in the wound was observed at days 1, 7 and 14 post-wounding. Figure 14 shows that there was very limited migration of MSCs into the dermis from where they were introduced. Over the course of the experiment, MSCs remained in the reticular region of the dermis. However it is noteworthy that although the MSCs did not home to the wound margins, they were still able to bring about wound healing in a similar fashion to those seeded directly into the wound (compare Figure 6.9 to Figure 6.6).

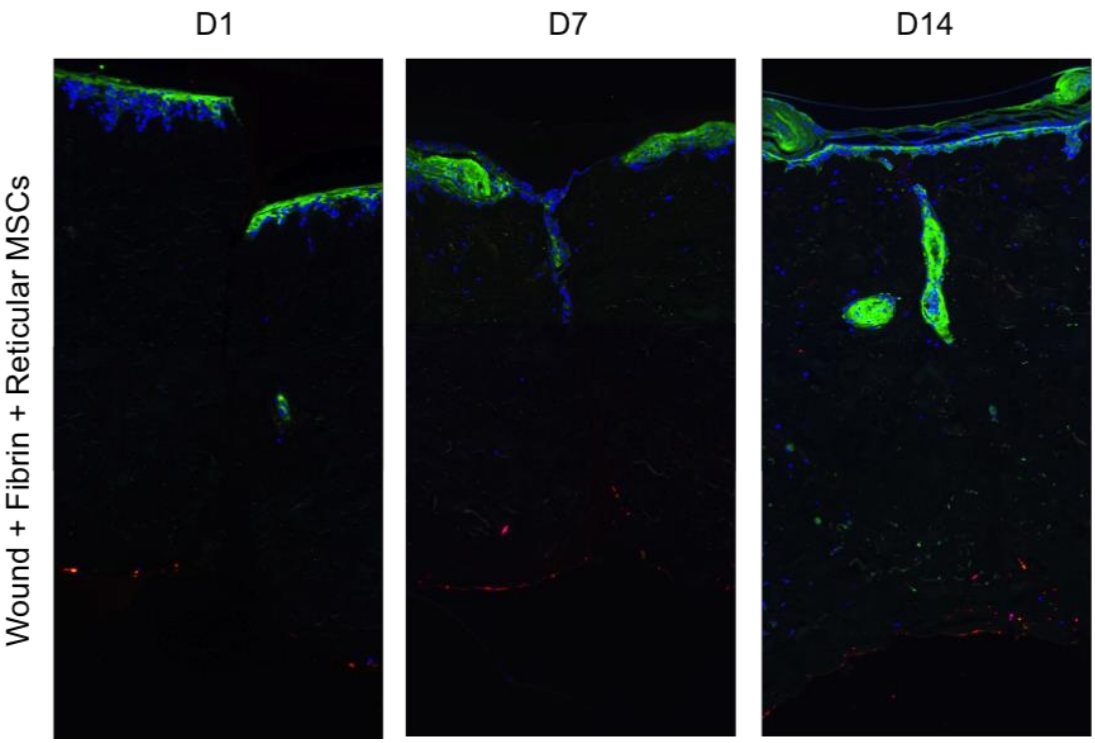

Figure 6.10. *Immunohistochemisty of wound models that contained reticular-seeded MSCs at days 1,7 and 14 post wounding. Blue= DAPI, Green= pan-cytokeratin, Red= RFP. (x 10 magnification).*

6.4. Discussion

Comparison of OCT to Histology

The use of OCT to non-invasively characterise wound healing in a wound model based on TE skin was evaluated in this study. Routine histology was still performed because this is the gold standard for assessment providing both cellular and structural information, and it was to this measure that the images acquired by OCT were compared.

OCT showed good correspondence to histological counterparts. OCT was able to discern essential morphological changes during wound healing of TE skin. Histology revealed the keratinised epithelium increased in thickness over time, and this matched the increase in the thickness of the hypolucid band (hyper reflective band) in the upper most region of the OCT images. By contrast, the acellular control samples (DED) did not exhibit a hypolucid band for the duration of the experiment. Similar observations have been made in previous studies *in vitro* using both collagen gels and TE skin (Jung *et al,* 2003; Yeh *et al,* 2004; Spoeler *et al,* 2006; Smith *et al,* 2010). In addition it has also been shown to be the case *in vivo*. Baui et al applied OCT to investigate wound healing/re-epithelialisation of DFUs and found that they were able to correlate the appearance of the hypolucid band with the onset of epidermal keratinisation and the expression of E-cadherin (Baui *et al*, 2012). Therefore the presence of the hypolucid band observed in this study can be attributed to the presence of keratinised epithelium. Also in common with others was the observation that unlike *in situ* or *ex vivo* skin, fewer details could be seen in TE skin via OCT (Gambichler *et al*, 2005; Krstajic *et al*, 2008).

However a novel finding of the study was that in the presence of MSCs, wounds reestablished their epithelium earlier and this event was detectable by OCT. Seven days after wounding, hypolucid bands were observed on top of the fibrin clots in both wound groups (with and without MSCs), however this band was much thinner in the wound-only group. Coincident with this observation was the finding that the MSC+ wounds contained a thicker epithelium and with more expression of pancytokeratin. Additionally, MSC+ wounds displayed a hypolucid band across the top of the fibrin clot several days earlier (day 3). Such a band was absent from the wound-only group. Although there was no histology (performed at D3) to verify that this was due to the presence of a thin keratinised epithelium, it is a plausible assumption given that this study and others have attributed the hypolucid band to the presence of epithelium. Therefore, OCT detected that MSCs accelerated re-epithelialisation in the wound model. The fact that MSCs accelerated epithelialisation holds clinical relevance because if keratinocytes fail to cover wounds, or if healing is considerably delayed, wounds are more susceptible to infection and dehydration, which adds further complications to healing.

Differences in Wound Healing: The Model Vs. *in Vivo*

Epidermis

In vivo, following injury, keratinocytes migrate from the leading edges of the wound and migrate laterally along the edge of the provisional matrix and down into the center of the wound, and in doing so they separate the eschar from the underlying healing tissue. There are two models by which this it thought to occur: the 'sliding' model (Vaughan and Trinkaus 1966) and the 'rolling' model (Krawczyk 1971). The sliding model proposes that the basal keratinocytes retract from the basement membrane and migrate into the wound, pulling the entire epidermis as sheets to close the wound by virtue of strong desmosomal attachments to the subprabasal keratinocytes and adjacent cells. In the rolling model, suprabasal cells are thought to be the primary participants in epidermal migration and they tumble over the basal keratinocytes pulling with them the overlying epidermis in a leapfrog fashion (Laplante *et al,* 2001).

One striking observation was that re-epithelialisation in the wound model occurred over the top of the fibrin clot as keratinocytes migrated across it and subsequently differentiated. This could be due to a number of limiting factors of the wound model. Although *in vitro* wound models are useful in studying many aspects of keratinocyte responses to injury, the model cannot fully mimic the complexity of the *in vivo* environment. For instance, there is no granulation tissue or activated platelets in the fibrin glue, and there are no macrophages/immune cells present in the wound model; all of these contribute a wealth of growth factors (Brissett and Hom 2003; Mosser and Edwards 2008). Therefore in the absence of the above cells, keratinocytes may be missing cues for migration under the clot. Nonetheless, lateral migration still occurred following wound healing and the epidermis could be reestablished over a short period in the model.

Dermis

It is unclear from the study if the dermis 'healed'. Although OCT was able to chart a reduction in the size of the fibrin clot and a change in the optical properties of the wound area, with scattering increasing over time, it was not clear if this was due to collagen deposition. Histology confirmed that there was no coincident increase in cellularity in the dermis as the fibrin clot regressed; this observation is often reported to accompany wound healing (Singer and Clark 1999). Therefore this suggests that neocollagen production was not entirely responsible for the re-appearance of collagen in the wounded area. For instance, the fibrin clot could have merely been in-filled with cellular material and degraded by cells, and given the dermis' elastic nature, as the clot gradually retreated, the edges of the wound may have been brought into apposition. Both fibroblasts and keratinocytes are known to degrade fibrin through the production of urokinase-type plasminogen activator

(uPA) which activates the fibrinolytic enzyme plasminogen thus stimulating plasmin-mediated fibrin degradation (Chen *et al,* 1993; Tuan *et al,* 1996). The clot did not regress in the absence of cells therefore cellular action is required for clot resolution.

The presence of newly formed collagen at the wound margin could be detected however by staining for type-III collagen at the wound site**.** Collagen III predominates in areas of neocollagen production following wounding, and as wounds mature, the collagen is replaced by collagen I (Peacock 1984). MSCs have previously been reported to exhibit increased levels of mRNA for collagen III in wound sites (Fathke *et al*, 2004; Volk *et al*, 2008). In addition wound-breaking strength (WBS) could be evaluated to determine if integrity was partly restored to the dermis. Several authors have demonstrated that after introducing MSCs into incisional wounds, the maximum force required to be applied across wounds to achieve breaking, was increased above that which was required to break tissues which healed without MSCs. Furthermore, the recorded WBSs in the presence of MSCs were closer to the WBS of unwounded tissue. (Stoff *et al*, 2008; Kwon *et al*, 2008; McFarlin *et al*, 2008), and these results have been associated with an increase in collagen production at the wound site (Kwon *et al*, 2008; McFarlin *et al*, 2008). Therefore it is expected that in the presence of MSCs, collagen production within the model would be increased. Furthermore, functional OCT may be applied to survey the wound area for collagen production in the model. Collagen is a birefringent (BF) material; it can polarise light into two parallel rays. Polarisation-sensitive OCT (PS-OCT) can detect the polarisation state of light backscattered from tissue in terms of BF amplitude and/or attenuation, and therefore can be used to monitor differences in collagen content between wounded and healthy tissue (Oh *et al,* 2006) .

MSCs have the capacity to home to wounds (Kwon *et al*, 2009; Sasaki *et a*l, 2008; Verstappen *et al*, 2011), therefore their ability to locate to the site of injury was evaluated in the wound model. By seeding the MSCs to the reticular side of the dermis, IHC could confirm if they re-located from this region to the wound site. The results demonstrated MSCs remained in the reticular region throughout the course of healing. It is not likely that the MSCs remained trapped in the fibrin glue because MSCs encapsulated in fibrin have been shown previously to express both plasminogen activators, and thus are able to partake in fibrinolysis and migrate through fibrin meshes (Neuss *et al*, 2011).

One possible explanation as to why the MSCs remained *in situ* is that the model may have been lacking in key chemokine/ growth factors to stimulate MSC mobilisation. Due to the absence of macrophages and endothelial cells in the model, factors such as PDGF-AB, RANTES, MDC (macrophage derived chemokine) and SDF-1 (stromal cell derived factor) may have been absent from the wound environment. Ponte et al demonstrated these factors positively affect BM-MSC migration, and in particular when the cells were pre-conditioned with TNF-α, the effect of RANTES, MDC and SDF-1 upon BM-

MSC mobilisation was potentiated via an increased expression of their respective receptors (Lopez Ponte *et al,* 2007).

Advantages of OCT Vs. Histology

Histology remains the gold standard in tissue assessment because the images obtained are very clear and not subject to ambiguous interpretation. However it is not free from several unavoidable drawbacks, which make recording an objective measurement of wound healing hard to achieve. Artifacts such as folding and fracture commonly occur especially in the wound area where structural integrity is diminished and the tissue area is increased in fragility. These artifacts become more apparent when thin sections of tissue are microtomed; for example all the images in figure 10 show foldings in the epidermal wound area. Additionally, although not shown to be the case with fibrin glue in this study, differential shrinkage between the tissue and the implanted material can result during processing which can lead to fracture and detachment of the implant from the tissue, and this can adversely affect objectivity in wound healing evaluation (Yuan *et al*, 2010). Moreover, histology is an experimental endpoint. Once a sample is designated for histology, it is necessarily removed from the experiment and the tissue lost to further experimentation. In contrast, OCT can track wound healing within a given sample over time; something which cannot be done via histology**.** All the images in for example Figure 2 are taken from one sample under each condition. Thus OCT has proven useful in this study in increasing the amount of data that can be rendered from a sample prior to histology.

ELISA

Hepatocyte Growth Factor

HGF, also known as scatter factor, was first characterised as a powerful hepatic mitogen and stimulator of epithelial cell dissociation (Sato *et al,* 1995). HGF is predominantly synthesised by mesenchymal cells and it is one of the most versatile dermis-derived growth factors involved in wound healing. As well as promoting keratinocyte proliferation and migration, under physiological calcium concentrations (Matsumoto *et al,* 1991), it also acts as a potent promoter of neoangiogensis (Conway *et al,* 2006), and can suppress inflammation (Di Nicola *et al,* 2002). As such, compromised HGF production is associated with impaired wound healing (Bevan *et al*, 2004).

ELISA performed on media from wound models containing MSCs, demonstrated HGF at levels above the controls over a period of 7 days. This observation is consistent with those of others that have previously shown human BM MSCs constitutively secrete HGF under standard culture conditions (Chen *et al*, 2008; Zang *et al*, 2010; Smith *et al*,

2012). Compared to dermal fibroblasts, MSCs secrete relatively greater amounts (Chen *et al*, 2008). Additionally, HGF can be found in elevated concentrations in wound environments that contained MSCs (Kinnaird *et al,* 2004; Nie *et al,* 2011). Therefore, given HGF's role in promoting keratinocyte migration, as outlined above, an elevated level of HGF may be associated with the earlier onset/ enhanced re-epithelialisation in the MSC wound models as observed by OCT and IHC.

Fibroblast Growth Factor- basic

bFGF, also known as FGF-2, is released into the wound environment in acute wounds. It is a potent mitogen and chemoattractant of endothelial cells, fibroblasts and keratinocytes, and plays an important role in granulation tissue formation, re-epithelialisation and dermal remodeling (Powers *et al,* 2000). *In vitro* studies have shown bFGF to regulate the synthesis and deposition of ECM components, and promote keratinocyte motility (Werner and Grose 2003; Xie *et al,* 2008) and *in vivo* administration of recombinant bFGF can accelerate both acute and chronic wound healing(Akita *et al,* 2008; Tan *et al,* 2008), thus demonstrating its importance in wound healing.

The results showed that levels of bFGF detected in the medium under all conditions remained similar to each other over seven days. One would have expected the level of bFGF to be found in elevated concentrations about the unwounded skin. It is possible that the wound environments did produce more bFGF than the control, though its effect may have been masked. Green's medium contains cholera toxin, an essential medium component for epithelial maturation, which amplifies levels of cyclic adenine monophosphate (cAMP) from cells, and such cAMP elevating agents have been shown to increase bFGF production from cells (Riva *et al,* 1997).

Interlukin-8

IL-8 is a pro-inflammatory cytokine that plays an important role in wound healing by encouraging skin re-epithelialisation through the promotion of keratinocyte migration (Michel *et al,* 1992) and proliferation (Tuschil *et al,* 1992). IL-8 was produced in the MSC-treated wounds at much greater concentrations than the other conditions over the first 72 h. It is known that MSCs constitutively secrete low amounts of IL-8 under standard culture conditions (Chen *et al*, 2008), therefore one might have expected the MSC-treated wounds to produce a smaller increase in the concentration of IL-8 above the wound-only samples.

TNF- α is another pro-inflammatory cytokine that is released during wound healing by keratinocytes and macrophages (Xu *et al,* 2013), and it has been shown to induce the secretion of a number of proteins from MSCs including: IL-6, IL-8, monocyte chemotactic protein-1, CXCL6, cathepsin L, and pentraxin-related protein 3, VEGF, IGF-1 and HGF (Wang *et al,* 2006; Lee *et al,* 2010). Heo *et al* (2011), recently demonstrated that if IL-6 or IL-8 were depleted from TNF-α conditioned medium (MSC culture medium + TNF-α), the effects the medium had on stimulating wound closure via re-epithelialisation, angiogenesis, cell proliferation ad immune cell infiltration were largely attenuated. Thus they suggest that TNF-α activates the healing potential of MSCs via IL-6 and IL-8 (Wang *et al,* 2006; Lee *et al,* 2010; Heo *et al,* 2011). Therefore it is possible that in the wound model, even in the absence of macrophages, that the damaged keratinocytes provide a sufficient concentration of TNF-α to enhance IL-8 production from the MSCs, thus the accelerated healing exhibited by the MSC containing wounds may be in part attributed to TNF-α, but this would require further investigation.

Limitations of the Data

Due to the constraints of time, the wound healing experiment was only performed once, therefore it is necessary to repeat the experimental series at least twice more to confirm if the data are reproducible and perform a reliable statistical analysis. However, despite this flaw the data appear to show some striking trends, which have been discussed, although it is necessary for much of the work to be repeated before solid conclusions can be drawn.

A further limitation was that the ELISA data was not normalised to cell number, therefore one cannot ascertain if the increased levels HGF and IL-8 observed in the wound models that contained MSCs arose simply because these models contained a greater number of cells which have the capacity to produce these soluble factors. It was however not possible to normalise the data to cell number because the number of cells that were present in the tissue are the start of the experiment was unknown; wounds were made in the tissue 7 days after seeding DED with fibroblasts and keratinocytes, and they would have proliferated over this time. Equally, the number of cells present at each experimental time-point was unknown because the extent to which the cells within the tissues and proliferated/ died was unquantifiable. For example, histology shows that over time the cellular make-up of the epidermis reduces as the keratinocytes committed to terminal differentiation, while the proportion of fibroblasts generally increases.

To understand if the MSC-containing wound models produced more HGF and IL-8 than wound models without MSCs in a manner that was not purely a product of an increased cell number in the tissue, it would be necessary to have an additional control i.e.

wound models containing an equal number of fibroblast to MSCs. Thus, if the wound models containing fibroblasts produced similar data to the MSC-containing would models, then one could say that the difference in results between wounded skin alone and wounded skin that contained cells was due to an increase in cell number and not due to the presence of a specific cell type.

6.5. Summary

- OCT could effectively be applied to evaluate wound healing. OCT could identify the regression of the fibrin clot from the wound area, and the re-establishment of the epithelium.

- MSCs did not benefit the wound in terms of advancing fibrin clot regression, however they did accelerate re-epithelialisation. In the presence of MSCs the epithelium was shown to be present, via OCT, as early as day 3. In the absence of MSCs the epithelium was only evident at day 7.

- The observation that MSCs accelerated re-epithelialisation was associated with increases in the wound-beneficial cytokines HGF and IL-8 found in the medium of wounds containing MSCs. I hypothesise that the production of these cytokines may be linked to the presence of TNF-α in the wound, however further investigation would be required.

- There were key differences between the healing of the model and how wounds would be expected to heal *in vivo*, which reflected some of the limitations of the model. Differences could be accounted for by the absence of endothelial cells, immune cells and true granulation tissue from the model. Future works could incorporate these cell types into the model to better model the *in vivo* environment.

- Further investigation would be required to determine the extent of neocollagen formation in the wounds and determine if there were differences between wound conditions.

Chapter Seven:
Future Work and Conclusions

7.1. Cell Delivery

Despite the promise of using MSCs as therapies to treat chronic skin conditions, there is still no consensus as to which is the most effective approach for cell delivery. Achieving efficient and safe cell delivery is essential to the success of cell therapies. The work undertaken in Chapter 3 was conducted as part of an EU consortium, which aimed to 'develop efficient, safe and secured methods of cultivating autologous and allogeneic MSCs according to GMP standards' in order to expediate the entry of 'off the shelf' cell-based therapeutics into the clinic.

Plasma polymerised acrylic acid (ppAAc) functionalised silicone substrates were found to promote the attachment of MSCs to medical grade silicone and it was found that ppAAc surfaces could effectively facilitate the transfer of MSCs to model wound beds composed of decellularised human dermis. Importantly, it was also discovered that the surface chemistry did not negatively affect the MSCs phenotype of functionality, and that once the MSCs arrived at the model wound bed they remained viable. Based on findings in the literature, I hypothesise that the ECM protein fibronectin, as opposed to vitronectin, which is adsorbed to the materials surface form serum, plays an essential role in facilitating MSC attachment. It would be interesting to test this hypothesis by performing functional blocking studies using antibodies directed to each ECM protein.

The findings of the study are of importance because these so-called cell 'carriers' are composed entirely from synthetic materials. This is a desirable characteristic as far as entering the clinic is concerned, since its manufacture is less open to batch-to-batch variation, as is the case with animal-based products, thus making adherence to GMP more easily achievable. In addition, the avoidance of animal based products reduces the risk to the patient. In the future, if this cell-delivery platform is introduced into the clinic it could be combined with the use of serum-free medium, so that animal based components are removed all together.

Since the publication of the work in Tissue Engineering, the carriers have been used to deliver adipose tissue derived stem cells to wounds *in vivo* (Jiang i 2013). Therefore it is possible that the carriers could be used to deliver stem cells from other origins to wounds, such as umbilical cord blood; MSCs derived from this tissue a have been shown to be beneficial in wound healing (Luo *et al,* 2010) In the future (next 2-5 years), I envisage there

will be 'off the shelf' MSC-derived products for the treatment of non-healing wounds.

An interesting finding of the study was that in the absence of keratinocytes, MSCs could not penetrate the basement membrane (BM). I propose that MSCs may behave similarly to dermal fibroblasts in that they may only express MMP-9, a gelatinase that can cleave collagen IV, which is the main constituent of the BM, when there is cross-talk with keratinocytes. This hypothesis could be tested firstly in a simple transwell study. Keratinocytes could be seeded in one chamber of the transwell and MSCs on the other, and an ELISA could be performed for MMP-9. The concentration of MMP-9 could then be compared to that detected from each cell type cultured in isolation. (Human dermal fibroblasts would also be co-cultured with the keratinocytes so that the MSCs' behavior could be compared to this other mesodermal cell type). In addition, it would be important to perform PCR for MMP-9 mRNA on the samples, to determine each cell types relative contribution to the protease concentration as detected via ELISA in the co-culture. Without this measure one could not confirm which cell-type had up-regulated MMP-9 production (if at all).

A further step would be to perform an ELISA for MMP-9 on the culture medium used to support co-cultures of keratinocytes and MSCs on decellularised dermis (DED), to determine if an increase in MMP-9 was associated with the observation that in the presence of keratinocytes the MSCs were able to traverse the BM. If this was found to be the case, one could provide evidence for a causal link between MMP-9 elevation and BM penetration by introducing specific inhibitors to MMP-9 to determine if MMP-9 retardation impacts the MSCs' migratory capacity.

7.2. Wound Model

TE skin could be used to study wound healing *in vitro* using fibrin glue to partly recreate the initial stages of wound healing. Because the wound model was able to demonstrate differences in the rate of re-epithelialisation between conditions, the model could be used to evaluate the potential of novel therapeutics, such as topical creams or hydrogels containing bioactive factors, to ameliorate wound healing. Therefore the wound model is not limited to the study of stem cell interactions and it has wider applications. For example, M. Shahbudin in our group is currently using the model developed herein to test the therapeutic potential of glucomannan, a naturally occurring plant-derived polysaccharide.

One of the main limitations of the model is that were no immune cells present such as macrophages, and there were no endothelial cells present. This limits the models reproduction of the *in vivo* environment. However, it may be possible to incorporate

macrophages and endothelial cells into the model to improve the models representation of the *in vivo* situation. Studies by the MacNeil group on incorporating endothelial cells are ongoing as are studies to incorporate immune cells. Also unlike *in vivo* wound healing, activated platelets were absent from the fibrin clot. Activated platelets release many growth factors into the wound, the chief one being PDGF, which stimulates keratinocyte proliferation. However in future studies it might be possible to produce a more physiologically relevant fibrin matrix through the incorporation of human recombinant PDGF into the fibrin clot.

7.3. The Use of MSCs in the Wound Model

A key finding of the study was that in the presence of MSCs, the wound re-epithelialised slightly earlier. This observation was associated with elevated levels of the cytokines IL-8 and HGF in the culture medium; both of these are beneficial to wound healing. I hypothesise that TNF-α may be responsible for the elevation in the production of these factors from the MSCs because it can increase the expression of these factors in 2D culture from MSCs (Wang *et al*, 208; Heo *et al*, 2011). Further investigation would be required to establish to what extent TNF-α was present in the medium from the wound models (+/- MSCs), and if this cytokine could stimulate IL-8 and HFG production in the wound model containing MSCs. I predict TNF-α would be present in elevated concentrations in the wound environment compared to undamaged tissue, even in the absence of macrophages (the main source of this inflammatory cytokine), because it is released from injured keratinocytes.

As mentioned previously, one of the limitations of the wound model was that there are no immune and endothelial cells present; this may have accounted for the observation that MSCs were not recruited to the wound site from the reticular dermis because factors secreted by these cells such as PDGF-AB, RANTES, MDC (macrophage derived chemokine) and SDF-1 (stromal cell derived factor) may have been absent from the wound environment. If macrophages and endothelial cells were incorporated into the wound models, MSC mobilisation may have been observed. An additional ELISA for the above factors would be required to substantiate the hypothesis that the MSCs did not migrate due to a lack of chemokines in the model.

One of the main reasons why chronic wounds fail to heal is due to poor vasculature, therefore attempts to re-establish vasculature in the wound bed is the mainstay of clinical intervention. MSCs have been shown to promote neo-angiogenesis, which can restore limb function and reduce the incidence of limb amputation. It would be interesting to incorporate endothelial cells into the wound model to evaluate if, in the wound environment, the MSCs could enhance their proliferation in the wound and the formation of vascular tubules.

Currently our lab is investigating the role MSCs play in making vasculature in TE skin by seeding MSCs with endothelial cells in TE skin. This is important to evaluate because MSCs, if incorporated into skin grafts for example, may encourage grafts to 'take', by stimulating angiogenesis and effectively integrating the grafted tissue into the wound site.

7.4. The Future of OCT

OCT could successfully be applied to image the TE wound model over the course of wound healing, and it could monitor wound healing both in terms of tracking the shrinkage of fibrin clots, and detecting the re-establishment of an epithelium over the wounded area. It is likely that in the future OCT will be preferred over histology as a method where the need to make gross morphological assessments of tissue is required, due to it being a rapid and non-invasive imaging platform. The OCT system employed in this thesis had an axial resolution of 10 μm, and a lateral resolution of 25 μm, which means that individual cells could not be resolved. However, recent developments in ultra-high resolution OCT have achieved resolutions equivalent to 1.8 μm axially and 3 μm transversely, which has allowed cells/cell nuclei to be identified (Pan *et al,* 2007). Furthermore through advancements in technology it may also be possible to couple functional OCT imaging into conventional OCT systems so that spatial and structural information can be gained from wounds (*in vitro* and *in vivo*) through the use of a single apparatus. Advancements in software and image processing in the future may also lead to faster image acquisition, allowing data to be collected and analysed more rapidly; in the current study the speed of processing was the main factor which determined and limited the number of image acquisitions from a sample.

References

Abbott, C.A., Garrow, A.P., Carrington, A.L., Morris, J., Van Ross, E.R.*, et al.* (2005). "Foot ulcer risk is lower in south-asian and african-caribbean compared with european diabetic patients in the uk the north-west diabetes foot care study". Diabetes Care. **28** (8): 1869-1875.

Abercrom, M. (1970). "Contact inhibition in tissue culture". In Vitro-Journal of the Tissue Culture Association. **6** (2): 128-&.

Abercrombie, M. (1967). "Contact inhibition: The phenomenon and its biological implications". Natl Cancer Inst Monogr. **26** 249-77.

Absolom, D.R., Zingg, W. and Neumann, A.W. (1987). "Protein adsorption to polymer particles - role of surface-properties". Journal of Biomedical Materials Research. **21** (2): 161-171.

Aggarwal, S. and Pittenger, M.F. (2005). "Human mesenchymal stem cells modulate allogeneic immune cell responses". Blood. **105** (4): 1815-1822.

Aguado, B.A., Mulyasasmita, W., Su, J., Lampe, K.J. and Heilshorn, S.C. (2011). "Improving viability of stem cells during syringe needle flow through the design of hydrogel cell carriers". Tissue Engineering Part A.

Ai, H., Meng, H.D., Ichinose, I., Jones, S.A., Mills, D.K.*, et al.* (2003). "Biocompatibility of layer-by-layer self-assembled nanofilm on silicone rubber for neurons". Journal of Neuroscience Methods. **128** (1-2): 1-8.

Ai, H., Mills, D.K., Jonathan, A.S. and Jones, S.A. (2002). "Gelatin-glutaraldehyde cross-linking on silicone rubber to increase endothelial cell adhesion and growth". In Vitro Cellular & Developmental Biology-Animal. **38** (9): 487-492.

Akela, A., Nandi, S.K., Banerjee, D., Das, P., Roy, S.*, et al.* (2012). "Evaluation of autologous bone marrow in wound healing in animal model: A possible application of autologous stem cells". International Wound Journal. **9** (5): 505-516.

Akita, S., Akino, K., Imaizumi, T. and Hirano, A. (2008). "Basic fibroblast growth factor accelerates and improves second-degree burn wound healing". Wound Repair and Regeneration. **16** (5): 635-641.

Alexander, M.R. and Duc, T.M. (1998). "The chemistry of deposits formed from acrylic acid plasmas". Journal of Materials Chemistry. **8** (4): 937-943.

Allen, L.T., Tosetto, M., Miller, I.S., O'Connor, D.P., Penney, S.C.*, et al.* (2006). "Surface-induced changes in protein adsorption and implications for cellular phenotypic responses to surface interaction". Biomaterials. **27** (16): 3096-3108.

Alster, T.S. (1999). "Clinical and histologic evaluation of six erbium : Yag lasers for cutaneous resurfacing". Lasers in Surgery and Medicine. **24** (2): 87-92.

Anderson, R.R. and Parrish, J.A. (1981). "The optics of human-skin". Journal of Investigative Dermatology. **77** (1): 13-19.

Antcliff, R.J., Stanford, M.R., Chauhan, D.S., Graham, E.M., Spalton, D.J.*, et al.* (2000). "Comparison between optical coherence tomography and fundus fluorescein angiography for the detection of cystoid macular edema in patients with uveitis". Ophthalmology. **107** (3): 593-599.

Apelqvist, J., Bakker, K., van Houtum, W.H., Schaper, N.C. and Int Working Grp Diabetic Foot, E. (2008). "Practical guidelines on the management and prevention of the diabetic foot - based upon the international consensus on the diabetic foot (2007) prepared by the international working group on the diabetic foot". Diabetes-Metabolism Research and Reviews. **24** S181-S187.

Argolo Neto, N.M., Del Carlo, R.J., Monteiro, B.S., Nardi, N.B., Chagastelles, P.C.*, et al.* (2012). "Role of autologous mesenchymal stem cells associated with platelet-rich plasma on healing of cutaneous wounds in diabetic mice". Clinical and Experimental Dermatology. **37** (5): 544-553.

Armstrong, D.G. and Lavery, L.A. (1998). "Diabetic foot ulcers: Prevention, diagnosis and classification". American Family Physician. **57** (6): 1325-1332.

Armstrong, D.G., Lavery, L.A. and Diabet Foot Study, C. (2005). "Negative pressure wound therapy after partial diabetic foot amputation: A multicentre, randomised controlled trial". Lancet. **366** (9498): 1704-1710.

Aschoff, R., Schmitt, J., Knuschke, P., Koch, E., Braeutigam, M.*, et al.* (2011). "Evaluation of the atrophogenic potential of hydrocortisone 1% cream and pimecrolimus 1% cream in uninvolved forehead skin of patients with atopic dermatitis using optical coherence tomography". Experimental Dermatology. **20** (10): 832-836.

Azzi, L., El-Alfy, M., Martel, C. and Labrie, F. (2005). "Gender differences in mouse skin morphology and specific effects of sex steroids and dehydroepiandrosterone". Journal of Investigative Dermatology. **124** (1): 22-27.

Badiavas, E.V. and Falanga, V. (2003). "Treatment of chronic wounds with bone marrow-derived cells". Archives of Dermatology. **139** (4): 510-516.

Baier, R.E. and Dutton, R.C. (1969). "Initial events in interactions of blood with a foreign surface". Journal of Biomedical Materials Research. **3** (1): 191-206.

Barshavit, R., Benezra, M., Eldor, A., Hyam, E., Fenton, J.W.*, et al.* (1990). "Thrombin immobilized to extracellular-matrix is a potent mitogen for vascular smooth-muscle cells - nonenzymatic mode of action". Cell Regulation. **1** (6): 453-463.

Bartholomew, A., Sturgeon, C., Siatskas, M., Ferrer, K., McIntosh, K.*, et al.* (2002). "Mesenchymal stem cells suppress lymphocyte proliferation in vitro and prolong skin graft survival in vivo". Experimental Hematology. **30** (1): 42-48.

Barui, A., Banerjee, P., Patra, R., Das, R.K., Dhara, S.*, et al.* (2011). "Swept-source optical coherence tomography of lower limb wound healing with histopathological correlation". Journal of biomedical optics. **16** (2):

Bashkatov, A.N., Genina, E.A., Kochubey, V.I. and Tuchin, V.V. (2005). "Optical properties of human skin, subcutaneous and mucous tissues in the wavelength range from 400 to 2000 nm". Journal of Physics D-Applied Physics. **38** (15): 2543-2555.

Bashkatov, A.N., Genina, E.A. and Tuchin, V.V. (2011). "Optical properties of skin, subcutaneous, and muscle tissues: A review". Journal of Innovative Optical Health Sciences. **4** (1): 9-38.

Bauer, E.A., Cooper, T.W., Huang, J.S., Altman, J. and Deuel, T.F. (1985). "Stimulation of invitro human skin collagenase expression by platelet-derived growth-factor". Proceedings of the National Academy of Sciences of the United States of America. **82** (12): 4132-4136.

Baum, C.L. and Arpey, C.J. (2005). "Normal cutaneous wound healing: Clinical correlation with cellular and molecular events". Dermatologic Surgery. **31** (6): 674-686.

Beamson, G. and Briggs, D. (1998). "Degradation of poly(vinyl alcohol) thin films during monochromatized xps: Substrate effects and x-ray intensity dependence". Surface and Interface Analysis. **26** (5): 343-351.

Bechara, F.G., Gambichler, T., Stucker, M., Orlikov, A., Rotterdam, S.*, et al.* (2004). "Histomorphologic correlation with routine histology and optical coherence tomography". Skin Research and Technology. **10** (3): 169-173.

Becker, J.C., Domschke, W. and Pohle, T. (2004). "Biological in vitro effects of fibrin glue: Fibroblast proliferation, expression and binding of growth factors". Scandinavian Journal of Gastroenterology. **39** (10): 927-932.

Bennett, N.T. and Schultz, G.S. (1993). "Growth-factors and wound-healing .2. Role in normal and chronic wound-healing". American Journal of Surgery. **166** (1): 74-81.

Bergers, G., Brekken, R., McMahon, G., Vu, T.H., Itoh, T.*, et al.* (2000). "Matrix metalloproteinase-9 triggers the angiogenic switch during carcinogenesis". Nature Cell Biology. **2** (10): 737-744.

Bieback, K., Hecker, A., Kocaoemer, A., Lannert, H., Schallmoser, K.*, et al.* (2009). "Human alternatives to fetal bovine serum for the expansion of mesenchymal stromal cells from bone marrow". Stem Cells. **27** (9): 2331-2341.

Bishop, A. (2008). "Role of oxygen in wound healing". Journal of wound care. **17** (9): 399-402.

Blomback, B., Hanson, L.A. (1976). "Plasma proteins". 43-54. ohn. Wiley & Sons.

Boppart, S.A., Herrmann, J., Pitris, C., Stamper, D.L., Brezinski, M.E.*, et al.* (1999). "High-resolution optical coherence tomography-guided laser ablation of surgical tissue". Journal of Surgical Research. **82** (2): 275-284.

Borena, B.M., Pawde, A.M., Amarpal, Aithal, H.P., Kinjavdekar, P.*, et al.* (2010). "Evaluation of autologous bone marrow-derived nucleated cells for healing of full-thickness skin wounds in rabbits". International Wound Journal. **7** (4): 249-260.

Botusan, I.R., Sunkari, V.G., Savu, O., Catrina, A.I., Grunler, J.*, et al.* (2008). "Stabilization of hif-1 alpha is critical to improve wound healing in diabetic mice". Proceedings of the National Academy of Sciences of the United States of America. **105** (49): 19426-19431.

Bouma, B.E., Tearney, G.J., Yabushita, H., Shishkov, M., Kauffman, C.R.*, et al.* (2003). "Evaluation of intracoronary stenting by intravascular optical coherence tomography". Heart. **89** (3): 317-320.

Bredfeldt, J.S., Vinegoni, C., Marks, D.L. and Boppart, S.A. (2005). "Molecularly sensitive optical coherence tomography". Optics Letters. **30** (5): 495-497.

Brem, H. and Tomic-Canic, M. (2007). "Cellular and molecular basis of wound healing in diabetes". Journal of Clinical Investigation. **117** (5): 1219-1222.

Breuss, J.M., Gallo, J., Delisser, H.M., Klimanskaya, I.V., Folkesson, H.G.*, et al.* (1995). "Expression of the beta-6 integrin subunit in development, neoplasia and tissue-repair suggests a role in epithelial remodeling". Journal of Cell Science. **108** 2241-2251.

Brezinski, M.E., Tearney, G.J., Weissman, N.J., Boppart, S.A., Bouma, B.E.*, et al.* (1997). "Assessing atherosclerotic plaque morphology: Comparison of optical coherence tomography and high frequency intravascular ultrasound". Heart. **77** (5): 397-403.

Brissett, A.E. and Hom, D.B. (2003). "The effects of tissue sealants, platelet gels, and growth factors on wound healing". Current opinion in otolaryngology & head and neck surgery. **11** (4): 245-50.

Broadley, K.N., Aquino, A.M., Woodward, S.C., Buckleysturrock, A., Sato, Y.*, et al.* (1989). "Monospecific antibodies implicate basic fibroblast growth-factor in normal wound repair". Laboratory Investigation. **61** (5): 571-575.

Bullock, A.J., Higham, M.C. and Macneil, S. (2006). "Use of human fibroblasts in the development of a xenobiotic-free culture and delivery system for human keratinocytes". Tissue Engineering. **12** (2): 245-255.

Calles-Escandon, J. and Cipolla, M. (2001). "Diabetes and endothelial dysfunction: A clinical perspective". Endocrine Reviews. **22** (1): 36-52.

Candi, E., Schmidt, R. and Melino, G. (2005). "The cornified envelope: A model of cell death in the skin". Nature Reviews Molecular Cell Biology. **6** (4): 328-340.

Capelli, C., Domenghini, M., Borleri, G., Bellavita, P., Poma, R.*, et al.* (2007). "Human platelet lysate allows expansion and clinical grade production of mesenchymal stromal cells from small samples of bone marrow aspirates or marrow filter washouts". Bone Marrow Transplantation. **40** (8): 785-791.

Caplan, A.I. (2007). "Adult mesenchymal stem cells for tissue engineering versus regenerative medicine". Journal of Cellular Physiology. **213** (2): 341-347.

Carter, D.C. and Ho, J.X. (1994). "Structure of serum-albumin". Advances in Protein Chemistry, Vol 45. **45** 153-203.

Castilla, D.M., Liu, Z.-J., Tian, R., Li, Y., Livingstone, A.S.*, et al.* (2012). "A novel autologous cell-based therapy to promote diabetic wound healing". Annals of Surgery. **256** (4): 560-572.

Catelas, I., Sese, N., Wu, B.M., Dunn, J.C.Y., Helgerson, S.*, et al.* (2006). "Human mesenchymal stem cell proliferation and osteogenic differentiation in fibrin gels in vitro". Tissue Engineering. **12** (8): 2385-2396.

Cavallo, C., Cuomo, C., Fantini, S., Ricci, F., Tazzari, P.L.*, et al.* (2011). "Comparison of alternative mesenchymal stem cell sources for cell banking and musculoskeletal advanced therapies". Journal of Cellular Biochemistry. **112** (5): 1418-1430.

Cavani, A., Zambruno, G., Marconi, A., Manca, V., Marchetti, M.*, et al.* (1993). "Distinctive integrin expression in the newly forming epidermis during wound-healing in humans". Journal of Investigative Dermatology. **101** (4): 600-604.

Chakrabarty, K.H., Heaton, M., Dalley, A.J., Dawson, R.A., Freedlander, E.*, et al.* (2001). "Keratinocyte-driven contraction of reconstructed human skin". Wound Repair and Regeneration. **9** (2): 95-106.

Chao, C.Y.L., Zheng, Y.-P. and Cheing, G.L.Y. (2011). "A novel noncontact method to assess the biomechanical properties of wound tissue". Wound Repair and Regeneration. **19** (3): 324-329.

Chastain, S.R., Kundu, A.K., Dhar, S., Calvert, J.W. and Putnam, A.J. (2006). "Adhesion of mesenchymal stem cells to polymer scaffolds occurs via distinct ecm ligands and controls their osteogenic differentiation". Journal of Biomedical Materials Research Part A. **78A** (1): 73-85.

Chau, A.H., Chan, R.C., Shishkov, M., MacNeill, B., Iftimiia, N.*, et al.* (2004). "Mechanical analysis of atherosclerotic plaques based on optical coherence tomography". Annals of Biomedical Engineering. **32** (11): 1494-1503.

Chen, C.S., Lyonsgiordano, B., Lazarus, G.S. and Jensen, P.J. (1993). "Differential expression of plasminogen activators and their inhibitors in an organotypic skin coculture system". Journal of Cell Science. **106** 45-53.

Chen, F.-M., Wu, L.-A., Zhang, M., Zhang, R. and Sun, H.-H. (2011). "Homing of endogenous stem/progenitor cells for in situ tissue regeneration: Promises, strategies, and translational perspectives". Biomaterials. **32** (12): 3189-3209.

Chen, J. and Lee, L. (2007). "Clinical applications and new developments of optical coherence tomography: An evidence-based review". Clinical and Experimental Optometry. **90** (5): 317-335.

Chen, J.S., Wong, V.W. and Gurtner, G.C. (2012). "Therapeutic potential of bone marrow-derived mesenchymal stem cells for cutaneous wound healing". Frontiers in immunology. **3** 192-192.

Chen, L.W., Tredget, E.E., Wu, P.Y.G. and Wu, Y.J. (2008). "Paracrine factors of mesenchymal stem cells recruit macrophages and endothelial lineage cells and enhance wound healing". Plos One. **3** (4):

Chieregato, K., Castegnaro, S., Madeo, D., Astori, G., Pegoraro, M.*, et al.* (2011). "Epidermal growth factor, basic fibroblast growth factor and platelet-derived growth factor-bb can substitute for fetal bovine serum and compete with human platelet-rich plasma in the ex vivo expansion of mesenchymal stromal cells derived from adipose tissue". Cytotherapy. **13** (8): 933-943.

Chin, G.A., Thigpin, T.G., Perrin, K.J., Moldawer, L.L. and Schultz, G.S. (2003). "Treatment of chronic ulcers in diabetic patients with a topical metalloproteinase inhibitor, doxycycline". Wounds-a Compendium of Clinical Research and Practice. **15** (10): 315-323.

Chmielowiec, J., Borowiak, M., Morkel, M., Stradal, T., Munz, B.*, et al.* (2007). "C-met is essential for wound healing in the skin". Journal of Cell Biology. **177** (1): 151-162.

Claridge, E., Cotton, S., Hall, P. and Moncrieff, M. (2003). "From colour to tissue histology: Physics-based interpretation of images of pigmented skin lesions". Medical Image Analysis. **7** (4): 489-502.

Clark, E.A., King, W.G., Brugge, J.S., Symons, M. and Hynes, R.O. (1998). "Integrin-mediated signals regulated by members of the rho family of gtpases". Journal of Cell Biology. **142** (2): 573-586.

Clark, R.A.F., Lanigan, J.M., Dellapelle, P., Manseau, E., Dvorak, H.F.*, et al.* (1982). "Fibronectin and fibrin provide a provisional matrix for epidermal-cell migration during wound reepithelialization". Journal of Investigative Dermatology. **79** (5): 264-269.

Cloutier, M., Girard, B., Peel, S.A.F., Wilson, D., Sandor, G.K.B.*, et al.* (2010). "Calvarial bone wound healing: A comparison between carbide and diamond drills, er:Yag and femtosecond lasers with or without bmp-7". Oral Surgery Oral Medicine Oral Pathology Oral Radiology and Endodontology. **110** (6): 720-728.

Colley, H., McArthur, S.L., Stolzing, A. and Scutt, A. (2012). "Culture on fibrin matrices maintains the colony-forming capacity and osteoblastic differentiation of mesenchymal stem cells". Biomedical Materials. **7** (4):

Colley, H.E., Mishra, G., Scutt, A.M. and McArthur, S.L. (2009). "Plasma polymer coatings to support mesenchymal stem cell adhesion, growth and differentiation on variable stiffness silicone elastomers". Plasma Processes and Polymers. **6** (12): 831-839.

Conway, K., Price, P., Harding, K.G. and Jiang, W.G. (2006). "The molecular and clinical impact of hepatocyte growth factor, its receptor, activators, and inhibitors in wound healing". Wound Repair and Regeneration. **14** (1): 2-10.

Cooper, D.M., Yu, E.Z., Hennessey, P., Ko, F. and Robson, M.C. (1994). "Determination of endogenous cytokines in chronic wounds". Annals of Surgery. **219** (6): 688-692.

Costa, R.A., Skaf, M., Melo, L.A.S., Calucci, D., Cardillo, J.A.*, et al.* (2006). "Retinal assessment using optical coherence tomography". Progress in Retinal and Eye Research. **25** (3): 325-353.

Cox, S., Cole, M. and Tawil, B. (2004). "Behavior of human dermal fibroblasts in three-dimensional fibrin clots: Dependence on fibrinogen and thrombin concentration". Tissue Engineering. **10** (5-6): 942-954.

Culav, E.M., Clark, C.H. and Merrilees, M.J. (1999). "Connective tissues: Matrix composition and its relevance to physical therapy". Physical Therapy. **79** (3): 308-319.

Cunningham, J.J., Nikolovski, J., Linderman, J.J. and Mooney, D.J. (2002). "Quantification of fibronectin adsorption to silicone-rubber cell culture substrates". Biotechniques. **32** (4): 876-+.

Cutler, A.J., Limbani, V., Girdlestone, J. and Navarrete, C.V. (2010). "Umbilical cord-derived mesenchymal stromal cells modulate monocyte function to suppress t cell proliferation". Journal of Immunology. **185** (11): 6617-6623.

Danaei, G., Finucane, M.M., Lu, Y., Singh, G.M., Cowan, M.J.*, et al.* (2011). "National, regional, and global trends in fasting plasma glucose and diabetes prevalence since 1980: Systematic analysis of health examination surveys and epidemiological studies with 370 country-years and 2.7 million participants". Lancet. **378** (9785): 31-40.

Danmark, S., Finne-Wistrand, A., Albertsson, A.C., Patarroyo, M. and Mustafa, K. (2012). "Integrin-mediated adhesion of human mesenchymal stem cells to extracellular matrix proteins adsorbed to polymer surfaces". Biomedical Materials. **7** (3):

Dash, N.R., Dash, S.N., Routray, P., Mohapatra, S. and Mohapatra, P.C. (2009). "Targeting nonhealing ulcers of lower extremity in human through autologous bone marrow-derived mesenchymal stem cells". Rejuvenation Research. **12** (5): 359-366.

Davidson, J.M., Broadley, K.N. and Quaglino, D., Jr. (1997). "Reversal of the wound healing deficit in diabetic rats by combined basic fibroblast growth factor and transforming growth factor-beta-1 therapy". Wound Repair and Regeneration. **5** (1): 77-88.

Daw, R., Candan, S., Beck, A.J., Devlin, A.J., Brook, I.M.*, et al.* (1998). "Plasma copolymer surfaces of acrylic acid 1,7 octadiene: Surface characterisation and the attachment of ros 17/2.8 osteoblast-like cells". Biomaterials. **19** (19): 1717-1725.

Dawson, J.B., Barker, D.J., Ellis, D.J., Grassam, E., Cotterill, J.A.*, et al.* (1980). "A theoretical and experimental-study of light-absorption and scattering by invivo skin". Physics in Medicine and Biology. **25** (4): 695-709.

Demidova-Rice, T.N., Hamblin, M.R. and Herman, I.M. (2012). "Acute and impaired wound healing: Pathophysiology and current methods for drug delivery, part 2: Role of growth factors in normal and pathological wound healing: Therapeutic potential and methods of delivery". Advances in Skin & Wound Care. **25** (8): 349-370.

Deng, G., Curriden, S.A., Wang, S.J., Rosenberg, S. and Loskutoff, D.J. (1996). "Is plasminogen activator inhibitor-1 the molecular switch that governs urokinase receptor-mediated cell adhesion and release?". Journal of Cell Biology. **134** (6): 1563-1571.

Descargues, P., Deraison, C., Bonnart, C., Kreft, M., Kishibe, M., *et al.* (2005). "Spink5-deficient mice mimic netherton syndrome through degradation of desmoglein 1 by epidermal protease hyperactivity". Nature Genetics. **37** (1): 56-65.

Deshpande, P., Notara, M., Bullett, N., Daniels, J.T., Haddow, D.B., *et al.* (2009). "Development of a surface-modified contact lens for the transfer of cultured limbal epithelial cells to the cornea for ocular surface diseases". Tissue Engineering Part A. **15** (10): 2889-2902.

Desmet, T., Morent, R., De Geyter, N., Leys, C., Schacht, E., *et al.* (2009). "Nonthermal plasma technology as a versatile strategy for polymeric biomaterials surface modification: A review". Biomacromolecules. **10** (9): 2351-2378.

Desmouliere, A., Geinoz, A., Gabbiani, F. and Gabbiani, G. (1993). "Transforming growth-factor-beta-1 induces alpha-smooth muscle actin expression in granulation-tissue myofibroblasts and in quiescent and growing cultured fibroblasts". Journal of Cell Biology. **122** (1): 103-111.

Di Nicola, M., Carlo-Stella, C., Magni, M., Milanesi, M., Longoni, P.D., *et al.* (2002). "Human bone marrow stromal cells suppress t-lymphocyte proliferation induced by cellular or nonspecific mitogenic stimuli". Blood. **99** (10): 3838-3843.

Diegelmann, R.F., Cohen, I.K. and Kaplan, A.M. (1981). "The role of macrophages in wound repair - a review". Plastic and Reconstructive Surgery. **68** (1): 107-113.

Dissemond, J. (2006). "Modern wound dressings for the therapy of chronic wounds". Hautarzt. **57** (10): 881-887.

Djouad, F., Charbonnier, L.-M., Bouffi, C., Louis-Plence, P., Bony, C., *et al.* (2007). "Mesenchymal stem cells inhibit the differentiation of dendritic cells through an interleukin-6-dependent mechanism". Stem Cells. **25** (8): 2025-2032.

Dominici, M., Le Blanc, K., Mueller, I., Slaper-Cortenbach, I., Marini, F.C., *et al.* (2006). "Minimal criteria for defining multipotent mesenchymal stromal cells. The international society for cellular therapy position statement". Cytotherapy. **8** (4): 315-317.

Doucet, C., Ernou, I., Zhang, Y.Z., Llense, J.R., Begot, L., *et al.* (2005). "Platelet lysates promote mesenchymal stem cell expansion: A safety substitute for animal serum in cell-based therapy applications". Journal of Cellular Physiology. **205** (2): 228-236.

Dowling, D.P., Miller, I.S., Ardhaoui, M. and Gallagher, W.M. (2011). "Effect of surface wettability and topography on the adhesion of osteosarcoma cells on plasma-modified polystyrene". Journal of Biomaterials Applications. **26** (3): 327-347.

Downing, D.T., Stewart, M.E., Wertz, P.W., Colton, S.W., Abraham, W., *et al.* (1987). "Skin lipids - an update". Journal of Investigative Dermatology. **88** (3): S2-S6.

Draper, B.K., Davidson, M.K. and Nanney, L.B. (2002). "Nmps and timp-1 are differentially expressed between acute murine excisional and laser wounds". Lasers in Surgery and Medicine. **30** (2): 106-116.

Drexler, W. (2004). "Ultrahigh-resolution optical coherence tomography". Journal of biomedical optics. **9** (1): 47-74.

Drnovsek-Olup, B., Beltram, M. and Pizem, J. (2004). "Repetitive er : Yag laser irradiation of human skin: A histological evaluation". Lasers in Surgery and Medicine. **35** (2): 146-151.

Du, J., Chen, X., Liang, X., Zhang, G., Xu, J., *et al.* (2011). "Integrin activation and internalization on soft ecm as a mechanism of induction of stem cell differentiation by ecm

elasticity". Proceedings of the National Academy of Sciences of the United States of America. **108** (23): 9466-9471.

Edwards, R. and Harding, K.G. (2004). "Bacteria and wound healing". Current Opinion in Infectious Diseases. **17** (2): 91-96.

Eltorai, I.M., Montroy, R.E., Kobayashi, M., Jakowatz, J. and Guttierez, P. (2002). "Marjolin's ulcer in patients with spinal cord injury". The journal of spinal cord medicine. **25** (3): 191-6.

Enfield, J., Jonathan, E. and Leahy, M. (2011). "In vivo imaging of the microcirculation of the volar forearm using correlation mapping optical coherence tomography (cmoct)". Biomedical Optics Express. **2** (5): 1184-1193.

Engler, A.J., Sen, S., Sweeney, H.L. and Discher, D.E. (2006). "Matrix elasticity directs stem cell lineage specification". Cell. **126** (4): 677-689.

Engrav, L.H., Garner, W.L. and Tredget, E.E. (2007). "Hypertrophic scar, wound contraction and hyper-hypopiginentation". Journal of Burn Care & Research. **28** (4): 593-597.

Epstein, E.H. and Munderloh, N.H. (1978). "Human-skin collagen - presence of type-i and type-iii at all levels of dermis". Journal of Biological Chemistry. **253** (5): 1336-1337.

Evans, D. and Land, L. (2001). "Topical negative pressure for treating chronic wounds: A systematic review". British Journal of Plastic Surgery. **54** (3): 238-242.

Eves, P., Layton, C., Hedley, S., Dawson, R.A., Wagner, M.*, et al.* (2000). "Characterization of an in vitro model of human melanoma invasion based on reconstructed human skin". British Journal of Dermatology. **142** (2): 210-222.

Eves, P.C., Beck, A.J., Shard, A.G. and MacNeil, S. (2005). "A chemically defined surface for the co-culture of melanocytes and keratinocytes". Biomaterials. **26** (34): 7068-7081.

Eves, P.C., Bullett, N.A., Haddow, D., Beck, A.J., Layton, C.*, et al.* (2008). "Simplifying the delivery of melanocytes and keratinocytes for the treatment of vitiligo using a chemically defined carrier dressing". Journal of Investigative Dermatology. **128** (6): 1554-1564.

Falanga, V., Iwamoto, S., Chartier, M., Yufit, T., Butmarc, J.*, et al.* (2007). "Autologous bone marrow-derived cultured mesenchymal stem cells delivered in a fibrin spray accelerate healing in murine and human cutaneous wounds". Tissue Engineering. **13** (6): 1299-1312.

Fang, J., Hodivala-Dilke, K., Johnson, B.D., Du, L.M., Hynes, R.O.*, et al.* (2005). "Therapeutic expression of the platelet-specific integrin, alpha iib beta 3, in a murine model for glanzmann thrombasthenia". Blood. **106** (8): 2671-2679.

Fathke, C., Wilson, L., Hutter, J., Kapoor, V., Smith, A.*, et al.* (2004). "Contribution of bone marrow-derived cells to skin: Collagen deposition and wound repair". Stem Cells. **22** (5): 812-822.

Fercher, A.F. (2010). "Optical coherence tomography – development, principles, applications". Zeitschrift für Medizinische Physik. **20** (4): 251-276.

Fercher, A.F., Hitzenberger, C.K., Kamp, G. and Elzaiat, S.Y. (1995). "Measurement of intraocular distances by backscattering spectral interferometry". Optics Communications. **117** (1-2): 43-48.

Ferraq, Y., Black, D., Lagarde, J.M., Schmitt, A.M., Dahan, S.*, et al.* (2007). "Use of a 3-d imaging technique for non-invasive monitoring of the depth of experimentally induced wounds". Skin Research and Technology. **13** (4): 399-405.

Ferraq, Y., Black, D.R., Theunis, J. and Mordon, S. (2012). "Superficial wounding model for epidermal barrier repair studies: Comparison of erbium:Yag laser and the suction blister method". Lasers in Surgery and Medicine. **44** (7): 525-532.

Filova, E., Bullett, N.A., Bacakova, L., Grausova, L., Haycock, J.W.*, et al.* (2009). "Regionally-selective cell colonization of micropatterned surfaces prepared by plasma polymerization of acrylic acid and 1,7-octadiene". Physiological Research. **58** (5): 669-684.

Fitzpatrick, T.B. and Breathnach, A.S. (1963). "The epidermal melanin unit system". Dermatologische Wochenschrift. **147** 481-9.

Forsea, A.-M., Carstea, E.M., Ghervase, L., Giurcaneanu, C. and Pavelescu, G. (2010). "Clinical application of optical coherence tomography for the imaging of non-melanocytic cutaneous tumors: A pilot multi-modal study". Journal of medicine and life. **3** (4): 381-9.

France, R.M., Short, R.D., Dawson, R.A. and MacNeil, S. (1998). "Attachment of human keratinocytes to plasma co-polymers of acrylic acid octa-1,7-diene and allyl amine octa-1,7-diene". Journal of Materials Chemistry. **8** (1): 37-42.

Freshney, R.I. (2000). "Culture of animal cells: A manual of basic technique". Wiley-LISS. New York.

Friedens.Aj, Chailakh.Rk, Latsinik, N.V., Panasyuk, A.F. and Keilissb.Iv. (1974). "Stromal cells responsible for transferring microenvironment of hematopoietic tissues - cloning invitro and retransplantation invivo". Transplantation. **17** (4): 331-340.

Friedens.Aj, Petrakov.Kv, Kuroleso.Ai and Frolova, G.P. (1968). "Heterotopic transplants of bone marrow - analysis of precursor cells for osteogenic and hematopoietic tissues". Transplantation. **6** (2): 230-&.

Fujimoto, J.G. (2001). "Optical coherence tomography". Comptes Rendus De L Academie Des Sciences Serie Iv Physique Astrophysique. **2** (8): 1099-1111.

Fujimoto, J.G. (2003). "Optical coherence tomography for ultrahigh resolution in vivo imaging". Nature Biotechnology. **21** (11): 1361-1367.

Gabbiani, G., Ryan, G.B. and Majno, G. (1971). "Presence of modified fibroblasts in granulation tissue and their possible role in wound contraction". Experientia. **27** (5): 549-&.

Galiano, R.D., Michaels, J., Dobryansky, M., Levine, J.P. and Gurtner, G.C. (2004a). "Quantitative and reproducible murine model of excisional wound healing". Wound Repair and Regeneration. **12** (4): 485-492.

Galiano, R.D., Tepper, O.M., Pelo, C.R., Bhatt, K.A., Callaghan, M.*, et al.* (2004b). "Topical vascular endothelial growth factor accelerates diabetic wound healing through increased angiogenesis and by mobilizing and recruiting bone marrow-derived cells". American Journal of Pathology. **164** (6): 1935-1947.

Galkowska, H., Olszewski, W.L., Wojewodzka, U., Rosinski, G. and Karnafel, W. (2006). "Neurogenic factors in the impaired healing of diabetic foot ulcers". Journal of Surgical Research. **134** (2): 252-258.

Gallagher, K.A., Liu, Z.-J., Xiao, M., Chen, H., Goldstein, L.J.*, et al.* (2007). "Diabetic impairments in no-mediated endothelial progenitor cell mobilization and homing are reversed by hyperoxia and sdf-1 alpha". Journal of Clinical Investigation. **117** (5): 1249-1259.

Gambichler, T., Hyun, J., Moussa, G., Tomi, N.S., Boms, S.*, et al.* (2007a). "Optical coherence tomography of cutaneous lupus erythematosus correlates with histopathology". Lupus. **16** (1): 35-38.

Gambichler, T., Jaedicke, V. and Terras, S. (2011). "Optical coherence tomography in dermatology: Technical and clinical aspects". Archives of Dermatological Research. **303** (7): 457-473.

Gambichler, T., Regeniter, P., Bechara, F.G., Orlikov, A., Vasa, R.*, et al.* (2007b). "Characterization of benign and malignant melanocytic skin lesions using optical coherence tomography in vivo". Journal of the American Academy of Dermatology. **57** (4): 629-637.

Gang, E.J., Jeong, J.A., Han, S., Yan, Q., Jeon, C.J.*, et al.* (2006). "In vitro endothelial potential of human uc blood-derived mesenchymal stem cells". Cytotherapy. **8** (3): 215-227.

Garcia, A.J., Vega, M.D. and Boettiger, D. (1999). "Modulation of cell proliferation and differentiation through substrate-dependent changes in fibronectin conformation". Molecular Biology of the Cell. **10** (3): 785-798.

Gawronska-Kozak, B., Bogacki, M., Rim, J.-S., Monroe, W.T. and Manuel, J.A. (2006). "Scarless skin repair in immunodeficient mice". Wound Repair and Regeneration. **14** (3): 265-276.

Geerlings, S.E. and Hoepelman, A.I.M. (1999). "Immune dysfunction in patients with diabetes mellitus (dm)". Fems Immunology and Medical Microbiology. **26** (3-4): 259-265.

Georgakoudi, I., Rice, W.L., Hronik-Tupaj, M. and Kaplan, D.L. (2008). "Optical spectroscopy and imaging for the noninvasive evaluation of engineered tissues". Tissue Engineering Part B-Reviews. **14** (4): 321-340.

Gholipour-Kanani, A., Bahrami, S.H., Samadi-Kochaksaraie, A., Ahmadi-Tafti, H., Rabbani, S.*, et al.* (2012). "Effect of tissue-engineered chitosan-poly(vinyl alcohol) nanofibrous scaffolds on healing of burn wounds of rat skin". Iet Nanobiotechnology. **6** (4): 129-135.

Ghosh, M.M., Boyce, S., Layton, C., Freedlander, E. and MacNeil, S. (1997). "A comparison of methodologies for the preparation of human epidermal-dermal composites". Annals of Plastic Surgery. **39** (4): 390-404.

Giattina, S.D., Courtney, B.K., Herz, P.R., Harman, M., Shortkroff, S.*, et al.* (2006). "Assessment of coronary plaque collagen with polarization sensitive optical coherence tomography (ps-oct)". International Journal of Cardiology. **107** (3): 400-409.

Gillery, P., Bellon, G., Coustry, F. and Borel, J.P. (1989). "Cultures of fibroblasts in fibrin lattices - models for the study of metabolic-activities of the cells in physiological conditions". Journal of Cellular Physiology. **140** (3): 483-490.

Glogau, R.G. (2000). "The risk of progression to invasive disease". Journal of the American Academy of Dermatology. **42** (1 Pt 2): 23-4.

Graaff, R., Aarnoudse, J.G., Zijp, J.R., Sloot, P.M.A., Demul, F.F.M.*, et al.* (1992). "Reduced light-scattering properties for mixtures of spherical-particles - a simple approximation derived from mie calculations". Applied Optics. **31** (10): 1370-1376.

Greenhalgh, D.G. (1996). "The role of growth factors in wound healing". Journal of Trauma-Injury Infection and Critical Care. **41** (1): 159-167.

Grinnell, F. (1994). "Fibroblasts, myofibroblasts, and wound contraction". Journal of Cell Biology. **124** (4): 401-404.

Grondahlhansen, J., Lund, L.R., Ralfkiaer, E., Ottevanger, V. and Dano, K. (1988). "Urokinase-type and tissue-type plasminogen activators in keratinocytes during wound reepithelialization invivo". Journal of Investigative Dermatology. **90** (6): 790-795.

Gross, T.J., Leavell, K.J. and Peterson, M.W. (1997). "Cd11b/cd18 mediates the neutrophil chemotactic activity of fibrin degradation product d domain". Thrombosis and Haemostasis. **77** (5): 894-900.

Gruber, R., Karreth, F., Kandler, B., Fuerst, G., Rot, A.*, et al.* (2004). "Platelet-released supernatants increase migration and proliferation, and decrease osteogenic differentiation of bone marrow-derived mesenchymal progenitor cells under in vitro conditions". Platelets. **15** (1): 29-35.

Gu, Z.Z., Cui, J., Brown, S., Fridman, R., Mobashery, S.*, et al.* (2005). "A highly specific inhibitor of matrix metalloproteinase-9 rescues laminin from proteolysis and neurons from apoptosis in transient focal cerebral ischemia". Journal of Neuroscience. **25** (27): 6401-6408.

Guo, L., Kawazoe, N., Hoshiba, T., Tateishi, T., Chen, G.*, et al.* (2008). "Osteogenic differentiation of human mesenchymal stem cells on chargeable polymer-modified surfaces". Journal of Biomedical Materials Research Part A. **87A** (4): 903-912.

Guo, S. and DiPietro, L.A. (2010). "Factors affecting wound healing". Journal of Dental Research. **89** (3): 219-229.

Haddow, D.B., Steele, D.A., Short, R.D., Dawson, R.A. and MacNeil, S. (2003). "Plasma-polymerized surfaces for culture of human keratinocytes and transfer of cells to an in vitro wound-bed model". Journal of Biomedical Materials Research Part A. **64A** (1): 80-87.

Halata, Z., Grim, M. and Bauman, K.I. (2003). "Friedrich sigmund merkel and his "merkel cell", morphology, development, and physiology: Review and new results". Anatomical Record Part a-Discoveries in Molecular Cellular and Evolutionary Biology. **271A** (1): 225-239.

Halme, D.G. and Kessler, D.A. (2006). "Fda regulation of stem-cell-based therapies". New England Journal of Medicine. **355** (16): 1730-1735.

Hamdoon, Z., Jerjes, W., Upile, T. and Hopper, C. (2011). "Optical coherence tomography-guided photodynamic therapy for skin cancer: Case study". Photodiagnosis and Photodynamic Therapy. **8** (1): 49-52.

Harris, A.K., Wild, P. and Stopak, D. (1980). "Silicone-rubber substrata- new wrinkle in the study of cell locomotion". Science. **208** (4440): 177-179.

Harrison, C.A., Gossiel, F., Layton, C.M., Bullock, A.J., Johnson, T.*, et al.* (2006). "Use of an in vitro model of tissue-engineered skin to investigate the mechanism of skin graft contraction". Tissue Engineering. **12** (11): 3119-3133.

Hartmann, I., Hollweck, T., Haffner, S., Krebs, M., Meiser, B.*, et al.* (2010). "Umbilical cord tissue-derived mesenchymal stem cells grow best under gmp-compliant culture conditions and maintain their phenotypic and functional properties". Journal of Immunological Methods. **363** (1): 80-89.

Haynes, C.A., Sliwinsky, E. and Norde, W. (1994). "Structural and electrostatic properties of globular-proteins at a polystyrene water interface". Journal of Colloid and Interface Science. **164** (2): 394-409.

Hedley, S.J., Layton, C., Heaton, M., Chakrabarty, K.H., Dawson, R.A.*, et al.* (2002). "Fibroblasts play a regulatory role in the control of pigmentation in reconstructed human skin from skin types i and ii". Pigment Cell Research. **15** (1): 49-56.

Heo, S.C., Jeon, E.S., Lee, I.H., Kim, H.S., Kim, M.B.*, et al.* (2011). "Tumor necrosis factor-alpha-activated human adipose tissue-derived mesenchymal stem cells accelerate

cutaneous wound healing through paracrine mechanisms". Journal of Investigative Dermatology. **131** (7): 1559-1567.

Herber, O.R., Schnepp, W. and Rieger, M.A. (2007). "A systematic review on the impact of leg ulceration on patients' quality of life". Health and Quality of Life Outcomes. **5**

Hernon, C.A., Dawson, R.A., Freedlander, E., Short, R., Haddow, D.B.*, et al.* (2006). "Clinical experience using cultured epithelial autografts leads to an alternative methodology for transferring skin cells from the laboratory to the patient". Regenerative Medicine. **1** (6): 809-821.

Hibst, R. (1992). "Mechanical effects of erbium - yag laser bone ablation". Lasers in Surgery and Medicine. **12** (2): 125-130.

Hieta, N., Impola, U., Lopez-Otin, C., Saarialho-Kere, U. and Kahari, V.M. (2003). "Matrix metalloproteinase-19 expression in dermal wounds and by fibroblasts in culture". Journal of Investigative Dermatology. **121** (5): 997-1004.

Higashiyama, R., Nakao, S., Shibusawa, Y., Ishikawa, O., Moro, T.*, et al.* (2011). "Differential contribution of dermal resident and bone marrow-derived cells to collagen production during wound healing and fibrogenesis in mice". Journal of Investigative Dermatology. **131** (2): 529-536.

Higham, M.C., Dawson, R., Szabo, M., Short, R., Haddow, D.B.*, et al.* (2003). "Development of a stable chemically defined surface for the culture of human keratinocytes under serum-free conditions for clinical use". Tissue Engineering. **9** (5): 919-930.

Higuchi, A., Takanashi, Y., Tsuzuki, N., Asakura, T., Cho, C.S.*, et al.* (2003). "Production of interferon-beta by fibroblast cells on membranes prepared with rgd-containing peptides". Journal of Biomedical Materials Research Part A. **65A** (3): 369-378.

Ho, W., Tawil, B., Dunn, J.C.Y. and Wu, B.M. (2006). "The behavior of human mesenchymal stem cells in 3d fibrin clots: Dependence on fibrinogen concentration and clot structure". Tissue Engineering. **12** (6): 1587-1595.

Hocking, A.M. and Gibran, N.S. (2010). "Mesenchymal stem cells: Paracrine signaling and differentiation during cutaneous wound repair". Experimental Cell Research. **316** (14): 2213-2219.

Hong, H.S., Kim, Y.H. and Son, Y. (2012). "Perspectives on mesenchymal stem cells: Tissue repair, immune modulation, and tumor homing". Archives of Pharmacal Research. **35** (2): 201-211.

Horwitz, E.M., Gordon, P.L., Koo, W.K.K., Marx, J.C., Neel, M.D.*, et al.* (2002). "Isolated allogeneic bone marrow-derived mesenchymal cells engraft and stimulate growth in children with osteogenesis imperfecta: Implications for cell therapy of bone". Proceedings of the National Academy of Sciences of the United States of America. **99** (13): 8932-8937.

Horwitz, E.M., Le Blanc, K., Dominici, M., Mueller, I., Slaper-Cortenbach, I.*, et al.* (2005). "Clarification of the nomenclature for msc: The international society for cellular therapy position statement". Cytotherapy. **7** (5): 393-395.

Hsiue, G.H., Lee, S.D., Wang, C.C., Shiue, M.H.I. and Chang, P.C.T. (1994). "Plasma-induced graft-copolymerization of hema onto silicone-rubber and tpx film improving rabbit corneal epithelial-cell attachment and growth". Biomaterials. **15** (3): 163-171.

Huang, D., Swanson, E.A., Lin, C.P., Schuman, J.S., Stinson, W.G.*, et al.* (1991). "Optical coherence tomography". Science. **254** (5035): 1178-1181.

Huang, S., Lu, G., Wu, Y., Jirigala, E., Xu, Y.*, et al.* (2012). "Mesenchymal stem cells delivered in a microsphere-based engineered skin contribute to cutaneous wound healing and sweat gland repair". Journal of Dermatological Science. **66** (1): 29-36.

Huijberts, M.S.P., Schaper, N.C. and Schalkwijk, C.G. (2008). "Advanced glycation end products and diabetic foot disease". Diabetes-Metabolism Research and Reviews. **24** S19-S24.

Ichioka, S., Kouraba, S., Sekiya, N., Ohura, N. and Nakatsuka, T. (2005). "Bone marrow-impregnated collagen matrix for wound healing: Experimental evaluation in a microcirculatory model of angiogenesis, and clinical experience". British Journal of Plastic Surgery. **58** (8): 1124-1130.

Ishida, Y., Kondo, T., Takayasu, T., Iwakura, Y. and Mukaida, N. (2004). "The essential involvement of cross-talk between ifn-gamma and tgf-beta in the skin wound-healing process". Journal of Immunology. **172** (3): 1848-1855.

Ishida-Yamamoto, A. and Iizuka, H. (1998). "Structural organization of cornified cell envelopes and alterations in inherited skin disorders". Experimental Dermatology. **7** (1): 1-10.

Itoh, T., Tanioka, M., Yoshida, H., Yoshioka, T., Nishimoto, H.*, et al.* (1998). "Reduced angiogenesis and tumor progression in gelatinase a-deficient mice". Cancer Research. **58** (5): 1048-1051.

Jakob, T., Brown, M.J. and Udey, M.C. (1999). "Characterization of e-cadherin-containing junctions involving skin-derived dendritic cells". Journal of Investigative Dermatology. **112** (1): 102-108.

Jameson, J. and Havran, W.L. (2007). "Skin gamma delta t-cell functions in homeostasis and wound healing". Immunological Reviews. **215** 114-122.

Jang, I.K., Bouma, B.E., Kang, D.H., Park, S.J., Park, S.W.*, et al.* (2002). "Visualization of coronary atherosclerotic plaques in patients using optical coherence tomography: Comparison with intravascular ultrasound". Journal of the American College of Cardiology. **39** (4): 604-609.

Javazon, E.H., Keswani, S.G., Badillo, A.T., Crombleholme, T.M., Zoltick, P.W.*, et al.* (2007). "Enhanced epithelial gap closure and increased angiogenesis in wounds of diabetic mice treated with adult murine bone marrow stromal progenitor cells". Wound Repair and Regeneration. **15** (3): 350-359.

Jiang, D., Qi, Y., Walker, N.G., Sindrilaru, A., Hainzl, A.*, et al.* (2013). "The effect of adipose tissue derived mscs delivered by a chemically defined carrier on full-thickness cutaneous wound healing". Biomaterials. **34** (10): 2501-2515.

Jiang, X.-Y., Lu, D.-B. and Chen, B. (2012). "Progress in stem cell therapy for the diabetic foot". Diabetes Research and Clinical Practice. **97** (1): 43-50.

Jiang, Y., Huang, S., Fu, X., Liu, H., Ran, X.*, et al.* (2011). "Epidemiology of chronic cutaneous wounds in china". Wound Repair and Regeneration. **19** (2): 181-188.

Jonasson, J.M., Ye, W., Sparen, P., Apelqvist, J., Nyren, O.*, et al.* (2008). "Risks of nontraumatic lower-extremity amputations in patients with type 1 diabetes - a population-based cohort study in sweden". Diabetes Care. **31** (8): 1536-1540.

Jorgensen, T.M., Tycho, A., Mogensen, M., Bjerring, P. and Jemec, G.B.E. (2008). "Machine-learning classification of non-melanoma skin cancers from image features obtained by optical coherence tomography". Skin Research and Technology. **14** (3): 364-369.

Jumper, J.M., Gallemore, R.P., McCuen, B.W. and Toth, C.A. (2000). "Features of macular hole closure in the early postoperative period using optical coherence tomography". Retina-the Journal of Retinal and Vitreous Diseases. **20** (3): 232-237.

Jung, S., Panchalingam, K.M., Rosenberg, L. and Behie, L.A. (2012). "Ex vivo expansion of human mesenchymal stem cells in defined serum-free media". Stem Cells International.

Jung, W.G., Kao, B., Kelly, K.M., Liaw, L.H.L., Nelson, J.S.*, et al.* (2003). "Optical coherence tomography for in vitro monitoring of wound healing after laser irradiation". Ieee Journal of Selected Topics in Quantum Electronics. **9** (2): 222-226.

Kalinin, A.E., Kajava, A.V. and Steinert, P.M. (2002). "Epithelial barrier function: Assembly and structural features of the cornified cell envelope". Bioessays. **24** (9): 789-800.

Kato, T., Kure, T., Chang, J.H., Gabison, E.E., Itoh, T.*, et al.* (2001). "Diminished corneal angiogenesis in gelatinase a-deficient mice". Febs Letters. **508** (2): 187-190.

Keenan, J., Pearson, D. and Clynes, M. (2006). "The role of recombinant proteins in the development of serum-free media". Cytotechnology. **50** (1-3): 49-56.

Kelly, J.M., Short, R.D. and Alexander, M.R. (2003). "Experimental evidence of a relationship between monomer plasma residence time and carboxyl group retention in acrylic acid plasma polymers". Polymer. **44** (11): 3173-3176.

Keselowsky, B.G., Collard, D.M. and Garcia, A.J. (2003). "Surface chemistry modulates fibronectin conformation and directs integrin binding and specificity to control cell adhesion". Journal of Biomedical Materials Research Part A. **66A** (2): 247-259.

Khetani, S.R. and Bhatia, S.N. (2006). "Engineering tissues for in vitro applications". Current Opinion in Biotechnology. **17** (5): 524-531.

Khoo, C., Micklem, K. and Watt, S. (2011). "A comparison of methods for quantifying angiogenesis in the matrigel assay in vitro.". Tissue Engineering. ((in press)):

Kim, C.H., Lee, J.H., Won, J.H. and Cho, M.K. (2011a). "Mesenchymal stem cells improve wound healing in vivo via early activation of matrix metalloproteinase-9 and vascular endothelial growth factor". Journal of Korean Medical Science. **26** (6): 726-733.

Kim, E.K., Li, G., Lee, T.J. and Hong, J.P. (2011b). "The effect of human adipose-derived stem cells on healing of ischemic wounds in a diabetic nude mouse model". Plastic and Reconstructive Surgery. **128** (2): 387-394.

Kim, K.H., Pierce, M.C., Maguluri, G., Park, B.H., Yoon, S.J.*, et al.* (2012). "In vivo imaging of human burn injuries with polarization-sensitive optical coherence tomography". Journal of biomedical optics. **17** (6):

Kim, S.S., Song, C.K., Shon, S.K., Lee, K.Y., Kim, C.H.*, et al.* (2009). "Effects of human amniotic membrane grafts combined with marrow mesenchymal stem cells on healing of full-thickness skin defects in rabbits". Cell and Tissue Research. **336** (1): 59-66.

Kim, W.-S., Park, B.-S., Sung, J.-H., Yang, J.-M., Park, S.-B.*, et al.* (2007). "Wound heating effect of adipose-derived stem cells: A critical role of secretory factors on human dermal fibroblasts". Journal of Dermatological Science. **48** (1): 15-24.

Kinnaird, T., Stabile, E., Burnett, M.S., Lee, C.W., Barr, S.*, et al.* (2004). "Marrow-derived stromal cells express genes encoding a broad spectrum of arteriogenic cytokines and promote in vitro and in vivo arteriogenesis through paracrine mechanisms". Circulation Research. **94** (5): 678-685.

Kirana, S., Stratmann, B., Lammers, D., Negrean, M., Stirban, A.*, et al.* (2007). "Wound therapy with autologous bone marrow stem cells in diabetic patients with ischaemia-induced tissue ulcers affecting the lower limbs". International Journal of Clinical Practice. **61** (4): 690-692.

Kirchner, L.M., Meerbaum, S.O., Gruber, B.S., Knoll, A.K., Bulgrin, J.*, et al.* (2003). "Effects of vascular endothelial growth factor on wound closure rates in the genetically diabetic mouse model". Wound Repair and Regeneration. **11** (2): 127-131.

Knighton, D.R., Ciresi, K.F., Fiegel, V.D., Austin, L.L. and Butler, E.L. (1986). "Classification and treatment of chronic nonhealing wounds - successful treatment with autologous platelet-derived wound-healing factors (pdwhf)". Annals of Surgery. **204** (3): 322-330.

Knuttel, A., Bonev, S. and Knaak, W. (2004). "New method for evaluation of in vivo scattering and refractive index properties obtained with optical coherence tomography". Journal of biomedical optics. **9** (2): 265-273.

Kobayashi, T., Watanabe, H., Yanagawa, T., Tsutsumi, S., Kayakabe, M.*, et al.* (2005). "Motility and growth of human bone-marrow mesenchymal stem cells during ex vivo expansion in autologous serum". Journal of Bone and Joint Surgery-British Volume. **87B** (10): 1426-1433.

Koch, P.J., de Viragh, P.A., Scharer, E., Bundman, D., Longley, M.A.*, et al.* (2000). "Lessons from loricrin-deficient mice: Compensatory mechanisms maintaining skin barrier function in the absence of a major cornified envelope protein". Journal of Cell Biology. **151** (2): 389-400.

Koenig, A.L., Gambillara, V. and Grainger, D.W. (2003). "Correlating fibronectin adsorption with endothelial cell adhesion and signaling on polymer substrates". Journal of Biomedical Materials Research Part A. **64A** (1): 20-37.

Koolwijk, P., vanErck, M.G.M., deVree, W.J.A., Vermeer, M.A., Weich, H.A.*, et al.* (1996). "Cooperative effect of tnf alpha, bfgf, and vegf on the formation of tubular structures of human microvascular endothelial cells in a fibrin matrix. Role of urokinase activity". Journal of Cell Biology. **132** (6): 1177-1188.

Korde, V.R., Bonnema, G.T., Xu, W., Krishnamurthy, C., Ranger-Moore, J.*, et al.* (2007). "Using optical coherence tomography to evaluate skin sun damage and precancer". Lasers in Surgery and Medicine. **39** (9): 687-695.

Kranke, P., Bennett, M.H., Martyn-St James, M., Schnabel, A. and Debus, S.E. (2012). "Hyperbaric oxygen therapy for chronic wounds". Cochrane Database of Systematic Reviews. (4):

Krawczyk, W.S. (1971). "Pattern of epidermal cell migration during wound healing". Journal of Cell Biology. **49** (2): 247-&.

Kume, T., Akasaka, T., Kawamoto, T., Watanabe, N., Toyota, E.*, et al.* (2005a). "Assessment of coronary intima-media thickness by optical coherence tomography - comparison with intravascular ultrasound". Circulation Journal. **69** (8): 903-907.

Kume, T., Akasaka, T., Kawamoto, T., Watanabe, N., Toyota, E.*, et al.* (2005b). "Visualization of neointima formation by optical coherence tomography". International Heart Journal. **46** (6): 1133-1136.

Kuo, Y.-R., Wang, C.-T., Cheng, J.-T., Wang, F.-S., Chiang, Y.-C.*, et al.* (2011). "Bone marrow-derived mesenchymal stem cells enhanced diabetic wound healing through recruitment of tissue regeneration in a rat model of streptozotocin-induced diabetes". Plastic and Reconstructive Surgery. **128** (4): 872-880.

Kuznetsov, S.A., Mankani, M.H. and Robey, P.G. (2000). "Effect of serum on human bone marrow stromal cells: Ex vivo expansion and in vivo bone formation". Transplantation. **70** (12): 1780-1787.

Kwon, D.S., Gao, X., Liu, Y.B., Dulchavsky, D.S., Danyluk, A.L.*, et al.* (2008). "Treatment with bone marrow-derived stromal cells accelerates wound healing in diabetic rats". International Wound Journal. **5** (3): 453-463.

Lamparter, S., Slight, S.H. and Weber, K.T. (2002). "Doxycycline and tissue repair in rats". Journal of Laboratory and Clinical Medicine. **139** (5): 295-302.

Lange, C., Cakiroglu, F., Spiess, A.-N., Cappallo-Obermann, H., Dierlamm, J.*, et al.* (2007). "Accelerated and safe expansion of human mesenchymal stromal cells in animal serum-free medium for transniantation and regenerative medicine". Journal of Cellular Physiology. **213** (1): 18-26.

Laplante, A.F., Germain, L., Auger, F.A. and Moulin, V. (2001). "Mechanisms of wound reepithelialization: Hints from a tissue-engineered reconstructed skin to long-standing questions". Faseb Journal. **15** (13): 2377-2389.

Larsson, J., Agardh, C.D., Apelqvist, J. and Stenstrom, A. (1998). "Long term prognosis after healed amputation in patients with diabetes". Clinical Orthopaedics and Related Research. (350): 149-158.

Laurens, N., Koolwijk, P. and De Maat, M.P.M. (2006). "Fibrin structure and wound healing". Journal of Thrombosis and Haemostasis. **4** (5): 932-939.

Lazarus, G.S., Cooper, D.M., Knighton, D.R., Margolis, D.J., Percoraro, R.E.*, et al.* (1994). "Definitions and guidelines for assessment of wounds and evaluation of healing". Wound Repair and Regeneration. **2** (3): 165-170.

Le Blanc, K., Rasmusson, I., Sundberg, B., Gotherstrom, C., Hassan, M.*, et al.* (2004). "Treatment of severe acute graft-versus-host disease with third party haploidentical mesenchymal stem cells". Lancet. **363** (9419): 1439-1441.

Lee, J.N., Jiang, X., Ryan, D. and Whitesides, G.M. (2004). "Compatibility of mammalian cells on surfaces of poly(dimethylsiloxane)". Langmuir. **20** (26): 11684-11691.

Lee, M.J., Kim, J., Kim, M.Y., Bae, Y.-S., Ryu, S.H.*, et al.* (2010). "Proteomic analysis of tumor necrosis factor-alpha-induced secretome of human adipose tissue-derived mesenchymal stem cells". Journal of Proteome Research. **9** (4): 1754-1762.

Lee, S.H., Lee, J.H. and Cho, K.H. (2011). "Effects of human adipose-derived stem cells on cutaneous wound healing in nude mice". Annals of Dermatology. **23** (2): 150-155.

Leitgeb, R., Hitzenberger, C.K. and Fercher, A.F. (2003). "Performance of fourier domain vs. Time domain optical coherence tomography". Optics Express. **11** (8): 889-894.

Leonardi, D., Oberdoerfer, D., Fernandes, M.C., Meurer, R.T., Pereira-Filho, G.A.*, et al.* (2012). "Mesenchymal stem cells combined with an artificial dermal substitute improve repair in full-thickness skin wounds". Burns. **38** (8): 1143-1150.

Li, H., Fu, X., Ouyang, Y., Cai, C., Wang, J.*, et al.* (2006). "Adult bone-marrow-derived mesenchymal stem cells contribute to wound healing of skin appendages". Cell and Tissue Research. **326** (3): 725-736.

Li, J. and Pei, M. (2012). "Cell senescence: A challenge in cartilage engineering and regeneration". Tissue Engineering Part B-Reviews. **18** (4): 270-287.

Li-Tsang, C.W.P., Lau, J.C.M. and Chan, C.C.H. (2005). "Prevalence of hypertrophic scar formation and its characteristics among the chinese population". Burns. **31** (5): 610-616.

Liang, C.-C., Park, A.Y. and Guan, J.-L. (2007). "In vitro scratch assay: A convenient and inexpensive method for analysis of cell migration in vitro". Nature Protocols. **2** (2): 329-333.

Liew, Y.M., McLaughlin, R.A., Gong, P., Wood, F.M. and Sampson, D.D. (2013). "In vivo assessment of human burn scars through automated quantification of vascularity using optical coherence tomography". Journal of biomedical optics. **18** (6):

Lindblad, W.J. (2008). "Considerations for selecting the correct animal model for dermal wound-healing studies". Journal of Biomaterials Science-Polymer Edition. **19** (8): 1087-1096.

Lister, T., Wright, P.A. and Chappell, P.H. (2012). "Optical properties of human skin". Journal of biomedical optics. **17** (9):

Liu, P., Deng, Z., Han, S., Liu, T., Wen, N.*, et al.* (2008). "Tissue-engineered skin containing mesenchymal stem cells improves burn wounds". Artificial Organs. **32** (12): 925-931.

Lobmann, R., Ambrosch, A., Schultz, G., Waldmann, K., Schiweck, S.*, et al.* (2002). "Expression of matrix-metalloproteinases and their inhibitors in the wounds of diabetic and non-diabetic patients". Diabetologia. **45** (7): 1011-1016.

Lobmann, R., Schultz, G. and Lehnert, H. (2005). "Proteases and the diabetic foot syndrome: Mechanisms and therapeutic implications". Diabetes Care. **28** (2): 461-471.

Loots, M.A.M., Kenter, S.B., Au, F.L., van Galen, W.J.M., Middelkoop, E.*, et al.* (2002). "Fibroblasts derived from chronic diabetic ulcers differ in their response to stimulation with egf, igf-i, bfgf and pdgf-ab compared to controls". European Journal of Cell Biology. **81** (3): 153-160.

Loots, M.A.M., Lamme, E.N., Mekkes, J.R., Bos, J.D. and Middelkoop, E. (1999). "Cultured fibroblasts from chronic diabetic wounds on the lower extremity (non-insulin-dependent diabetes mellitus) show disturbed proliferation". Archives of Dermatological Research. **291** (2-3): 93-99.

Loots, M.A.M., Lamme, E.N., Zeegelaar, J., Mekkes, J.R., Bos, J.D.*, et al.* (1998). "Differences in cellular infiltrate and extracellular matrix of chronic diabetic and venous ulcers versus acute wounds". Journal of Investigative Dermatology. **111** (5): 850-857.

Lopez Ponte, A., Marais, E., Gallay, N., Langonne, A., Delorme, B.*, et al.* (2007). "The in vitro migration capacity of human bone marrow mesenchymal stem cells: Comparison of chemokine and growth factor chemotactic activities". Stem Cells. **25** (7): 1737-1745.

Lu, D., Chen, B., Liang, Z., Deng, W., Jiang, Y.*, et al.* (2011). "Comparison of bone marrow mesenchymal stem cells with bone marrow-derived mononuclear cells for treatment of diabetic critical limb ischemia and foot ulcer: A double-blind, randomized, controlled trial". Diabetes Research and Clinical Practice. **92** (1): 26-36.

Luo, G., Cheng, W., He, W., Wang, X., Tan, J.*, et al.* (2010). "Promotion of cutaneous wound healing by local application of mesenchymal stem cells derived from human umbilical cord blood". Wound Repair and Regeneration. **18** (5): 506-513.

Lynch, S.E., Colvin, R.B. and Antoniades, H.N. (1989). "Growth-factors in wound-healing - single and synergistic effects on partial thickness porcine skin wounds". Journal of Clinical Investigation. **84** (2): 640-646.

Ma, K., Liao, S., He, L., Lu, J., Ramakrishna, S.*, et al.* (2011). "Effects of nanofiber/stem cell composite on wound healing in acute full-thickness skin wounds". Tissue Engineering Part A. **17** (9-10): 1413-1424.

Maas-Szabowski, N., Stark, H.J. and Fusenig, N.E. (2000). "Keratinocyte growth regulation in defined organotypic cultures through il-1-induced keratinocyte growth factor expression in resting fibroblasts". Journal of Investigative Dermatology. **114** (6): 1075-1084.

MacDonald, D.E., Deo, N., Markovic, B., Stranick, M. and Somasundaran, P. (2002). "Adsorption and dissolution behavior of human plasma fibronectin on thermally and chemically modified titanium dioxide particles". Biomaterials. **23** (4): 1269-1279.

MacNeill, B.D., Jang, I.K., Bouma, B.E., Iftimia, N., Takano, M.*, et al.* (2004). "Focal and multi-focal plaque distributions in patients with macrophage acute and stable presentations of coronary artery disease". Journal of the American College of Cardiology. **44** (5): 972-979.

Madden, J.W. and Peacock, E.E. (1968). "Studies on biology of collagen during wound healing .I. Rate of collagen synthesis and deposition in cutaneous wounds of rat". Surgery. **64** (1): 288-&.

Madison, K.C. (2003). "Barrier function of the skin: "La raison d'etre" of the epidermis". Journal of Investigative Dermatology. **121** (2): 231-241.

Maharlooei, M.K., Bagheri, M., Solhjou, Z., Jahromi, B.M., Akrami, M.*, et al.* (2011). "Adipose tissue derived mesenchymal stem cell (ad-msc) promotes skin wound healing in diabetic rats". Diabetes Research and Clinical Practice. **93** (2): 228-234.

Mansilla, E., Marin, G.H., Sturla, F., Drago, H.E., Gil, M.A.*, et al.* (2005). "Human mesenchymal stem cells are tolerized by mice and improve skin and spinal cord injuries". Transplantation Proceedings. **37** (1): 292-294.

Marekov, L.N. and Steinert, P.M. (1998). "Ceramides are bound to structural proteins of the human foreskin epidermal cornified cell envelope". Journal of Biological Chemistry. **273** (28): 17763-17770.

Mareschi, K., Novara, M., Rustichelli, D., Ferrero, I., Guido, D.*, et al.* (2006). "Neural differentiation of human mesenchymal stem cells: Evidence for expression of neural markers and eag k+ channel types". Experimental Hematology. **34** (11): 1563-1572.

Maricich, S.M., Wellnitz, S.A., Nelson, A.M., Lesniak, D.R., Gerling, G.J.*, et al.* (2009). "Merkel cells are essential for light-touch responses". Science. **324** (5934): 1580-1582.

Marieb, E.N., and Hoehn, K. . (2007). "The integumentary system. In human anatomy and physiology". (2ed) 151-158. Pearson Benjamin Cummings. San Francisco.

Marques, C.M.D. (2010). "Tissue engineered human skin models to study the effect of inflammation on melanoma invasion". Thesis (Type) Department of Engineering Materials. Univerisity of Sheffield.

Marschall, S., Sander, B., Mogensen, M., Jorgensen, T.M. and Andersen, P.E. (2011). "Optical coherence tomography-current technology and applications in clinical and biomedical research". Analytical and Bioanalytical Chemistry. **400** (9): 2699-2720.

Martin, P. (1997). "Wound healing - aiming for perfect skin regeneration". Science. **276** (5309): 75-81.

Martin-Rendon, E., Sweeney, D., Lu, F., Girdlestone, J., Navarrete, C.*, et al.* (2008). "5-azacytidine-treated human mesenchymal stem/progenitor cells derived from umbilical cord, cord blood and bone marrow do not generate cardiomyocytes in vitro at high frequencies". Vox Sanguinis. **95** (2): 137-148.

Mason, C., Markusen, J.F., Town, M.A., Dunnill, P. and Wang, R.K. (2004). "Doppler optical coherence tomography for measuring flow in engineered tissue". Biosensors & Bioelectronics. **20** (3): 414-423.

Mast, B.A. and Schultz, G.S. (1996). "Interactions of cytokines, growth factors, and proteases in acute and chronic wounds". Wound Repair and Regeneration. **4** (4): 411-420.

Matcher, S.J. (2010). ""Pratical aspects of oct imaging in tissue engineering" in: 3d cell cultre methods and protocols". (Haycok Ed) 261-281. Humana Press. New York.

Matsumoto, K., Hashimoto, K., Yoshikawa, K. and Nakamura, T. (1991). "Marked stimulation of growth and motility of human keratinocytes by hepatocyte growth-factor". Experimental Cell Research. **196** (1): 114-120.

McFarlin, K., Gao, X., Liu, Y.B., Dulchavsky, D.S., Kwon, D.*, et al.* (2006). "Bone marrow-derived mesenchymal stromal cells accelerate wound healing in the rat". Wound Repair and Regeneration. **14** (4): 471-478.

Medeiros, F.A., Zangwill, L.M., Bowd, C., Vessani, R.M., Susanna, R.*, et al.* (2005). "Evaluation of retinal nerve fiber layer, optic nerve head, and macular thickness measurements for glaucoma detection using optical coherence tomography". American Journal of Ophthalmology. **139** (1): 44-55.

Meglinski, I.V. and Matcher, S.J. (2002). "Quantitative assessment of skin layers absorption and skin reflectance spectra simulation in the visible and near-infrared spectral regions". Physiological Measurement. **23** (4): 741-753.

Meirelles, L.d.S., Fontes, A.M., Covas, D.T. and Caplan, A.I. (2009). "Mechanisms involved in the therapeutic properties of mesenchymal stem cells". Cytokine & Growth Factor Reviews. **20** (5-6): 419-427.

Menke, N., Ward, K., Witten, T., Bonchev, D. and Diegelmann, R. (2007a). "Impaired wound healing". Clinics in Dermatology. **25** (1): 19-25.

Menke, N.B., Ward, K.R., Witten, T.M., Bonchev, D.G. and Diegelmann, R.F. (2007b). "Impaired wound healing". Clinics in Dermatology. **25** (1): 19-25.

Menko, A.S. and Boettiger, D. (1987). "Occupation of the fibronectin receptor is a control point for myogenic differentiation". Journal of Cell Biology. **105** (4 PART 2): 47A-47A.

Meszaros, A.J., Reichner, J.S. and Albina, J.E. (2000). "Macrophage-induced neutrophil apoptosis". Journal of Immunology. **165** (1): 435-441.

Michel, G., Kemeny, L., Peter, R.U., Beetz, A., Ried, C.*, et al.* (1992). "Interleukin-8 receptor-mediated chemotaxis of normal human epidermal-cells". Febs Letters. **305** (3): 241-243.

Mills, R.E., Taylor, K.R., Podshivalova, K., McKay, D.B. and Jameson, J.M. (2008). "Defects in skin gamma delta t cell function contribute to delayed wound repair in rapamycin-treated mice". Journal of Immunology. **181** (6): 3974-3983.

Mirastschijski, U., Impola, U., Jahkola, T., Karlsmark, T., Agren, M.S.*, et al.* (2002). "Ectopic localization of matrix metalloproteinase-9 in chronic cutaneous wounds". Human Pathology. **33** (3): 355-364.

Misra, R.D.K., Girase, B., Nune, V.K.C. and Xu, W. (2012). "Cellular interactions and modulated osteoblasts functions mediated by protein adsorption". Advanced Engineering Materials. **14** (5): B247-B257.

Miyahara, Y., Nagaya, N., Kataoka, M., Yanagawa, B., Tanaka, K.*, et al.* (2006). "Monolayered mesenchymal stem cells repair scarred myocardium after myocardial infarction". Nature Medicine. **12** (4): 459-465.

Miyajima, S., Shirai, A., Yamamoto, S., Okada, N. and Matsushita, T. (2006). "Risk factors for major limb amputations in diabetic foot gangrene patients". Diabetes Research and Clinical Practice. **71** (3): 272-279.

Mizuno, N., Shiba, H., Ozeki, Y., Mouri, Y., Niitani, M.*, et al.* (2006). "Human autologous serum obtained using a completely closed bag system as a substitute for foetal calf serum in human mesenchymal stem cell cultures". Cell Biology International. **30** (6): 521-524.

Mogensen, M., Morsy, H.A., Nurnberg, B.M. and Jemec, G.B.E. (2008a). "Optical coherence tomography imaging of bullous diseases". Journal of the European Academy of Dermatology and Venereology. **22** (12): 1458-1464.

Mogensen, M., Morsy, H.A., Thrane, L. and Jemec, G.B.E. (2008b). "Morphology and epidermal thickness of normal skin imaged by optical coherence tomography". Dermatology. **217** (1): 14-20.

Mogensen, M., Nurnberg, B.M., Forman, J.L., Thomsen, J.B., Thrane, L.*, et al.* (2009a). "In vivo thickness measurement of basal cell carcinoma and actinic keratosis with optical coherence tomography and 20-mhz ultrasound". British Journal of Dermatology. **160** (5): 1026-1033.

Mogensen, M., Thrane, L., Joergensen, T.M., Andersen, P.E. and Jemec, G.B.E. (2009b). "Optical coherence tomography for imaging of skin and skin diseases". Seminars in Cutaneous Medicine and Surgery. **28** (3): 196-202.

Mogensen, M., Thrane, L., Jorgensen, T.M., Andersen, P.E. and Jemec, G.B.E. (2009c). "Oct imaging of skin cancer and other dermatological diseases". Journal of biophotonics. **2** (6-7): 442-451.

Moisan, M., Barbeau, J., Crevier, M.C., Pelletier, J., Philip, N.*, et al.* (2002). "Plasma sterilization. Methods mechanisms". Pure and Applied Chemistry. **74** (3): 349-358.

Monsaingeon, A. and Molimard, R. (1976). "Wound-healing - comparison of healing rates of burn wounds and excisional wounds". European Surgical Research. **8** (4): 337-343.

Montagna, W. and Carlisle, K. (1991). "The architecture of black-and-white facial skin". Journal of the American Academy of Dermatology. **24** (6): 929-937.

Montandon, D., D'Andiran, G. and Gabbiani, G. (1977). "The mechanism of wound contraction and epithelialization: Clinical and experimental studies". Clinics in Plastic Surgery. **4** (3): 325-46.

Morent, R., De Geyter, N., Trentesaux, M., Gengembre, L., Dubruel, P.*, et al.* (2010). "Stability study of polyacrylic acid films plasma-polymerized on polypropylene substrates at medium pressure". Applied Surface Science. **257** (2): 372-380.

Morent, R., De Geyter, N., Van Vlierberghe, S., Vanderleyden, E., Dubruel, P.*, et al.* (2009). "Deposition of polyacrylic acid films by means of an atmospheric pressure dielectric barrier discharge". Plasma Chemistry and Plasma Processing. **29** (2): 103-117.

Morgner, U., Drexler, W., Kartner, F.X., Li, X.D., Pitris, C.*, et al.* (2000). "Spectroscopic optical coherence tomography". Optics Letters. **25** (2): 111-113.

Morsy, H., Kamp, S., Thrane, L., Behrendt, N., Saunder, B.*, et al.* (2010). "Optical coherence tomography imaging of psoriasis vulgaris: Correlation with histology and disease severity". Archives of Dermatological Research. **302** (2): 105-111.

Mosmann, T. (1983). "Rapid colorimetric assay for cellular growth and survival - application to proliferation and cyto-toxicity assays". Journal of Immunological Methods. **65** (1-2): 55-63.

Mosser, D.M. and Edwards, J.P. (2008). "Exploring the full spectrum of macrophage activation". Nature Reviews Immunology. **8** (12): 958-969.

Moustafa, M., Bullock, A.J., Creagh, T.M., Heller, S., Jeffcoate, W.*, et al.* (2007). "Randomized, controlled, single-blind study on use of autologous keratinocytes on a transfer dressing to treat nonhealing diabetic ulcers". Regenerative Medicine. **2** (6): 887-902.

Moustafa, M., Simpson, C., Glover, M., Dawson, R.A., Tesfaye, S.*, et al.* (2004). "A new autologous keratinocyte dressing treatment for non-healing diabetic neuropathic foot ulcers". Diabetic Medicine. **21** (7): 786-789.

Mulder, G.D., Lee, D.K. and Jeppesen, N.S. (2012). "Comprehensive review of the clinical application of autologous mesenchymal stem cells in the treatment of chronic wounds and diabetic bone healing". International Wound Journal. **9** (6): 595-600.

Müller, J., Mollenhauer, J., Tuan, R. and Benz, K. (2012). "Quality control for mesenchymal stromal cells: Chondrogenesis as a
standard condition?". Rheumatology. **S3**

Nagase, H. and Woessner, J.F. (1999). "Matrix metalloproteinases". Journal of Biological Chemistry. **274** (31): 21491-21494.

Nakagawa, H., Akita, S., Fukui, M., Fujii, T. and Akino, K. (2005). "Human mesenchymal stem cells successfully improve skin-substitute wound healing". British Journal of Dermatology. **153** (1): 29-36.

Nambu, M., Ishihara, M., Nakamura, S., Mizuno, H., Yanagibayashi, S.*, et al.* (2007). "Enhanced healing of mitomycin c-treated wounds in rats using inbred adipose tissue-derived stromal cells within an atelocollagen matrix". Wound Repair and Regeneration. **15** (4): 505-510.

Nambu, M., Kishimoto, S., Nakamura, S., Mizuno, H., Yanagibayashi, S.*, et al.* (2009). "Accelerated wound healing in healing-impaired db/db mice by autologous adipose tissue-derived stromal cells combined with atelocollagen matrix". Annals of Plastic Surgery. **62** (3): 317-321.

Nemes, Z. and Steinert, P.M. (1999). "Bricks and mortar of the epidermal barrier". Experimental and Molecular Medicine. **31** (1): 5-19.

Nemeth, K., Leelahavanichkul, A., Yuen, P.S.T., Mayer, B., Parmelee, A.*, et al.* (2009). "Bone marrow stromal cells attenuate sepsis via prostaglandin e-2-dependent reprogramming of host macrophages to increase their interleukin-10 production". Nature Medicine. **15** (1): 42-49.

Neuss, S., Schneider, R.K.M., Tietze, L., Knuechel, R. and Jahnen-Dechent, W. (2010). "Secretion of fibrinolytic enzymes facilitates human mesenchymal stem cell invasion into fibrin clots". Cells Tissues Organs. **191** (1): 36-46.

Nguyen, M., Arkell, J. and Jackson, C.J. (2001). "Human endothelial gelatinases and angiogenesis". International Journal of Biochemistry & Cell Biology. **33** (10): 960-970.

Nie, C., Yang, D., Xu, J., Si, Z., Jin, X.*, et al.* (2011). "Locally administered adipose-derived stem cells accelerate wound healing through differentiation and vasculogenesis". Cell Transplantation. **20** (2): 205-216.

Norisugi, O., Makino, T., Hara, H., Matsui, K., Furuichi, M.*, et al.* (2011). "Evaluation of skin atrophy associated with linear atrophoderma of moulin by ultrasound imaging". Journal of the American Academy of Dermatology. **65** (1): 232-233.

Nwomeh, B.C., Yager, D.R. and Cohen, I.K. (1998). "Physiology of the chronic wound". Clinics in Plastic Surgery. **25** (3): 341-+.

O'Loughlin, A., Kulkarni, M., Dockery, P., Shaw, G., Mooney, E.*, et al.* (2011). "Mesenchymal stem cell therapy for diabetic foot ulceration". Irish Journal of Medical Science. **180** S493-S493.

Oh, J.-T., Lee, S.-W., Kim, Y.-S., Suhr, K.-B. and Kim, B.-M. (2006). "Quantification of the wound healing using polarization-sensitive optical coherence tomography". Journal of biomedical optics. **11** (4):

Oishi, K., Noguchi, H., Yukawa, H. and Hayashi, S. (2009). "Differential ability of somatic stem cells". Cell Transplantation. **18** (5-6): 581-589.

Olmedo, J.M., Warschaw, K.E., Schmitt, J.M. and Swanson, D.L. (2006). "Optical coherence tomography for the characterization of basal cell carcinoma in vivo: A pilot study". Journal of the American Academy of Dermatology. **55** (3): 408-412.

Opalenik, S.R. and Davidson, J.M. (2005). "Fibroblast differentiation of bone marrow-derived cells during wound repair". Faseb Journal. **19** (9): 1561-+.

Orbay, H., Takami, Y., Hyakusoku, H. and Mizuno, H. (2011). "Acellular dermal matrix seeded with adipose-derived stem cells as a subcutaneous implant". Aesthetic Plastic Surgery. **35** (5): 756-763.

Oren, A., Ganz, T., Liu, L. and Meerloo, T. (2003). "In human epidermis, beta-defensin 2 is packaged in lamellar bodies". Experimental and Molecular Pathology. **74** (2): 180-182.

Oswald, J., Boxberger, S., Jorgensen, B., Feldmann, S., Ehninger, G.*, et al.* (2004). "Mesenchymal stem cells can be differentiated into endothelial cells in vitro". Stem Cells. **22** (3): 377-384.

Otoole, L., Beck, A.J. and Short, R.D. (1996). "Characterization of plasma polymers of acrylic acid and propanoic acid". Macromolecules. **29** (15): 5172-5177.

Owen, M.J. (1990). "Silicon-based polymer science: A comprehensive resource". American Chemical Society. Washington.

Palmer, C.N.A., Irvine, A.D., Terron-Kwiatkowski, A., Zhao, Y.W., Liao, H.H.*, et al.* (2006). "Common loss-of-function variants of the epidermal barrier protein filaggrin are a major predisposing factor for atopic dermatitis". Nature Genetics. **38** (4): 441-446.

Pan, Y.T., Wu, Z.L., Yuan, Z.J., Wang, Z.G. and Du, C.W. (2007). "Subcellular imaging of epithelium with time-lapse optical coherence tomography". Journal of biomedical optics. **12** (5):

Pandey, A.C., Semon, J.A., Kaushal, D., O'Sullivan, R.P., Glowacki, J.*, et al.* (2011). "Microrna profiling reveals age-dependent differential expression of nuclear factor kappa b and mitogen-activated protein kinase in adipose and bone marrow-derived human mesenchymal stem cells". Stem Cell Research & Therapy. **2**

Parhi, P., Golas, A. and Vogler, E.A. (2010). "Role of proteins and water in the initial attachment of mammalian cells to biomedical surfaces: A review". Journal of Adhesion Science and Technology. **24** (5): 853-888.

Park, B.H., Saxer, C., Srinivas, S.M., Nelson, J.S. and de Boer, J.F. (2001). "In vivo burn depth determination by high-speed fiber-based polarization sensitive optical coherence tomography". Journal of biomedical optics. **6** (4): 474-479.

Paunescu, V., Deak, E., Herman, D., Siska, I.R., Tanasie, G.*, et al.* (2007). "In vitro differentiation of human mesenchymal stem cells to epithelial lineage". Journal of Cellular and Molecular Medicine. **11** (3): 502-508.

Peacock, E.E. (1984). "Wound repair". (3ed) Saunders. Philadelphia.

Pechter, P.M., Gil, J., Valdes, J., Tomic-Canic, M., Pastar, I.*, et al.* (2012). "Keratin dressings speed epithelialization of deep partial-thickness wounds". Wound Repair and Regeneration. **20** (2): 236-242.

Phadnis, S.M., Joglekar, M.V., Venkateshan, V., Ghaskadbi, S.M., Hardikar, A.A.*, et al.* (2006). "Human umbilical cord blood serum promotes growth, proliferation, as well as differentiation of human bone marrow-derived progenitor cells". In Vitro Cellular & Developmental Biology-Animal. **42** (10): 283-286.

Piaggesi, A., Viacava, P., Rizzo, L., Naccarato, G., Baccetti, F.*, et al.* (2003). "Semiquantitative analysis of the histopathological features of the neuropathic foot ulcer - effects of pressure relief". Diabetes Care. **26** (11): 3123-3128.

Pierce, M.C., Sheridan, R.L., Park, B.H., Cense, B. and de Boer, J.F. (2004). "Collagen denaturation can be quantified in burned human skin using polarization-sensitive optical coherence tomography". Burns. **30** (6): 511-517.

Pittenger, M.F., Mackay, A.M., Beck, S.C., Jaiswal, R.K., Douglas, R.*, et al.* (1999). "Multilineage potential of adult human mesenchymal stem cells". Science. **284** (5411): 143-147.

Plow, E.F., Haas, T.K., Zhang, L., Loftus, J. and Smith, J.W. (2000). "Ligand binding to integrins". Journal of Biological Chemistry. **275** (29): 21785-21788.

Podoleanu, A.G. (2005). "Optical coherence tomography". British Journal of Radiology. **78** (935): 976-988.

Poloni, A., Maurizi, G., Rosini, V., Mondini, E., Mancini, S.*, et al.* (2009). "Selection of cd271+ cells and human ab serum allows a large expansion of mesenchymal stromal cells from human bone marrow". Cytotherapy. **11** (2): 153-162.

Posnett, J., and Franks, P.J. (2007). "The costs of skin breakdown and ulceration in the uk". In skin breakdown: The silent epidemic". Smith & Nephew Foundation. Hull

Postlethwaite, A.E. and Kang, A.H. (1976). "Collagen-induced and collagen peptide-induced chemotaxis of human-blood monocytes". Journal of Experimental Medicine. **143** (6): 1299-1307.

Pountos, I. and Giannoudis, P.V. (2005). "Biology of mesenchymal stem cells". Injury. **36 Suppl 3** S8-S12.

Povazay, B., Bizheva, K., Unterhuber, A., Hermann, B., Sattmann, H.*, et al.* (2002). "Submicrometer axial resolution optical coherence tomography". Optics Letters. **27** (20): 1800-1802.

Powers, C.J., McLeskey, S.W. and Wellstein, A. (2000). "Fibroblast growth factors, their receptors and signaling". Endocrine-Related Cancer. **7** (3): 165-197.

Pradhan, L., Nabzdyk, C., Andersen, N.D., LoGerfo, F.W. and Veves, A. (2009). "Inflammation and neuropeptides: The connection in diabetic wound healing". Expert Reviews in Molecular Medicine. **11**

Prichard, H.L., Reichert, W.M. and Klitzman, B. (2007). "Adult adipose-derived stem cell attachment to biomaterials". Biomaterials. **28** (6): 936-946.

Prockop, D.J. (2007). ""Stemness" does not explain the repair of many tissues by mesenchymal stem/multipotent stromal (mscs)". Clinical Pharmacology & Therapeutics. **82** (3): 241-243.

Proksch, E., Brandner, J.M. and Jensen, J.-M. (2008). "The skin: An indispensable barrier". Experimental Dermatology. **17** (12): 1063-1072.

Prompers, L., Schaper, N., Apelqvist, J., Edmonds, M., Jude, E.*, et al.* (2008). "Prediction of outcome in individuals with diabetic foot ulcers: Focus on the differences between individuals with and without peripheral arterial disease. The eurodiale study". Diabetologia. **51** (5): 747-755.

Puolakkainen, P.A., Twardzik, D.R., Ranchalis, J.E., Pankey, S.C., Reed, M.J.*, et al.* (1995). "The enhancement in wound-healing by transforming growth factor-beta(1) (tgf-beta(1)) depends on the topical delivery system". Journal of Surgical Research. **58** (3): 321-329.

Quattrini, C., Jeziorska, M., Boulton, A.J.M. and Malik, R.A. (2008). "Reduced vascular endothelial growth factor expression and intra-epidermal nerve fiber loss in human diabetic neuropathy". Diabetes Care. **31** (1): 140-145.

Rafii, S. and Lyden, D. (2003). "Therapeutic stem and progenitor cell transplantation for organ vascularization and regeneration". Nature Medicine. **9** (6): 702-712.

Rasulov, M.F., Vasil'chenkov, A.V., Onishchenko, N.A., Krasheninnikov, M.E., Kravchenko, V.I.*, et al.* (2005). "First experience in the use of bone marrow mesenchymal stem cells for the treatment of a patient with deep skin burns". Bulletin of Experimental Biology and Medicine. **139** (1): 141-144.

Ratner, B.D. (2004). "A history of biomaterials". In: Biomaterials science-an introduction to materials in medicine". (2ed) 10-19. Academic Press.

Ravari, H., Hamidi-Almadari, D., Salimifar, M., Bonakdaran, S., Parizadeh, M.R.*, et al.* (2011). "Treatment of non-healing wounds with autologous bone marrow cells, platelets, fibrin glue and collagen matrix". Cytotherapy. **13** (6): 705-711.

Reddy, K.B., Bialkowska, K. and Fox, J.E.B. (2001). "Dynamic modulation of cytoskeletal proteins linking integrins to signaling complexes in spreading cells - role of skelemin in initial integrin-induced spreading". Journal of Biological Chemistry. **276** (30): 28300-28308.

Regar, E., van Beusekom, H.M.M., van der Giessen, W.J. and Serruys, P.W. (2005). "Optical coherence tomography findings at 5-year follow-up after coronary stent implantation". Circulation. **112** (23): E345-E346.

Reinhardt, J., Stuehler, A. and Bluemel, J. (2011). "Safety of bovine sera for production of mesenchymal stem cells for therapeutic use". Human Gene Therapy. **22** (6): 775-775.

Reinoso, R.F., Telfer, B.A. and Rowland, M. (1997). "Tissue water content in rats measured by desiccation". Journal of Pharmacological and Toxicological Methods. **38** (2): 87-92.

Richardson, D.L., Pepper, D.S. and Kay, A.B. (1976). "Chemotaxis for human monocytes by fibrinogen-derived peptides". British Journal of Haematology. **32** (4): 507-513.

Ries, C., Egea, V., Karow, M., Kolb, H., Jochum, M.*, et al.* (2007). "Mmp-2, mti-mmp, and tmp-2 are essential for the invasive capacity of human mesenchymal stem cells: Differential regulation by inflammatory cytokines". Blood. **109** (9): 4055-4063.

Ries, C., Popp, T., Egea, V., Kehe, K. and Jochum, M. (2009). "Matrix metalloproteinase-9 expression and release from skin fibroblasts interacting with keratinocytes: Upregulation in response to sulphur mustard". Toxicology. **263** (1): 26-31.

Rinnerthaler, M., Duschl, J., Steinbacher, P., Salzmann, M., Bischof, J.*, et al.* (2013). "Age-related changes in the composition of the cornified envelope in human skin". Experimental Dermatology. **22** (5): 329-335.

Riva, M.A., Molteni, R. and Racagni, G. (1997). "L-deprenyl potentiates camp-induced elevation of fgf-2 mrna levels in rat cortical astrocytes". Neuroreport. **8** (9-10): 2165-2168.

Robson, M.C. (1997). "The role of growth factors in the healing of chronic wounds". Wound Repair and Regeneration. **5** (1): 12-17.

Rochefort, G.Y., Delorme, B., Lopez, A., Herault, O., Bonnet, P.*, et al.* (2006). "Multipotential mesenchymal stem cells are mobilized into peripheral blood by hypoxia". Stem Cells. **24** (10): 2202-2208.

Rodriguez, P.G., Felix, F.N., Woodley, D.T. and Shim, E.K. (2008). "The role of oxygen in wound healing: A review of the literature". Dermatologic Surgery. **34** (9): 1159-1169.

Rogers, L.C., Bevilacqua, N.J. and Armstrong, D.G. (2008). "The use of marrow-derived stem cells to accelerate healing in chronic wounds". International Wound Journal. **5** (1): 20-25.

Rogowska, J., Patel, N., Plummer, S. and Brezinski, M.E. (2006). "Quantitative optical coherence tomographic elastography: Method for assessing arterial mechanical properties". British Journal of Radiology. **79** (945): 707-711.

Romani, N., Clausen, B.E. and Stoitzner, P. (2010). "Langerhans cells and more: Langerin-expressing dendritic cell subsets in the skin". Immunological Reviews. **234** 120-141.

Romer, J., Lund, L.R., Eriksen, J., Pyke, C., Kristensen, P.*, et al.* (1994). "The receptor for urokinase-type plasminogen-activator is expressed by keratinocytes at the leading skin during reepithilialization". Journal of Investigative Dermatology. **102** (4): 519-522.

Roskelley, C.D., Srebrow, A. and Bissell, M.J. (1995). "A hierarchy of ecm-mediated signaling regulates tissue-specific gene-expression". Current Opinion in Cell Biology. **7** (5): 736-747.

Sabatino, M., Ren, J., David-Ocampo, V., England, L., McGann, M.*, et al.* (2012). "The establishment of a bank of stored clinical bone marrow stromal cell products". Journal of Translational Medicine. **10**

Sahu, K., Verma, Y., Sharma, M., Rao, K.D. and Gupta, P.K. (2010). "Non-invasive assessment of healing of bacteria infected and uninfected wounds using optical coherence tomography". Skin Research and Technology. **16** (4): 428-437.

Sarasua, J.G., Lopez, S.P., Viejo, M.A., Basterrechea, M.P., Rodriguez, A.F.*, et al.* (2011). "Treatment of pressure ulcers with autologous bone marrow nuclear cells in patients with spinal cord injury". Journal of Spinal Cord Medicine. **34** (3): 301-307.

Sasaki, K.M., Aoki, A., Ichinose, S., Yoshino, T., Yamada, S.*, et al.* (2002). "Scanning electron microscopy and fourier transformed infrared spectroscopy analysis of bone removal using er : Yag and co2 lasers". Journal of Periodontology. **73** (6): 643-652.

Sasaki, M., Abe, R., Fujita, Y., Ando, S., Inokuma, D.*, et al.* (2008). "Mesenchymal stem cells are recruited into wounded skin and contribute to wound repair by transdifferentiation into multiple skin cell type". Journal of Immunology. **180** (4): 2581-2587.

Sato, C., Tsuboi, R., Shi, C.M., Rubin, J.S. and Ogawa, H. (1995). "Comparative-study of hepatocyte growth-factor scatter factor and keratinocyte growth-factor effects on human keratinocytes". Journal of Investigative Dermatology. **104** (6): 958-963.

Sawicki, G., Marcoux, Y., Sarkhosh, K., Tredget, E. and Ghahary, A. (2005). "Interaction of keratinocytes and fibroblasts modulates the expression of matrix metalloproteinases-2 and-9 and their inhibitors". Molecular and Cellular Biochemistry. **269** (1-2): 209-216.

Schindler, M., Nur-E-Kamal, A., Ahmed, I., Kamal, J., Liu, H.Y.*, et al.* (2006). "Living in three dimensions - 3d nanostructured environments for cell culture and regenerative medicine". Cell Biochemistry and Biophysics. **45** (2): 215-227.

Schmitt, J.M. (1999). "Optical coherence tomography (oct): A review". Ieee Journal of Selected Topics in Quantum Electronics. **5** (4): 1205-1215.

Segre, J.A. (2006). "Epidermal barrier formation and recovery in skin disorders". Journal of Clinical Investigation. **116** (5): 1150-1158.

Selmani, Z., Naji, A., Zidi, I., Favier, B., Gaiffe, E.*, et al.* (2008). "Human leukocyte antigen-g5 secretion by human mesenchymal stem cells is required to suppress t lymphocyte and natural killer function and to induce cd4(+)cd25(high)foxp3(+) regulatory t cells". Stem Cells. **26** (1): 212-222.

Shafaei, H., Esmaeili, A., Mardani, M., Razavi, S., Hashemibeni, B.*, et al.* (2011). "Effects of human placental serum on proliferation and morphology of human adipose tissue-derived stem cells". Bone Marrow Transplantation. **46** (11): 1464-1471.

Shahdadfar, A., Fronsdal, K., Haug, T., Reinholt, F.P. and Brinchmann, J.E. (2005). "In vitro expansion of human mesenchymal stem cells: Choice of serum is a determinant of cell proliferation, differentiation, gene expression, and transcriptome stability". Stem Cells. **23** (9): 1357-1366.

Sharma, U., Chang, E.W. and Yun, S.H. (2008). "Long-wavelength optical coherence tomography at 1.7 mu m for enhanced imaging depth". Optics Express. **16** (24): 19712-19723.

Shaw, J.E., Sicree, R.A. and Zimmet, P.Z. (2010). "Global estimates of the prevalence of diabetes for 2010 and 2030". Diabetes Research and Clinical Practice. **87** (1): 4-14.

Shechter, R. and Schwartz, M. (2013). "Cns sterile injury: Just another wound healing?". Trends in Molecular Medicine. **19** (3): 135-143.

Shepherd, J., Douglas, I., Rimmer, S., Swanson, L. and MacNeil, S. (2009). "Development of three-dimensional tissue-engineered models of bacterial infected human skin wounds". Tissue Engineering Part C-Methods. **15** (3): 475-484.

Shepherd, J., Sarker, P., Rimmer, S., Swanson, L., MacNeil, S.*, et al.* (2011). "Hyperbranched poly(nipam) polymers modified with antibiotics for the reduction of bacterial burden in infected human tissue engineered skin". Biomaterials. **32** (1): 258-267.

Shokrgozar, M.A., Fattahi, M., Bonakdar, S., Kashani, I.R., Majidi, M.*, et al.* (2012). "Healing potential of mesenchymal stem cells cultured on a collagen-based scaffold for skin regeneration". Iranian Biomedical Journal. **16** (2): 68-76.

Si, Y.-L., Zhao, Y.-L., Hao, H.-J., Fu, X.-B. and Han, W.-D. (2011). "Mscs: Biological characteristics, clinical applications and their outstanding concerns". Ageing Research Reviews. **10** (1): 93-103.

Singer, A.J. and Clark, R.A.F. (1999). "Mechanisms of disease - cutaneous wound healing". New England Journal of Medicine. **341** (10): 738-746.

Singer, A.J., Wang, Z., McClain, S.A. and Pan, Y. (2007). "Optical coherence tomography: A noninvasive method to assess wound reepithelialization". Academic Emergency Medicine. **14** (5): 387-391.

Singh, N., Armstrong, D.G. and Lipsky, B.A. (2005). "Preventing foot ulcers in patients with diabetes". Jama-Journal of the American Medical Association. **293** (2): 217-228.

Smiell, J.M., Wieman, T.J., Steed, D.L., Perry, B.H., Sampson, A.R.*, et al.* (1999). "Efficacy and safety of becaplermin (recombinant human platelet-derived growth factor-bb) in patients with nonhealing, lower extremity diabetic ulcers: A combined analysis of four randomized studies". Wound Repair and Regeneration. **7** (5): 335-346.

Smith, L.E., Bonesi, M., Smallwood, R., Matcher, S.J. and MacNeil, S. (2010). "Using swept-source optical coherence tomography to monitor the formation of neo-epidermis in tissue-engineered skin". Journal of Tissue Engineering and Regenerative Medicine. **4** (8): 652-658.

Smith, S.A. and Dale, B.A. (1986). "Immunological localization of filaggrin in human oral epithelia and correlation with keratinization". Journal of Investigative Dermatology. **86** (2): 168-172.

Song, Q., Bai, J., Garvin, M.K., Sonka, M., Buatti, J.M.*, et al.* (2013). "Optimal multiple surface segmentation with shape and context priors". Ieee Transactions on Medical Imaging. **32** (2): 376-386.

Sorrell, J.M. and Caplan, A.I. (2010). "Topical delivery of mesenchymal stem cells and their function in wounds". Stem Cell Research & Therapy. **1**

Sotiropoulou, P.A., Perez, S.A., Salagianni, M., Baxevanis, C.N. and Papamichail, M. (2006). "Characterization of the optimal culture conditions for clinical scale production of human mesenchymal stem cells". Stem Cells. **24** (2): 462-471.

Spoeler, F., Foerst, M., Marquardt, Y., Hoeller, D., Kurz, H.*, et al.* (2006). "High-resolution optical coherence tomography as a non-destructive monitoring tool for the engineering of skin equivalents". Skin Research and Technology. **12** (4): 261-267.

Srinivas, S.M., de Boer, J.F., Park, H., Keikhanzadeh, K., Huang, H.E.L.*, et al.* (2004). "Determination of burn depth by polarization-sensitive optical coherence tomography". Journal of biomedical optics. **9** (1): 207-212.

Stadelmann, W.K., Digenis, A.G. and Tobin, G.R. (1998). "Physiology and healing dynamics of chronic cutaneous wounds". American Journal of Surgery. **176** (2A): 26S-38S.

Staton, C.A., Brown, N.J. and Lewis, C.E. (2003). "The role of fibrinogen and related fragments in tumour angiogenesis and metastasis". Expert Opinion on Biological Therapy. **3** (7): 1105-1120.

Steed, D.L., Webster, M.W., Ricotta, J.J., Luterman, A., Brown, S.*, et al.* (1995). "Clinical-evaluation of recombinant human platelet-derived growth-factor for the treatment of lower-extremity diabetic ulcers". Journal of Vascular Surgery. **21** (1): 71-81.

Steele, J.G., Dalton, B.A., Johnson, G. and Underwood, P.A. (1995). "Adsorption of fibronectin and vitronectin onto primaria(tm) and tissue-culture polystyrene and relationship

to the mechanism of initial attachment of human vein endothelial-cells and bhk-21 fibroblasts". Biomaterials. **16** (14): 1057-1067.

Steinberg, J.P., Hong, S.J., Geringer, M.R., Galiano, R.D. and Mustoe, T.A. (2012). "Equivalent effects of topically-delivered adipose-derived stem cells and dermal fibroblasts in the ischemic rabbit ear model for chronic wounds". Aesthetic Surgery Journal. **32** (4): 504-519.

Steiner, R., Kunzi-Rapp, K. and Scharffetter-Kochanek, K. (2003). "Optical coherence tomography: Clinical applications in dermatology". Medical Laser Application. **18** (3): 249-259.

Steinstraesser, L., Sorkin, M., Niederbichler, A.D., Becerikli, M., Stupka, J.*, et al.* (2010). "A novel human skin chamber model to study wound infection ex vivo". Archives of Dermatological Research. **302** (5): 357-365.

Stoff, A., Rivera, A.A., Banerjee, N.S., Moore, S.T., Numnum, T.M.*, et al.* (2009). "Promotion of incisional wound repair by human mesenchymal stem cell transplantation". Experimental Dermatology. **18** (4): 362-369.

Stolzing, A., Colley, H. and Scutt, A. (2011). "Effect of age and diabetes on the response of mesenchymal progenitor cells to fibrin matrices". International journal of biomaterials. **2011** 378034-378034.

Streuli, C.H., Bailey, N. and Bissell, M.J. (1991). "Control of mammary epithelial differentiation - basement-membrane induces tissue-specific gene-expression in the absence of cell cell-interaction and morphological polarity". Journal of Cell Biology. **115** (5): 1383-1395.

Stute, N., Holtz, K., Bubenheim, M., Lange, C., Blake, F.*, et al.* (2004). "Autologous serum for isolation and expansion of human mesenchymal stem cells for clinical use". Experimental Hematology. **32** (12): 1212-1225.

Sugata, K., Kitahara, T. and Takema, Y. (2008). "Changes of human skin in subepidermal wound healing process". Skin Research and Technology. **14** (4): 436-439.

Sun, T.T., Eichner, R., Nelson, W.G., Vidrich, A. and Woodcock-Mitchell, J. (1983). "Keratin expression during normal epidermal differentiation". Current problems in dermatology. **11** 277-91.

Sundin, M., Ringden, O., Sundberg, B., Nava, S., Gotherstrom, C.*, et al.* (2007). "No alloantibodies against mesenchymal stromal cells, but presence of anti-fetal calf serum antibodies, after transplantation in allogeneic hematopoietic stem cell recipients". Haematologica-the Hematology Journal. **92** (9): 1208-1215.

Surmely, J.F., Takeda, T., Ito, T., and Suzuki, T. . (2007). ""Acute oct findings after stenting". In optical coherence tomography in cardiovascular research". 171-182. Informa Healthcare. London.

Swartzendruber, D.C., Wertz, P.W., Madison, K.C. and Downing, D.T. (1987). "Evidence that the corneocyte has a chemically bound lipid envelope". Journal of Investigative Dermatology. **88** (6): 709-713.

Takiwaki, H. (1998). "Measurement of skin color: Practical application and theoretical considerations". Journal of Medical Investigation. **44** (3-4): 121-126.

Tan, G., Shim, W., Gu, Y., Qian, L., Chung, Y.Y.*, et al.* (2010). "Differential effect of myocardial matrix and integrins on cardiac differentiation of human mesenchymal stem cells". Differentiation. **79** (4-5): 260-271.

Tan, Y., Xiao, J., Huang, Z., Xiao, Y., Lin, S.*, et al.* (2008). "Comparison of the therapeutic effects recombinant human acidic and basic fibroblast growth factors in wound healing in diabetic patients". Journal of Health Science. **54** (4): 432-440.

Tandara, A.A. and Mustoe, T.A. (2004). "Oxygen in wound healing - more than a nutrient". World Journal of Surgery. **28** (3): 294-300.

Tang, L., Sierra, J.O., Kelly, R., Kirsner, R.S. and Li, J. (2012). "Wool-derived keratin stimulates human keratinocyte migration and types iv and vii collagen expression". Experimental Dermatology. **21** (6): 458-460.

Tanigawa, J., Barlis, P. and Di Mario, C. (2007). "Intravascular optical coherence tomography: Optimisation of image acquisition and quantitative assessment of stent strut apposition". EuroIntervention : journal of EuroPCR in collaboration with the Working Group on Interventional Cardiology of the European Society of Cardiology. **3** (1): 128-36.

Tateishi-Yuyama, E., Matsubara, H., Murohara, T., Ikeda, U., Shintani, S.*, et al.* (2002). "Therapeutic angiogenesis for patients with limb ischaemia by autologous transplantation of bone-marrow cells: A pilot study and a randomised controlled trial". Lancet. **360** (9331): 427-435.

Tearney, G.J., Yabushita, H., Houser, S.L., Aretz, H.T., Jang, I.K.*, et al.* (2003). "Quantification of macrophage content in atherosclerotic plaques by optical coherence tomography". Circulation. **107** (1): 113-119.

Tekkatte, C., Gunasingh, G.P., Cherian, K.M. and Sankaranarayanan, K. (2011). ""Humanized" stem cell culture techniques: The animal serum controversy". Stem Cells International.

Terhorst, D., Maltusch, A., Stockfleth, E., Lange-Asschenfeldt, S., Sterry, W.*, et al.* (2011). "Reflectance confocal microscopy for the evaluation of acute epidermal wound healing". Wound Repair and Regeneration. **19** (6): 671-679.

Thom, S.R., Bhopale, V.M., Velazquez, O.C., Goldstein, L.J., Thom, L.H.*, et al.* (2006). "Stem cell mobilization by hyperbaric oxygen". American Journal of Physiology-Heart and Circulatory Physiology. **290** (4): H1378-H1386.

Thomsen, S., Pearce, J.A. and Cheong, W.F. (1989). "Changes in birefringence as markers of thermal-damage in tissues". Ieee Transactions on Biomedical Engineering. **36** (12): 1174-1179.

Thornton, D.J.A., Harrison, C.A., Heaton, M.J., Bullock, A.J. and MacNeil, S. (2008). "Inhibition of keratinocyte-driven contraction of tissue-engineered skin in vitro by calcium chelation and early restraint but not submerged culture". Journal of Burn Care & Research. **29** (2): 369-377.

Todorovic, M., Jiao, S., Ai, J., Pereda-Cubian, D., Stoica, G.*, et al.* (2008). "In vivo burn imaging using mueller optical coherence tomography". Optics Express. **16** (14): 10279-10284.

Tomlins, P.H. and Wang, R.K. (2005). "Theory, developments and applications of optical coherence tomography". Journal of Physics D-Applied Physics. **38** (15): 2519-2535.

Toriseva, M. and Kahari, V.M. (2009). "Proteinases in cutaneous wound healing". Cellular and Molecular Life Sciences. **66** (2): 203-224.

Tsai, W.B., Grunkemeier, J.M., McFarland, C.D. and Horbett, T.A. (2002). "Platelet adhesion to polystyrene-based surfaces preadsorbed with plasmas selectively depleted in fibrinogen, fibronectin, vitronectin, or von willebrand's factor". Journal of Biomedical Materials Research. **60** (3): 348-359.

Tseng, S.C.G., Jarvinen, M.J., Nelson, W.G., Huang, J.W., Woodcockmitchell, J.*, et al.* (1982). "Correlation of specific keratins with different types of epithelial differentiation - monoclonal-antibody studies". Cell. **30** (2): 361-372.

Tu, Z., Li, Q., Bu, H. and Lin, F. (2010). "Mesenchymal stem cells inhibit complement activation by secreting factor h". Stem Cells and Development. **19** (11): 1803-1809.

Tuan, T.L., Zhu, J.Y., Sun, B., Nichter, L.S., Nimni, M.E.*, et al.* (1996). "Elevated levels of plasminogen activator inhibitor-1 may account for the altered fibrinolysis by keloid fibroblasts". Journal of Investigative Dermatology. **106** (5): 1007-1011.

Tuschil, A., Lam, C., Haslberger, A. and Lindley, I. (1992). "Interleukin-8 stimulates calcium transients and promotes epidermal-cell proliferation". Journal of Investigative Dermatology. **99** (3): 294-298.

Uchino, E., Uemura, A. and Ohba, N. (2001). "Initial stages of posterior vitreous detachment in healthy eyes of older persons evaluated by optical coherence tomography". Archives of Ophthalmology. **119** (10): 1475-1479.

Van den Steen, P.E., Dubois, B., Nelissen, I., Rudd, P.M., Dwek, R.A.*, et al.* (2002). "Biochemistry and molecular biology of gelatinase b or matrix metalloproteinase-9 (mmp-9)". Critical Reviews in Biochemistry and Molecular Biology. **37** (6): 375-536.

Vargas, O., Chan, E.K., Barton, J.K., Rylander, H.G. and Welch, A.J. (1999). "Use of an agent to reduce scattering in skin". Lasers in Surgery and Medicine. **24** (2): 133-141.

Vaughan, R.B. and Trinkaus, J.P. (1966). "Movements of epithelial cell sheets in vitro". Journal of Cell Science. **1** (4): 407-&.

Versari, D., Daghini, E., Virdis, A., Ghiadoni, L. and Taddei, S. (2009). "Endothelial dysfunction as a target for prevention of cardiovascular disease". Diabetes Care. **32** S314-S321.

Veves, A., Sheehan, P., Pham, H.T. and Promogran Diabetic Foot Ulcer, S. (2002). "A randomized, controlled trial of promogran (a collagen/oxidized regenerated cellulose dressing) vs standard treatment in the management of diabetic foot ulcers". Archives of Surgery. **137** (7): 822-827.

Vicente-Manzanares, M., Choi, C.K. and Horwitz, A.R. (2009). "Integrins in cell migration - the actin connection". Journal of Cell Science. **122** (2): 199-206.

Vin, F., Teot, L. and Meaume, S. (2002). "The healing properties of promogran in venous leg ulcers". Journal of wound care. **11** (9): 335-41.

Vo-Dinh, T. (2003). "Biomedical photonics handbook". (1ed) CRC Press. Boca Raton.

Vojtassak, J., Danisovic, L.u., Kubes, M., Bakos, D., Jarabek, L.u.*, et al.* (2006). "Autologous biograft and mesenchymal stem cells in treatment of the diabetic foot". Neuroendocrinology Letters. **27** 134-137.

Volk, S.W., Radu, A., Zhang, L. and Liechty, K.W. (2007). "Stromal progenitor cell therapy corrects the wound-healing defect in the ischemic rabbit ear model of chronic wound repair". Wound Repair and Regeneration. **15** (5): 736-747.

Walter, M.N.M., Wright, K.T., Fuller, H.R., MacNeil, S. and Johnson, W.E.B. (2010). "Mesenchymal stem cell-conditioned medium accelerates skin wound healing: An in vitro study of fibroblast and keratinocyte scratch assays". Experimental Cell Research. **316** (7): 1271-1281.

Wang, M., Crisostomo, P.R., Herring, C., Meldrum, K.K. and Meldrum, D.R. (2006). "Human progenitor cells from bone marrow or adipose tissue produce vegf, hgf, and igf-i in response to tnf by a p38 mapk-dependent mechanism". American Journal of Physiology-Regulatory Integrative and Comparative Physiology. **291** (4): R880-R884.

Wang, N., Li, Q., Zhang, L., Lin, H., Hu, J.*, et al.* (2012). "Mesenchymal stem cells attenuate peritoneal injury through secretion of tsg-6". Plos One. **7** (8):

Wang, Z., Pan, H., Yuan, Z., Liu, J., Chen, W.*, et al.* (2008). "Assessment of dermal wound repair after collagen implantation with optical coherence tomography". Tissue engineering. Part C, Methods. **14** (1): 35-45.

Weeks, S., Kulkarni, A., Smith, H., Whittall, C., Yang, Y.*, et al.* (2012). "The effects of chemokine, adhesion and extracellular matrix molecules on binding of mesenchymal stromal cells to poly(l-lactic acid)". Cytotherapy. **14** (9): 1080-1088.

Wei, X., Schneider, J.G., Shenouda, S.M., Lee, A., Towler, D.A.*, et al.* (2011). "De novo lipogenesis maintains vascular homeostasis through endothelial nitric-oxide synthase (enos) palmitoylation". Journal of Biological Chemistry. **286** (4): 2933-2945.

Wei, Y., Eble, J.A., Wang, Z.M., Kreidberg, J.A. and Chapman, H.A. (2001). "Urokinase receptors promote beta 1 integrin function through interactions with integrin alpha 3 beta 1". Molecular Biology of the Cell. **12** (10): 2975-2986.

Weisel, J.W., Francis, C.W., Nagaswami, C. and Marder, V.J. (1993). "Determination of the topology of factor-xiiia-induced fibrin gamma-chain cross-links by electron-microscopy of ligated fragments". Journal of Biological Chemistry. **268** (35): 26618-26624.

Welzel, J. (2001). "Optical coherence tomography in dermatology: A review". Skin Research and Technology. **7** (1): 1-9.

Welzel, J., Reinhardt, C., Lankenau, E., Winter, C. and Wolff, H.H. (2004). "Changes in function and morphology of normal human skin: Evaluation using optical coherence tomography". British Journal of Dermatology. **150** (2): 220-225.

Werb, Z., Tremble, P.M., Behrendtsen, O., Crowley, E. and Damsky, C.H. (1989). "Signal transduction through the fibronectin receptor induces collagenase and stromelysin gene-expression". Journal of Cell Biology. **109** (2): 877-889.

Werdin, F., Tenenhaus, M. and Rennekampff, H.-O. (2008). "Chronic wound care". Lancet. **372** (9653): 1860-1862.

Werner, S. and Grose, R. (2003). "Regulation of wound healing by growth factors and cytokines". Physiological Reviews. **83** (3): 835-870.

Westermarck, J. and Kahari, V.M. (1999). "Regulation of matrix metalloproteinase expression in turner invasion". Faseb Journal. **13** (8): 781-792.

Whittle, J.D., Short, R.D., Douglas, C.W.I. and Davies, J. (2000). "Differences in the aging of allyl alcohol, acrylic acid, allylamine, and octa-1,7-diene plasma polymers as studied by x-ray photoelectron spectroscopy". Chemistry of Materials. **12** (9): 2664-2671.

Wilson, C.J., Clegg, R.E., Leavesley, D.I. and Pearcy, M.J. (2005). "Mediation of biomaterial-cell interactions by adsorbed proteins: A review". Tissue Engineering. **11** (1-2): 1-18.

Winter, G.D. (1995). "Formation of the scab and the rate of epithelisation of superficial wounds in the skin of the young domestic pig. 1962". Journal of wound care. **4** (8): 366-7; discussion 368-71.

Wong, V., Sorkin, M., Glotzbach, J.P., Longaker, M.T. and Gurtner, G.C. (2011). "Surgical approaches to create murine models of human wound healing". Journal of Biomedicine and Biotechnology.

Woodcockmitchell, J., Eichner, R., Nelson, W.G. and Sun, T.T. (1982). "Immunolocalization of keratin polypeptides in human-epidermis using monoclonal-antibodies". Journal of Cell Biology. **95** (2): 580-588.

Wu, Y.J., Chen, L., Scott, P.G. and Tredget, E.E. (2007). "Mesenchymal stem cells enhance wound healing through differentiation and angiogenesis". Stem Cells. **25** 2648-2659.

Xie, J.L., Bian, H.N., Qi, S.H., De Chen, H., Li, H.D.*, et al.* (2008). "Basic fibroblast growth factor (bfgf) alleviates the scar of the rabbit ear model in wound healing". Wound Repair and Regeneration. **16** (4): 576-581.

Xie, X., McGregor, M. and Dendukuri, N. (2010). "The clinical effectiveness of negative pressure wound therapy: A systematic review". Journal of wound care. **19** (11): 490-5.

Xu, F., Zhang, C. and Graves, D.T. (2013). "Abnormal cell responses and role of tnf-alpha in impaired diabetic wound healing". BioMed research international. **2013** 754802.

Xu, Y., Huang, S. and Fu, X. (2012). "Autologous transplantation of bone marrow-derived mesenchymal stem cells: A promising therapeutic strategy for prevention of skin-graft contraction". Clinical and Experimental Dermatology. **37** (5): 497-500.

Yabushita, H., Bourna, B.E., Houser, S.L., Aretz, T., Jang, I.K.*, et al.* (2002). "Characterization of human atherosclerosis by optical coherence tomography". Circulation. **106** (13): 1640-1645.

Yager, D.R., Chen, S.M., Ward, S.I., Olutoye, O.O., Diegelmann, R.F.*, et al.* (1997). "Ability of chronic wound fluids to degrade peptide growth factors is associated with increased levels of elastase activity and diminished levels of proteinase inhibitors". Wound Repair and Regeneration. **5** (1): 23-32.

Yager, D.R., Zhang, L.Y., Liang, H.X., Diegelmann, R.F. and Cohen, I.K. (1996). "Wound fluids from human pressure ulcers contain elevated matrix metalloproteinase levels and activity compared to surgical wound fluids". Journal of Investigative Dermatology. **107** (5): 743-748.

Yamaguchi, Y., Kubo, T., Murakami, T., Takahashi, M., Hakamata, Y.*, et al.* (2005). "Bone marrow cells differentiate into wound myofibroblasts and accelerate the healing of wounds with exposed bones when combined with an occlusive dressing". British Journal of Dermatology. **152** (4): 616-622.

Yang, Y., Dubois, A., Qin, X.P., Li, J., El Haj, A.*, et al.* (2006). "Investigation of optical coherence tomography as an imaging modality in tissue engineering". Physics in Medicine and Biology. **51** (7): 1649-1659.

Yasuda. (1985). "Plasma polymerisation". Academic Press.

Yeh, A.T., Kao, B.S., Jung, W.G., Chen, Z.P., Nelson, J.S.*, et al.* (2004). "Imaging wound healing using optical coherence tomography and multiphoton microscopy in an in vitro skin-equivalent tissue model". Journal of biomedical optics. **9** (2): 248-253.

Yoda, R. (1998). "Elastomers for biomedical applications". Journal of Biomaterials Science, Polymer Edition. **9** 561-626.

Yoshikawa, T., Mitsuno, H., Nonaka, I., Sen, Y., Kawanishi, K.*, et al.* (2008). "Wound therapy by marrow mesenchymal cell transplantation". Plastic and Reconstructive Surgery. **121** (3): 860-877.

Yuan, Z., Zakhaleva, Julia., Ren, Hugang., Liu, Jingxuan., Chen, Weiliam., Pan, Yingtian. (2010). "Noninvasive and high-resolution optical monitoring of healing of diabetic dermal excisional wounds implanted with biodegradable in situ gelable hydrogels". Tissue Engineering Part C-Methods. **16** (2): 237-247.

Yun, J.K., Defife, K., Colton, E., Stack, S., Azeez, A.*, et al.* (1995). "Human monocyte-macrophage adhesion and cytokine production on surface-modified poly(tetrafluoroethylene hexafluoropropylene) polymers with and without protein preadsorption". Journal of Biomedical Materials Research. **29** (2): 257-268.

Zaulyanov, L. and Kirsner, R.S. (2007). "A review of a bi-layered living cell treatment (apligraf (r)) in the treatment of venous leg ulcers and diabetic foot ulcers". Clinical Interventions in Aging. **2** (1): 93-98.

Zelzer, M., Albutt, D., Alexander, M.R. and Russell, N.A. (2012). "The role of albumin and fibronectin in the adhesion of fibroblasts to plasma polymer surfaces". Plasma Processes and Polymers. **9** (2): 149-156.

Zelzer, M., Majani, R., Bradley, J.W., Rose, F., Davies, M.C.*, et al.* (2008). "Investigation of cell-surface interactions using chemical gradients formed from plasma polymers". Biomaterials. **29** (2): 172-184.

Zhang, M., Methot, D., Poppa, V., Fujio, Y., Walsh, K.*, et al.* (2001). "Cardiomyocyte grafting for cardiac repair: Graft cell death and anti-death strategies". Journal of Molecular and Cellular Cardiology. **33** (5): 907-921.

Zhang, Y.Y., Fisher, N., Newey, S.E., Smythe, J., Tatton, L.*, et al.* (2009). "The impact of proliferative potential of umbilical cord-derived endothelial progenitor cells and hypoxia on vascular tubule formation in vitro". Stem Cells and Development. **18** (2): 359-375.

Zhu, N., Warner, R., Simpson, C., Glover, M., Hernon, C.*, et al.* (2005). "Treatment of burns and chronic wounds using a new cell transfer dressing for delivery of autologous keratinocytes". European Journal of Plastic Surgery. **28** (5): 319-330.

Zou, J.-P., Huang, S., Peng, Y., Liu, H.-W., Cheng, B.*, et al.* (2012). "Mesenchymal stem cells/multipotent mesenchymal stromal cells (mscs): Potential role in healing cutaneous chronic wounds". International Journal of Lower Extremity Wounds. **11** (4): 244-253.

Zysk, A.M., Nguyen, F.T., Oldenburg, A.L., Marks, D.L. and Boppart, S.A. (2007). "Optical coherence tomography: A review of clinical development from bench to bedside". Journal of biomedical optics. **12** (5): 051403.